
# Molecular Visualization and Localization of Ribosomal Subunits Interaction in Cells

**KHALID AL-JUBRAN**

**Supervised by Dr. Saverio Brogna**

January 2010

School of Biosciences
The University of Birmingham
Birmingham, B15 2TT

This dissertation is submitted for the degree of
DOCTOR OF PHILOSOPHY

## Summary

Eukaryotic cells are highly compartmentalized, so that some steps of gene expression occur in the nucleus and others in the cytoplasm, i.e., transcription and pre-mRNA processing are spatially separated from translation which occurs in the cytoplasm. Ribosome subunits and several translation factors are present in the nucleus but it is understood that they can interact to form the functional ribosome only during translation in the cytoplasm. Recent studies, however, have suggested that translation may occur also in the nucleus. That functional ribosomes may exist also in the nucleus has been suggested by studies in the field of nonsense mediated mRNA decay (NMD) and, more directly, by reports that ribosomal proteins are found associated with nascent transcripts on *Drosophila* polytene chromosome and that amino acids are incorporated at transcription sites.

My project aimed to investigate further the question of whether there are functional ribosomes in the nucleus; and also to confirm the presence of ribosomal proteins at active transcription sites. To address these issues, I have developed a system to visualize ribosomal subunits interaction at the molecular level. The technique consists in tagging pair of ribosomal proteins, located at interaction surface of the 40S and 60S subunits, with split fragments of yellow fluorescent protein so that bimolecular fluorescence complementation (BiFC) occurs only when the subunits join to form a 80S ribosome. With this technique I was able to visualize translation sites in *Drosophila* S2 cells and in transgenic flies. Translation sites are most apparent in the cytoplasm, however in cells in which export of ribosomal subunits was blocked by drug treatment a clear signal is visible also in the nucleoplasm. Notably, I also I

detected a strong signal in the nucleolus. These observations suggest that either there is translation in the nucleolus or that, contrary to what is currently understood, ribosome subunits can join together during ribosome biogenesis.

In summary, with the technique I have developed I was able to find further evidence that functional ribosomes are present in the nucleus. This technique and these first results shall aid future investigations into the fundamental issue of whether ribosomes have a function in the nucleus and also to monitor translation changes in living cells.

## Acknowledgements

Firstly, I would like to thank all the people who have encouraged and helped me during my PhD study. I would especially like to express my sincere thanks and gratitude to my supervisor, Dr. Saverio Brogna, for his direct and close supervision and guidance, and his understanding of my needs for the four years of my PhD, which have had a great effect in overcoming many obstacles that I could not have overcome without his help. I would also like to thank Dr Robin May, who was close to me through his kind and humble personality.

I would also like to thank all of people on 6$^{th}$ floor in general, but especially Dr Alicia Hidalgo, for her cooperation and help in writing genetic protocols, and Preethi Ramanathan for her technical help in polysome experiment and generally I would like to extend my thanks to the other members of Saverio's lab, Sandip De, Jiannan Guo, Gavin Ross, Jikai Wen, and Karl Kemp, for their discussions, support and kind friendship.

I would like to thank the government of Saudi Arabia for funding my studentship. Also thanks to the School of Biosciences, University of Birmingham.

Finally I would also like to thank all the members of my family who have sacrificed a lot in order for me to complete my study.

KHALID AL JUBRAN

January 2010

# Abbreviations

| | |
|---|---|
| **40S** | Eukaryotic small ribosomal subunit |
| **60S** | Eukaryotic large ribosomal subunit |
| **80S** | Eukaryotic ribosomes |
| **BiFC** | Bimolecular fluorescence complementation |
| **BSA** | Bovine serum albumin |
| **CBC** | Cap binding complex |
| **CBP** | Cap binding protein |
| **ChIP** | Chromatin immunoprecipitation |
| **Cryo-EM** | Cryo-electron microscopy |
| **DAPI** | 4'-6-diamidino-2-phenylinodole |
| **DBA** | Diamond blackfan anemia |
| **DDAB** | Dimethyl dioctadecyl ammonium bromide |
| **DFC** | Dense fibrillar component |
| **DSE** | Downstream sequence |
| **EDTA** | Ethylenediaminotetra-acetic acid |
| **eEF1 / eEF2/ eEF3** | Eukaryotic translation elongation factors |
| **eIF3/eIF4AIII/eIF4G** | Eukaryotic translation initiation factors |
| **EJC** | Exon-exon junction complex |
| **ER** | Endoplasmic reticulum |
| **eRF1/eRF3** | Eukaryotic release factor 1 and 3 |
| **FBS** | Fetal bovine serum |
| **FC** | Fibrillar component |

| | |
|---|---|
| **FITC** | Fluorescein isothiocyanate |
| **FLIM** | Fluorescence lifetime imaging microscopy |
| **FRET** | Fluorescence resonance energy transfer |
| **GC** | Granular component |
| **GFP** | Green fluorescent protein |
| **HRP** | Horseradish peroxidase |
| **LMB** | Leptomycin B |
| **NMD** | Nonsense-mediated mRNA decay |
| **NPC** | Nuclear pore complex |
| **PABPC** | Poly(A) binding protein, cytoplasm |
| **Pol (I, II, and III).** | RNA polymerases (I, II, and III). |
| **PTC** | Premature termination Condon |
| **RPs** | Ribosomal proteins |
| **SDS** | Sodium dodecyl sulfate |
| **TBS** | Tris-buffered saline |
| **TRIS** | Tris(hydromethyl-amino)ethane |
| **UAS** | Upstream activating sequences |
| **UPF** | Up-frame shift |
| **UTR** | Untranslated region |
| **WGA** | Wheat germ agglutinin |
| **WT** | Wild-type |
| **YC** | C-terminal half of YFP |
| **YFP** | Yellow fluorescent protein |
| **YN** | N-terminal half of YFP |

# Table of Contents

# Chapter 1. Introduction

## 1.1 Eukaryotic gene expression and pre-mRNA processing

Gene expression involves transcription of DNA into mRNA and translation of mRNA into protein. In prokaryotes, the mRNA is translated as soon as it emerges from the RNA polymerase. Instead, in eukaryotes the primary transcript, the precursor of the mRNA (pre-mRNA), undergoes several post-transcriptional modifications before it is exported to the cytoplasm and translated (Moore and Proudfoot, 2009).

All pre-mRNAs undergo 5′-end capping and 3′-end processing and many transcripts (the majority in higher eukaryotes like humans or *Drosophila*) are, in addition, spliced to remove introns (Moore and Proudfoot, 2009). Pre-mRNA processing is coupled to transcription elongation. The first RNA processing event is 5' end capping, which converts the pppN 5' terminus of the primary transcript to 7meGpppN (Shuman, 2001). Processing at the 3' end involves cleavage of the pre-mRNA and addition of a poly(A) tail (Colgan and Manley, 1997). The poly (A) site is specified by an evolutionarily conserved flanking sequence, the best conserved and the most characterized being the polyadenylation signal AAUAAA, which is located 30-40 nt before the polyadenylation site (Colgan and Manley, 1997). Polyadenylation probably facilitates mRNA release from the transcription site and export through the nuclear pore complexes (NPCs) (Jensen et al., 2003). In the cytoplasm the poly(A) tail is required for efficient translation and mRNA stability (Moore, 2005). In eukaryotes, most protein-coding genes contain intervening sequences called introns, which split the pre-mRNA into two or more exons (Berget et al., 1977; Chow et al., 1977). The splicing reaction that removes introns from the pre-mRNA is catalyzed by a

macromolecular complex called the spliceosome (Zhou et al., 2002). In eukaryotes, such as in human cells, genes can be alternatively spliced, whereby a single pre-mRNA molecule gives rise to multiple mRNAs, which may encode for different proteins (Stamm et al., 2005). Alternative splicing can generate many more proteins than the number of genes in the genome. This might explain why more complex organisms like humans do not have significantly more genes than flies or worms , alternative splicing is very frequent in humans and might generate the protein diversity required to account for this increased level of complexity (Hui, 2009).

After pre-mRNA processing, the mature mRNA is exported to the cytoplasm where it can be translated into proteins by the ribosome. The export of mRNA requires association with proteins to form the export competent mRNA protein complex (mRNP) (Brodsky and Silver, 2000). Eukaryotic gene expression is a highly interconnected process that can be controlled at multiple steps (Hagiwara and Nojima, 2007; Moore and Proudfoot, 2009). The coupling of pre-mRNA processing with transcription, along with the link with downstream events like export, mRNA stability and translation, depends on the structure and composition of the mRNP. The assembly of the mRNP starts co-transcriptionally and impinges upon seemingly unconnected events such as mRNA localization and translation (Moore and Proudfoot, 2009). The observation that pre-mRNA splicing affects translation and nonsense mediated mRNA decay (NMD) is major evidence for the existence of a link between pre-mRNA processing in the nucleus and cytoplasmic events (these key studies are reviewed in the NMD section below).

## 1.2 Translation

For protein-encoding genes, the final step of gene expression is translation. Translation is the process that decodes the genetic sequence on the mRNA into proteins, and this process is carried out by the ribosome, a large macromolecular machine that consists of both RNA and proteins (see below). In both eukaryotic and prokaryotic cells, translation of a single mRNA is a very complex mechanism that can be divided into four major phases: initiation, elongation, termination and recycling (Kapp and Lorsch, 2004) (Figure 1.1). Whereas elongation in prokaryotes and eukaryotes involves similar factors and proceeds by similar mechanisms, the initiation, termination, and ribosome recycling mechanisms appear to be quite different between these types of organisms. Initiation is a complicated and highly regulated process (Rodnina and Wintermeyer, 2009). In the first step, the initiator tRNA binds to the 40S ribosomal subunit to form the 43S complex, and then this 43S complex associates with the eukaryotic initiation factor eIF4E that is bound with the 7-methylguanosine (m7G) cap of the mRNA. The recruitment of the 43S complex is mediated by an interaction with eIF4G, which is a scaffold protein that interacts with both eIF4E and with eIF3 on the 43S. Once on the mRNA, the 43S complex scans the 5' UTR until the initiation codon is detected. At this point, the large ribosomal subunit (60S) joins the complex to form a translation competent 80S in which the initiation codon is paired with the anticodon of the initiator-tRNA in the peptidyl (P) site of the ribosome. Protein synthesis occurs during the elongation phase, in which the ribosome pairs codons with cognate aa-tRNAs and catalyses peptide bond formation between the incoming amino acid and the peptidyl-tRNAs (Acker and Lorsch, 2008; Kapp and Lorsch, 2004).

As mentioned above, the elongation phase of translation is similar across all the kingdoms of life (Ramakrishnan, 2002). Elongation involves three steps: 1) binding of the cognate aminoacyl-tRNA in the aminoacyl (A) site, 2) peptide bond formation, and 3) translocation of the peptidyl-tRNA complex from the A site to the P site. The process of elongation requires two proteins that are conserved between prokaryotes and eukaryotes. In eukaryotes these are eEF1 and eEF2 (in yeast a third protein, eEF3, is required). Both cognate and noncognate aminoacyl tRNAs can bind to the ribosomal A site, but several mechanisms involving codon-anticodon base pairing and conformational changes in the decoding center of the 40S ensure that only the cognate aa-tRNA is attached to the nascent peptide (Rodnina and Wintermeyer, 2001). Peptide bond formation between the incoming amino acid and the P site peptidyl-tRNA is catalyzed by the ribosomal peptidyl transferase center in the large ribosomal subunits (Beringer and Rodnina, 2007).

Following peptide bond formation, tRNAs and mRNA move through the ribosome between the A, P and exit (E) sites of the ribosome in a process called translocation (Beringer and Rodnina, 2007). During translocation, which is catalyzed by eEF2, the ribosome repositions the A site over the next codon in the mRNA, the peptidyl-tRNA moves to the P site and the deacylated tRNA leaves the ribosome through the E site.

Elongation stops when the ribosome reaches a stop codon. There are no tRNAs to interact with the stop codon and instead the release factor eRF1 enters the A site and, together with eRF3, they trigger the release of the nascent peptide (Pisareva et al., 2006).

In eukaryotes there is cumulative evidence that translation occurs on mRNA that is kept in a closed-loop conformation whereby it has been suggested that, after

termination, the 40S subunit is recycled on the same mRNA and not released into the cytosol (Wells et al., 1998). The 40S subunit may be shuttled across or over the poly(A) tail back to the 5'-end of the mRNA via the 5'- and 3'-end-associated factors (Kapp and Lorsch, 2004). Recently, the eIF3 has been reported essential for the splitting of 80S ribosomes into 40S and 60S subunits (Pisarev et al., 2007)

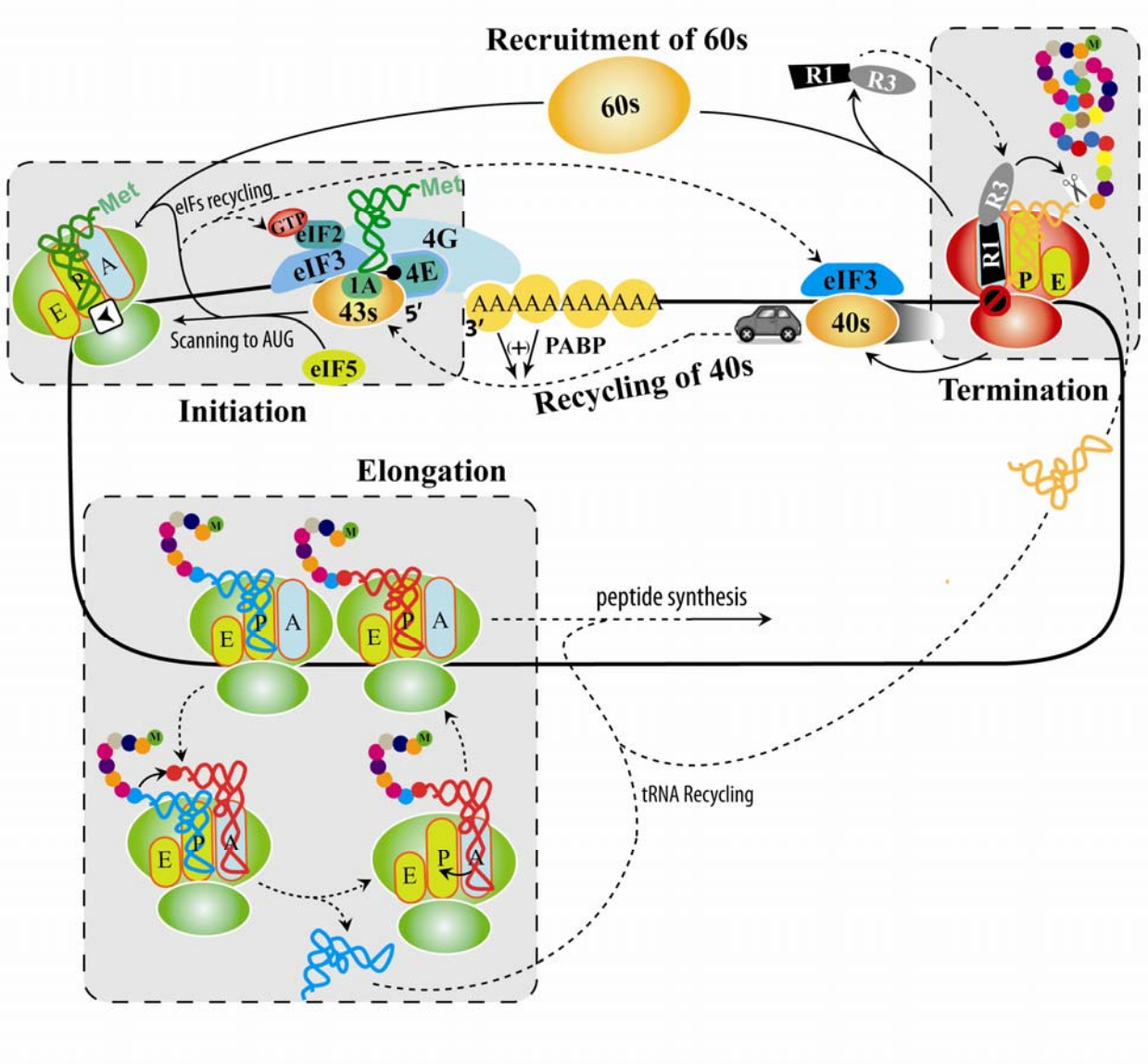


**Figure 1.1 Schematic diagram of translation phases in eukaryotes.**

In the initiation steps the initiator methionyl tRNA is brought to the 40S subunit by eIF-2 to form 43S. The mRNA is recognized and brought to the 43S by the eIF-4 group of factors associated with the 5' end cap. The 43S intiation complex then scans down to identify the first initiation codon, where the 60S subunit binds to the 40S subunit to form the 80S initiation complex. During elongation, peptide bonds are formed between the amino acids while the ribosome moves along the mRNA. This movement translocates the peptidyl tRNA to the P site and the uncharged tRNA to the E site, leaving an empty A site ready for addition of the next amino acid until a stop codon is reached, which is recognized by releasing factors, tRNA is then released, and the ribosomal subunits and the template mRNA dissociate to be reutilized in new round of translation.

## 1.3 Eukaryotic cell compartmentalization and translation

In contrast to prokaryotic cells, eukaryotic cells are highly compartmentalized, with many steps of gene expression being restricted either to the nucleus or to the cytoplasm. It is commonly accepted that transcription and RNA processing take place in the nucleus, but that translation occurs only in the cytoplasm. It was, therefore, believed that there is no direct link between nuclear events, such as pre-mRNA splicing, and cytoplasmic events, such as translation and mRNA destruction. As mentioned previously, this dogma has been challenged in recent years by reports that indicate that the nature of the nuclear mRNP also impinges on cytoplasmic events such as translation and NMD (Moore and Proudfoot, 2009). In addition, there are reports that translation, or a translation-like mechanism, may exist within the nucleus. In the next two sections I review published data which suggest the existence of translation in the nucleus. In the first section I review a set of studies coming from the NMD field. In the second, I review data that appears to provide direct evidence that ribosome components are associated with the nascent transcript and that translation can occur in the nucleus.

### 1.3.1. Nonsense mediated mRNA decay and translation

NMD describes the translation coupled mechanism by which the presence of a nonsense mutation in the transcript often leads to a reduction in mRNA levels (Brogna and Wen, 2009). NMD works as an mRNA quality control mechanism, which selectively degrades mRNA harbouring premature translation termination codons (PTCs). This phenomenon has been observed in all organisms that have been so far investigated. It has been best studied in *D. melanogaster*, *S. cerevisiae*, *C. elegans*,

and mammalian cells (Amrani et al., 2004; Belgrader et al., 1993; Brogna et al., 1999; Buhler et al., 2006; Carter et al., 1996; Gatfield et al., 2003; Kertesz et al., 2006; Le Hir et al., 2001; Le Hir et al., 2000; Maquat, 1995; Pulak and Anderson, 1993). As an evolutionarily conserved mechanism, NMD probably evolved to protect the cell from the potentially deleterious effect of truncated proteins. PTCs can be generated by nucleotide mutations (substitution, insertion or deletion), RNA transcription error or by abnormal pre-mRNA processing. Mutations that alter splicing signals generate nonsense mutations, frequently due to the retention of intronic sequences (Holbrook et al., 2004; Mendell and Dietz, 2001). Abnormally spliced mRNAs are probably the most frequent NMD substrates in cells (McGlincy and Smith, 2008). Inactivation of NMD in *S. cerevisiae* causes an accumulation of many unspliced mRNAs indicating that NMD might contribute to splicing regulation (Atmakuri et al., 2003; Sayani et al., 2008). NMD is an active process that requires specific trans-acting factors that were first recognized in *S. cerevisiae* and *C. elegans* (Culbertson et al., 1980; Hodgkin et al., 1989). The better known factors are the proteins encoded by the *UPF1, UPF2* and *UPF3* (Upstream frameshift) genes. These three proteins associate together to form the UPF complex, which constitutes the conserved core of the NMD mechanism from yeast to humans (Conti and Izaurralde, 2005). The interaction between UPF1 and UPF3 is bridged by UPF2 (Chamieh et al., 2008; He et al., 1997; Weng et al., 1996). Deletion or silencing of these genes results in the stabilization of mRNAs containing PTCs and prevents NMD in all tested eukaryotic organisms (Conti and Izaurralde, 2005) . In both *S. cerevisiae* and mammalian cells, UPF1 has been reported to associate with the ribosome via an interaction with eukaryotic translation release factors eRF1 and eRF3 (Kashima et al., 2006). In addition to the conserved UPF core

complex, additional proteins have been shown to be involved in NMD in higher eukaryotes (Conti and Izaurralde, 2005)

#### 1.3.1.1 NMD requires translation

Since translating ribosomes are the only known means of detecting termination codons, NMD requires translation. The mechanism that links NMD and translation is, however, still puzzling; but is clear that translation of the mRNA is required: for example, tRNA suppressors, antibiotics and hairpins in the 5'-UTR that inhibit translation also abolish NMD (Belgrader et al., 1993; Lim and Maquat, 1992; Qian et al., 1993). The key question that remains to be addressed in the field is how the ribosome is able to differentiate normal translation termination from premature termination (Brogna and Wen, 2009).

##### 1.3.1.1.1 PTC recognition and NMD mechanisms

Studies in mammalian cells indicated that PTC recognition is linked to pre-mRNA splicing (Maquat, 2004). In many studies, it has been found that introns enhanced NMD when positioned after the PTC (Carter et al., 1996; Zhang and Maquat, 1996; Zhang et al., 1998). It appears that PTCs are distinguished from normal stop codons by their position relative to the last exon-exon junction: PTC can trigger NMD only when located upstream of at least one intron (Zhang et al., 1998). Consistent with this model, insertion of an intron downstream from the normal stop codon triggers NMD (Thermann et al., 1998), this manipulation makes a normal stop codon look like a PTC (Hentze and Kulozik, 1999). The finding that mRNAs derived from naturally intronless genes are immune to NMD is also consistent with this model (Maquat and Li, 2001). The link between NMD and splicing is probably mediated by RNA binding proteins that bind the pre-mRNA in the nucleus and remain associated with the mature

mRNA in the cytoplasm. Consistent with this view, it has been found that pre-mRNA splicing deposits multiple proteins about 20-24 nt upstream of the exon-exon junction site, and these proteins form a well defined complex called the exon-exon junction complex (EJC) (Le Hir et al., 2001). In addition to NMD, the EJC has a role in mRNA export and localization (Degot et al., 2004; Giorgi et al., 2007; Hachet and Ephrussi, 2004; Palacios et al., 2004).

The EJC binds NMD UPF2 and UPF3 and provides a direct link between splicing and translation (Brogna and Wen, 2009; Le Hir et al., 2001). The interaction between the EJC and NMD factors is proposed to promote UPF1 recruitment (Figure 1.2A) and activation the NMD inducing complex that commits the mRNA for decay (Chamieh et al., 2008). The position of the PTC relative to the exon–exon junction is critical, as NMD occurs when translation terminates more than 50–55 nucleotides upstream of the 3'-most exon–exon junction. In contrast, mRNA is immune to NMD if translation terminates less than 50–55 nucleotides upstream of the 3'- exon–exon junction or downstream of the junction (Zhang and Maquat, 1996; Zhang et al., 1998).

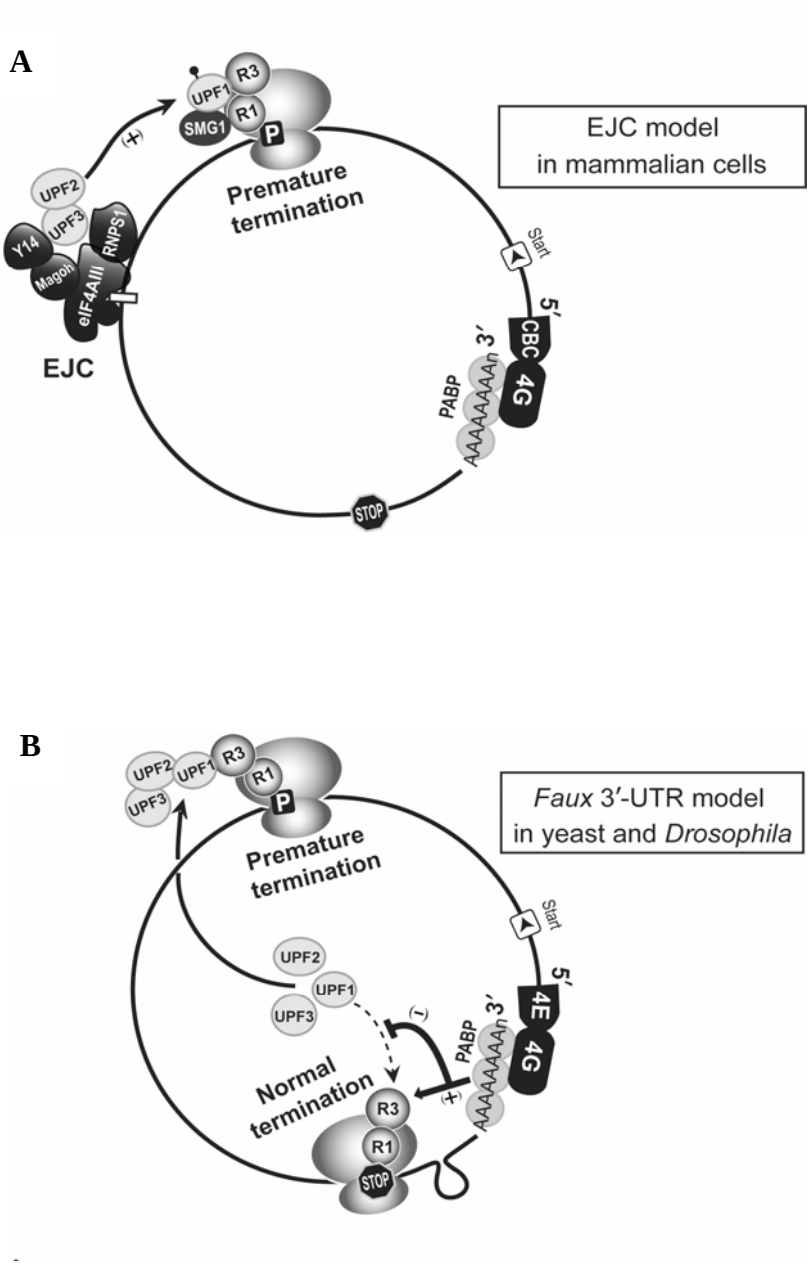


**Figure 1.2 Mechanisms that distinguish between normal and premature termination codons.** (A) EJC model in mammalian cells. A PTC triggers NMD only if it is located upstream of an intron; the EJC accelerates the recruitment of UPF proteins. The association of UPF proteins triggers rapid mRNA decay. (B) *Faux* 3' UTR model in *S. cerevisiae* and *D. melanogaster*. During normal translation termination the terminating ribosome is in close proximity to the 3' end poly (A) tail-bound PABPC, which stimulate termination. If termination is far away from the poly (A) tail, termination is aberrant because of lack of interaction with PABC and triggers rapid mRNA decay (NMD). The main factors and complexes involved in NMD are shown above (see text for details).

#### 1.3.1.1.2 (EJC) independent NMD

Unlike mammalian genomes, the yeast genome has very few introns and lacks an EJC homologue (Kressler et al., 1997). It was proposed that in yeast it is the presence of a downstream sequence element (DSE) that distinguishes NMD inducing PTCs from normal stop codons (Zhang et al., 1995). The DSE function is analogous to that of the EJC in mammalian cells; it is proposed that the DSE associates with some RNA binding proteins that in turn recruit NMD factors (Ruiz-Echevarria et al., 1998).

NMD is the most apparent with 5' proximal PTCs but not with mutations located further downstream. This polarity phenomenon has been documented and the general conclusion is that nonsense mutations in the 5' half of the mRNA cause strong and rapid mRNA decay, whereas mutations in the second half of the gene behave like a normal stop codon (Amrani et al., 2006; Brogna and Wen, 2009). In adddition, it was reported that mRNAs with extended 3' UTRs are also NMD substrates in *S. cerevisiae* and *C. elegans* (Muhlrad and Parker, 1999). This and other similar findings are explained by the the *faux* 3' UTR model of NMD (Amrani et al., 2004; Behm-Ansmant et al., 2007; Buhler et al., 2006; Eberle et al., 2008; Kebaara and Atkin, 2009; Muhlrad and Parker, 1999; Singh et al., 2008) This model proposes that the distinction between normal and premature termination might simply depend on the distance between the stop codon and the 3' end of mRNA (Figure 1.2 B). In agreement with this model, efficient termination and mRNA stability appear to require an interaction between a terminating ribosome and a poly(A) binding protein (PABC), whereas inefficient termination is due to the lack of an interaction between the terminating ribosome and PABPC, and it is this lack of interaction that triggers NMD (Amrani et al., 2004). In higher organisms, this model could explain the NMD

polarity observed in the alcohol dehydrogenase (*Adh*) gene in *D. melanogaster*, the chloramphenicol acetyltransferase (*Cat*) gene in *Drosophila* S2 cells, and the immunoglobulin μ gene (Ig-μ) in human cells (Behm-Ansmant et al., 2007; Brogna et al., 1999; Buhler et al., 2006; Gatfield and Izaurralde, 2004).

A number of recent reports have questioned the applicability of the EJC model and proposed that the *faux* 3' UTR model explains NMD better than the EJC model also in S2 cells and NMD in mammalian cells (Buhler et al., 2006; Eberle et al., 2008; Singh et al., 2008).

#### 1.3.1.2 NMD in the nucleus

As reviewed above, there is compelling evidence for the fact that proteins that associate with the mRNA in the nucleus can affect translation and NMD in the cytoplasm. An important issue, however, is whether the reverse interaction can also occur: does translation affect pre-mRNA processing? A number of studies have reported data suggesting that this may also occur. In mammalian cells, there is early data suggesting that NMD may take place in the nucleus (Chang and Kan, 1979). Further early studies support the suggestion that NMD is a nucleus-associated event (Belgrader et al., 1994; Cheng et al., 1994; Cheng and Maquat, 1993). Other observations have also reported that PTCs can affect both the nuclear and cytoplasmic mRNA fractions, supporting nuclear NMD or NMD during nuclear export (Maquat, 1995). Some studies in human cells indicate that NMD occurs while the mRNA is still associated with the nuclear cap binding complex (CBC, formed by CBP80 and CBP20), before CBC is replaced by the cytoplasmic cap binding protein, eIF4E (Ishigaki et al., 2001). The EJC appears to associate with CBP80-bound mRNA but not with eIF4E-bound mRNA (Lejeune et al., 2002). These studies, therefore, indicate

that CBP80 is required for NMD in mammalian cells. RNAi depletion of CBP80 stabilizes NMD substrates (Hosoda et al., 2005). This first round of translation of CBC-associated mRNA was called the pioneer round of translation and it may happen while the mRNA is still associated with the nuclear envelope. Therefore, it is feasible that seemingly nuclear NMD is simply due to a pioneer round of translation of mRNA not yet released from the nuclear envelope. However, it is feasible that nonsense mutation recognition could occur while the transcript is still in the nucleus. In particular, it has been proposed that PTC can be recognised on nascent mRNA. This possibility is supported by a study showing that PTCs can affect pre-mRNA 3'end processing - the closer the premature stop codon is to the 5'end the longer the poly(A) tail is (Brogna et al., 1999); and by another study showing that PTCs lead to an accumulation of pre-mRNA at the site of transcription (Li et al., 2002; Muhlemann et al., 2001). Observations that PTCs can affect pre-mRNA splicing are consistent with the suggestion that translation might occur also in the nucleus (Li et al., 2002).

### 1.3.2 Coupling of transcription and translation in eukaryotes

If, as reported above, NMD can occur in the nucleus, presumably there must be some translation occurring in the nucleus. Here I review old and new studies that suggest the existence of translation in the nucleus. The notion that translation might occur also in the nucleus is not new as evidence of nuclear polysomes and translation was reported more than three decades ago (Allen and Wong, 1978; Goldstein, 1970). Functional polyribosomes have been found in the nuclei of the slime mould *Dictyostelium discoideum* (Mangiarotti, 1999). Furthermore, in *D. discoideum*, newly assembled 40S and 60S ribosomal subunits, that are still associated with pre-rRNA, appear to be fully active in protein synthesis and the pre-rRNA is often detected in

80S monosomes and even polyribosomes *in vivo* and *in vitro* (Mangiarotti and Chiaberge, 1997). Direct evidence for nuclear translation was provided by experiments that allow visualization of translation sites in mammalian cells (Iborra et al., 2001). It was reported that fluorescently labelled amino acids could be incorporated into nascent peptides in highly purified nuclei. In this assay, putative translation sites were readily visible under a fluorescence microscope and appeared as distinct fluorescent foci. The occurrence of this nuclear fluorescence and of fluorescent dots was prevented by translation inhibitor drugs. Putative translation was found close to transcription sites and was found to be sensitive to transcription inhibitors. These observation were interpreted as evidence that, like in prokaryotes , translation might be coupled to transcription in the nucleus (Iborra et al., 2001). In agreement with this conclusion, a later study reported that several NMD, transcription and translation factors copurify in biochemical procedures and colocalize in electron microscopy (EM)-immunostaining assays (Iborra et al., 2004). Similar observations were also reported in *Drosophila*. It was found that [$^{35}$S]methionine/cysteine was rapidly incorporated at active transcription sites of polytene chromosomes and in the nucleolus; this incorporation is sensitive to translation inhibitor drugs (Brogna et al., 2002). In this latter study, it was also reported that many ribosomal proteins and some translation factors are found associated with transcription sites. In addition, it was also shown by in situ hybridization that rRNA is also present at these chromosomal sites (Brogna et al., 2002). These experiments support the view that translation also might be coupled to transcription in eukaryotes.

The view that translation might occur in the nucleus is controversial. It has been argued that the seemingly nuclear translation reported by Iborra et al. (2001) is due to contamination of the nuclei with endoplasmic reticulum (ER), as the ER is attached to

the nuclear envelope and is difficult to strip away from the nuclei(Dahlberg et al., 2003). The nuclear signal could be an artifact of over-permeabilization of the nuclei, which might lead to entry of cytoplasmic ribosomes into the nucleus (Nathanson et al., 2003). Similarly to the Iborra study, the study by Brogna et al was criticized; it was argued that the antibodies used were not specific for ribosomal proteins and that the immunostaining procedure allows artificial access of cytoplasmic materials into the nucleus (Dahlberg et al., 2003). However, in agreement with the study by Brogna et al. (2002), a later study also found evidence that ribosomal proteins are associated with chromatin (Schroder and Moore, 2005). It was found that ribosomal proteins copurify with the linker histone H1 in *Drosophila* cells (Ni et al., 2006). Ribosomal proteins were reported to be associated with nascent transcripts in *S. cerevisiae.* It was found, using chromatin immunoprecipitation (ChIP) assays, that ribosomal proteins associate with chromatin via RNA (Schroder and Moore, 2005). Surprisingly, ribosomal proteins were found to associate with both protein- and non-protein-encoding genes.

In summary, it is apparent that ribosomal components and translation factors are present in the nucleus at active transcription sites, the issue is whether this localization reflects fully assembled ribosomes or merely free ribosomal proteins. In addition, it has been pointed out that the absence of a key translation factor would be sufficient to preclude translation in the nucleus. A study with mammalian cells has concluded that key translation factors are actively excluded from the nucleus (Bohnsack et al., 2002). However, the issue is still open and we await further evidence before a conclusion can be drawn. In my PhD project I studied this issue further. In particular, I aimed to visualize the interaction of ribosomal subunits *in vivo* and to test whether the subunits can interact in the nucleus.

## 1.4 Ribosome structure

Ribosomes are large ribonucleoprotein complexes consisting of ~ 65% ribosomal RNA and ~ 35% ribosomal proteins (RPs) in eukaryotes. Each ribosome is composed of a large ribosomal subunit (50S in prokaryotes and 60S in eukaryotes) and a small ribosomal subunit (30S in prokaryotes and 40S in eukaryotes). The large subunit contains the catalytic centre (peptidyltransferase centre) that drives peptide bond formation, while the small subunit contains the decoding domain, which pairs the codon triplet on the mRNA with the anticodon of the corresponding tRNA (Maguire and Zimmermann, 2001).

The level of understanding of the structure of the ribosome has improved significantly following the publication of high-resolution crystallography structures of prokaryotic ribosomes. Knowing the structure of the ribosome has revolutionized the ribosome field and now allows investigation of the ribosome functions at the atomic level .The first high-resolution structure of the 50S subunit from *Haloarcula marismortui* was reported in the year 2000 at the level of 2.4 Å resolution (Ban et al., 2000). Two high-resolution structures of the *Thermus thermophilus* 30S subunit at 3.3 Å and 3.0 Å have been reported (Schluenzen et al., 2000; Wimberly et al., 2000), and the complete structure of the *T. thermophilus* 70S ribosome in the presence of mRNA and tRNAs bound in the A, P and E sites has also been reported (Yusupov et al., 2001). The two subunits have a number of shared features, such as that the interface side of both subunits is largely free of proteins and that most of the proteins in the subunits have a globular domain, are found generally on the solvent side of the subunit and have long extensions that pass through and interact with ribosomal RNA (rRNA) and stabilise its tertiary structure (Figure 1.3).

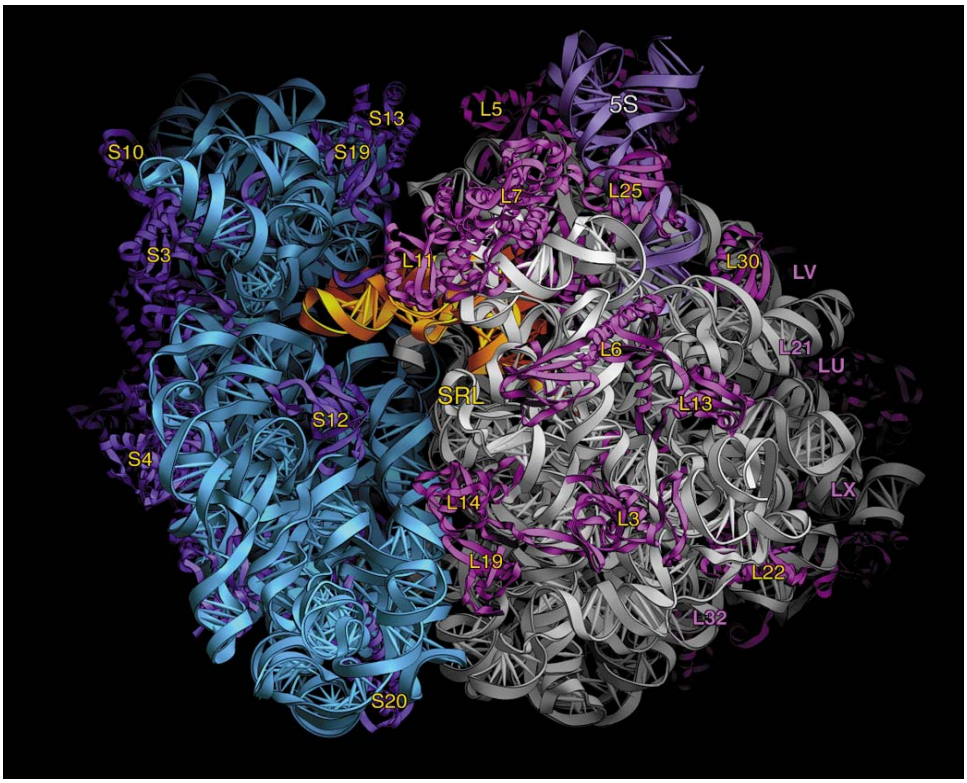


**Figure 1.3 An overview of the complete crystal structure of the two subunits of the bacterial 70S ribosome**. The structure is showing the subunits interface cavity, with the 50S subunit on the right and the 30S subunit on the left. The anticodon arm of the A-tRNA (gold) is visible in the interface cavity (Yusupov et al., 2001).

Due to the evolutionary conservation of both rRNA and ribosomal proteins between prokaryotes and eukaryotes, the structure of the eukaryotic ribosome is expected to be similar to the prokaryotic one; and it can be expected that the fundamental mechanism of ribosome biosynthesis is common in prokaryotes and eukaryotes. But the actual degree of similarity is not yet known and in fact there are significant differences: eukaryotic ribosomes have 20-30 more RPs and the rRNA is larger than its prokaryotic counterpart. In terms of function, there are differences between eukaryotic and prokaryotic ribosomes, as mentioned above, apart from elongation the other translation phases are quite different. In general, the translation cycle in eukaryotes is more complex than in prokaryotes (Ramakrishnan, 2002). The atomic structure has not yet been obtained for any eukaryotic ribosome, but there are high quality cryo-electron microscopy (cryo- EM) structures available. The first high-resolution (15 Å) cryo-EM reconstruction of a eukaryotic ribosome has been reported for the *S. cerevisiae* 80S (Spahn et al., 2001); and more recently also for the mammalian 80S ribosome at 8.7Å resolution(Chandramouli et al., 2008). The mammalian ribosome is larger than the yeast ribosome, but mammalian and yeast ribosomes contain a similar number of proteins and the difference in size is due to expansion segments in the large subunit rRNA (Chandramouli et al., 2008). These studies revealed the positions of all the major rRNA expansion elements, as well as of additional proteins and inter subunit bridges, they also revealed that the 18S rRNA is 256 nt longer than the 16S rRNA of *E. coli* and that the 40S subunit contains 11 more proteins than the 30S subunit; 15 of the ribosomal proteins of the 40S subunit have a homologue in bacteria while 17 have not (Table1). The 60S subunit is made from a 25S rRNA, a 5.8S rRNA, a 5S rRNA and 45 ribosomal proteins; there are 12 more ribosomal proteins in the

eukaryotic 60S subunit than in the *E.coli* 50S subunit. The 25S rRNA is 646 nucleotides longer than its *E. coli* counterpart. These rRNA expansion segments are located at the surface of the subunits. Twenty eight of the 60S RPs have a homologue in bacteria while 17 do not (Table2). There are 33 RPs that are conserved between *D.melanogaster*, *S. cerevisiae* and *E.coli* (Table 3). RNA domains and ribosomal proteins present at the interface between subunits form intersubunit bridges, which are important for the movement of the subunits during translation. All the bridges discovered in bacterial ribosomes are conserved in eukaryotes and involve RNA-RNA interactions, protein-RNA interaction and one protein-protein interaction (Merryman et al., 1999; Mitchell et al., 1992; Yusupov et al., 2001). The protein-protein bridge (B1b/c) is formed by RpS18 (RpS13 in prokaryotes) and RpL11 (RpL5 in prokaryotes) and connects the head of the 40S subunit to the central protuberance of the 60S subunit (Spahn et al., 2001) (Figure 1.4). Recently, another protein-protein bridge was observed from the cryo-EM map of the wheat germ 80S ribosome; this bridge (eb9) is formed by RpS13 (RpS15 ) and RpL30 (Halic et al., 2005).

**Table 1. 40S RPs with a homologue in Bacteria**

**(Spahn et al., 2001)**

| *S. cerevisiae* (Rp) | *E.coli* (Rp) | Sequence Identity (%) |
|---|---|---|
| **S0** | S2 | **30** |
| **S2** | S5 | **29** |
| **S3** | S3 | **27** |
| **S5** | S7 | **32** |
| **S9** | S4 | **21** |
| **S11** | S17 | **36** |
| **S13** | S15 | **20** |
| **S14** | S11 | **41** |
| **S15** | S19 | **34** |
| **S16** | S9 | **43** |
| **S18** | S13 | **31** |
| **S20** | S10 | **28** |
| **S22** | S8 | **25** |
| **S23** | S12 | **36** |
| **S29** | **S14** | **37** |

**Table 2. 60S RPs with a homologue in Bacteria**

**(Spahn et al., 2001)**

| *S. cerevisiae* (Rp) | *E.coli* (Rp) | *Sequence Identity (%)* |
|---|---|---|
| **L1** | L1 | **20** |
| **L2** | L2 | **46** |
| **L3** | L3 | **35** |
| **L4** | L4 | **36** |
| **L5** | L18 | **39** |
| **L7** | L30 | **21** |
| **L8** | L7 | **26** |
| **L9** | L6 | **32** |
| **L10** | L10 | **29** |
| **L11** | L5 | **37** |
| **L12** | L11 | **21** |
| **L15** | L15 | **38** |
| **L16** | L13 | **35** |
| **L17** | L22 | **30** |
| **L18** | L18 | **28** |
| **L19** | L19 | **36** |
| **L21** | L21 | **23** |
| **L23** | L14 | **41** |
| **L24** | L24 | **30** |
| **L25** | L23 | **42** |
| **L26** | L24 | **34** |
| **L28** | L15 | **23** |
| **L31** | L31 | **33** |
| **L32** | L32 | **33** |
| **L35** | L29 | **27** |
| **L37** | L37 | **56** |
| **L42** | L44 | **26** |
| **L43** | **L37** | **40** |

**Table 3 The orthology of D.*melanogaster* Rps with *S.cerevisiae* and *E.coli***

**RPG(Ribosomal Protein Gene data base)**

| ***E.coli* (Rp)** | ***S.cerevisiae* (Rp)** | ***D.melanogaster* (Rp)** |
|---|---|---|
| RPS2 | RPS0A<br>RPS0B | sta |
| RPS3 | RPS3 | RpS3 |
| RPS4 | RPS9A<br>RPS9B | RpS9 |
| RPS5 | RPS2 | sop |
| RPS7 | RPS5 | RpS5a<br>RpS5b |
| RPS8 | RPS22A<br>RPS22B | RpS15Ab<br>RpS15Aa |
| RPS9 | RPS16A<br>RPS16B | RpS16 |
| RPS10 | RPS20 | RpS20 |
| RPS11 | RPS14A<br>RPS14B | RpS14a<br>RpS14b |
| RPS12 | RPS23A<br>RPS23B | RpS23 |
| RPS13 | RPS18A<br>RPS18B | RpS18 |
| RPS14 | RPS29A<br>RPS29B | RpS29 |
| RPS15 | RPS13 | RpS13 |
| RPS17 | RPS11A<br>RPS11B | RpS11 |
| RPS19 | RPS15 | RpS15 |
| RPL1 | RPL1A<br>RPL1B | RpL10Ab<br>RpL10Aa |
| RPL2 | RPL2A<br>RPL2B | RpL8 |
| RPL3 | RPL3 | RpL3 |
| RPL5 | RPL11A<br>RPL11B | RpL11 |
| RPL6 | RPL9A<br>RPL9B | RpL9 |
| RPL10 | RPP0 | RpLP0 |
| RPL11 | RPL12A<br>RPL12B | RpL12 |
| RPL7/L12 | RPP1A<br>RPP1B | RpLP1 |
| RPL13 | RPL16A<br>RPL16B | RpL13A |
| RPL14 | RPL23A<br>RPL23B | RpL23 |
| RPL15 | RPL28 | RpL27A |
| RPL16 | RPL10 | Qm |
| RPL18 | RPL5 | RpL5 |
| RPL22 | RPL17A<br>RPL17B | RpL17 |
| RPL23 | RPL25 | RpL23A |
| RPL24 | RPL26A<br>RPL26B | RpL26 |
| RPL29 | RPL35A<br>RPL35B | RpL35 |
| RPL30 | RPL7A<br>RPL7B | RpL7 |

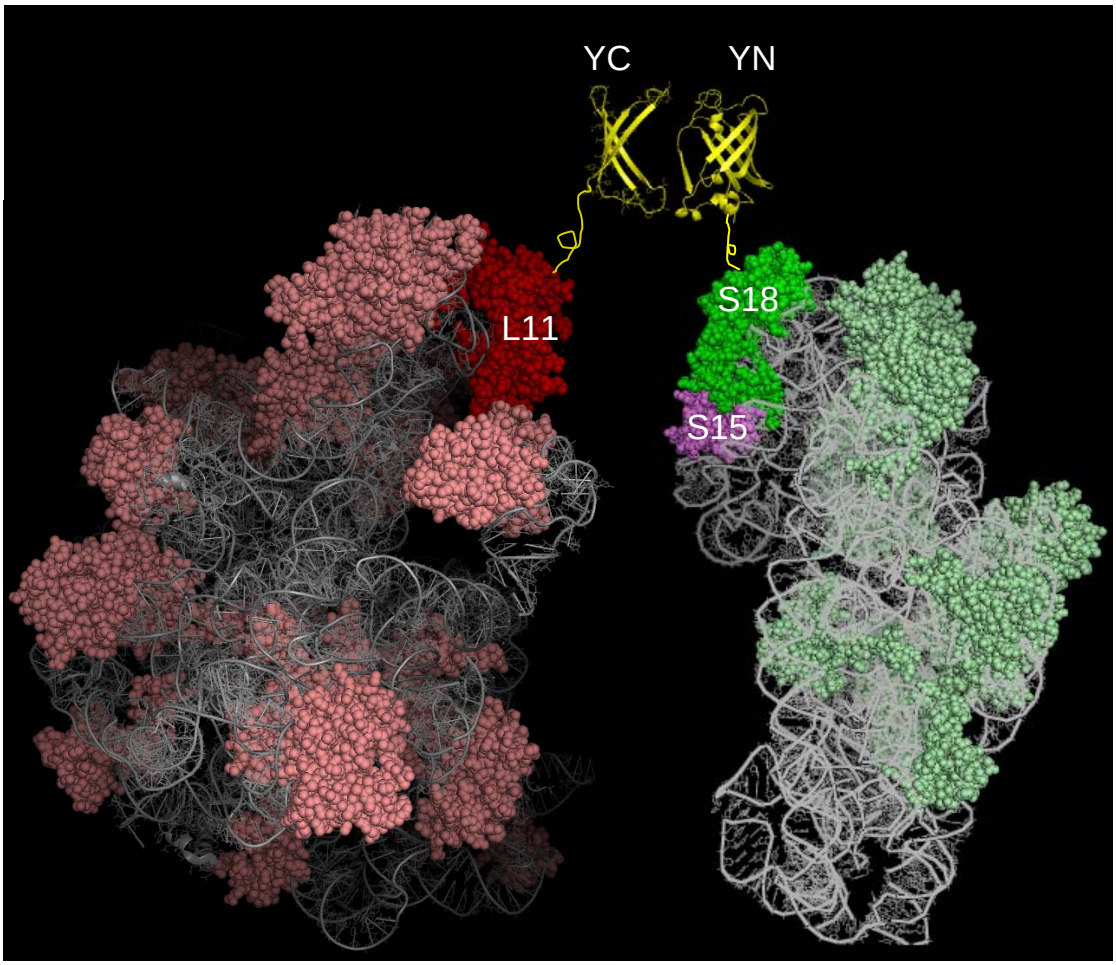


**Figure 1.4 The 15Å cryo-EM structure of the yeast 80S ribosome.** The model is viewed from the right hand side, showing the subunit interface cavity, with the 60S subunit on the left and the 40S subunit on the right. The RPs that are involved in the interaction of the ribosomal subunits, L11, S18 and S15 (labeled with the BiFC fragments, YC and YN) are indicated The structure was visualized with PyMol (www.pymol.org) using the pdb files deposited in the RCSB Protein Data Bank by Spahn et al (Spahn et al., 2001); accession codes 1K5X, 1K5Y, and 1K5Z.

## 1.5 Ribosome biogenesis

Eukaryotic ribosome biogenesis is a very dynamic, highly coordinated multi-step process. Biogenesis requires synthesis, processing and modification of the pre-rRNA, and assembly with ribosomal proteins and other non-ribosomal factors. Ribosomal subunit assembly in eukaryotes mainly takes place in the nucleolus, a specialized sub-nuclear compartment (Tschochner and Hurt, 2003).

Ribosome biogenesis is significantly more complex in eukaryotes compared with their prokaryotic counterparts. For instance, whereas a single RNA polymerase synthesizes all rRNAs and mRNAs in bacteria, in eukaryotes, ribosome biogenesis requires the action and coordination of all three RNA polymerases (I, II, and III). The rRNA is transcribed by Pol I as a polycistronic pre-rRNA transcript in the nucleolus, instead the 5S rRNA is transcribed by RNA polymerase III from a separate locus in the nucleoplasm. And the ribosomal protein genes are transcribed by Pol II. Ribosomal proteins are synthesized in the cytoplasm and rapidly imported into the nucleus, where they associate with rRNAs to form pre-ribosomal subunits (Lam et al., 2007; Tschochner and Hurt, 2003). The pre-rRNA is transcribed first as a 35S precursor, which folds into a 90S pre-ribosomal particle (Perez-Fernandez et al., 2007; Schneider et al., 2007). The pre-rRNA then undergoes a series of endo- and exonucleolytic cleavage reactions in the spacer region, between the sequences of the 18S rRNA and the 5.8S rRNA, which splits the 90S pre-ribosome into a pre-40S and a pre-60S particle (Chu et al., 1994; Lygerou et al., 1996). In some cases, for example, in yeast under active growth conditions, the 35S RNA is cleaved co-transcriptionally in the internal transcribed spacer, thereby releasing pre-40S particles without prior 90S

particle formation (Osheim et al., 2004) and more recently the immature pre-40S was reported competent to initiate the translation in *S. cerevisiae,* (Soudet et al., 2009).The 5S rRNA binds ribosomal proteins RpL5 and RpL11 forming a subcomplex in the nucleolus before assembling to the 90S pre-ribosome (Zhang et al., 2007).

Ribosome biogenesis involves a number of additional maturation and assembly steps, which require the intervention of a large number of non-ribosomal proteins, small RNAs and *trans*-acting factors, which transiently participate in ribosome biogenesis at different stages (Venema and Tollervey, 1999). The 90S pre-ribosome is the first intermediate in the ribosome biogenesis pathway; at this stage most of the small subunit RPs are already associated (Ferreira-Cerca et al., 2007). It is generally believed that many RPs associate very early with the nascent pre-rRNA, probably in the dense fibrillar component (DFC) of the nucleolus (Huang, 2002) (Figure 1.5). Other studies, however, have reported that this assembly takes place in the granular component (GC) (Figure 1.5), which is the nucleolar region in which later pre-ribosomal RNA processing steps take place (Kruger et al., 2007). It is believed that additional maturation steps, for both pre-40S and pre-60S, occur in the nucleoplasm. The two subunit precursors are transported separately into the cytoplasm through the nuclear pore complex (NPC) where final maturation events occur (Zemp and Kutay, 2007).

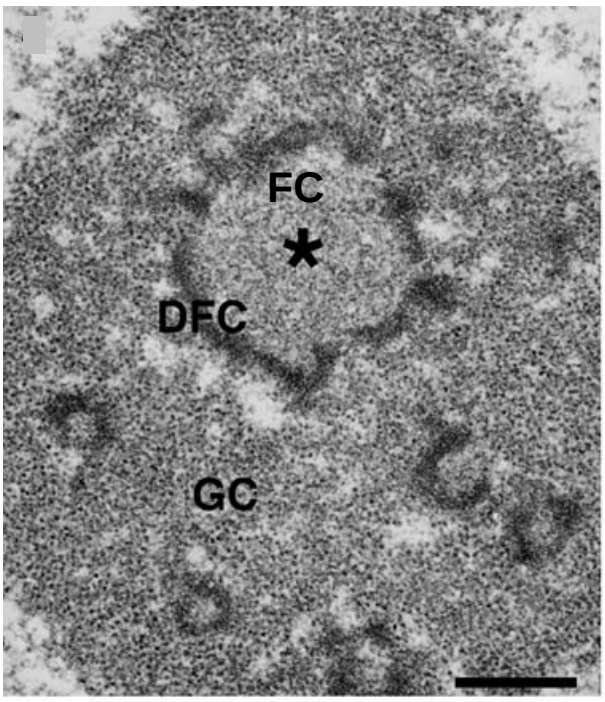


**Figure 1.5 A EM micrograph of mammalian cell nucleolus**. The EM picture shows the three main nucleolar components, fibrillar center (FC), the dense fibrillar component (DFC) and the granular component (GC). FCs of different sizes are visible, the largest is indicated by an *asterisk*. The FCs are surrounded by the DFC and are embedded in the GC. Picture taken from (Sirri et al., 2008)

### 1.5.1 Ribosomal proteins (RPs)

Evolutionarily, many RPs are highly conserved from bacteria to humans; their nucleotide and peptide sequences are valuable for studying phylogenetic relationships between organisms (Veuthey and Bittar, 1998). The first eukaryotic RPs that have been characterized in detail are from rat ribosomes (Wool, 1979). Human RPs have also been well characterized, and their amino acid sequences and biochemical properties have been described (Nakao et al., 2004; Wool et al., 1995). All RPs but one are present as single copy proteins per ribosome (Wool, 1979). The RPs of *D. melanogaster* were first studied in the 1970s and up to 78 individual RPs have been documented using two-dimensional gel electrophoresis (Lambertsson, 1975). In a later study only 52 RPs were identified in highly purified ribosomes using high-resolution two-dimensional gels coupled with mass spectrometry (Alonso and Santaren, 2006), A detailed genetic characterization of RP genes in *Drosophila* has recently been reported (Marygold et al., 2007). On the basis of this latest study, in *Drosophila* there are 79 RPs (32 from the small subunit and 47 from the large subunit). The proteins are encoded by 88 genes distributed across the entire genome, which have orthologues in mammalian genomes (Marygold et al., 2007). While the majority of RPs are encoded by single genes in *Drosophila,* nine are encoded by two distinct genes, and they are distinguished by a lowercase '*a*' or '*b*' suffix to the gene symbol, for example, *RpL37a* and *RpL37 b* are different genes that encode the same protein (McConkey et al., 1979; Wool et al., 1991). Theses duplicated genes likely have originated by either gene transposition or retrotransposition of a copy of the ancestral gene. Both genes are functional, but the one with higher similarity to its

human counterpart is ubiquitously moreexpressed , while the other is expressed in specific tissues, and it may have other functions other than ribosome biogenesis (Marygold et al., 2007). The genes were named according to the standard metazoan gene nomenclature proposed by the Wool group (Wool et al., 1991). RP genes are given an '*Rp*' prefix. In *D. melanogaster*, mutations in genes encoding RPs have been shown to cause an array of cellular and developmental defects called 'Minute' syndrome. 'Minute' defects are a common class of haplo-insufficient mutations characterized by prolonged development, short and thin bristles, and poor fertility and viability. It has been known that some haplo-insufficient *Minute* loci of *Drosophila* correspond to the genes encoding RPs (Lambertsson, 1998). In the recent study by Marygold et al., it was reported that all but one of the minute loci are linked to mutated RP genes; the minute phenotype is probably a consequence of suboptimal protein synthesis due to a reduced level of functional ribosomes (Marygold et al., 2007). Under normal conditions the cells require high concentrations of functional ribosomes to maintain proper cellular functions. RP mRNAs are among the most abundant cellular transcripts, and can account for 50% of all RNA polymerase II-mediated transcription (Warner, 1999).

Recent studies in mammalian cells revealed that RPs are expressed in excess, and that cells contain more RPs than rRNA. This generates a pool of free RPs in the nucleoplasm, which is subject to proteosomal degradation (Lam et al., 2007).

### 1.5.2 The role of RPs in ribosome biogenesis

Until recently, the role of RPs in ribosome biogenesis was largely unexplored. Certain ribosomal proteins have been shown to affect ribosome biogenesis at different stages; RpS18 and RpS15 are required early in 40S biogenesis, RpS18 depletion leads to a

nucleolar maturation defect and RpS15 depletion causes nucleoplasmic accumulation of 20S pre-rRNA (Leger-Silvestre et al., 2004).

Recent studies have systematically analysed the role RPs in 40S biogenesis (Ferreira-Cerca et al., 2005; Henras et al., 2008). These studies revealed that most of the RPs of the 40S subunit play distinct and essential roles in rRNA maturation, export and overall small ribosomal subunit biogenesis, and nuclear export. RpS0, RpS2, RpS3, RpS10, RpS15 and RpS26 appear to be required for nuclear export of pre-40S particles; 20S pre-rRNA accumulated in the nucleus of cells lacking any of these RPs, and 20S pre-rRNA accumulated in cytoplasm upon RpS20 depletion, suggesting that Rps20 is necessary for 20S pre-rRNA cytoplasmic processing but not required for nuclear export. In yeast, depletion of any small subunit RPs impairs ribosome biogenesis, due to a failure either in rRNA processing, ribosome assembly or ribosome subunit export (Ferreira-Cerca et al., 2005).

Although the role of RPs in 60S subunit maturation has not yet been systematically analysed, many 60S RPs have been studied individually and appear also to be required for ribosome production. RpL1 is required for the association and stability of the 5S rRNA with 60S (Deshmukh et al., 1995). RpL25 is required for efficient pre-rRNA processing, whereas the depletion of RpL25 blocks conversion of the 27S pre-rRNA precursor to 5.8S and 25S rRNA (van Beekvelt et al., 2001). RpL10 is involved in recycling of 60S exportation adaptor protein Nmd3p and the subsequent 60S subunit joining (West et al., 2005). RpL3 has an essential role in the assembly of early pre-60S particles and depletion of RpL3 results in a marked decrease in 27S rRNA levels, which impairs the export of pre-60S ribosomal particles (Rosado et al., 2007).

It has also been shown that RpL5 and RpL11 are necessary for assembly of 5S rRNA into 90S preribosomes (Zhang et al., 2007).

The importance of ribosomal proteins is also apparent in *D. melanogaster* where, as mentioned above, the deletion of one copy of the ribosomal protein genes results in the 'Minute' syndrome. In humans, mutations in many RPs cause an inherited red cell aplasia called Diamond Blackfan Anemia (DBA). Six genes encoding RpS19, RpS17 and RpS24, and RpL11, RpL5and RpL35a, were found to be mutated in patients with DBA (Robledo et al., 2008). The disease is probably caused by haploinsufficiency of these RPs (Gazda et al., 2004). The RPs associated with DBA could have a function in the biogenesis of either the large or small ribosomal subunit. Pre-RNA cleavage is impaired at various steps of rRNA processing, leading to the accumulation of different rRNA precursors in DBA patients (Choesmel et al., 2007). DBA is probably caused by suboptimal concentrations of RPs, which can affect both the quality and quantity of ribosomes in the cell (Robledo et al., 2008).

## 1.6 Ribosomal proteins with extra-ribosomal functions

Beside the main role of RPs in ribosome biogenesis and cell growth, many RPs also play extra-ribosomal functions that are independent of ribosome function. Findings from several groups show that some RPs function in DNA repair, transcription, apoptosis, mRNA processing, development and tumorigenesis (Lindstrom, 2009; Wool, 1996). RPs that were found to be involved in extra-ribosomal function usually interact either with some non-ribosomal component of the cell, either RNA or proteins, and the interaction has a physiological impact on the cell (Warner and McIntosh, 2009). Some ribosomal proteins appear to be involved in transcription

control, for example, over-expression of RpL11 results in it binding to the oncoprotein Myc and inhibits Myc-mediated transcriptional activation of target genes (Dai et al., 2007). In *Drosophila*, RpL22 is found associated with linker histone H1 on condensed chromatin. Depletion of RpL22 results in transcriptional up-regulation, while over-expression of either RpL22 or H1 results in suppression of transcription (Ni et al., 2006). Other ribosomal proteins have been implicated in apoptosis and cancer (Lindstrom, 2009). Over expression of RpL11, RpL5, RpL23 and RpS7 activate the tumour suppressor gene p53, which is involved in cell cycle control and apoptotic regulation (Dai and Lu, 2004). However, other RPs have protective effects, preventing cell death; several studies have identified a correlation between over-expression of RpL13, RpL35a, RpS13, and RpS9, and suppression of apoptosis (Kim et al., 2003; Lopez et al., 2002; Shi et al., 2004). Feedback mechanisms have also been described, for example, RpL7 inhibits translation of specific mRNAs as well as of its own mRNA, and RpS13 auto regulates its own pre-mRNA splicing (Malygin et al., 2007).

# Chapter 2 Materials and Methods

## 2.1 Solutions and buffers

Unless otherwise described, the composition of all buffers and media, plus common protocols, are as described in Molecular Cloning 2nd edition (Sambrook et al., 1989). The Gateway Technology and protocols can be found on the Invitrogen website (http://www.invitrogen.com). Solutions were prepared using analytical grade reagents supplied by Sigma-Aldrich, VWR or Fluka. All of the solutions and buffers were made in deionised water (Elix 5, Millipore) and sterilized by either autoclaving or filtration (0.22 μm, Millipore).

## 2.2 DNA cloning in *Escherichia coli*

Most standard protocols were as described in Molecular Cloning 2nd edition (Sambrook et al., 1989).

### 2.2.1 *E. coli* strains

*DH5α* and *XL1-cell blue* strains were used as the host for general cloning. The *DB3.1* strain was used for propagation of Gateway plasmids carrying the killer *ccdB* gene (Invitrogen, CA, USA).

### 2.2.2 Bacterial growth media

Recipes for LB broth, LB agar-plates and SOC are given in Appendix I.

### 2.2.3 Ligation and *E. coli* transformation

Ligation of DNA fragments was typically performed in a 20 μl reaction containing 100 ng of linearized plasmid and a four fold molar excess of the insert DNA, typically with 10 units of T4 DNA ligase (New England Biolabs, NEB). The ligation reaction was kept at 18°C overnight or at room temperature for 2 hours. 100 μl of *E. coli* competent cells were typically transformed with 5 μl of ligation mixture as follows: the ligation mixture was mixed with competent cells and kept on ice for 20 minutes; the cells were then heat shocked at 42°C for 45 seconds and cooled on ice for 2 minutes; the competent cells were mixed with 0.5 ml of SOC media and incubated at 37°C for 1 hour, with gentle shaking. The cells were briefly centrifuged and then spread on an LB plate containing 100 μg/ml ampicillin.

### 2.2.4 Small-scale preparation of plasmids

A single colony was inoculated into 2 ml of LB broth containing 100 μg/ml ampicillin and grown overnight. Plasmid DNA was typically purified from a 1 ml aliquot of this culture using the following boiling-prep method:

1. 1 ml of the cell culture was transferred into a fresh 1.5 ml tube and spun briefly at 13000 rpm and the supernatant discarded.

2. 110 μl of ice cold STET buffer (8% sucrose, 50 mM Tris pH 8.0, 50 mM EDTA pH 8.0, 5% Triton X-100) containing 5 μl of 20 mg/ml lyzozyme was added into each sample and the pellet was then completely resuspended by pipetting up and down.

3. The samples were placed in boiling water for 20 seconds and then centrifuged at 13000 rpm for 10 minutes. The pellets were removed using sterile toothpicks.

4. 110 μl of isopropanol was added to the supernatant, mixed and centrifuged at 13000 rpm for 15 minutes.

5. The supernatant was discarded. The pellet was washed with 70% ethanol, air-dried and resuspended in 40 μl TE (10 mM Tris/Cl pH 8.0, 1 mM EDTA pH 8.0) containing 1 μl of 1 mg/ml RNase A stock. The DNA samples were incubated at 65°C for 20 minutes to remove the RNase and stored at -20 °C if required for future use.

### 2.2.5 Large-scale preparation of plasmid DNA

Typically a single colony was inoculated into 1 ml of LB broth containing 100 μg/ml ampicillin and grown overnight, then 200 μl of the overnight culture was inoculated into 100 ml of LB broth containing 100 μg/ml ampicillin and grown over-night. Plasmid DNA was then prepared from the culture using commercial kits (typically QIA filter Plasmid Midi Kit, Qiagen). The extracted plasmid DNA was resuspended in 500 μl TE, pH 8.0, and the concentration of plasmid DNA was measured with a spectrophotometer. (ND-1000, NanoDrop).

### 2.2.6 Restriction enzyme digestion

All restriction enzymes used in this study were obtained from NEB. Restriction enzyme digestions were carried out in a 10-50 μl reaction. The conditions of the single enzyme or double enzyme digestion were followed according to the NEB

enzyme instructions. For a sequential digestion, the initial reaction contained the enzyme that is active in the buffer with the lowest salt concentration. After the reaction had proceeded for 2 hours, the second enzyme and the buffer with the higher salt concentration were added and the reaction continued for a further 1 hour.

### 2.2.7 Dephosphorylation of DNA

Antarctic phosphatase (NEB) was used to remove the 5' terminal phosphates of the DNA. This procedure was generally applied to prevent self-ligation of digested plasmid DNA. Following the restriction enzyme digestion, 1 μl of antarctic phosphatase (5 units/μl) was added into the reaction and incubated at 37°C for 1 hour. The DNA samples was then inactivated at 65°C for 15 minutes or purified by gel electrophoresis and gel extraction using a silica powder based technique (see below).

### 2.2.8 DNA Purification

Two methods were used to perform DNA purifications following PCR and restriction digestion. One is the polyethylene glycol (PEG) method, and the other is gel extraction.

#### 2.2.8.1 PEG purification

1. Add an equal volume of the PEG solution (13% PEG8000 (w/v), 0.6 M NaAc, and 6mM $MgCl_2 \cdot 6H_2O$) to the DNA sample and mix by vigorous vortexing. Keep at room temperature for 20 minutes. If the DNA fragment size was less than 300 bp, three volumes of the PEG solution was used instead.

2. The sample was centrifuged at 13000 rpm for 20 minutes and the supernatant was completely removed using a Pasteur pipette, without touching the pellet.

3. The DNA pellet was washed with 1 ml of 96% ethanol and centrifuged at 13000 rpm for 3 minutes, and then washed again with 70% ethanol.

4. The pellet was air-dried and dissolved in 20-30 μl TE buffer.

#### 2.2.8.2 Gel purification

The DNA fragment was sliced-out of the gel and placed into a 1.5 ml eppendorf tube. The DNA was then purified by silica powder as described in the manufacturers instructions (Silica Bead DNA Gel Extraction Kit, Fermentas).

### 2.2.9 Standard PCR

All of the primers used in my study are shown in Appendix III, table 1. The primers were purchased from either Sigma or MWG. The polymerase chain reaction (PCR) was used to amplify DNA. DNA polymerase enzymes used in my study included *Taq* polymerase (Bioline) and *Phusion* DNA polymerase (NEB). Taq polemerase was used when proof reading was not required or when high fidelity PCR failed. *Phusion* DNA polymerase was used if the fragments being amplified were to be cloned .The PCR conditions varied, depending on the DNA polymerase used, the melting temperature ($T_m$) of the primer and the length of amplified DNA. PCRs were run in a thermal cycler (PTC-200, DNA Engine) and the products analyzed by agarose gel electrophoresis.

#### 2.2.9.1 PCR for colony screening

For a bacterial colony PCR, the fresh colonies were mixed with 10 μl of PCR solutions, which contained 1× PCR buffer, dNTP mixture (0.2 mM of each dNTP),

1.5 mM $MgCl_2$, 2 μM primers and 0.25 U Taq DNA polymerase (typically GoTaq, Promega), and amplified using standard cycling parameters.

#### 2.2.9.2 PCR for cloning

Phusion DNA polymerase (NEB) was used to amplify DNA fragments from *Drosophila* cDNA Library. ~1 ng of plasmid DNA was used as template and amplified in 50 μl reactions which contained 1× HB buffer, dNTP mixture (0.2 mM of each), 2 μM primers and 1 U Phusion DNA polymerase. The PCR amplification was as follows: 98°C denaturation for 1 minute; 98°C for 5 seconds, Tm °C as the annealing temperature for 20 seconds, 72°C extension for 0.5 minute/kb of the expected DNA length and run for 25 or 30 cycles; 72°C extension for 5 minutes.

#### 2.2.9.3 Single fly DNA preparation for PCR

A single fly ($CO_2$ anesthetized) was placed in a 1 ml tube and mashed for 10 seconds using a yellow pipette tip that contains 50 μl of squashing buffer (10 mM Tris-Cl pH 8.2, 1 mM EDTA, 25 mM NaCl and 200 μg /ml Proteinase K). Only expel the squashing buffer from pipette tip after fly mashing as sufficient liquid would escape from tip. The solution was then incubated at 30-37°C for 20-30 minutes and was then incubated at 95°C to inactivate proteinase K. 28-30 cycles of PCR reaction gives maximum yield. The preparation can be stored at 4°C for several weeks

### 2.2.10 Agarose gel electrophoresis of DNA

Following restriction enzyme digestion or PCR, DNA samples were run on the agarose gels to confirm and separate the correct bands by molecular weight. DNA samples and the loading control were mixed with DNA loading buffer (10× stock,

20% glycerol, 0.1 M EDTA, pH8.0, 1.0% SDS, 0.25% bromophenol blue and 0.25% xylene cyanol), loaded onto the 0.8% -2% (w/v) horizontal agarose gel and run in TAE buffer (40 mM Tris base, 40 mM acetic acid and 2 mM EDTA) with 0.5 μg/ml ethidium bromide at a constant voltage of 90 V. The 1kb DNA ladder was used as the loading control (NEB).

### 2.2.11 DNA sequencing

The Big Dye cycle sequencing kit was used to do the sequencing PCR reaction. 200 to 500 ng of plasmid DNA was mixed with 8 μl terminator ready reaction mix, 3.2 pmoles primer, and sterile water to 20 μl final volume. The PCR was run following recommended cycle condition. After the sequencing PCR was finished, the PCR products were mixed with 1 μl 500 mM EDTA and 64 μl 95 % ethanol, and then vortexed briefly. The mixtures were incubated at room temperature for at least 15 minutes, and centrifuged at 13,200 rpm. for 20 minutes. Immediately the supernatants were carefully removed since the pellets may not be visible. 250 μl of 70 % ethanol was used to wash the pellets twice and then they were centrifuged at 13,200 rpm. for 10 minutes. The supernants were removed carefully and the pellets were dried in the dark. 10 μl loading solution was added to each sample, the tubes were wrapped in foil and kept at room temperature for 30 minutes, before sending the samples for sequencing in the Functional Genomics and Proteomics Unit of the School of Biosciences. Later in the project, some sequencing was done using an outside company (GATC Biotech AG, Germany).

## 2.3 Plasmid construction

### 2.3.1 Outline of the Gateway cloning system

In order to facilitate the cloning steps I used the Gateway cloning technology (Invitrogen, CA, USA). The Gateway system conveniently and efficiently enables cloning of several genes into different vectors without the requirement for restriction endonucleases and ligase treatment. This technology is a universal cloning system based on bacteriophage lambda site-specific recombination (Landy, 1989), and provides a highly efficient way to move DNA sequences into multiple vector systems for functional analysis and protein expression (Hartley et al., 2000). Two *in vitro* recombination reactions constitute the basis of this cloning system (Figure 2.1). The first uses BP Clonase enzyme mix to recombine the DNA fragment of interest (typically PCR amplified) into a plasmid donor vector (pDONR221). This reaction is between *att*B recombination sites at the end of the DNA insert and *att*P sites on the plasmid donor vector. This first reaction generate an intermediate plasmid called the entry clone in which the DNA insert is flanked by *att*L recombination sites. The second step is the LR reaction, which uses LR Clonase enzyme mix, recombines the DNA sequence of interest in the entry clone, with the attR1 and attR2 recombination sites in the final destination vector. Several destination vectors are available; I have used some that allow expression in *Drosophila* (see below). In both steps, the result is a "swap" of the DNA insert with the cassette containing the killer ccdB gene (which expresses a protein toxic to *E. coli*); only plasmids that have recombined out the *ccdB* gene will grow. The orientation of the gene is maintained throughout the subcloning, because *att*L1 reacts only with *att*R1, and *att*L2 reacts only with *att*R2. Detailed protocols are available on the Invitrogen website (www.invitrogen.com).

**A**


**B**


**Figure 2.1 Schematic of the Gateway recombination reactions.** (A) BP reaction: recombination of an *att*B substrate (*att*B plasmid clone or *att*B-PCR product) with an *att*P substrate (donor vector) in the presence of BP Clonase mix to generate an *att*L-containing entry clone. (B) LR reaction: recombining of an *att*L substrate (entry clone) with an *att*R substrate (destination vector) in the presence of LR Clonase mix to create an *att*B-containing expression clone (Schematic taken from the Gateway manual, www.invitrogen.com).

#### 2.3.1.1 Construction of plasmids expressing tagged RPs under the control of the Actin-5C promoter

The coding regions of RP genes were at first amplified by PCR from cDNA libraries obtained from the *Drosophila* Genomics Resource Centre (DGRC) (www.dgrc.cgb.indiana.edu) using primers flanked with *att*B recombination sites (see Appendix III, table 1). I first generated entry clones in the pDONR-221 vector and then the DNA inserts were recombined into either the destination vector pAGW (N-terminal GFP fusions) (Figure 2.2) or into pAWG (GFP C-terminal fusions) (Figure 2.3). Both pAGW and pAWG were obtained form DGRC; these plasmids are part of the *Drosophila* Gateway[a] Vector Collection produced by Dr Terence Murphy (www.ciwemb.edu/labs/murphy/Gateway%20vectors.html)

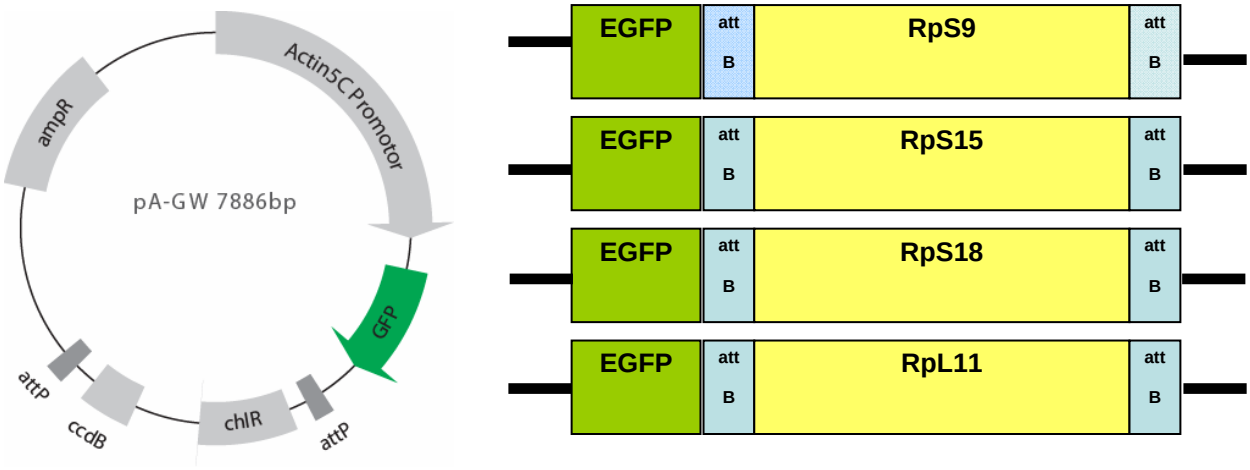


**Figure 2.2** Schematic representation of Gateway destination plasmids expressing RpS9, RpS15, RpS18 and RpL11 fused to EGFP at the N-terminus. The map on the left is that of the destination pAGW vector used to generate the RP expression constructs indicated on the right.

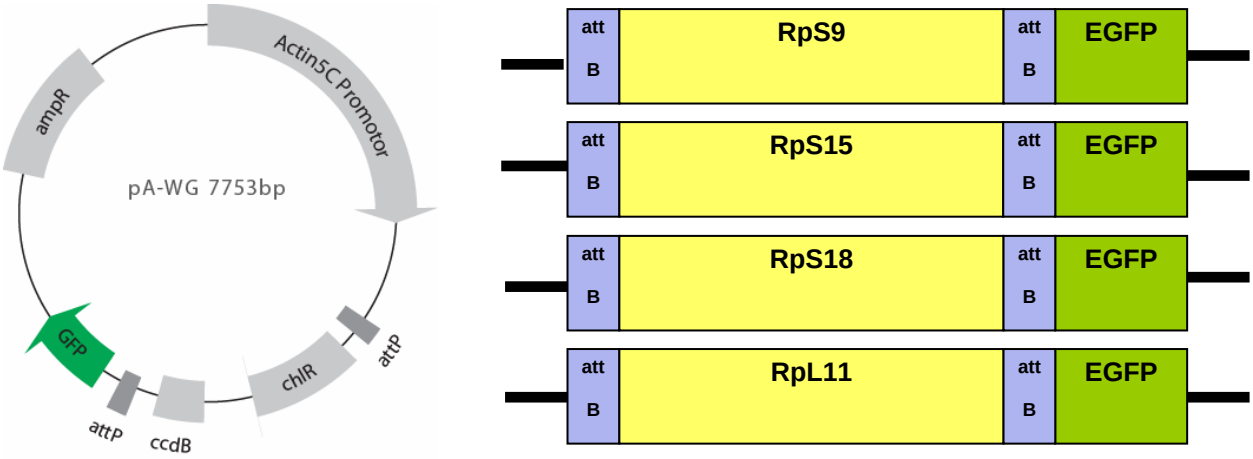


**Figure 2.3** Schematic of Gateway destination plasmids expressing RpS9, RpS15, RpS18 and RpL11 fused to EGFP at the C-terminus. The map on the left is that of the destination pAWG vector used to generate the RP expression constructs indicated on the right.

### 2.3.1.2 Construction of *Drosophila* transformation plasmids expressing tagged RPs under the UAS promoter

The GAL4/UAS system is a powerful genetic tool commonly used in *Drosophila* to control the expression of transgenes (see bellow for more details). To generate transgenic flies expressing tagged RPs under the control of the UAS promoter, I cloned the RPs-fusion constructs into the pUAST vector (or derivatives, details below). This plasmid carry P-element inverted repeats which allow transposase mediated germline transformation (Rubin and Spradling, 1982) These transformation vectors contains a red-eye marker (the product of the *white* gene) which allow for identification of transformant flies (O'Hare and Rubin, 1983).To generate these constructs, I used entry clones described above and used the LR clonase enzyme mix to recombine the RPs constructs into the pUAST derivatives-pTWG (C-terminal GFP fusions) and pTWR (C-terminal RFP fusions) (Figure 2.4).

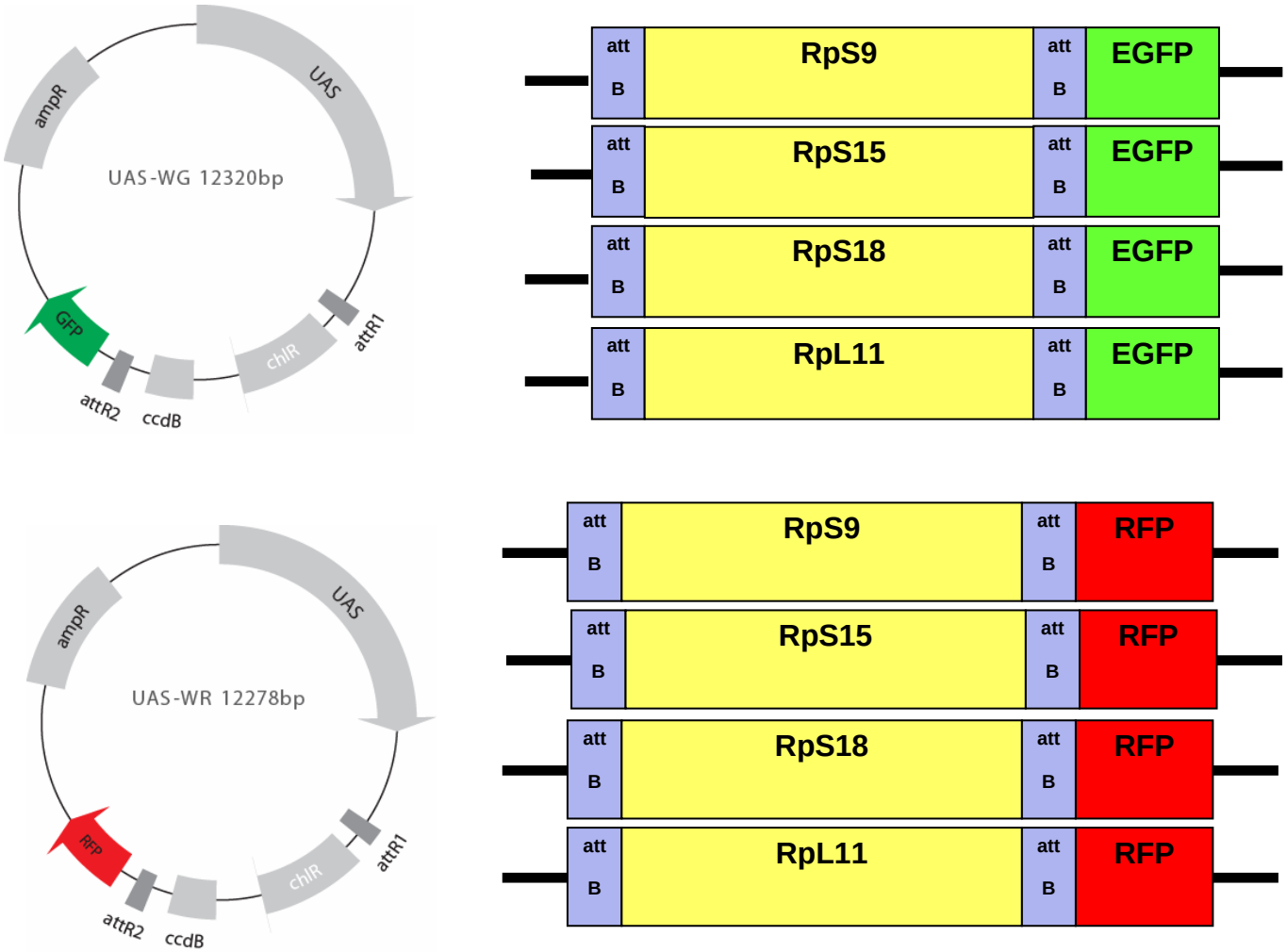


**Figure 2.4** Schematic of Gateway destination plasmids expressing RpS9, RpS15, RpS18 and RpL11 fused at the C-terminal end to EGFP (top panel) and to mRFP (bottom panel). The map on the left is that of the destination pTWG (top) and pTWR (bottom) vectors used to generate the RP expression constructs indicated on the right.

### 2.3.2 Construction of new Gateway destination vectors allowing PhiC31 mediated germline transformation

In P-element transformation constructs can insert randomly in the genome, so that expression of the transgene is often affected by flanking enhancers or silencers, leading to a phenomenon called position effect whereby the expression of constructs varies depending on the insert position. We wanted to prevent this variation so that we can better compare the expression of different RPs fusion constructs. To overcome this limitation of the P element trasformation, I have made additional transformation constructs that rely on PhiC31 integrase-mediated transgenesis systems which based on the site-specific bacteriophage PhiC31 integrase (Bischof et al., 2007). The PhiC13 system allows integration by sequence-specific recombination at sites introduced at known locations in the genome. The recombination is between a specific *att*B sequence on the plasmid and an *att*P sequence in the genome. The recombination is catalysed by PhiC13 integrase provided by a transgene in the host embryos. The PhiC13 system allows integration of all transgenes at the same position. Fly lines with *att*P sites at different chromosomal positions are available from the Basler lab (www.flyc31.frontiers-in-genetics.org). To generate pUAST derivatives compatible with the PhiC13 transformation system, I inserted the full length Gateway recombination cassette from pTWG and pTWR into the PhiC13-compatible pUAST derivative (pUAST*att*B).

The Gateway recombination cassette including the GFP and RFP regions (*attR1-Cmr-ccdB-attR2-GFP*) and (*attR1-Cmr-ccdB-attR2-RFP*) were PCR amplified from pTWG and pTWR with primers KJ67 and KJ68 (see Appendix III, table 1) (Figure 2.5A).

Both primers carry KpnI restriction sites at their 5`- and 3`-ends. The PCR products were digested with KpnI and inserted into the KpnI site in the multiple cloning site of pUAST*att*B (Figure 2.5A). This step generated pUAST.*att*B.WG and pUAST.*att*B.WR. To clone the RPs sequences into these new destination vectors. I PCR amplified RpS2, RpS5a, RpS11, RpS13, RpL8, RpL23, RpL32and RpL36 by PCR from cDNA libraries obtained from DGRC. The *attB*-containing primers were: KJ64&KJ66;KJ51&KJ53;KJ58 &KJ60;KJ54& KJ57;KJ39& KJ41;KJ48& KJ50;KJ42& KJ44;KJ36& KJ38, (see Appendix III, table 1). Following the production of the entry clones I recombined the 40S RPs sequences into pUAST.*att*B.WG (GFP fusions) and 60S RPs into pUAST.*att*B.WR (RFP fusions) (Figure 2.5B)

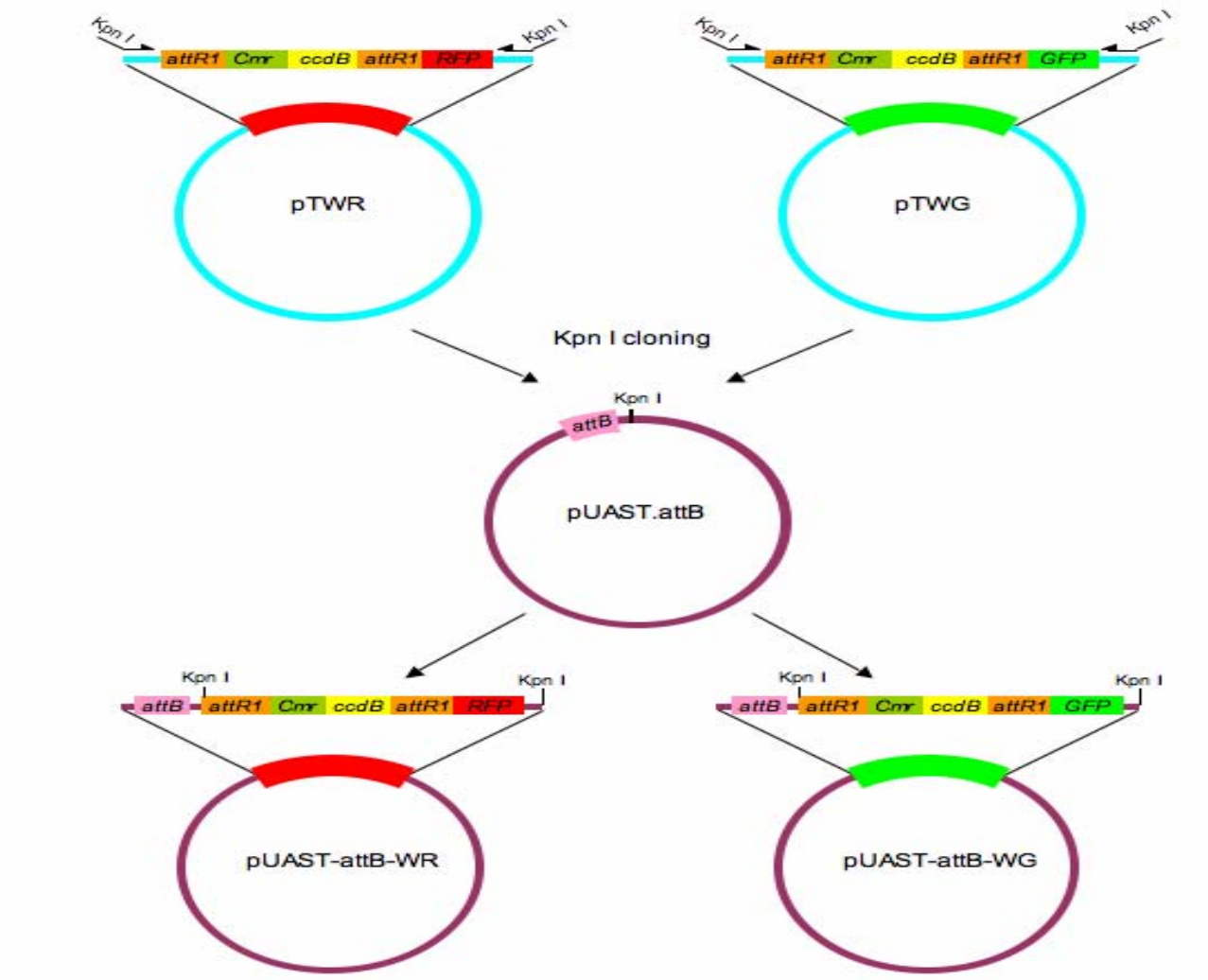


**2.5A Schematic of the construction of pUAST.*att*B.WG and pUAST.*att*B.WR**

The Gateway recombination cassette, the GFP or RFP coding regions were PCR amplified from pTWR or pTWG with KpnI-tailed specific primers (see text) and cloned into the KpnI site located in the multiple cloning site of expression vector pUAST.*att*B.

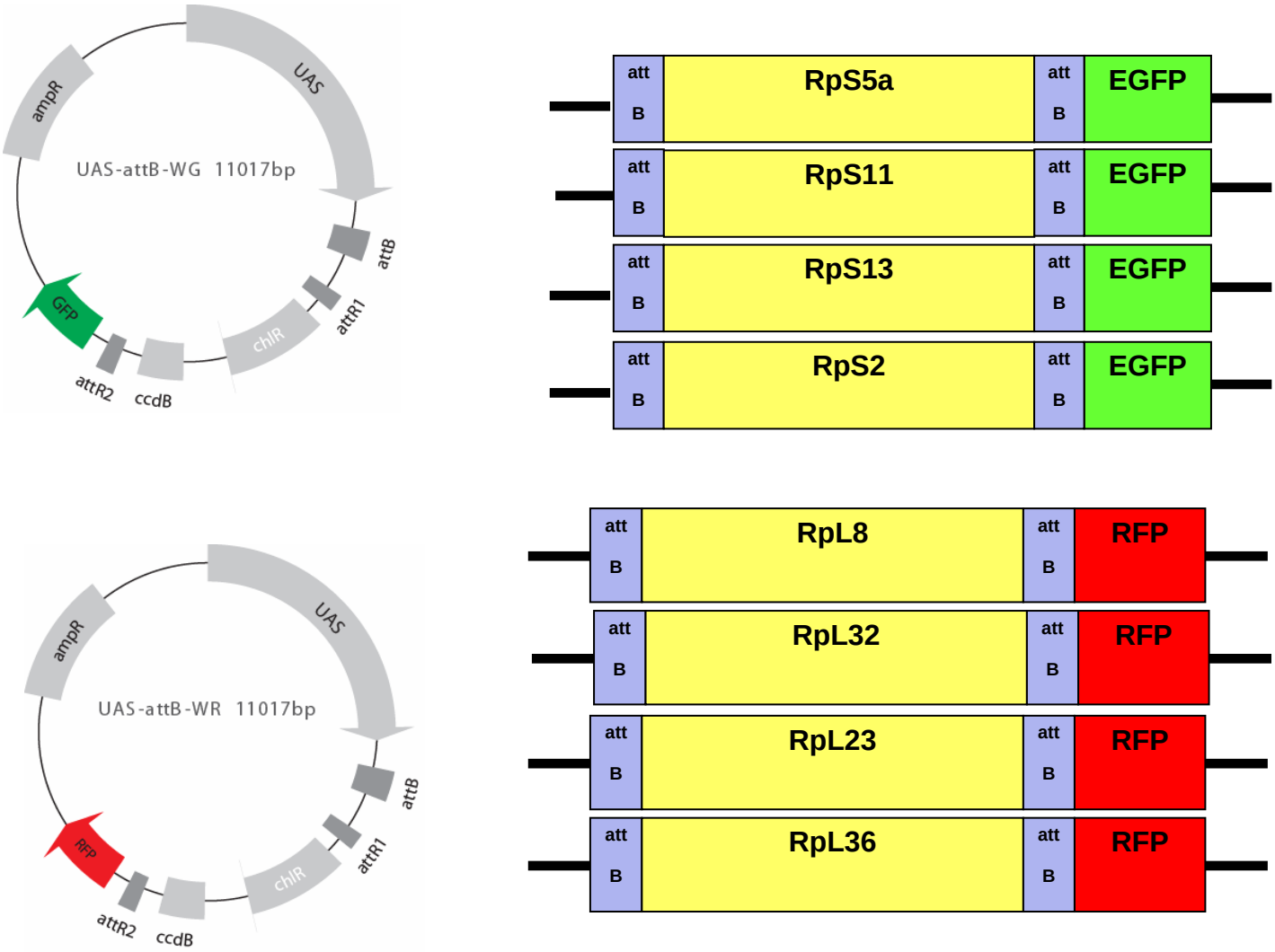


**Figure 2.5B** Schematic of Gateway destination plasmids expressing RpS5a, RpS11, RpS13 and RpS2 fused to EGFP at the C-terminal end (top panel) or RpL8, RpL32, RpL23and RpL36 fused to mRFP at their C-terminal ends (bottom panel). The map on the left is that of the destination pUAST-*att*B-WG (top) and pUAST-*att*B-WR (bottom) vectors used to generate the RPs expression constructs indicated on the right.

## 2.4 *In vivo* protein-protein interaction techniques

The most popular method to investigate protein–protein interactions in cells uses microscopy fluorescence resonance energy transfer (FRET) assays, which are based on changes in the excitation characteristics of fluorescent proteins when they are in close proximity, such as when they are fused to interacting proteins (Sekar and Periasamy, 2003). However, FRET assays are technically difficult and sensitivity is affected by various, unpredictable factors, including autofluorescence and photobleaching (Bhat et al., 2006). A relatively simple alternative to FRET is bimolecular fluorescence complementation (BiFC). The BiFC approach is to split a fluorescent protein into two non-fluorescent fragments, and to fuse each fragment to one of a pair of potentially interacting partners (Figure 2.6). When co-expressed in cells, interaction of the two partners drives the non-fluorescent fragments into close proximity, leading to the reconstitution of an intact fluorescent protein and enabling visualization of the interaction sites (Shyu et al., 2008). Compared to FRET analysis, which generally requires higher levels of protein expression, the BiFC assay has increased sensitivity and enables analysis of protein interactions at concentrations similar to their normal levels in the cell. In addition, there is essentially no background since fluorescence does not occur unless the fused BiFC fragments interact with one another.The BiFC approach can be used for the analysis of interactions between many types of proteins and does not require information about the structures of the interaction partners (Kerppola, 2006b). Many different fluorescent protein fragments have been identified that can be used in BiFC assays, such as GFP, enhanced cyan fluorescent protein, Cerulean, enhanced yellow fluorescent protein (EYFP), Citrine, Venus and mRFP1, and have been shown to

support fluorescent protein complementation in other cells and organisms (Shyu et al., 2006; Zhang et al., 2004).For most purposes, fragments of YFP truncated at residue 155 (YN155, N-terminal residues 1–154 and YC155, C-terminal residues 155– 238) are recommended, as they produce relatively bright fluorescence signals in complexes formed by many interaction partners (Kerppola, 2008). The advantage of the BiFC approach compared to other complementation methods is that the assembled complex has strong intrinsic fluorescence that allows direct visualization of the protein in their normal cellular environment at levels comparable to their endogenous counterparts without exogenous fluorogenic or chromogenic agents avoiding potential artifacts associated with cell lysis or fixation (Hiatt et al., 2008) . Complexes formed by complementation require maturation time before they become flourescent and this can be considered as a limitation for the BiFC technique where it does not allow real-time detection. Furthermore, in many cases the association of the fluorescent protein fragments can stabilize the interaction association between associated parteners; it been reported that *in vitro* in many cases the BiFC complex is irreversible. However while this feature prevent real-time assays, it makes it possible to detect transient and weak interactions (Hu et al., 2002; Morell et al., 2007). After using the BiFC approach successfully to detect the subcellular localization of the interaction among transcription factors in mammalian cell (Hu et al., 2002) this method has been implemented for the detection of protein–protein interactions in bacteria (Atmakuri et al., 2003); in plants(Andersen et al., 2005); and in a variety of model systems such as *D. melanogaster* (Benton et al., 2006) and *Xenopus* (Saka et al., 2007) and for diverse families of proteins (Kerppola, 2006a). In this project the use of a BiFC assay to study the *in vivo* formation of complexes between ribosomal subunits and this will enable me to study the subcellular localization of ribosomal subunit interaction. Based on

available ribosome structures, RpS18 and RpL11 are predicted to interact upon ribosome subunits joining in both prokaryotes and eukaryotes (Spahn et al., 2001; Yusupov et al., 2001). I have tagged RpS18 with an amino terminal YFP fragment (YN), and RpL11 with the carboxy terminal fragment (YC) fusions to both the N- and C-terminal ends of the ribosomal proteins (see Figure 5.3 in Chapter 5). The BiFC fragments were expected to fold into a functional YFP fluorescent protein only upon ribosome subunit association.

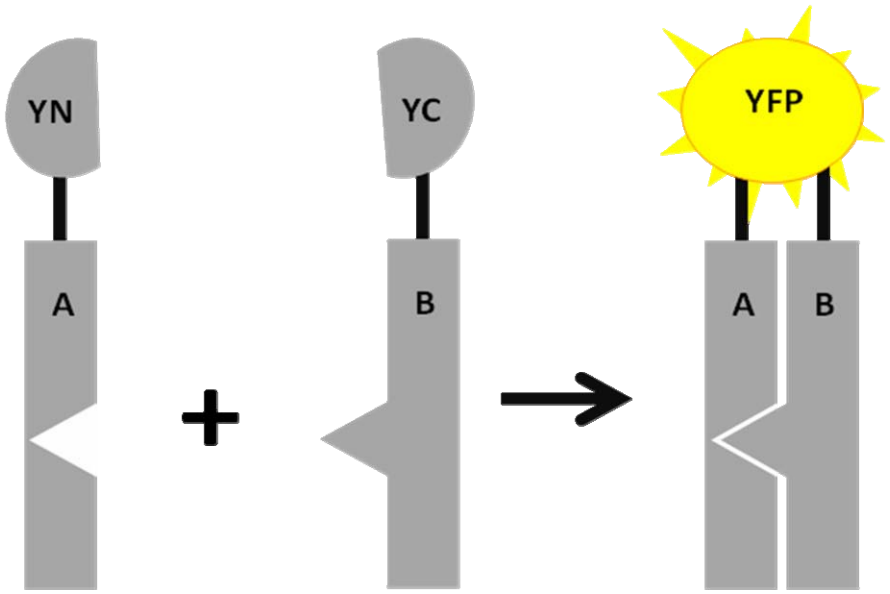


**Figure 2.6 Schematic illustration of the principle of the BiFC assay.** The YN and YC fragments of YFP are fused to putative interaction partners (A and B). Upon the association of these putative interaction partners (A and B), the non fluorescent YN and YC fragments will complement, forming a bimolecular fluorescent complex.

### 2.4.1 Generation of constructs expressing BiFC tagged RPs

To generate plasmids expressing RPs tagged at either the N or C terminus with YFP-derived BiFC fragments (Figure 2.7A and B), I PCR amplified the N-terminal (YN) and C-terminal (YC) domains of YFP from two previously described plasmids, pBiFC Jun-YN and pBiFC Fos-YC (Hu et al., 2002), (see Appendix III, table 2 for a list of all constructs); the plasmids were kindly provided by Dr. Kerppola , University of Michigan, USA. In the first cloning step, the YN fragment (corresponding to residues 1-154) was PCR amplified with primers KJ32 and KJ33 (see Appendix III, table 1 for a list of all primers). The KJ32 primer corresponds to the beginning of the YFP coding region and the KJ33 to the reverse complement of the 3' end of the YN fragment, flanked with an in frame sequence encoding RSIAT, the same linker as between Jun and YN in the previously described pBiFC Jun-YN construct (Hu et al., 2002). Similarly, the YC (residues 155-239) fragment was PCR amplified with the KJ34 and KJ35 primers. The KJ34 primer corresponds to the beginning of the YC fragment and the KJ35 primer is the reverse complement of the end of the YC fragment, flanked with the in frame sequence encoding KQKVMNH, the same linker as between Foss and YC in pBiFC Foss-YC (Hu et al., 2002). Both KJ32 and KJ34 are 5' tailed with a Bgl II recognition site, and KJ33 and KJ35 with a Bam HI site. Next I inserted both the YN and YC fragments into the BamH1 site located in the multiple cloning site of pBluescript II KS+ (pBS, Stratagene). This step generated the intermediate plasmids pBS-YN and pBS-YC (Figure 2.8). In parallel, the coding regions for RpS9, RpS15, RpS18 and RpL11 were PCR amplified from cDNA libraries obtained from the DGRC using specific forward primers (KJ1, KJ6, KJ11

and KJ17) that correspond to the beginning of the RPs coding regions, and reverse primers (KJ3, KJ7, KJ12 and KJ18) that correspond to the end of the RPs sequences (including the stop codon). Both forward and reverse primers are 5' and 3' tailed with a BamHI recognition site. I then cloned these RP fragments into the BamHI site of the previously produced pBS-YN and pBS-YC (Figure 2.8). In this step I generated plasmid clones carrying in-frame fusions of RpS9, RpS15 and RpS18 with YN, and RpL11 fused to YC. In the final step, I sub-cloned the RPs BiFC-fusions into the NotI-KpnI sites located in the polylinker of pUAST (Figure 2.8). The identity of all constructs was verified by sequencing with inserts  forword primers, and KJ73, a reverse primer in pUAST 3' of the KpnI site, and reconfirmed again with the reverse primers used to make the inserts and a forward primer, KJ74, corresponding  to the pUAST backbone.

Following a similar strategy, I generated C-terminal tagged RP constructs fused with YN and YC. To make YN C-terminal tagged constructs, I PCR amplified the YN sequence with primers KJ28 and KJ29. The KJ28 primer corresponds to the beginning of YFP flanked with an in-frame sequence encoding RSIAT, and KJ29 corresponds to the reverse complement of the end the YN fragment. YC was PCR amplified with KJ30 and KJ31. The KJ30 primer corresponds to the beginning of the YC fragment flanked with an in-frame sequence encoding KQKVMNH, and the KJ31 primer is the reverse complement of the end of the YC fragment (including a stop codon) (see Appendix II, Figure S1). Both KJ28 and KJ30 are 5' tailed with a BamHI recognition site and KJ29 and KJ31 with a BglII site. Next I inserted bothYN or YC into the BamH1 site located in the polylinker of pBS – this recreates an in-frame BamHI site at the beginning of the BiFC fragments. In parallel, I PCR amplified the sequence of Rps18 and RpL11 from cDNA libraries using the KJ11 and KJ17 forward primers that

correspond to the beginning of the RPs, and the KJ15 and KJ19 reverse primers that correspond to the end of the RPs, the forward primers were tailed with a BamHI recognition site and the reverse primers with a Bgl II site. I then cloned the RpS18 and RpL11 sequences into the BamH1 site of pBS.YN and pBS.YC respectively. As for the N-terminal fusions, in the last step I subcloned the NotI-KpnI fragment containing the fusion into pUAST (Figure 2.9). The identity of the constructs was verified by sequencing with the forward primer used to PCR the inserts, and a reverse primer, KJ73, corresponding to the pUAST backbone, and reconfirmed again with the inserts reverse primers and a forward primer, KJ74, corresponding to the pUAST backbone.

Next I generated constructs expressing only the free YN and YC fragments, so that they can be used as a negative control (Figure 2.7C). To make the YN expressing construct, I PCR amplified the YN sequence with primers KJ69 and KJ70; the KJ69 primer corresponds to the beginning of YFP (see Appendix III, table 1), and KJ70 to the reverse complement of the end of the YN fragment. The YC fragment was PCR amplified with KJ71 and KJ72. The KJ71 primer corresponds to the beginning of the YC fragment and the KJ72 primer is the reverse complement of the end of the YC fragment. Both KJ69 and KJ71 are 5' tailed with a NotI recognition site and KJ70 and KJ72 with a KpnI site. Both fragments were cloned into the NotI and KpnI sites located in the polylinker of pUAST (Figure 2.10). The constructs were verified by sequencing as described above.

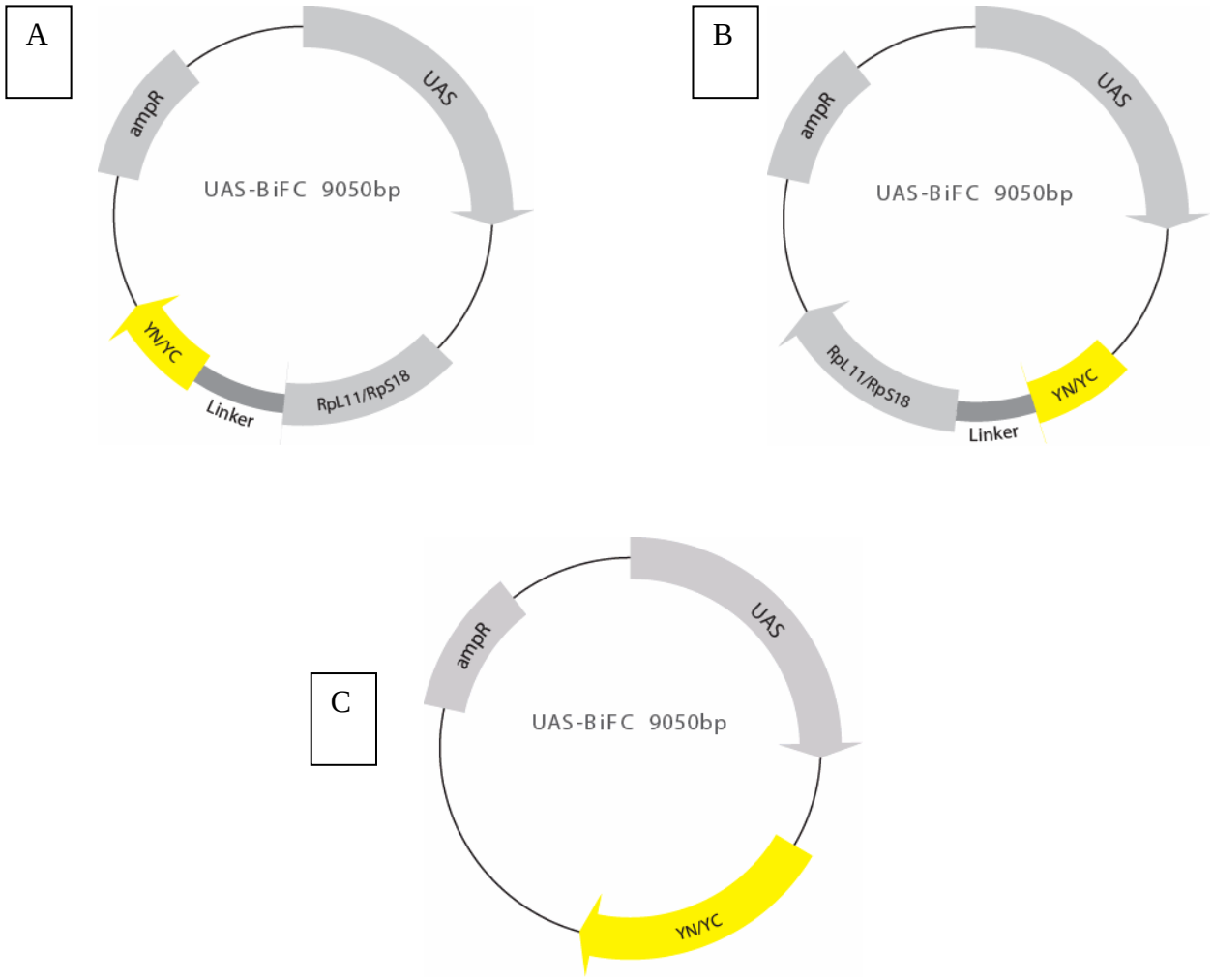


**Figure 2.7 Schematic of the constructs expressing BiFC-tagged RPs**

(A) Map of the BiFC expression constructs pUAST-RpL11-YC and pUAST-RpS18-YN - (C-terminally tagged).

(B) Map of the BiFC expression constructs pUAST-YC-RpL11, pUAST-YN-RpS18 (N-terminally tagged).

(C) Map of the expression constructs expressing free YC and YN peptides pUAST-YC, pUAST-YN (not fused to interacting proteins).

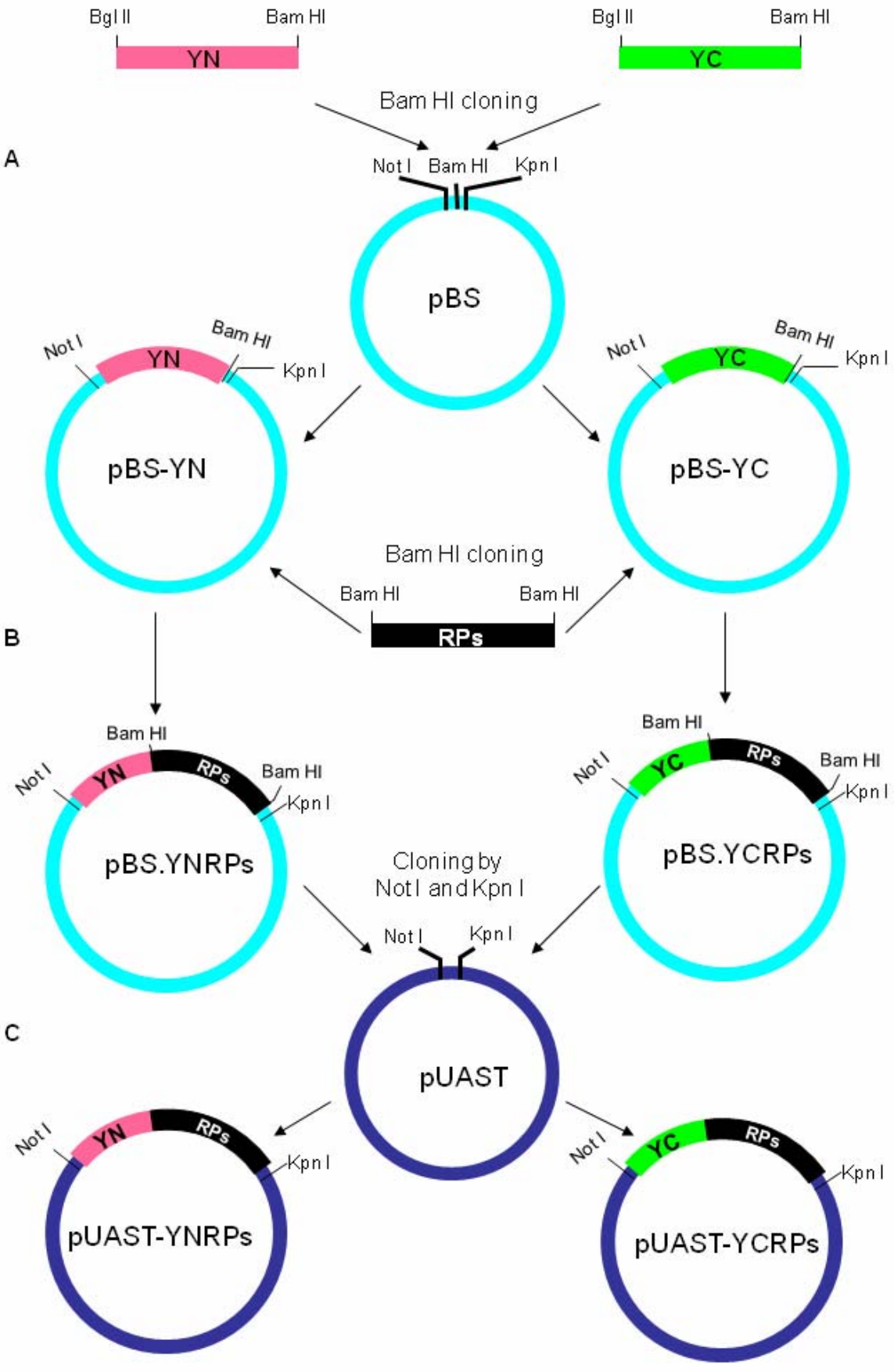
Bgl II
Bam HI
YN
Bgl II
Bam HI
YC
Bam HI cloning
A
Not I
Bam HI
Kpn I
pBS
Not I
Bam HI
YN
Kpn I
pBS-YN
Not I
Bam HI
YC
Kpn I
pBS-YC
Bam HI cloning
Bam HI
Bam HI
RPs
B
Bam HI
Not I
YN
RPs
Bam HI
Kpn I
pBS.YNRPs
Bam HI
Not I
YC
RPs
Bam HI
Kpn I
pBS.YCRPs
Cloning by
Not I and Kpn I
Not I
Kpn I
C
pUAST
Not I
YN
RPs
Kpn I
pUAST-YNRPs
Not I
YC
RPs
Kpn I
pUAST-YCRPs

**Figure 2.8 Outline of the cloning strategy used to generate the constructs expressing N-terminally tagged BiFC fusion RPs.**

(A) The YN and YC coding regions were PCR amplified with specific primers (see the text) tailed with 5' BglII and 3' BamHI sites and cloned into the BamHI site of pBluescript KS II. (B) The RPs coding regions (including stop codon) were PCR amplified with specific primers (see the text) tailed with BamHI sites and cloned into the BamHI sites of pBS-YN or pBS-YC constructs generated in the previous step (A). (C) To generate constructs suitable for *Drosophila* expression/transformation, the YN-RPs and YC-RPs sequences from the previous step (B) were subcloned into the NotI-KpnI sites in pUAST.

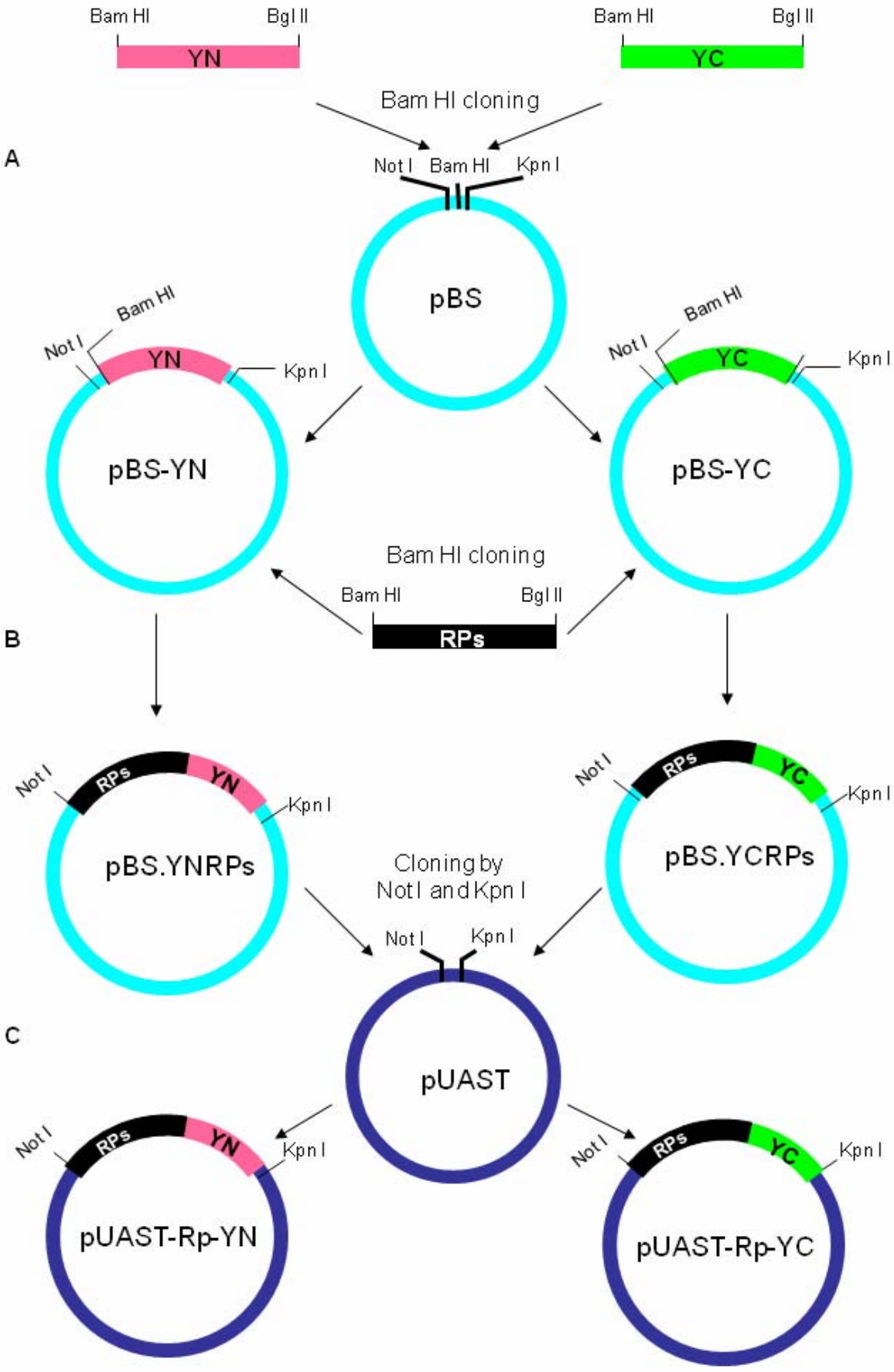
Bam HI
Bgl II
YN
Bam HI
Bgl II
YC
Bam HI cloning
A
Not I
Bam HI
Kpn I
pBS
Not I
Bam HI
YN
Kpn I
pBS-YN
Not I
Bam HI
YC
Kpn I
pBS-YC
Bam HI cloning
Bam HI
Bgl II
RPs
B
Not I
RPs
YN
Kpn I
pBS.YNRPs
Not I
RPs
YC
Kpn I
pBS.YCRPs
Cloning by
Not I and Kpn I
Not I
Kpn I
C
pUAST
Not I
RPs
YN
Kpn I
pUAST-Rp-YN
Not I
RPs
YC
Kpn I
pUAST-Rp-YC

**Figure 2.9 Outline of the cloning strategy used to generate C-terminally tagged BiFC-RP fusion constructs.**

(A) The YN and YC coding regions were PCR amplified with specific primers (see the text ) tailed with 5' BamHI and 3'BglII sites and cloned into the BamHI site of pBluescript KS II. (B) The RPs coding regiona without stop codons were PCR amplified with specific primers (see the text) tailed with 5' BamHI and 3' BglII sites and cloned into the BamHI site of pBS-YN or pBS-YC constructs generated in the previous step (A). (C) To generate constructs suitable for *Drosophila* expression/transformation, the RPs-YN and RPs-YC sequences from the previous step (B) were subcloned into the NotI-KpnI sites in pUAST.

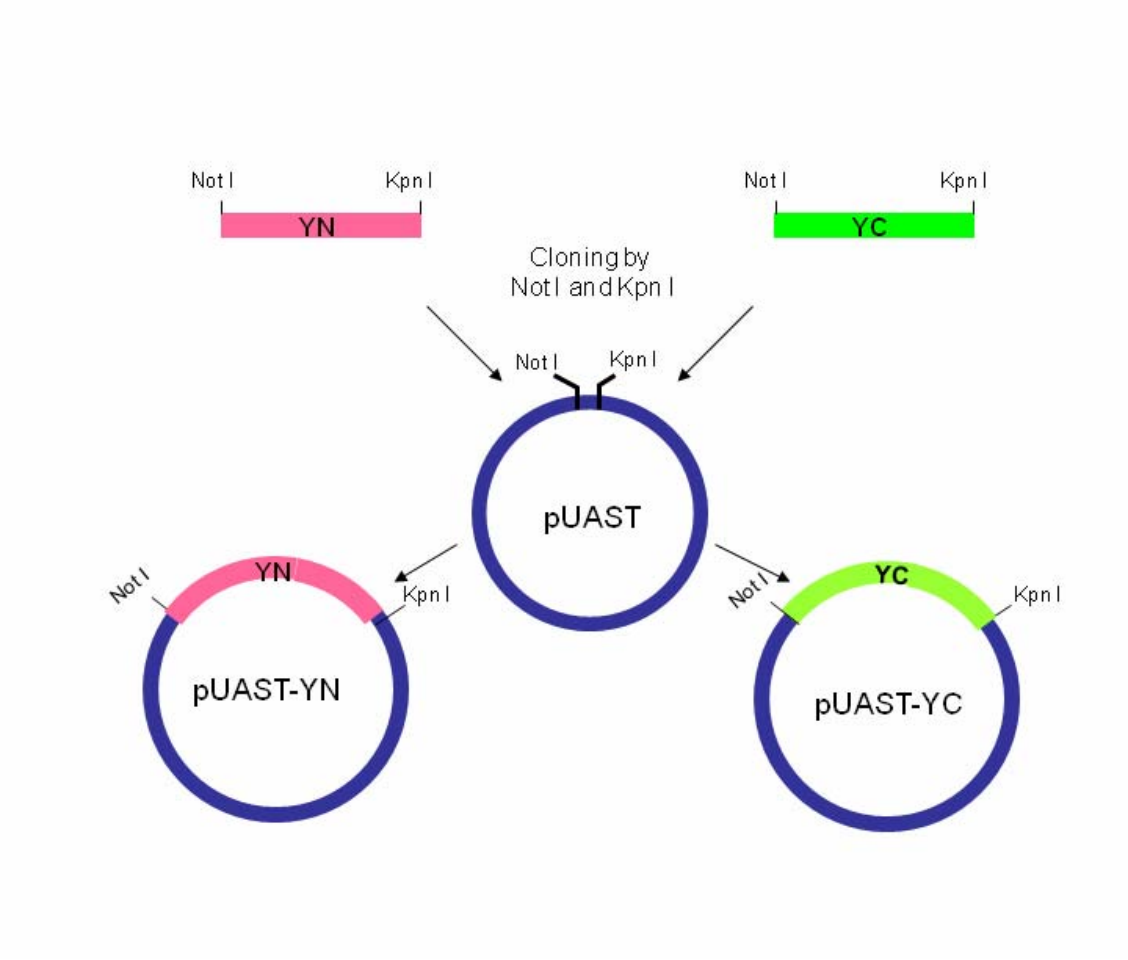


**Figure 2.10 Outline of the cloning strategy used to generate the constructs expressing unfused BiFC fragments (YN and YC)**

The YN and YC coding regions were PCR amplified with specific primers (see the text) tailed with 5' NotI and 3'KpnI sites and cloned directly into the NotI-KpnI sites located in the multiple cloning site of the expression vector pUAST suitable for *Drosophila* expression/transformation.

## 2.5 Polysome analysis

### 2.5.1 Cell fractionation

Transfected cells (typically one day after transfection) were treated with 100 μg/ml cycloheximide 15 min before harvesting. Cells were chilled on ice and then pelleted at 4°C. The pellet was washed in cold PBS and then lysed in 1x lysis buffer containing 20 mM Hepes.KOH pH 7.4, 2 mM magnesium acetate, 100 mM Potassium acetate, 1 mM dithiothreitol (DTT), 250 μg/ml Heparin, 0.05 mM aurintricarboxylic acid (ATA, Sigma), 0.25 % Triton X-100 and 100 μg/ml cycloheximide. The lysis buffer also contained an EDTA-free protease inhibitor cocktail (Roche). When required, cells were treated with 100 μg/ml puromycin for 15 minutes. In this case, the lysis buffer and the gradient also contained 100 μg/ml puromycin. The lysate was cleared by centrifugation at 13,000 rpm for 20 minutes and the $A_{260}$ of the extracts was determined. The lysate was then centrifuged through a 10%-50% sucrose gradient at 38,000 rpm for 3 hours in a Beckman SW40Ti rotor. All of the above steps were done at 4°C. After centrifugation, the gradients were pumped (from the bottom, using a steel capillary) through a flow-through UV spectrophotometer (Pharmacia LKB-Optical Unit UV-1) with a peristaltic pump (P-1, Pharmacia) at a speed of 1.2 ml/min. The $A_{254}$ was recorded as the fractions passed through the flow cell.

### 2.5.2 Protein precipitation.

After fractionation, the proteins were precipitated using the trichloroacetic acid (TCA) and Na-deoxycholate (DOC) method as described in (Bensadoun and Weinstein, 1976) with some modifications as described. To 1ml of fractions, 10μl of 1.25% Na-

deoxycholate (DOC) was added to a final concentration of 125µg /ml, vortexed and allowed to sit at room temperature for 15 minutes. 350µl of 24% TCA was added, vortexed and centrifuged at 4°C at maximum speed for 30 minutes. The supernatant was carefully removed and the precipitate was washed with ice cold acetone by spinning for 2 minutes at 4°C. The precipitate was then resuspended in 40µl of 2x SDS gel loading buffer with 5% $\beta$-mercaptoethanol and the protein denatured by boiling for 5 minutes. The protein extract was kept on ice for 2 minutes and centrifuged at 4°C for 5 minutes before loading.

### 2.5.3 Western blotting

The protein samples were resolved by SDS-PAGE and transferred to a nitrocellulose membrane (Protran BA-85, Geneflow) using a wet blotting apparatus (Biorad). The membrane was blocked in 5% milk made in 1x TBST (Tris-buffered Saline containing 0.05% Tween-20) for 2 hours at room temperature. After blocking, the membranes were incubated overnight at 4°C in the primary antibody goat anti-GFP (AbD Serotec) or mouse monoclonal anti-GFP (3E1Cancer Research UK) diluted 1:2000 in 1x TBST. Then the membranes were washed and incubated with the appropriate secondary antibody (polyclonal rabbit anti-goat IgG, HRP conjugated or HRP-conjugated anti-mouse IgG,).The blots were then incubated with West Pico chemiluminescent substrate (Thermo Scientific) and then visualized with a CCD camera and Quantity One software (Biorad).

## 2.6 Schneider S2 cells transfection and immunostaining

### 2.6.1 Cell culture and transfection

*D. melanogaster* Schneider line-2 cells (S2 cells) were grown in Insect-XPRESS medium (Cambrex) supplemented with 4% fetal bovine serum, 1% penicillin/streptomycin/glutamine mix (Cambrex), and grown at 27°C without $CO_2$. Transfection was typically done in 6-well plates seeded with $3x10^6$ cells /well and grown over night to almost complete confluence. Transfection with plasmids was done at a final concentration of 3.75 μg/ml diluted in serum-free media. Cells were transfected using dimethyl dioctadecyl ammonium bromide (DDAB, Sigma) (Han, 1996). DDAB was added to the diluted DNA mix and incubated for 30 minutes at room temperature. During this time the cells were washed twice with media without serum and kept in 0.875 ml of the serum-free media. At the end of the incubation, the transfection mix was added and incubated at 27°C for 5 hours. After 5 hours, the media was removed and replaced with 2 ml of media complete with serum and antibiotics. This was then incubated over 1 or 2 nights at 27°C.

### 2.6.2 Fixation of S2 cells

Cells grown on coverslips for 24-48h were fixed with 2-4% formaldehyde in PBS, pH 7.4, for 15 minutes at 20°C ,washed in PBS, pH 7.4, three times, 10 minutes each, permeabilized in 0.05% Tween 20 in PBS for 5 minutes on ice, and then washed in PBS three times, 10 minutes each . At the second time of rinsing after incubation ,DAPI (4'-6-diamidino-2-phenylinodole) (Sigma-Aldrich) was added to PBS in a 1:10,000 dilution (0.1 μg /ml) to stain the DNA. The coverslip was mounted with a drop of mounting medium (PromoFluor Antifade Reagent from PromoKine bioscience www.promokine.info/home/). The coverslip was sealed with clear nail

polish to prevent drying and movement under the microscope. Glass slides were cleaned with 100% ethanol, 70% ethanol and water, respectively if needed. Slides are kept in the dark if they are not to be viewed immediately.

### 2.6.3 Fluorescent immunostaining

After transfection, S2 cells were fixed as described above. Fixed cells were washed with 50mM $NH_4Cl$ to reduce the background then washed three times in PBS for10 min. After blocking in 4% BSA for 10 minutes wash in three times in PBS for 10 minutes. Incubate with primary antibody at a dilution of 1:100 for 2 hours at room temp in a humidified chamber. If using 22mm X 22mm square coverslips, 30 μl of diluted antibody is placed on the coverslip and the coverslip is inverted onto a glass slide. The slide is then placed in the humidified chamber, which is incubated at room temperature. Wash three times in PBS for 10 minutes. Incubate in secondary antibody, 1:500 dilution, in the dark for 1 hour in a humidified chamber at room temperature or overnight at 4°C.Wash three times in PBS for 10 minutes. DAPI was added to TBS at a 1:10,000 dilution (0.1 μg/ml) to stain DNA in the second wash. Mount the coverslip as described above.

## 2.7 Salivary gland manipulation

### 2.7.1 Salivary gland dissection and polytene chromosome squashing

#### 2.7.1.1 Dissection solutions

Solution A (for dissection): 100 μl 10x Buffer A, 100 μl 10% Triton X-100, 800 μl distilled water. Buffer A (1X): 15 mM Hepes pH 7.4, 60 mM KCl, 15 mM NaCl, 1.5 mM Spermine, 1.5 mM Spermidine.

Solution B (Fixing solution): 100 µl 10x Buffer A, 100 µl 10% Triton X-100, 231 µl 4% Paraformaldehyde and 569 µl distilled water.

Solution G (Squashing solution): 500 µl Acetic acid and 500 µl distilled water

#### 2.7.1.2 Salivary gland dissection

For larval dissection, third-instar wandering larvae that start climbing out of food were dissected; for high resolution imaging of polytene chromosomes the selected larva should look fat and healthy. Larvae were then placed in a glass dissecting dish containing distilled water on ice to put them to sleep and for cleaning, and the larvae were then dissected using sharp forceps in a glass dissecting depression-slide containing 20 µl solution A. Removal of any dark fat bodies around the glands was required as they would interfere with imaging. After dissection, salivary glands were transferred into 50 µl solution B for 30 seconds. After that, glands were washed in spreading solution G by being dipped into it and then transferred into a small drop (10 µl) of solution G on a glass coverslip. Glands were left in solution G for 2-3 minutes, and then with microscope slide gently touch the droplet on the coverslip until the coverslip adheres to the slide.

#### 2.7.1.3 Squashing

Salivary glands were broken by tapping on the coverslip with the blunt end of forceps (or a similar pointed object) to break the nuclei and spread the chromosomes. Using a folded tissue on the slide, the glands were squashed vertically against a table surface using a thumb. Slides containing squashed salivary glands were checked with a microscope under a phase contrast objective. Well squashed slides were selected and dipped into liquid nitrogen for about a minute. Then coverslips were removed with a razor blade. The position of the coverslip was marked on the slide with a diamond

pencil, then the slide submerged in 95% ethanol in a Coplin jar (or similar) and stored at -20˚C (the slide can be processed straight away for immunostaining or kept for 1-2 days in the freezer).

#### 2.7.1.4 Immunostaining

Prior to immunostaining, the slides were rehydrated by immersing them in 50% ethanol, 50% TBS solution for 10 minutes, and then rinsed twice with TBS (150 mM NaCl, 10 mM Tris-Cl pH 7.0-7.5, 0.05% Tween). Rehydrated slides were blocked in blocking solution containing TBS, 10% Fetal Bovine Serum (FBS) and 0.05% sodium azide ($NaN_{3)}$ for 50-60 minutes at room temperature. 20 µl of diluted primary antibody (1:100) in 4% blocking solution was put on a clean coverslip on the bench as a droplet. Tissue dried (outside the chromosome area) slides were carefully lowered onto the coverslip, to pick them up in the chromosome region of slide that was marked by the diamond pencil. Slides were then incubated in humid chamber that contained TBS at room temperature for 1-2 hours. After incubation, coverslips were removed by tapping the slide on the side of a beaker and slides were rinsed three times in TBS for 10 minutes each time at room temperature. The secondary antibody procedure was similar to the primary antibody staining; it was diluted 1:400 in 4% blocking solution. Slides were incubated with secondary antibody at room temperature for 1-2 hours. Due to photosensitivity of the secondary antibody, the humid chambers needed to be covered by tin foil during incubation. At the second time rinsing after incubation (three times in total), DAPI was added to TBS at a 1:10,000 dilution (0.1 µg /ml) to stain DNA. Slides from the TBS rinsing were dried in air, and with tin foil covered. A small amount of mounting medium was applied to a coverslip. The dried slide was then placed onto the coverslip, ensuring the region

containing the chromosome was covered precisely. Coverslips were sealed with clear nail polish to prevent drying and movement under the microscope, and then slides could be stored horizontally at 4°C for months. The protocol for chromosome squashing and staining is a modification of one that has been previously published (Shopland and Lis, 1996).

#### 2.7.1.5 Antibodies

The primary antibody specific to EGFP was Anti-GFP rabbit IgG (Molecular Probes, Invitrogen), the antibody specific to mRFP was a rabbit IgG anti-RFP (Millipore), and the primary antibody used for RNA polymerase II was an anti-polymerase II mouse IgM (H5, purchased from BabCO).The secondary antibodies used were either fluorescein isothiocyanate (FITC) conjugated (goat anti mouse IgM) or Cyanine 3 (Cy3) conjugated donkey anti-rabbit IgG. All secondary antibodies were purchased from Jackson Immuno Research Technologies and used as recommended by the manufacturer.

#### 2.7.1.6 Fluorescence microscopy/image processing

Stained polytene chromosomes were inspected with a fluorescence microscope (Leica, DMIRE2), with a 40X dry objective lens. Images were captured with a CCD camera (HAMAMATSU C4743-95) using the Open Lab software (Improvision). Images were subsequently processed using the ImageJ software (rsbweb.nih.gov/ij/).

### 2.7.2 Dissection and fixation of intact salivary glands for fluorescent imaging

Salivary glands were dissected from third instar larvae in PBS, using a transparent dissection plates, allowing a limit of 2 dissected larvae per well to avoid contamination.

The salivary glands were fixed by washing the glands for 3 minutes in a 4% formaldehyde solution diluted in PBS, and a 3 minutes PBS wash. The glands then were permeablised for 3 min in 10% Triton X-100 (Sigma, Cat. No T9284), and then transfer to 0.1 μg /ml PBS/DAPI solution for 10 minutes to stain the nuclei of the cells. After these steps the salivary glands were placed using the forceps on a microscope slide and covered with 20 μl mounting medium along with a cover slip placed on the top.

### 2.7.3 Confocal microscopy/image processing

All the salivary gland imagings were taken with a confocal inverted microscope Leica DMIRE2 with a 40X and 63X oil objective lenses. Images were acquired with the Leica Confocal Software Suite. All image processing was carried out with ImageJ software (rsbweb.nih.gov/ij/).

### 2.7.4 *Drosophila* heat shock induction protocol

Heat shock induction was used in order to express the BiFC genes in the fly two days before dissection. The strongest signal was with two pulses of heat shock at 37°C for 30 minutes with a 3 hour interval; this was done on the eighth day after egg laying, then heat shocked again 24 hours later at 37°C for 30 minutes. Larvae can be dissected 24 hours later. Before and after heat shock, larvae were grown in a 18°C incubator (this temperature is optimal for BiFC fragment maturation).

## 2.8 Genetics

All fly experiments were done with *D. melanogaster*. All fly stocks were maintained on standard corn meal medium seeded with dry yeast, in 18°C or 25°C incubators

with 60–70% relative humidity and stocks were transferred every 28 or 21 days respectively. See Appendix III for the list of all stocks

### 2.8.1 Balancer and marker

Balancer chromosomes are the valuable genetic tools that put the fly genetics apart from other organisms: balancer are multiply inverted chromosomes that prevent crossing over and recombination and carry marker mutations (Greenspan, 2004). Balancers are used to allow invisible mutation to be followed through genetic protocols and allow stable heterozygous stocks to be established from homozygous lethal lines. Balancers are available for all chromosomes except the fourth, which is very short and less likely involved homologous recombination (balancer stock used are listed in Appendix III, table 3)

### 2.8.2 GAL4/UAS expression system

In *Drosophila* the GAL4/UAS system is commonly used to drive the expression of transgenes in specific tissues/cells at given times during development. Gal4 is a yeast transcription activator that bind the yeast upstream activating sequences (UAS) and induces transcription (Duffy, 2002). Gal4 can be expressed with different endogenous promoters active in different cells. If the transgene is flanked by the UAS sequence, it will be expressed only in the cells expressing Gal4. Typically to drive the expression of UAS transgenes, the UAS line is crossed with a selected Gal4 driver line.The Gal4 drivers used in this study are listed in (Appendix III, table 3)

### 2.8.3 Virgin collection

We normally keep fly stocks in glass vials at 18°C; stocks are transferred to fresh food every 4 weeks (or every 2 weeks if stocks were kept at 25°C). Virgin female

flies were typically collected twice a day, normally at 9am and 5pm. During the night the fly vials or bottles were kept at 18°C to delay hatching;, virgins were kept in a 18°C incubator overnight. To collect the maximum number of virgins in the shortest period of time, virgin collecting lines were kept in a 25°C incubator between 9am and 5pm to accelerate hatching.

### 2.8.4 Setting up crosses

With the GAL4/UAS expression system, the desired transgenic lines need to be crossed with the selected Gal4 line to allow expression of the tagged RPs. To express tagged RPs in salivary glands, I have tested different Gal4 drivers (Appendix III, table 3). The best expression was obtained with SG-Gal4 and a heat shock-Gal4 driver. Typically, 5 males were crossed with 10 virgin females in glass vials. Crosses were kept in the 18°C incubator and transferred to fresh tubes every 2 days (larvae grow better at 18°C and develop bigger salivary glands). Third instar larvae were then dissected on the $10^{th}$ day after egg laying. For BiFC experiments, the same procedure was followed.

### 2.8.5 *Drosophila* germline transformation

In my project the transgenes were generated by germ line transformation, using either P-element mediated integration in the *yw* host strain; or generated by PhiC31 integrase-mediated homologous recombination (Bischof et al., 2007). The transformations were done by BestGene Inc. (Chino Hills, U.S.A.).

# Chapter 3. Visualization of the subcellular distribution of ribosomal proteins in S2 cells and salivary glands

## 3.1 Introduction

As reviewed in the Introduction, in eukaryotes, about 80 RPs associate with ribosomal RNA (rRNA) to produce 40S and 60S ribosomal subunits (Tschochner and Hurt, 2003). The RPs are mostly located on the surface of the ribosomal subunits and apart from their important function in ribosome assembly and maintenance of the structural integrity of the ribosome, RPs also play important roles in ribosome biogenesis. RPs are synthesised in the cytoplasm and rapidly imported into the nucleus, where they accumulate in the nucleolus, and assemble with nascent rRNA (Tschochner and Hurt, 2003). Cumulative observations from many studies using immunostaining and electron microscopy have revealed that RPs are most abundant in the cytoplasm and nucleolus (Jakel and Gorlich, 1998; Kruger et al., 2007; Lam et al., 2007; Plafker and Macara, 2002).

Although most ribosomal proteins are essential for viability, several studies have indicated that it is feasible to tag the termini of a number of these proteins with GFP or other peptides without preventing incorporation into functional ribosomes (Hurt et al., 1999; Inada et al., 2002; Lam et al., 2007). We were interested in visualizing ribosomal subunits in cells. Therefore, to track ribosome subunits in the cells, I have tagged several ribosomal proteins with GFP or other fluorescent proteins in *Drosophila*. The results of this study indicate that tagging of ribosomal proteins in *Drosophila* does not affect incorporation into ribosomes. Therefore, the genetically

tagged proteins we have tested provide a feasible tool to track ribosomal subunits in *Drosophila* cells.

## 3.2 Results

### 3.2.1 Visualization of tagged ribosomal proteins in S2 cells

To generate constructs expressing tagged RPs I used the Gateway cloning system (Invitrogen, see Material and Methods). In brief, I cloned selected ribosomal proteins (RpS9, RpS15, RpS18 and RpL11) into a destination vector producing GFP tagged constructs (pAWG with GFP at the C-terminus). A schematic of the constructs is shown in Figure 3.1, see Material and Methods for more details. I transiently transfected S2 cells with these plasmid constructs and with a control expressing GFP alone. Using some of the transfected cells, I assayed the expression of the fusion protein by Western blot analysis using an antibody against GFP. I found that all of the constructs produced a band of the right size, confirming that these proteins are well expressed in S2 cells (Figure 3.2). With the remaining cells, which were attached to a cover slip, I visualized the RPs tagged with GFP under the fluorescence microscope. All four tagged proteins showed the expected sub-cellular localization pattern: most of the signal was in the nucleolus and in the cytoplasm in 80-90% of the transfected cells (Figure 3.3). In contrast, GFP, accumulates all over the cell when is not fused to any RPs, showing a high concentration in the nucleus (Figure 3.3, panels M-O). In agreement with previous reports that both endogenous and GFP-tagged ribosomal proteins are also present in the nucleoplasm (Brogna et al., 2002; Lam et al., 2007), our tagged RPs are also present in the nucleoplasm. Not all cells show nucleolus localization, presumably because the nucleolus is a dynamic structure that changes, or

disappears, during the cell cycle, this pattern of expression represents 5-10% of transfecte cells (Figure 3.5).

Again, using the Gateway technology, I also constructed N-terminal fusions of the same four ribosomal proteins: RpS9, RpS15, RpS18 and RpL11. To do this I used a different destination vector (pAGW with GFP at the N-terminus) (Figure 3.1). These plasmid constructs were transfected into S2 cells and the cells were assayed by Western blotting. As for the C-terminal fusions, a clear single band of the right size was observed in all transfected cells (Figure 3.2). Fluorescence microscopy inspection showed that the N-terminal fusions are also most abundant in the nucleolus and in the cytoplasm (Figures 3.4). As seen for the transfections with the C-terminal fusion constructs, not all of the transfected cells show the same pattern of distribution; the intensity of the signal in the nucleolus varied between cells; figure 3.5 shows example of cells in which the RPs are not concentarted in the nucleolus (this pattern was found in a small fraction of cells and the frequency varied between different fusion proteins).

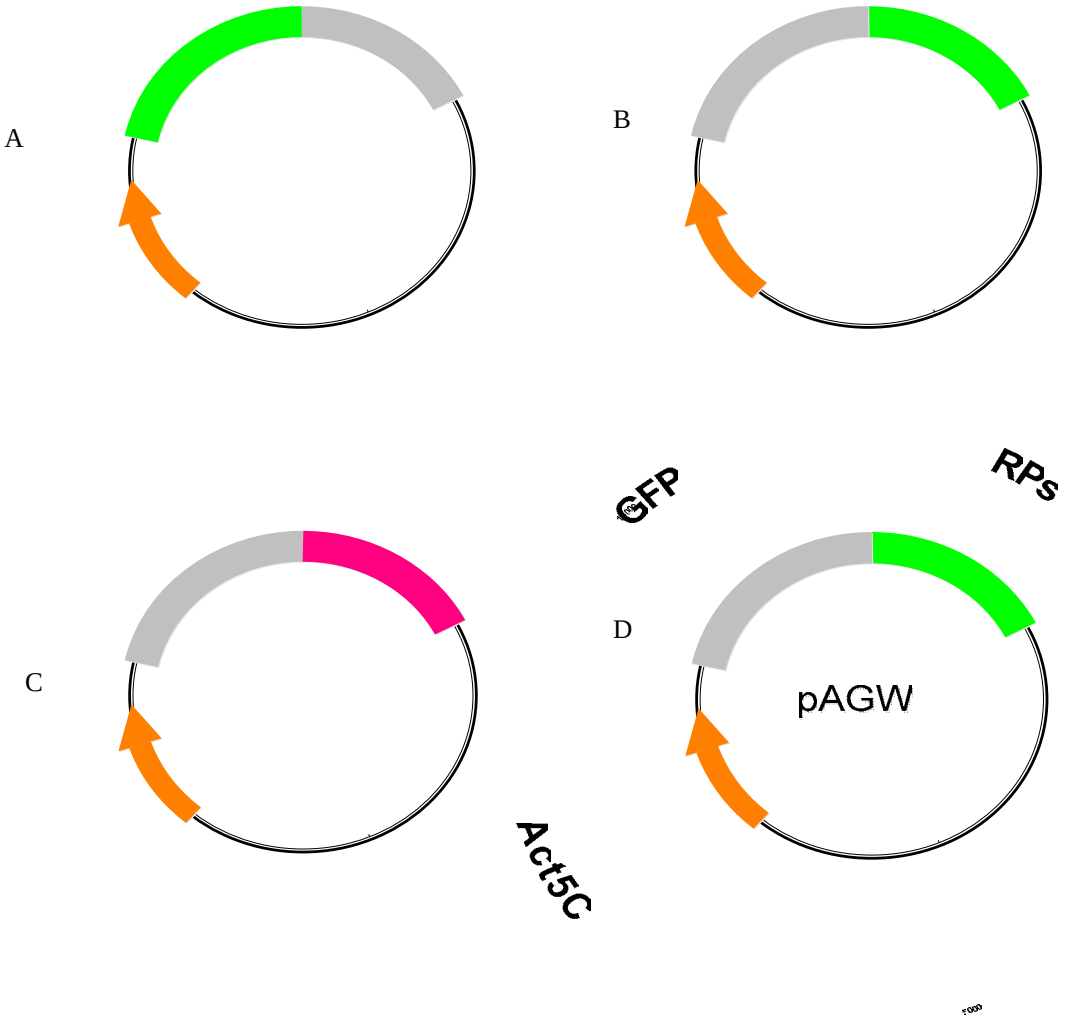


**Figure 3.1 Schematic of the constructs used to express RPs in S2 cells**. (A) and (B) two generic maps of constructs regulated by the Act5c promoter (Invitrogen); the conscructs express N-terminal and C- terminal GFP-tagged RPs. (C) and (D ) show similar construct as above but regulated by the UAST promoter. The constructs were generated using the Gateway recombination system.

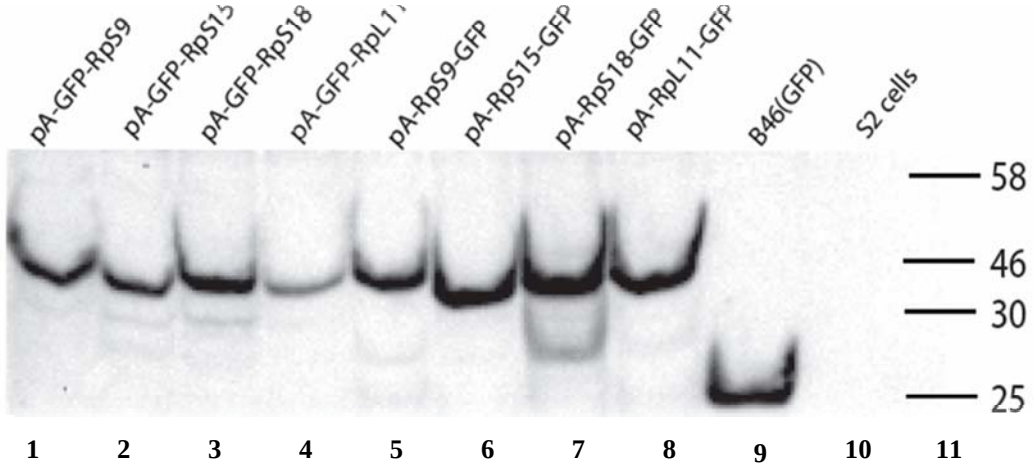


**Figure 3.2 Western blot analysis of S2 cells expressing different RPs fusions.** Proteins were detectd with an anti-GFP antibody (see Material and Methods). From left to right, Lane1, pA-GFP-RpS9 (43.4 kDa), Lane 2, pA-GFP-RpS15 (38.4 kDa) ,Lane 3 , pA-GFP-RpS18 (39.1 kDa), Lane 4, pA-GFP-RpL11 (42.3 kDa), Lane 5, pA-RpS9-GFP (43.4 kDa), Lane 6, pA-RpS15-GFP (38.4 kDa), Lane 7, pA-RpS18-GFP (39.1 kDa), Lane 8, pA-RpL11-GFP (42.3 kDa), Lane 9, GFP alone control and Lane 10, untransfected S2 cells, Lane 11, protein ladder.

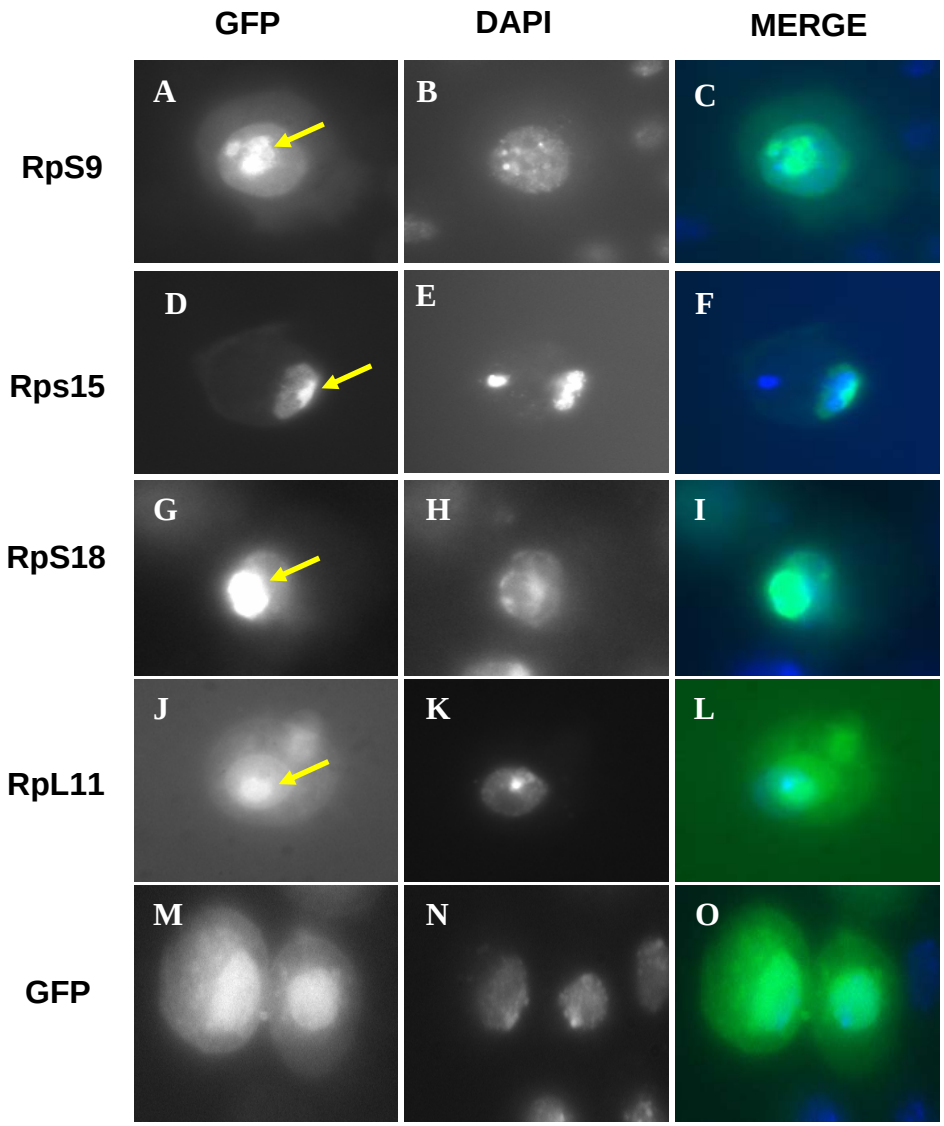


**Figure 3.3 Fluorescence imaging of S2 expressing C-terminal fusions of different RPs.**Image of cells transiently transfectd with Act5c regulating constructes expressing the GFP C-terminal fusions of the RP indicated on the left.The bottom row shows cells expressing GFP alone, as a control. Arrows point to the nucleoli. The GFP signals are on left column, DAPI staining in the middle and the merged image on the right. Images were taken using a fluorescence microscope with a 60X oil immersion objective.

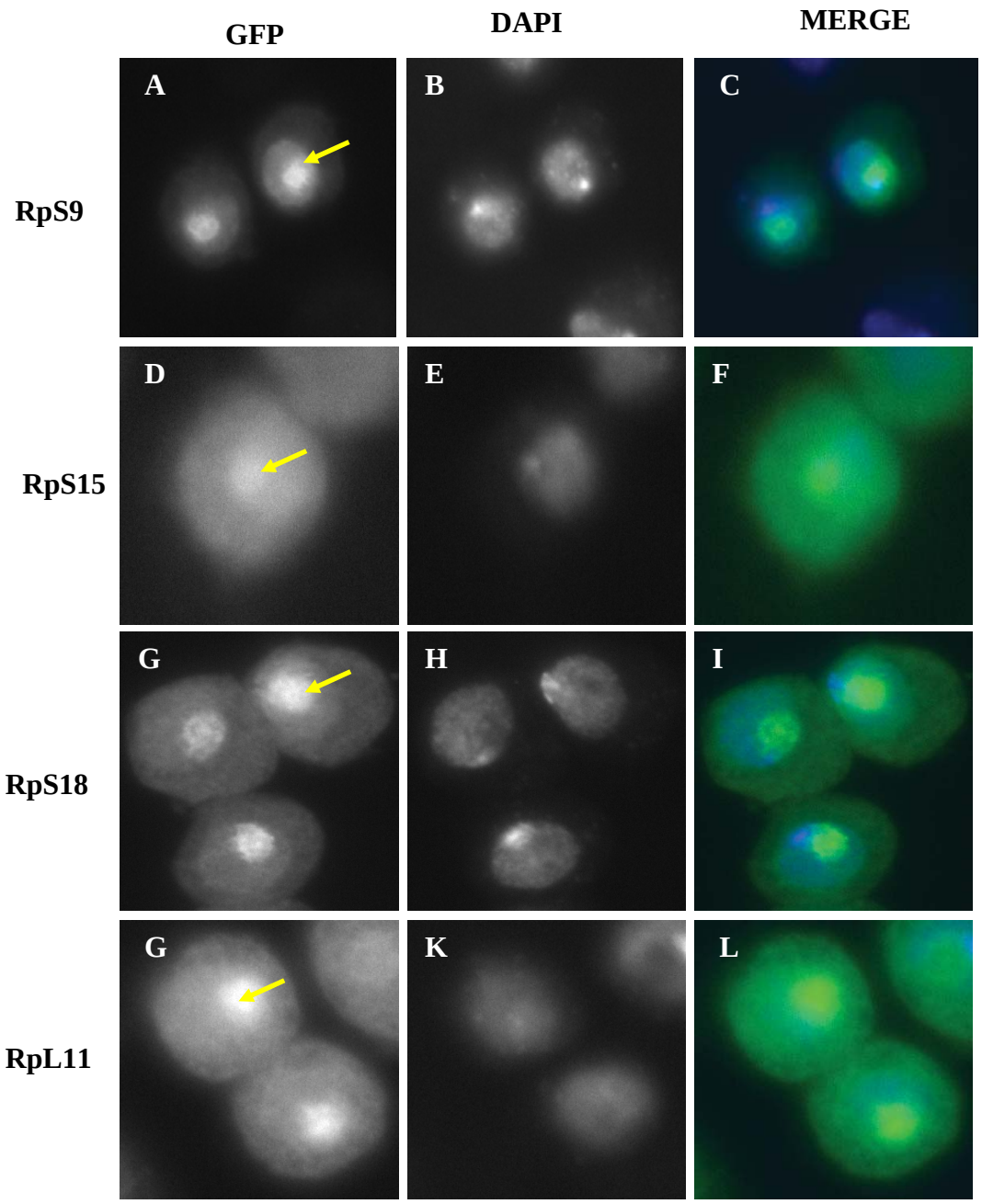


**Figure 3.4 Fluorescence imaging of S2 expressing N-terminal fusions of different RPs.**Image of cells transiently transfectd with Act5c regulating constructes expressing the GFP N-terminal fusions of the RP indicated on the left. Arrows point to the nucleoli. The GFP signals are on left column, DAPI staining in the middle and the merged image on the right. Images were taken using a fluorescence microscope with a 60X oil immersion objective.

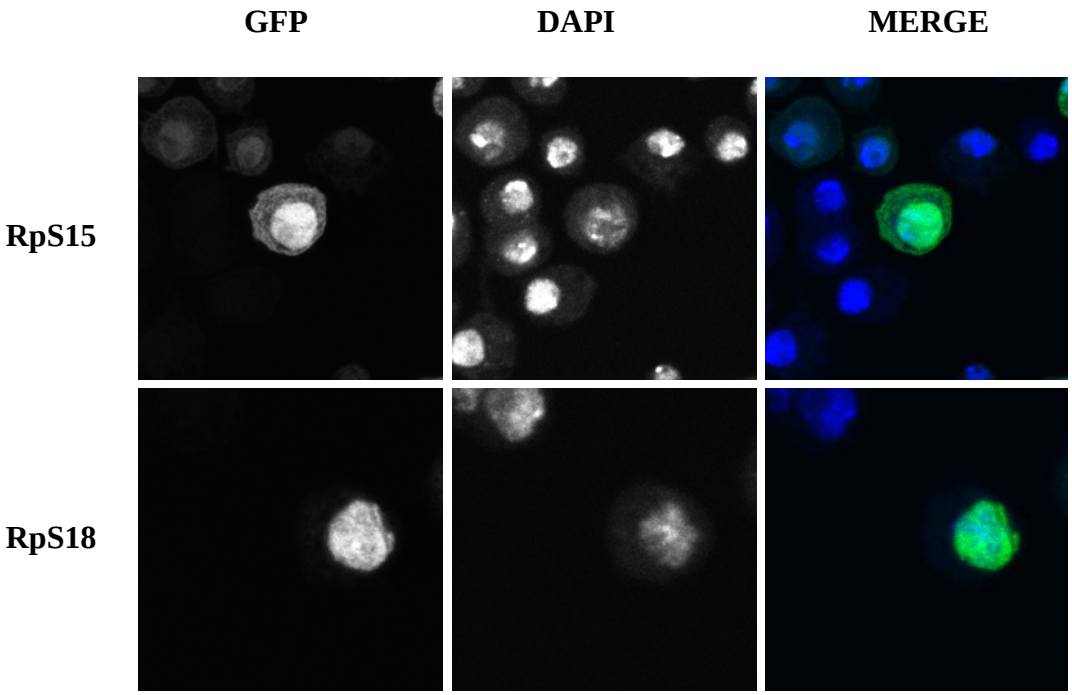


**Figure 3.5 Fluorescence imaging of S2 cells transiently transfected with C-terminal fusions of the indicated RPs**. The signal distribution was not restricted to the nucleolus and cytoplasm but is also shown clearly in nucleoplasm:. Localization is shown by GFP signals (left column), DAPI staining (middle column) and the merged image (right column). Images were taken using a fluorescence microscope with a 60X oil immersion objective.

Given that we were planning to express tagged RPs in flies, we also tested whether these tagged proteins could be efficiently expressed with the UAST promoter. By using the UAS/Gal4 system, the UAST promoter allows expression of the tagged proteins in the tissue of choice and at specific times of development (Brand and Perrimon, 1993) (more information in the Materials and Methods). UAST-driven constructs were generated using the Gateway technique as before, by transferring the four constructs described above (S9, S15, S18 and L11) into a destination vector with a UAS promoter (Figure 3.1) (see Figure 2.4 in Materials and Methods)

In addition, other constructs expressing eight more ribosomal proteins (RpS2, RpS5a, RpS11, RpS13, RpL8, RpL23, RpL32 and RpL36) were generated. These selected ribosomal proteins are encoded by single genes which correspond toMinute mutations (Marygold et al., 2007). The Minute phenotype of the heterozygous mutations and the lethality of the homozigotes shall allow to test for functionality of our fusion RPs proteins by genetic complementation.

The 40S proteins were tagged with GFP and the 60S proteins with RFP, in both cases at the C-terminus. By tagging the two subunits with different colour fluorescent proteins, it would be possible to visualize the two subunits contemporaneously in the cell, and potentially, to allow the use of fluorescence resonance energy transfer assay (FRET) to visualize the subunit interaction (see below). As for the previous constructs, these eight additional plasmids were generated using the Gateway system, using a different destination vector. These plasmids contain the PhiC31 recombination cassette that allows germ line transformation using the novel PhiC31-integrase mediated system; see Material & Methods for details (Bischof et al., 2007). The

advantage of the PhiC31-system is that it allows integration of the transgenes at defined chromosomal loci, therefore minimizing unwanted differences in expression levels between the constructs.

To assess whether these tagged ribosomal proteins are well expressed, I transiently transfected S2 cells with these plasmid constructs and with the control expressing GFP alone. Then, from half of the cells, I extracted proteins and assayed expression of the proteins by Western blotting. The constructs express the expected fusion proteins: a single band of the expected size was present in all cases (Figure 3.6). The remaining cells, which were attached to a cover slip, were viewed with a fluorescence microscope. All protein fusions with both GFP (Figure 3.7) and with RFP (Figure 3.8) show the expected sub-cellular localization:  high concentration in the nucleolus and in the cytoplasm. The localization pattern was similar to that seen with the previously tagged RPs (Figures 3.3 and 3.4).

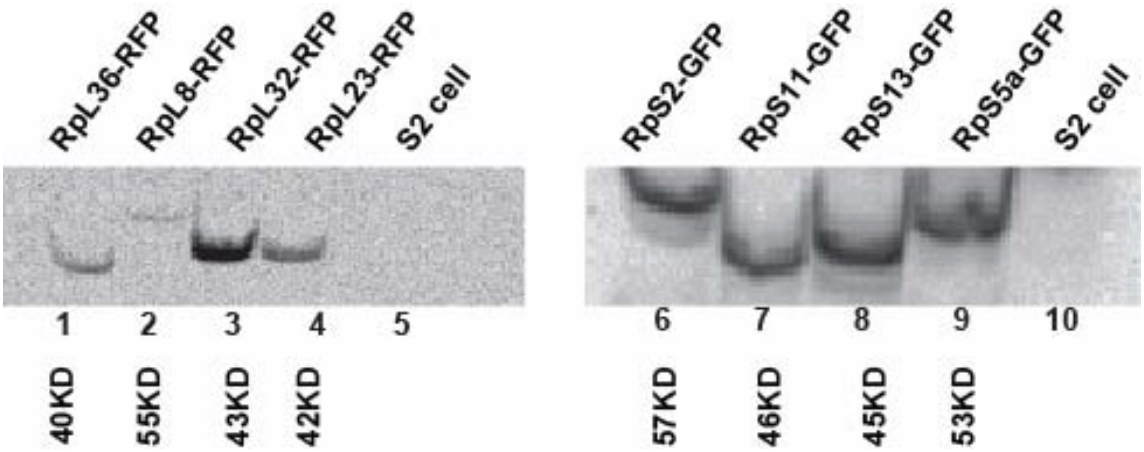


**Figure 3.6 Western blot analysis of RFP and GFP fused RPs isolated from transfected S2 cells**. Left to right: Lane 1, UAS-RpL36-RFP (40 kDa), Lane 2, UAS-RpL8-RFP (55 kDa), Lane 3, UAS-RpL32-RFP (43 kDa), Lane 4, UAS-RpL23-RFP (42 kDa), Lane 5, untransfected S2 cells, Lane 6, UAS-RpS2-GFP (57 kDa), Lane 7, UAS-RpS11-GFP (46 kDa), Lane 8, UAS-RpS13-GFP (45 kDa), Lane 9, UAS-RpS5a-GFP (53 kDa), Lane 10, untransfected S2 cells.

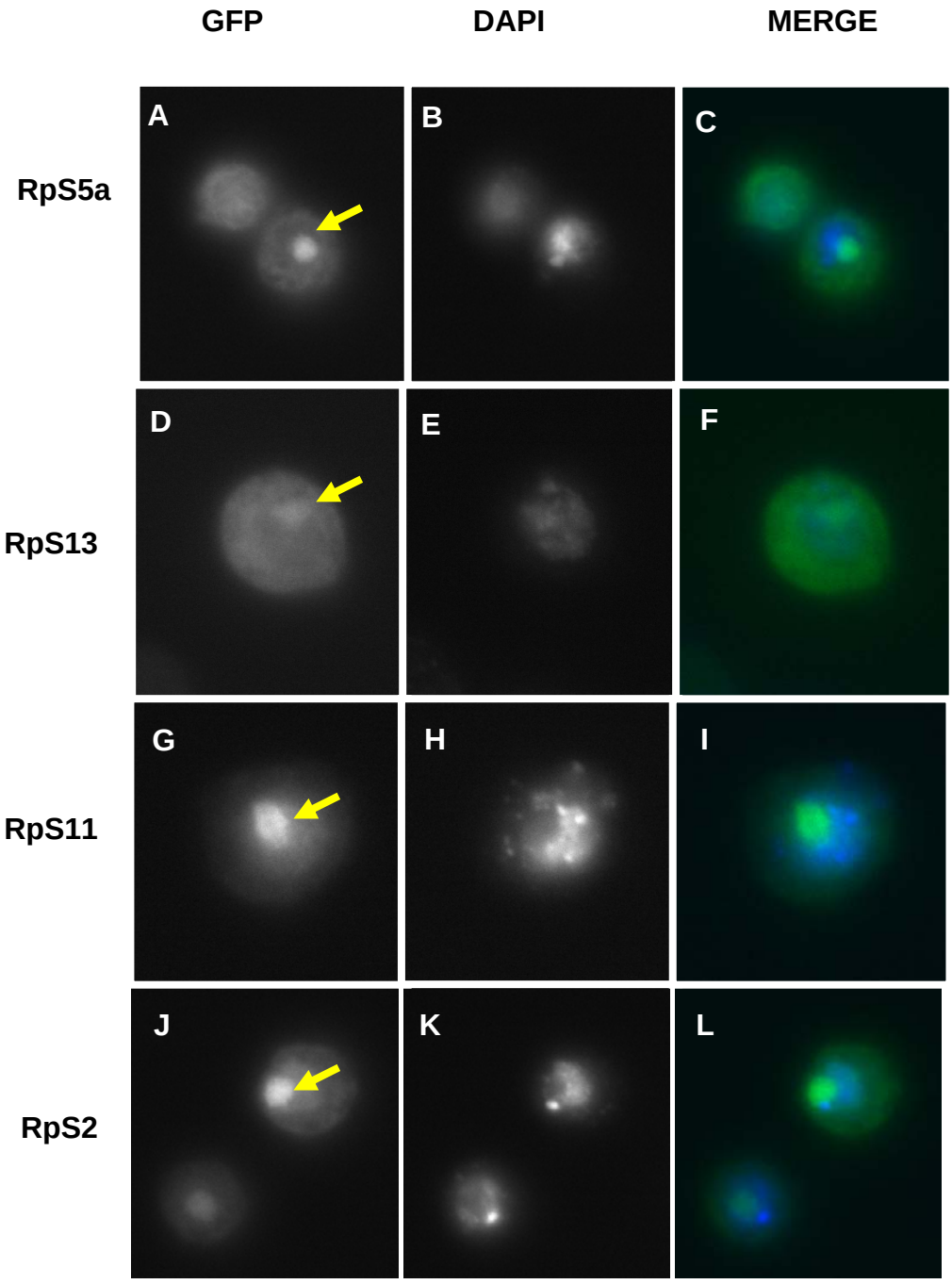


**Figure 3.7 Fluorescence imaging of S2 expressing C-terminal fusions of different RPs** .Image of cells transiently transfected with UAST-regulated constructs expressing the GFP C-terminal fusions of the RP indicated on the left. Arrows point to the nucleoli. The GFP signals are on left column, DAPI staining in the middle and the merged image on the right. Images were taken using a fluorescence microscope with a 60X oil immersion objective.

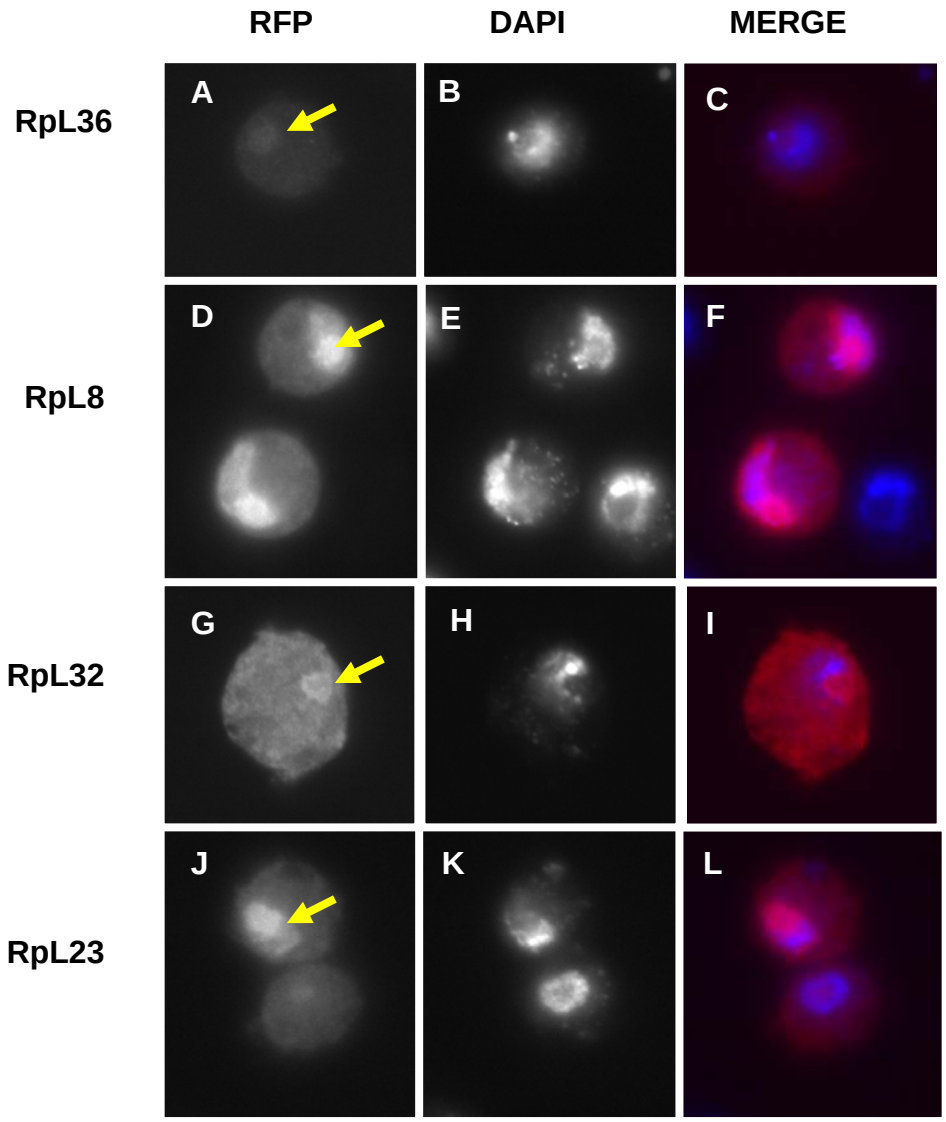


**Figure 3.8 Fluorescence imaging of S2 expressing C-terminal fusions of different RPs** .Image of cells transiently transfected with UAST-regulated constructs expressing the RFP C-terminal fusions of the RP indicated on the left. Arrows point to the nucleoli. The RFP signals are on left column, DAPI staining in the middle and the merged image on the right. Images were taken using a fluorescence microscope with a 60X oil immersion objective.

### 3.2.2 Tagged ribosomal proteins are incorporated into functional ribosomes

The finding that the tagged RPs are well expressed, and that their sub-cellular localization pattern is the same as that reported for endogenous RPs, indicates that these proteins are incorporated into ribosomes. To assess the functionality of the proteins more directly, I tested whether the fusion proteins are incorporated into polysomes. During the translation cycle, a small 40S and large 60S ribosomal subunit associate with mRNA to form an 80S complex (monosome). This ribosome moves along the mRNA during translational elongation (Ramakrishnan, 2002). Throughout elongation, additional ribosomes can initiate translation on the same mRNA to form polysomes (Arava et al., 2005). Each polysomal complex can contain from two to over twenty ribosomes, and it is the number of ribosomes that determines the mass of each complex. Therefore, the fraction of polysomes within the cell can be separated by sucrose density gradient centrifugation on the basis of the loading of ribosomes on the mRNA.

As reviwed in the Introduction, RpS18, RpS15 and RpL11 are located at the ribosomal subunit interface; RpS18 and RpL11 are expected to interact upon ribosome subunits joining. Instead RpS9 is located at the opposite side of the interacting surface. Cell extracts of S2 cells expressing the GFP C-terminal fusions of the RPs were separated by sucrose gradient centrifugation and the fractions corresponding to free proteins, 40S, 60S, 80S subunits, and polysome fractions were analysed by Western blotting with tag-specific antibodies (see Material and Methods). We found that all four tagged proteins associate with the polysome fraction, indicating that these tagged RPs can be incorporated into functional ribosomes (Figure 3.9).

The extent to which the proteins were incorporated into polysomes varied between constructs, wherase most of the protein was associated with ribosome fractions, fraction of the protein was also found in lighter fractions, probably corresponding to free proteins not associated with ribosomes.

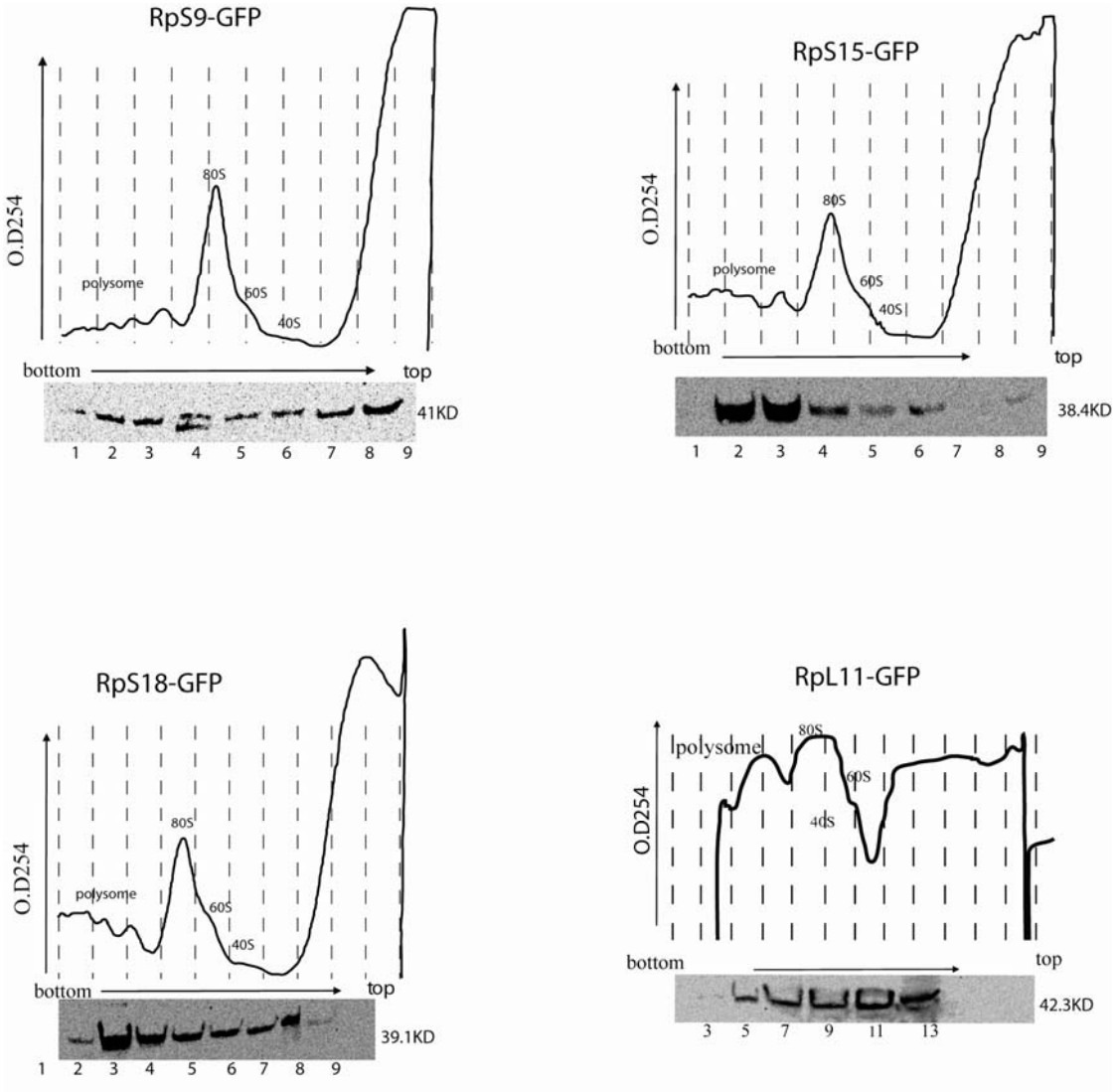


**Figure 3.9 Tagged RPs associate with polysomes**

Polysome fractionation of cell extracts of cells expressing the indicated RP fusions: RPS9-GFP, RPS15-GFP, RPS18-GFP and RPL11-GFP. Cell extracts were separated on sucrose (50-10%) gradients and fractionated into 1 ml fractions following $OD_{254}$ monitoring (top panels). Fractions were TCA precipitated and analyzed by Western blotting with an anti- GFP antibody (panel below the $OD_{254}$ profile). (This experiment was done with technical assistance of Preethi Ramanathan)

### 3.2.3 Localization of ribosomal proteins in transgenic flies

#### 3.2.3.1 Generation of transgenic *Drosophila* expressing fluorescent ribosomal proteins

After having demonstrated that the constructs with the RP fusions are well expressed in S2 cells and that these proteins can be incorporated into ribosomes, I used these constructs to generate transgenic flies. The transgenes were generated by germ line transformation, using either P-element mediated integration or, as mentioned above, the PhiC31 system (more info in Materials and Methods). In all instances expression of the constructs was under the control of the UAS promoter. The GAL4/UAS system allowed me to express the tagged ribosomal proteins in the salivary glands by crossing the UAS transgenes with a strain expressing Gal4 in salivary glands throughout larval development (SG-Gal4) (see Table 3 in Appendix III) The salivary gland cells are very large and are amenable as a system to visualize the subcellular localization of proteins.

#### 3.2.3.2 Localization of ribosomal protein in salivary glands

The transgenes encoding RpL11-RFP, RpS18-GFP and RpS9-GFP were first crossed with a strain carrying GMR-Gal4. The GMR-Gal4 driver is expressed at a high level in the developing eye (Freeman, 1996). Over-expression in the eye is a very sensitive assay to visualize eventually toxic effects associated with the expression of transgenes. None of the transgenes showed roughening of the eye, indicating that overexpressing these fusion proteins is not detrimental for the cell. Next I crossed my transgenic flies with a SG-Gal4 strain that allows tissue-specific expression in the

salivary glands of mid third instar larvae. Fluorescence imaging showed a sub-cellular localization pattern of small subunit RPs (RpS9, RpS18, RpS13, RpS2, RpS11, and RpS5a) fused with GFP (Figure3.10) and large subunit RPs (RpL36, RpL11, RpL8, and RpL32) fused with RFP (Figure 3.11). Unlike in transfected S2 cells where not all cells show a high concentration of RPs in the nucleolus, in salivary glands, all RPs show a prominent signal in the nucleolus where most of the events of ribosome biogenesis take place. The high signal intensity of tagged RPs can be attributed to the stage of larvae development – at this stage (third instar), the salivary glands secrete high levels of glue protein synthesis to form a sticky matrix that allows the larva to adhere itself to solid surfaces to prepare for pupation. As for S2 cells, signal was also detected in cytoplasm. For several of the tagged RPs a clear signal was also apparent in the nucleoplasm, and this was most apparent for RpS18-GFP, RpS5a-GFP and RpL11-RFP (Figures 3.10 and 3.11). The nucleoplasm signal is less intense than the signal seen in the nucleolus, but is comparable and, in some instances, even stronger than in the cytoplasm where fluorescence seems to be faint. The low cytoplasmic signal is probably artifactual: the salivary glands cells are replete with vesicles, which in fluorescent micrographs appears as black regions devoid from fluorescent protein signal.

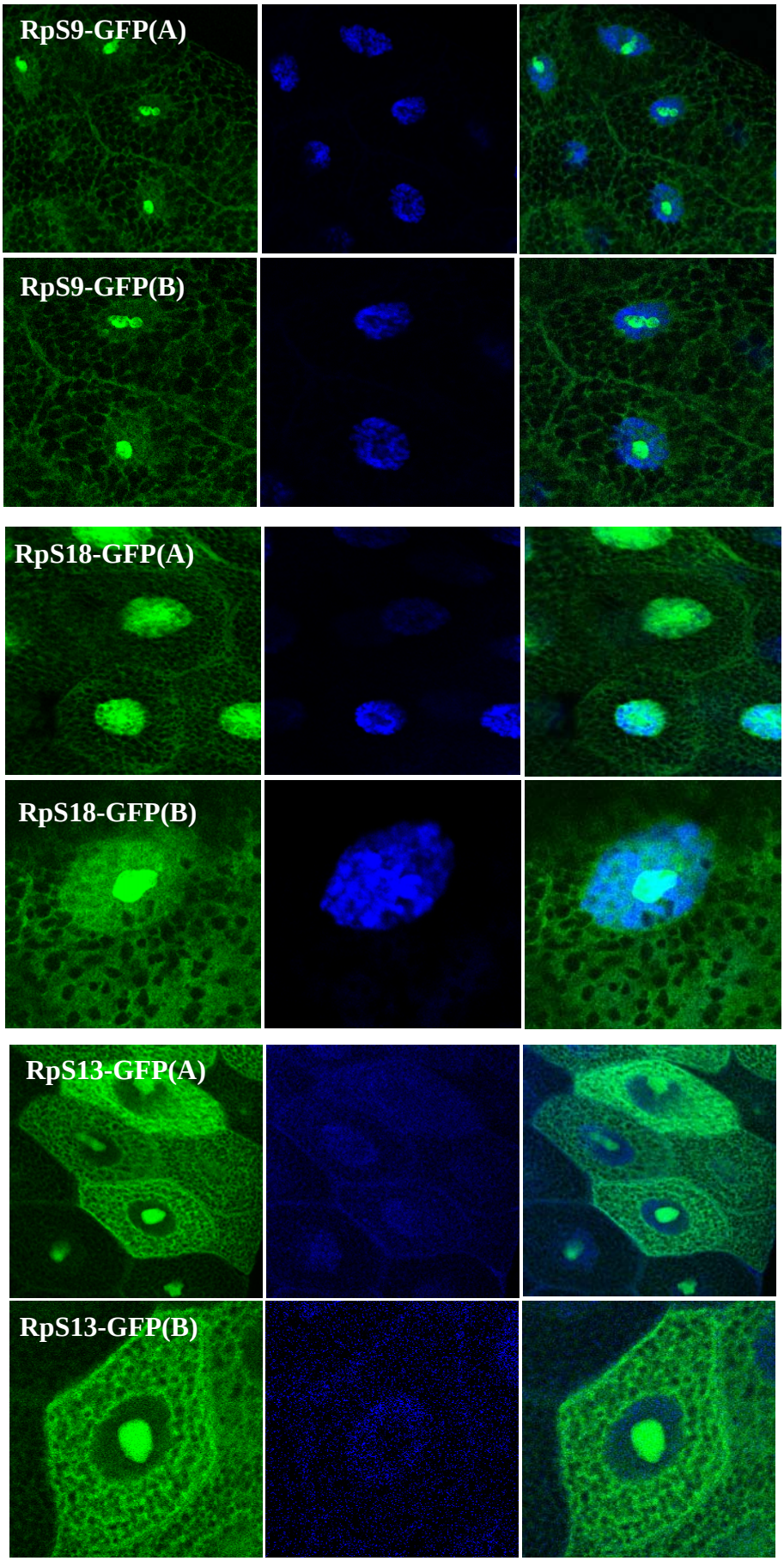


**Figure 3.10 Salivary glands cells expressing C-terminal GFP-fusions of 40S RPs**.

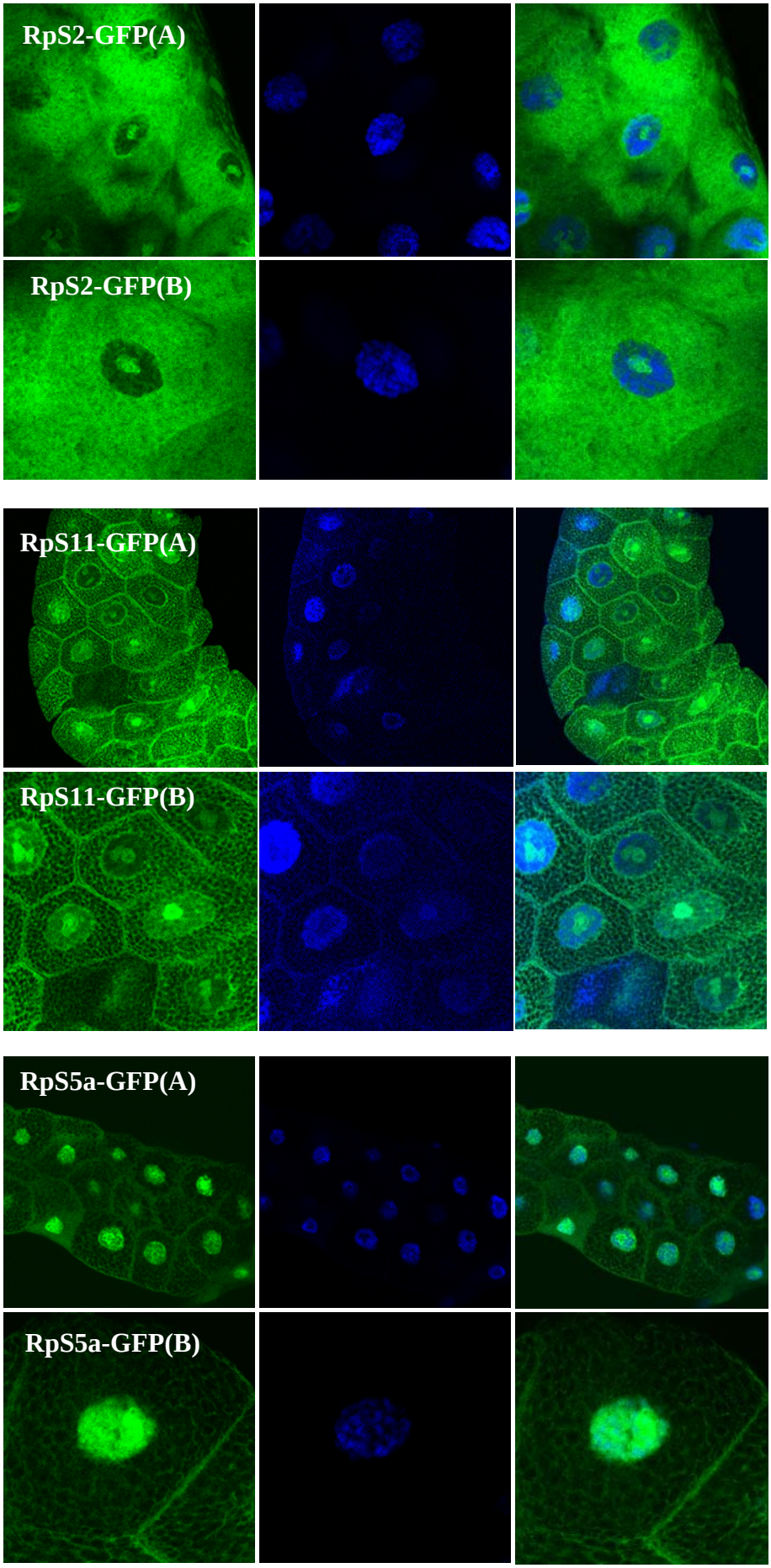


**Figure 3.10 Salivary glands cells expressing C-terminal GFP-fusions of 40S RPs.**

**Figure 3.10 Micrographs of salivary glands cells expressing C-terminal GFP-fusions of 40S RPs**. The RPs shown are RpS9-GFP, RpS18-GFP, RpS13-GFP, RpS2-GFP, RpS11-GFP and RpS5a-GFP. The RPs expression was achieved by crossing the UAS transgens with the SG-Gal4 driver expressed specifically in the salivary glands. Two different images are shown for each RP, taken with a 40X oil immersion objective, at either low (A) or high zoom (B).The GFP signals are shown in the left column, DAPI staining in the middle and the merged image on the right. All images were taken with a confocal microscope.

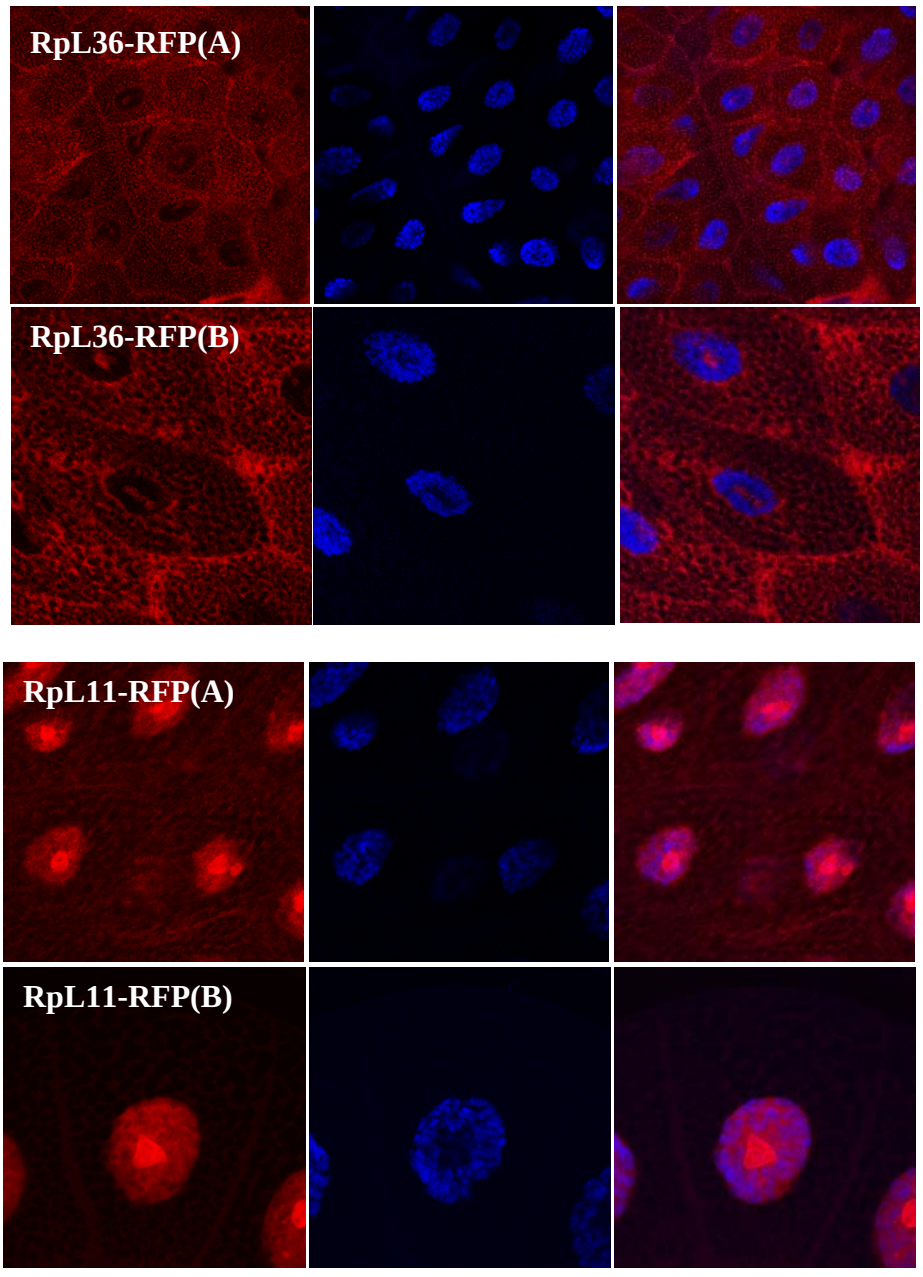


**Figure 3.11 Salivary glands cells expressing C-terminal RFP-fusions of 60S RPs**.

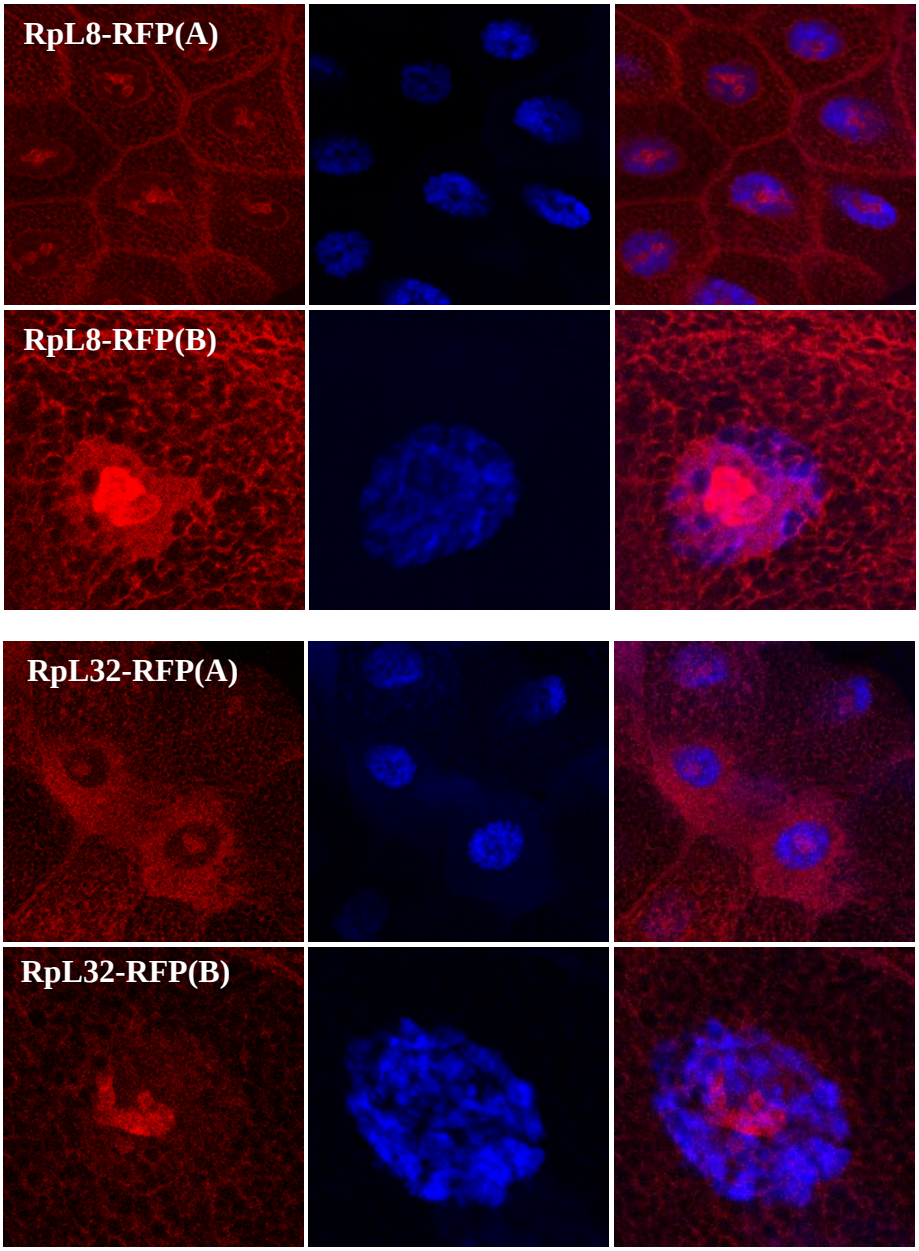


**Figure 3.11 Micrographs of salivary glands cells expressing C-terminal RFP-fusions of 60S RPs**. The RPs shown are RpL36-RFP, RpL11-RFP, RpL8-RFP and RpL32-RFP. The RPs expression was achieved by crossing the UAS transgens with the SG-Gal4 driver expressed specifically in the salivary glands. Two different images are shown for each RP, taken with a 40X oil immersion objective, at either low (A) or high zoom (B).The RFP signals are shown in the left column, DAPI staining in the middle and the merged image on the right. All images were taken with a confocal microscope.

## 3.3 Discussion

As reviewed in the Introduction (Chapter I), RPs are synthesized in the cytoplasm and imported into the nucleus. In the nucleus, RPs concentrate in the nucleolus where they associate with rRNA during ribosome biogenesis. Therefore, we expected that, if tagging has no detrimental effects, the tagged RPs should show a clear cytoplasmic distribution and a high concentration in the nucleolus. In this chapter, I report the development of a number of gene constructs expressing ten RPs in *Drosophila* cells. Some of the proteins were tagged with GFP, while others were tagged with RFP, and some with both, either at the N- or C-terminus. These tagged proteins accumulate in the S2 cell cytoplasm and are highly concentrated in the nucleolus. Many previous studies have reported that the nucleolar localization of ribosomal proteins depends on active rRNA transcription (Andersen et al., 2005; Lam et al., 2007); therefore, accumulation in the nucleolus is a first indication that these tagged RPs are functional and capable of interacting with rRNA. Furthermore, upon treatment with Actinomycin D, the nucleolar signal is reduced considerably (unpublished work by other members of the Brogna laboratory); this observation indicate that the nucleolar accumulation of these RPs depends, as expected, on rRNA synthesis. A further indication that these tagged RPs are functional is that we found them associated with polysomes (Figure 3.9). However, in transfected S2 cells, the tagged RPs did not appear to concentrate in the nucleolus in small fraction of cells, even though they were present at a high level in the nucleoplasm. I speculate that, in the cells without a clear nucleolus signal, the nucleolus is simply disassembled .The nucleolus is a dynamic structure that changes or disappears during the cell cycle or in response to stress, leading to redistribution of

the ribosomal proteins to the nucleoplasm (Heix et al., 1998; Lam et al., 2007; Rubbi and Milner, 2003; Sirri et al., 2008).

In the salivary gland cells all RPs I have are most concentrated in the nucleolus (I have never observed cells without a strong nucleolar signal). The salivary gland cells have polytenic nuclei and very large nucleoli. These secretory cells are very metabolically active and must require a high rate of protein synthesis and ribosome production. All cells in the salivary gland have a nucleolus; in salivary glands, the nucleolus is a stable component as these cells differentiate by increasing the volume (cell size) of individual cells without further cell division (Andrew et al., 2000).

As for S2 cells, I found that some tagged RPs clearly accumulate in the nucleoplasm as well as in the cytoplasm and nucleolus. This was particularly apparent with RpS18-GFP, RpS5a-GFP and RpL11-RFP. The nucleoplasm accumulation could be due to the overexpressed of the tagged RPs. Recent data suggest that several endogenous RPs are also expressed in excess and are normally degraded by the nuclear proteasome, and that only a fraction re-enters the cytoplasm as components of the ribosome through 40s and 60S exportation (Lam et al., 2007; Schubert et al., 2000). The presence of RPs in the nucleoplasm, however, is also consistent with the previous finding that ribosome components are present at transcription sites and that translation might also occur in the nucleus (Brogna et al., 2002; Iborra et al., 2001). This issue is investigated further in the Discussion (Chapter 6).

# Chapter 4. Ribosomal proteins associate with active transcription sites

## 4.1 Introduction

In this chapter I investigated whether RPs associate with transcription sites. To do this I have analysed the association of RpS9, RpS18 and RpL11 with polytene chromosomes in transgenic flies..

In recent years, there has been some controversy regarding the presence of ribosomal proteins at sites of transcription. One study reported that many ribosomal proteins are present at transcription sites, most probably associated with nascent RNA (Brogna et al., 2002). In addition this study reported that rRNA and some translation factors are also present at these sites. Therefore, these data suggest that ribosomal subunits are associated with nascent mRNA and that translation is occurring at these sites. In agreement with this conclusion, it has also been reported that amino acids are incorporated at chromosomal sites (Iborra et al., 2001). As reviewed in the Introduction the notion that translation might occur also in the nucleus was reported more than three decades ago (Allen and Wong, 1978; Goldstein, 1970). The two recent studies, however, were hotly debated. Some authors have suggested that the seemingly nuclear translation in mammalian cells reporter by Iborra et al. might have been an artefact of the cell permeabilization procedure required for the uptake of modified charged amino acids (Dahlberg and Lund, 2004). As for the study by Brogna et al., it has been argued that the antibodies used were not sufficiently specific for the ribosomal proteins and that the chromosomal staining was due to cross reactivity with other proteins (Dahlberg and Lund, 2004). In the *Drosophila* study, the

immunostaining experiments in question involved the use of primary antibodies directed against endogenous proteins, and it was difficult to exclude rigorously the possibility that the staining was due to some residual cross-reactivity, because there was no negative control, such as a mutant fly missing the protein under investigation, as the RPs are essential for viability. Here I have readdressed the issue of whether ribosomal proteins are present at transcription sites on polytene chromosomes using chromosomal immunostaining of the polytene chromosomes of transgenic flies expressing RPs tagged with either GFP or RFP. The RPs were detected by chromosomal immunostaining with antibodies directed against either GFP or RFP. Unlike the previous study, this approach allows the specificity of the antibodies to be rigorously assessed in chromosomes from flies that do not express the fusion protein.

## 4.2 Results

### 4.2.1 Visualization of transcription sites on polytene chromosomes

The *Drosophila* polytene chromosomes from third instar larval salivary glands are a powerful tool to investigate the association of proteins with transcription sites and nascent transcripts. On polytene chromosomes, the transcribed regions (interbands) are cytologically distinct from regions which are not transcribed (bands) (Zhimulev et al., 2004). This feature provides a great opportunity to study the recruitment of specific proteins that might be involved in transcription, RNA processing and other transcription site processes. The interbands are particularly apparent upon immunostaining with antibodies directed against RNA polymerase II (Pol II). Preparation of chromosomes squashes and immunostaining are technically demanding techniques and, therefore, I first optimised the protocol using an antibody specific for the hyper-phosphorylated alpha subunit of RNA polymerase II (H5), which specifically stains active transcription sites (Weeks et al., 1993). For optimisation purposes, the salivary glands were dissected from a *yellow white* fly strain(see Materials and Methods) The primary antibody (H5) was a mouse IgM and was detected with a FITC conjugated anti-mouse IgM secondary antibody (more information in Materials and Methods). Inspection with a fluorescence microscope revealed the expected pattern of distribution of RNA polymerase II: a distinct banding pattern, corresponding to interbands (Figure 4.1). The green FITC bands are complementary to the DAPI banding pattern; this confirms that the Pol II decondensed regions of the chromosome are where active genes are found. These data indicate that the squashing and immunostaining techniques used were effective and

could be used to assay the presence of the tagged RPs on polytene chromosomes. To verify that the primary antibodies used are indeed specific to GFP and RFP respectively, and that there was no cross reaction, control squashes were prepared from glands of flies not expressing the tags. The antibodies I used did not show any cross reactivity, neither on the chromosomes or any other component of the salivary gland cells (see Figure 4.2).

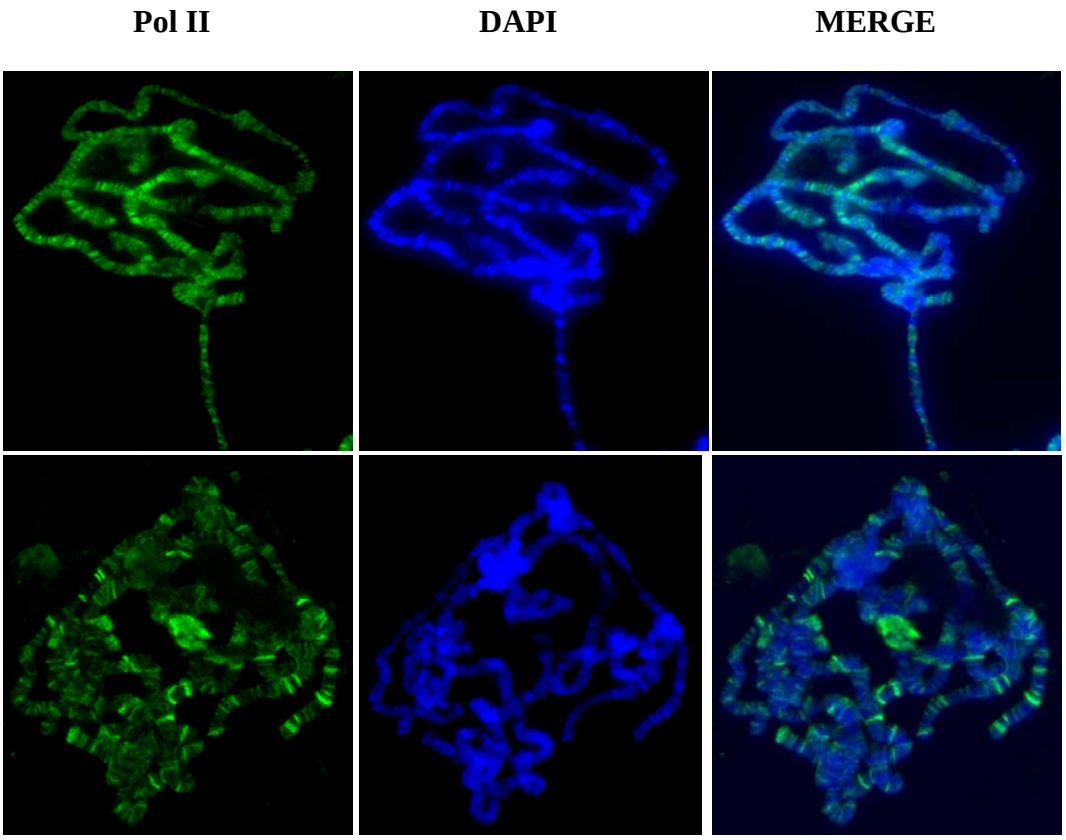


**Figure 4.1 Localization of Pol II on polytene chromosomes.** Immunostaining of polytene chromosomes with H5, an antibody specific for hyperphosphorylated Pol II and a FITC-conjugated secondary antibody. The panels on the left show the FITC (green filter) signal corresponding to Pol II; the middle panels show the DAPI of the DNA (blue filter); and panels on the right show a merged image of the FITC and DAPI signals. Polytene chromosomes were dissected from control larvae not carrying any transgenes (a standard *yw* lab strain); the two rows show the result of two different squashes. Images were taken with a fluorescence microscope under a 40X objective lens.

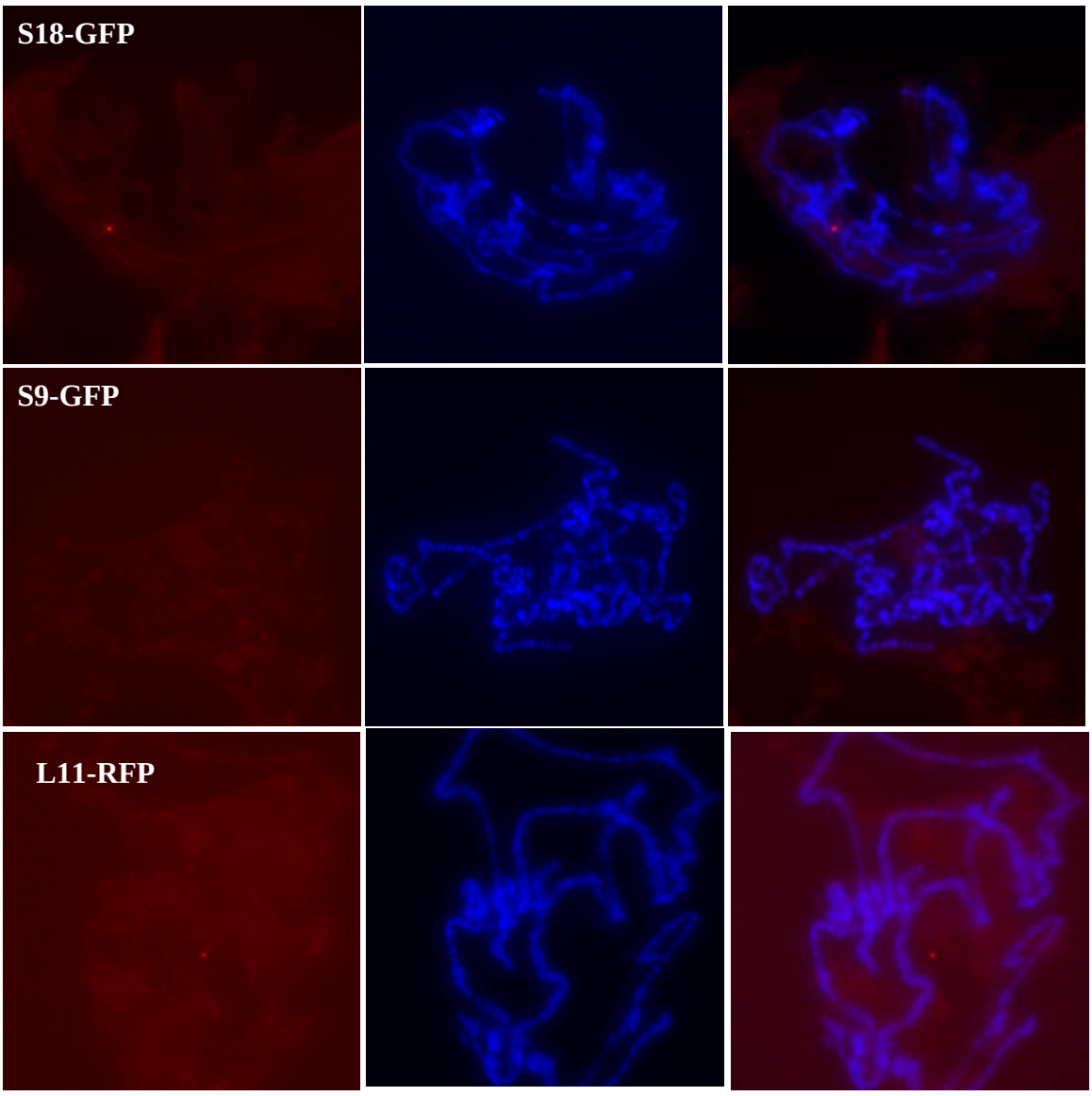


**Figure 4.2 The GFP and RFP antibodies do not cross react with endogenous components of the polytene chromosomes**. The panels on the left show indirect immunofluorescence using an anti GFP or RFP primary antibody and Cy3 conjugated secondary antibody (red), the middle panels show the DAPI of the DNA (blue filter), and the panels on the right show a merged image of the anti-FP-Cy3 and DAPI images. Polytene chromosomes were dissected from non-fluorescent larvae that were selected from each of the crosses of the transgenes with the Gal4 line. Images were taken with an fluorescence microscope, under a 40X objective lens.

### 4.2.2 Tagged ribosomal proteins associate with active transcription sites

To localize the tagged RPs, I followed the optimized immunostaining procedures used above for Pol II localization. Transgenic flies expressing the following tagged proteins were used: UAS-Rps9-GFP, UAS-RpS18-GFP and UAS-RpL11-RFP. The transgenes were expressed by crossing them with the salivary gland Gal4 driver described above (SG-Gal4, Chapter 3), which is active in mid third instar larvae. The larval progeny of the SG-Gal4 X UAS Rp-GFP/RFP crosses were examined under a UV dissecting microscope using appropriate filters, RFP for L11 and GFP for S18 and S9. Salivary glands were dissected from larvae that appeared as brightly fluorescent under the fluorescence dissecting microscope. Polytene chromosomes squashes were prepared as above. The tagged RPs were visualized with either anti-GFP or anti-RFP antibodies; in some experiments the chromosomes were also stained with the anti-Pol II antibody (since both the GFP and RFP antibodies were rabbit IgG, the anti-Pol II, which is a mouse IgM, could be used contemporaneously (for more details, see Materials and Methods). The immunostaining showed that the tagged ribosomal proteins RpS9-GFP, RpS18-GFP and RpL11-RFP are present on the chromosomes at sites that colocalize with Pol II (Figures 4.3, 4.4 and 4.5).

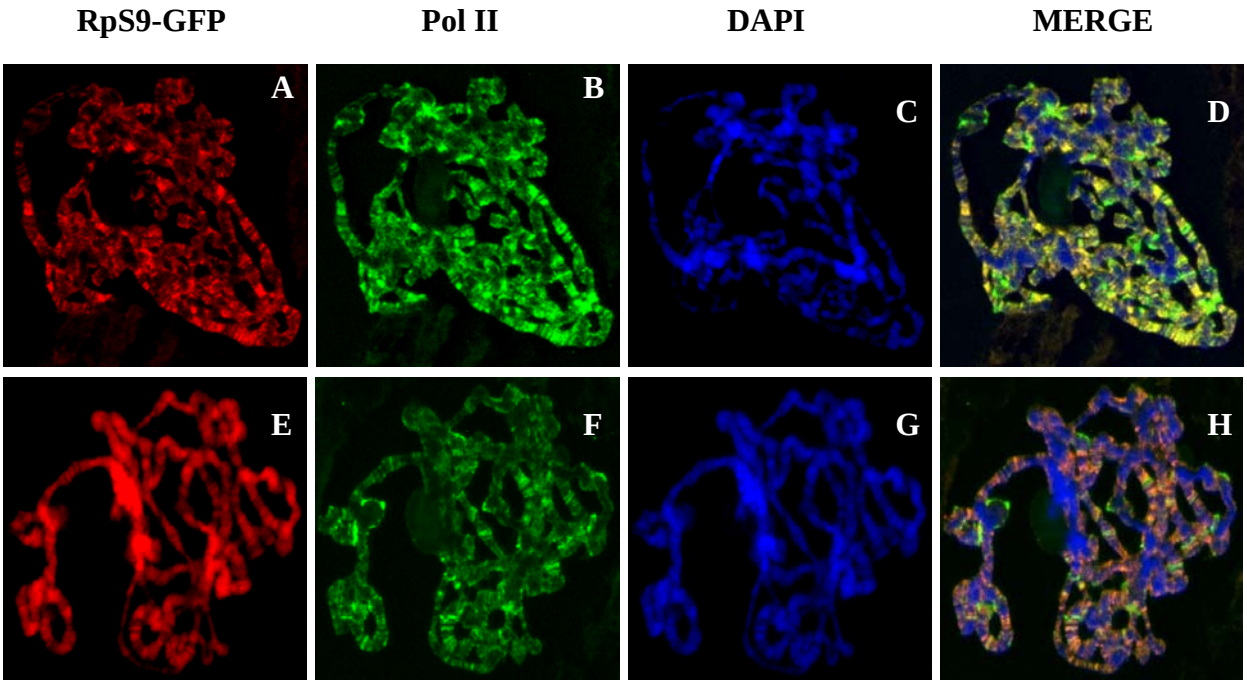


**Figure 4.3 RpS9-GFP associates with sites of transcription**. In the figure, the panels on the left show indirect immunofluorescence using an anti GFP primary antibody and Cy3-conjugated secondary antibody (red), the panels in the second column show staining with anti- Pol II and FITC conjugated secondary antibody (green), the panels in the third column show DAPI staining, and the panels on the right show merged pictures of the RpS9-GFP, Pol II and DAPI images, with the orange colour indicating colocalization of RpS9-GFP and Pol II at interbands. The two rows show results from two different squashes. Images were taken with a fluorescence microscope with a 40X objective**.**

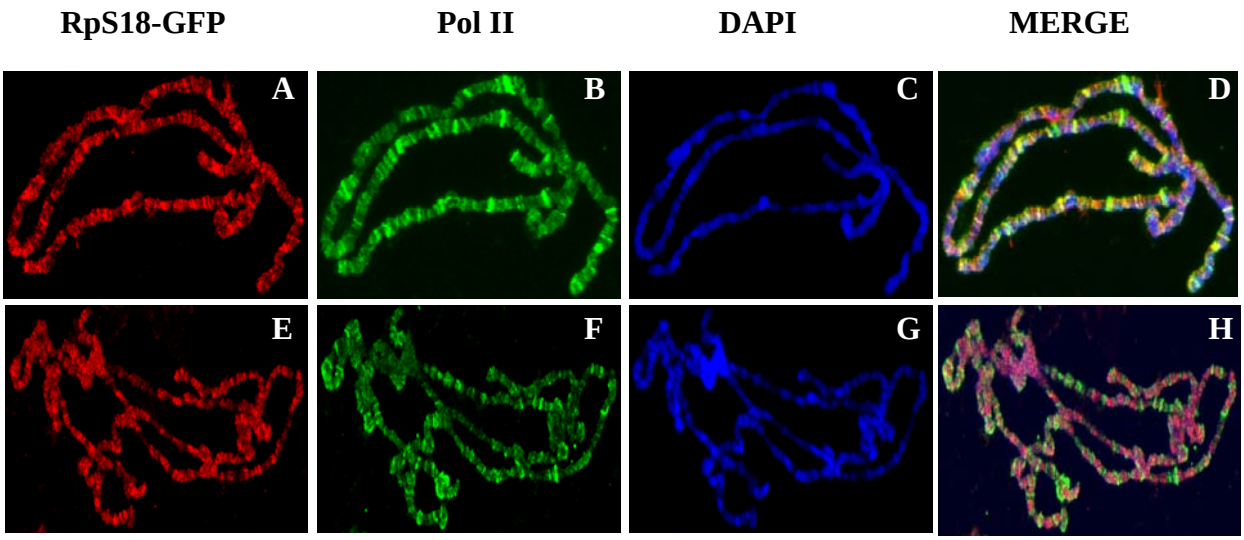


**Figure 4.4 RpS18-GFP associates with sites of transcription**. In the figure, the panels on the left show indirect immunofluorescence using an anti GFP primary antibody and Cy3-conjugated secondary antibody (red), the panels in the second column show staining with anti- Pol II and FITC conjugated secondary antibody (green), the panels in the third column show DAPI staining, and the panels on the right show merged pictures of the RpS18-GFP, Pol II and DAPI images, with the orange colour indicating colocalization of RpS18-GFP and Pol II at interbands. The two rows show results from two different squashes. Images were taken with a fluorescence microscope with a 40X objective**.**

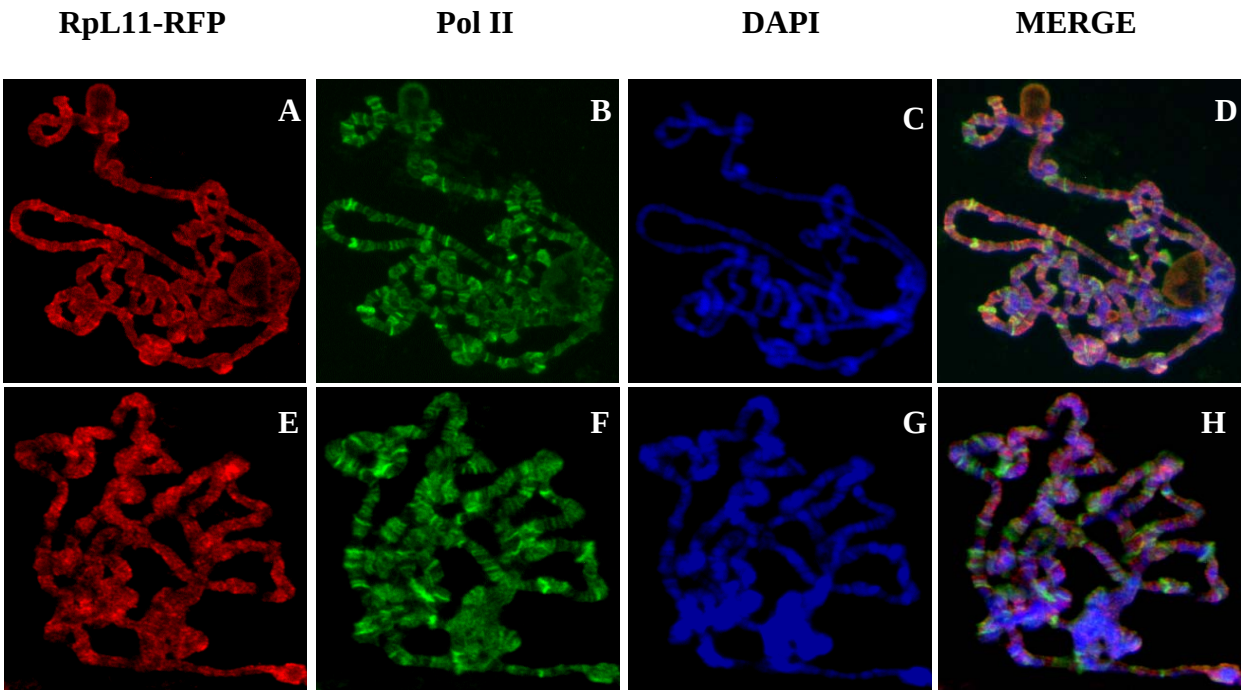


**Figure 4.5 RpL11-RFP associates with sites of transcription**. In the figure, the panels on the left show indirect immunofluorescence using an anti RFP primary antibody and Cy3-conjugated secondary antibody (red), the panels in the second column show staining with anti- Pol II and FITC conjugated secondary antibody (green), the panels in the third column show DAPI staining, and the panels on the right show merged pictures of the RpL11-RFP, Pol II and DAPI images, with the orange colour indicating colocalization of RpL11-RFP and Pol II at interbands. The two rows show results from two different squashes. Images were taken with a fluorescence microscope with a 40X objective**.**

These data demonstrate that tagged RPs are present at the chromosomes and colocalize with RNA Pol II (the staining is apparent in interbands showing as dark regions weakly stained by DAPI) .The colocalization is apparent in the merged pictures of the green and red signal, indicating colocalization of Pol II and tagged ribosomal proteins. However, not all the Pol II bands (green) show a GFP signal (red), and this can be seen in the merged image where green bands can be distinguished.

The one concern that needed to be addressed was the possibility that the GFP or RFP signal could be an artefact caused by bleed through (a common artefact in experiments in which the signal from one fluorophore can be seen with the filter for the other); in my immunostaining, this can occur due to the relative signal intensity difference between Cy3 and FITC that corresponds to tagged RPs and Pol II respectively where the weak Cy3 signal can be bleed through of the strong FITC signal. Therefore, the banding pattern seen under the Cy3 filter could be simply a reflection of the pattern seen under the FITC filter. To check that the RPs signal is not due to bleed through of the more intense Pol II signal, the experiments were repeated staining only for the RPs, without counterstaining for Pol II. The results were similar to the experiments above: the RPs could be visualized at the interbands. These results confirm that GFP-tagged RpS9 (Figure 4.6), RpS18 (Figure 4.7), and RpL11 (Figure 4.8) are present at transcription sites in polytene chromosomes.

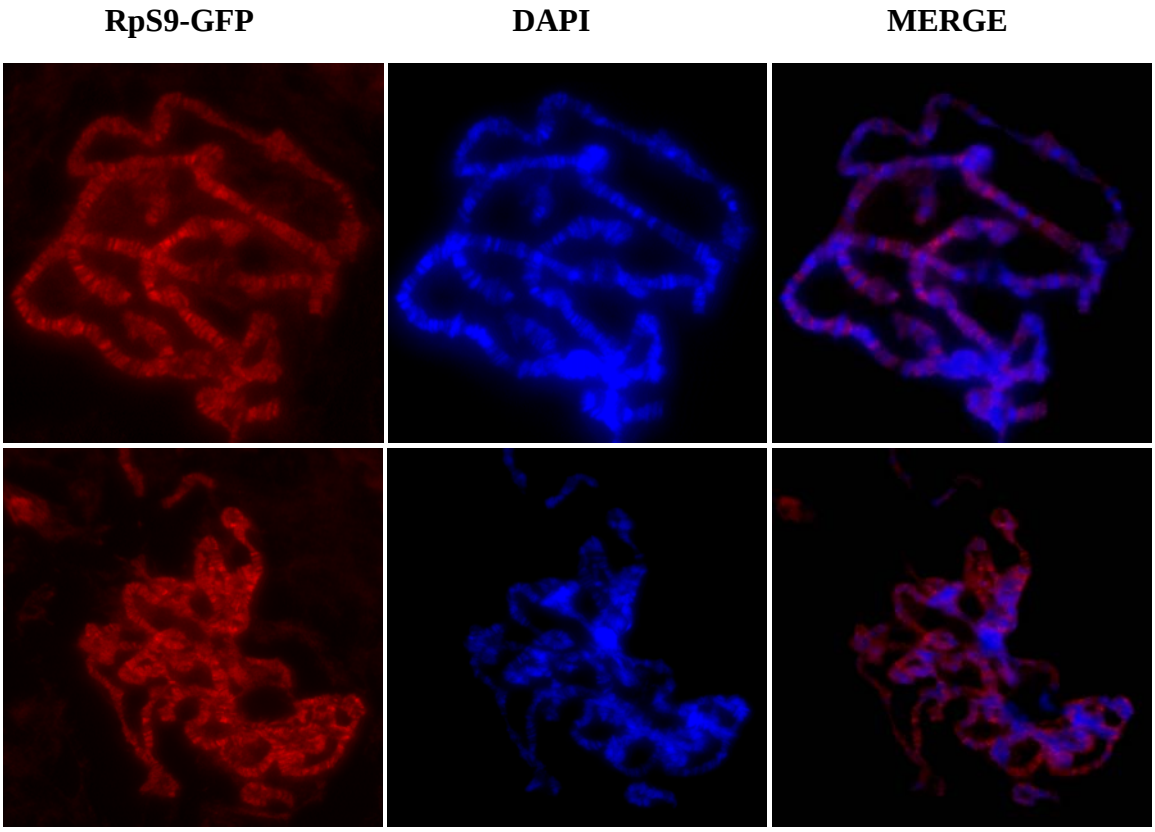


**Figure 4.6 RpS9 is confirmed to be associated with sites of transcription**. Left panels, indirect immunofluorescence using an anti -GFP primary antibody and Cy3 conjugated secondary antibody (red). Middle panels show the DAPI of the DNA (blue filter); and right panels show merge of the pictures on the left. The two rows show two different squashes. Images were taken with a fluorescence microscope, under a 40X objective lens.

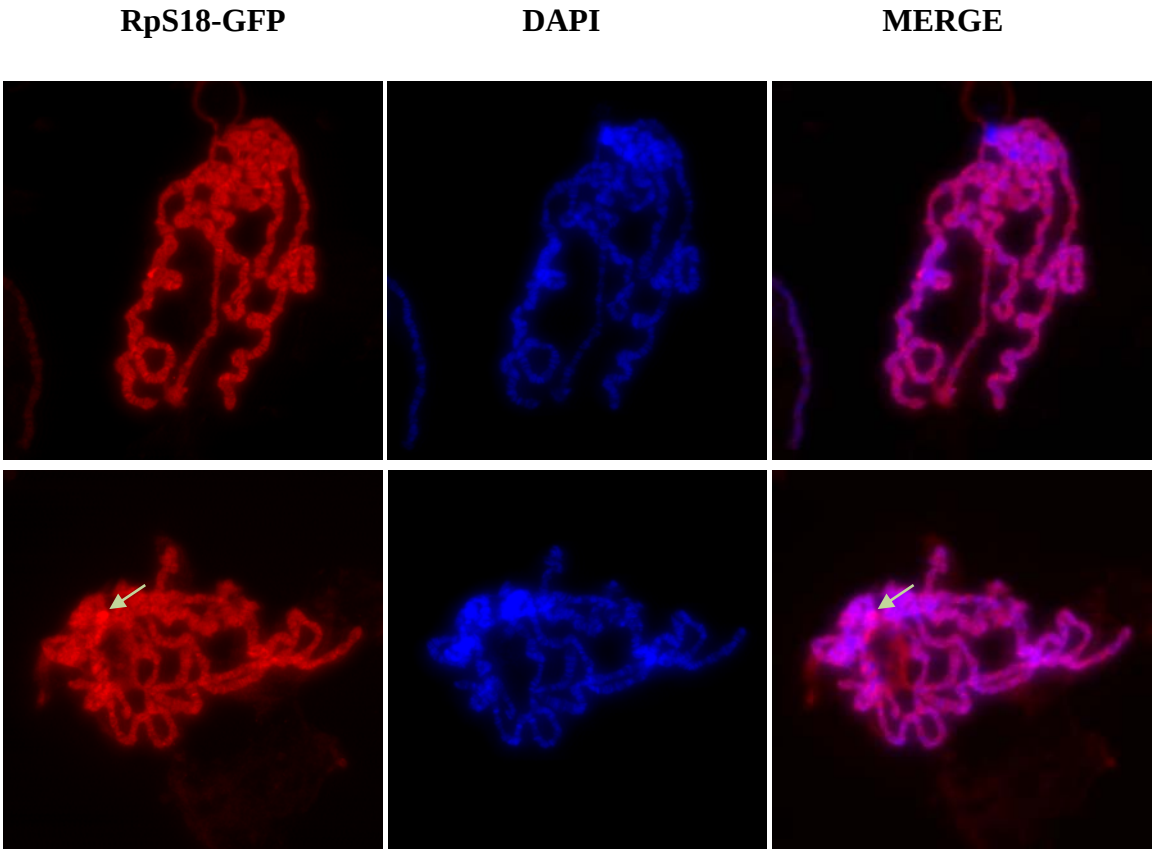


**Figure 4.7 RpS18 is confirmed to be associated with sites of transcription**. Left panels, indirect immunofluorescence using an anti -GFP primary antibody and Cy3 conjugated secondary antibody (red). Middle panels show the DAPI of the DNA (blue filter); and right panels show merge of the pictures on the left. The two rows show two different squashes. The arrows indicate chromosome puffs, and this specific puff is thought to be attributed to the heat shock protein, which has been induced in the salivary glands as a result of the dissection technique. Images were taken with a fluorescence microscope, under a 40X objective lens.

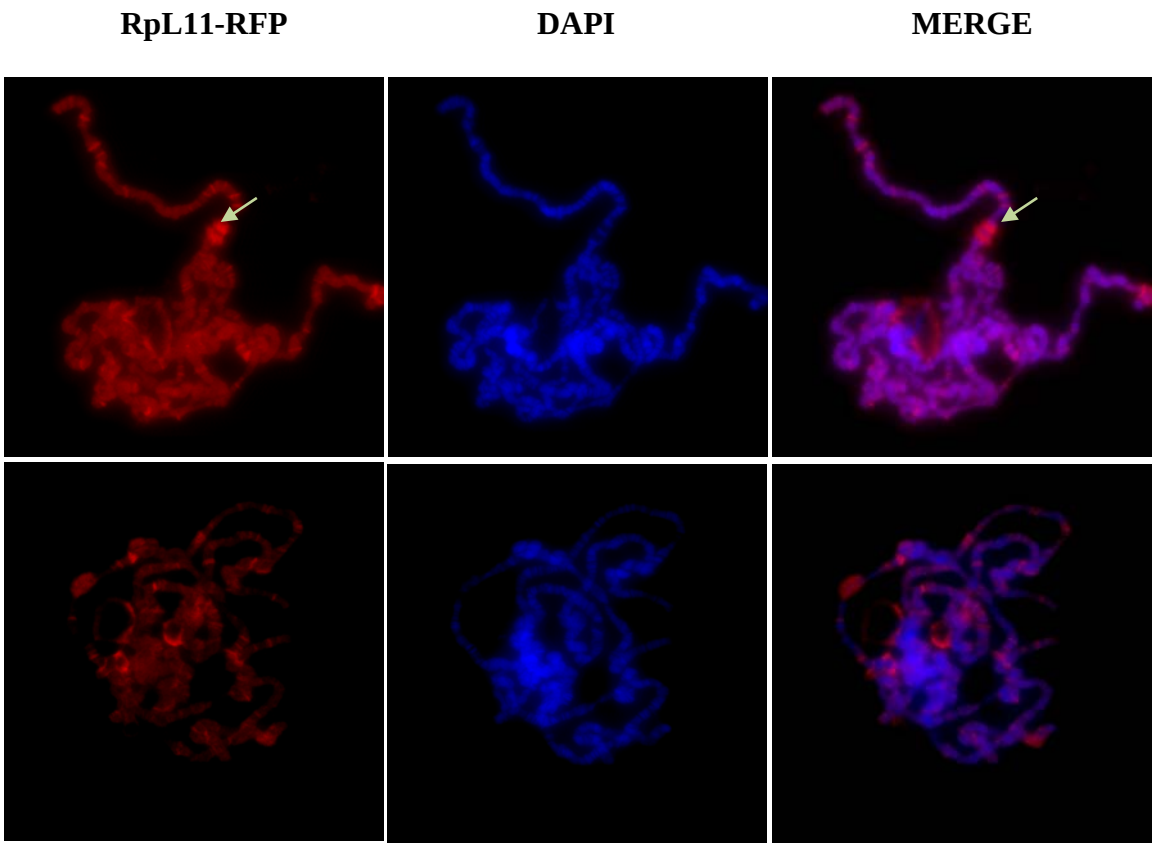


**Figure 4.8 RpL11 is confirmed to be associated with sites of transcription**. Left panels, indirect immunofluorescence using an anti RFP primary antibody and Cy3-conjugated secondary antibody (red). Middle panels show the DAPI of the DNA (blue filter); and right panels show merge of the pictures on the left. The two rows show two different squashes. The arrows indicate chromosome puffs, and this specific puff is thought to be attributed to the heat shock protein, which has been induced in the salivary glands as a result of the dissection technique. Images were taken with a fluorescence microscope, under a 40X objective lens.

The RPs signal corresponds to euchromatin regions of the polytene chromosome (darker region, poorly stained by DAPI). In some nuclei it was apparent that RPs are highly concentrated at heat shock puffs (Figures 4.7 and 4.8). These puffs are regions of the chromosomes that encode heat shock proteins and appear as areas of loosely packed chromatin (Zhimulev et al., 2004). The strong staining at the chromosome puff indicates that the RPs association strongly correlates to transcription activity.

## 4.3 Discussion

In this Chapter, I have provided further evidence that RPs are associated with transcription sites of the polytene chromosomes of *Drosophila*. These results are consistent with the earlier study by Brogna et al. (2002), which indicated the presence of many RPs at these sites. While the earlier study used antibodies directed against endogenous RPs, here I visualized the tagged RPs using antibodies specific for either GFP or RFP. The antibodies are very specific; no cross-reactivity was seen in flies that did not express the RP transgenes (Figure 4.2). I have tested three tagged RPs: RpS9-GFP, RpS18-GFP, and RpL11-RFP. These are the same RPs that I previously assayed in S2 cells and that appeared to be incorporated in functional ribosomes (Chapter 3). Here, I show that these RPs clearly associate with interbands (euchromatic regions). At this stage of the project, the issue was whether the RPs we detected at the sites of transcription are actually part of complete ribosome subunits. While, as suggested by previous studies, the presence of RPs might indicate the presence of a ribosome at these sites (see Introduction above), the RPs could be detached from rRNA; the chromosome association might be due to some non-ribosomal function of these RPs. As reviewed in the Introduction (Chapter 1) several ribosomal proteins are known to have extra-ribosomal functions, for instance, having a role in apoptosis, DNA repair and transcription. Out of the RPs I have analyzed here, only for RpL11 is there evidence that the protein has extra-ribosomal functions (Warner and McIntosh, 2009). It is even possible that the association with the chromatin is an artefact of over-expression. In fact, a recent study has suggested that even endogenous RPs are produced in excess and that those that fail to be incorporated into ribosomes accumulate in the nucleus, where they are subject to

proteosome degradation (Lam et al., 2007). In order to further investigate the issue of whether ribosomal subunits are present at these sites; during my PhD I developed a system to visualize the interaction of ribosomal subunits in cells and this work is discussed in the next Chapter.

# Chapter 5. Ribosomal subunit interaction at sub-cellular sites

## 5.1 Introduction

The data presented in Chapter 4 clearly indicate that many RPs can associate with transcription sites. These observations are consistent with the view that ribosomal subunits may be present at these sites (Brogna et al., 2002). These data alone, however, do not distinguish whether the presence of these proteins reflects the presence of ribosome subunits or instead if there is a non-ribosomal function of these proteins at these sites (Schroder and Moore, 2005). The 60S and 40S ribosome subunits are mostly assembled in the nucleolus but mRNA binding and 80S formation are believed to occur only in the cytoplasm during translation (Zemp and Kutay, 2007). To investigate the issue of whether ribosome subunits interact in the nucleus, I have developed an imaging procedure to visualize ribosome subunit interaction in cells.

To track ribosome subunit association, we have tagged ribosomal proteins located near the interface of the subunits, with bimolecular fluorescence complementation (BiFC) fragments, which are expected to fold into a functional fluorescent protein upon association of the ribosome subunits. BiFC relies on the reconstitution of a fluorescent YFP protein by the association of two non-fluorescent YFP half-molecules; typically the two non-fluorescent fragments complement only when they are individually linked to interacting proteins (Hu et al., 2002).

## 5.2 Results

### 5.2.1 Generation of constructs expressing combinations of BiFC-tagged RPs

Initially, the aim was to generate constructs expressing BiFC-tagged versions of RpL11 and RpS18, which, based on the available structures of yeast 80S and bacterial 70S ribosomes are expected to interact upon ribosomal subunit joining (Figure 5.1) (Chandramouli et al., 2008; Spahn et al., 2001; Yusupov et al., 2001). First, I generated constructs expressing RpL11 fused to the C-terminal half of EYFP (YC), corresponding to residues 155–238, and RpS18 fused to the N-terminal half of EYFP (YN), corresponding to residues 1 -154 (see Material and Methods). The EYFP fragments were fused either to the N- or C-terminaus of the ribosomal proteins (Figure 5.2). These fusion constructs were cloned into the standard *Drosophila* pUAST vector, which contains a UAS promoter that can be activated by co-expressing the yeast transcription factor Gal4 in the same cell (see Materials and Methods). In addition to RpL11 and RpS18, I tagged RpS15 with YN, which based on the available structures is adjacent to RpS18 on the 40S (Figure 5.1) (Chandramouli et al., 2008; Spahn et al., 2001). I reasoned that this would increase the chance of finding an efficient BiFC pair. In addition, I tagged RpS9 with YN, which is located away from the interaction surface (Figure 5.1); RpS9 was expected to work as a negative control and not to yield BiFC complementation. In all of the constructs, the two coding regions were connected by a linker encoding the peptide sequence RSIAT (for the YN fusions) or KQKVMNH (for the YC fusions) (Figure 5.2). These linkers are expected to allow flixable mobility of the BiFC fragments after fused proteins forming complex (Hiatt et al., 2008) (for more details see Materials and Methods).

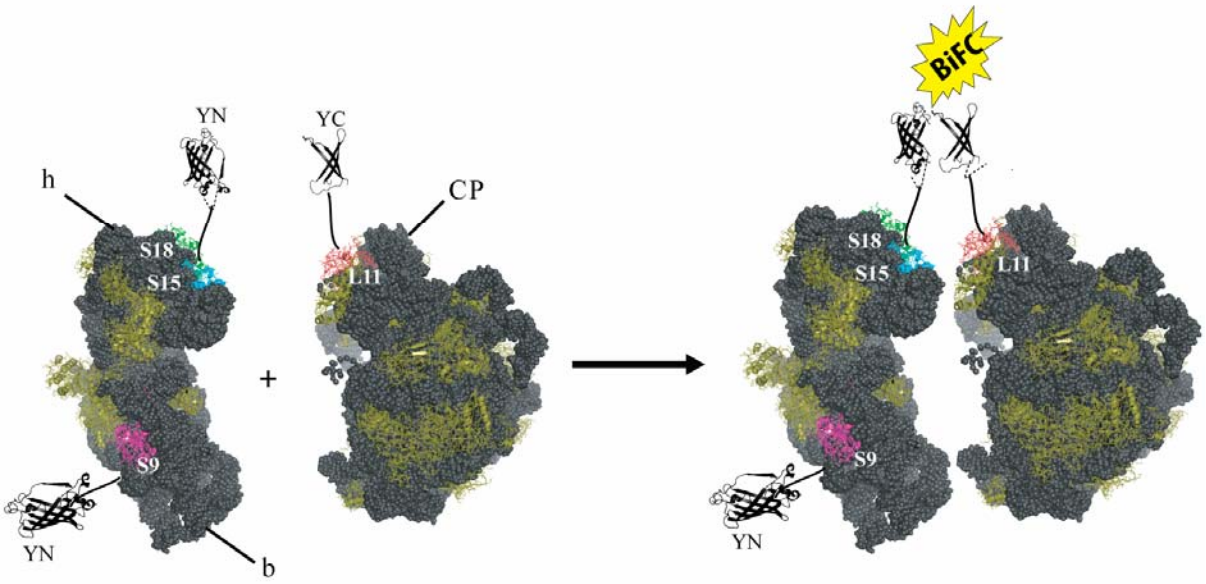


**Figure 5.1 Schemating of the BiFC ribosomal subunits interaction technique**. Structures of the yeast 40S and 60S subunits are shown with a cartoon of the BiFC tagged RPs. The YN fragment was fused to RpS18 and RpS15, located on the head (h) of the 40S, and to RpS9 on the body (b) of the subunit. The YC fragment was fused to RpL11, located on the central protuberance (CP) of the 60S subunits. Interaction of the ribosomal subunits puts RpS18 ,RpS15 and RpL11 in direct contact and would bring the YC and YN fragments into close proximity, allowing reconstitution of an intact fluorescent protein YFP (illustrated on the right). The structures were generated with Pymol using the following structural data files, 1K5X and 1K5Y. Deposited in the RCSB Protein Data Bank (Spahn et al., 2001).

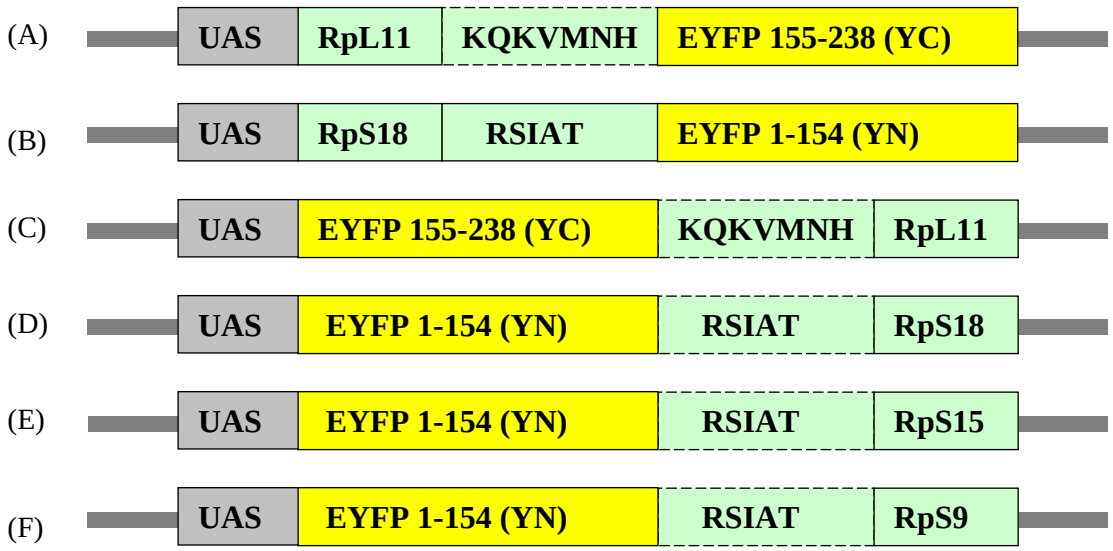


**Figure 5.2 Schematic of the constructs expressing BiFC-tagged RPs.**

(A) and ( C) show RpL11 fused with YC fragment of EYFP, at either the C or N terminus; (B) and (D) show RpS18 fused with YN fragment of EYFP at either the C or N terminal ends, ; (E) and (F) show RpS15and RpS9 fused with YN at their N terminus. The vector backbone is pUAST (see Materials and Methods).

### 5.2.2. Visualization of ribosome subunit interaction in *Drosophila* S2 cells

After generating the different BiFC constructs with different orientations (Figure 5.2), I transfected these plasmids (together with a Gal4 expressing plasmid) into S2 cells to find out which pair yields the most intense BiFC signal. The best complementation was observed between RpL11 and RpS18 with the YC and YN fragments fused to their respective C-terminals (pUAS-RpS18-YN and pUAS-RpL11-YC) (Figure 5.3). The YFP signal was localized mostly in the cytoplasm in about 90% of the transfected cells, while in about 10% of the cells, I detected clear YFP fluorescence also in the nucleolus (Figure 5.3 C and D). In addition to the optimal pUAS-RpS18-YN and pUAS-RpL11-YC pair, a clear YFP signal in cytoplasm was seen when S2 cells were cotransfected with pUAS-RpS18-YN and pUAS-Rp-YC-L11 (Figure 5.4 A). Out of the other combinations tested (see Figure 5.2), I observed a clear cytoplasmic BiFC fluorescence when cells were cotransfected with the following pairs: pUAS-YN-RpS18 and pUAS-YC-RpL11 (Figure5.4B), pUAS-YN-RpS18 and pUAS–RpL11-YC (Figure 5.4C), pUAS-YN-RpS15 and pUAS-YC-RpL11 (Figure 5.4D). The BiFC signal was undetectable when S2 cells were cotransfected with pUAS-YN-RpS15 and pUAS-RpL11-YC (Figure 5.4 E). Additionally, I found no YFP signal in the cytoplasm of cells transfected with YN-RpS9 and RpL11-YC or YN-RpS9 and YC-RpL11. However, this combination of proteins produced a strong signal in the nucleolus (Figure 5.4 F and 5.4 G).

To test whether the BiFC-fusion proteins are well expressed, I assayed their expression by Western blot analysis of total cell extracts. The expected fusion-proteins were produced with all constructs (the proteins were detected with an anti-

GFP antibody; see Materials and Methods). A single band of the right size was detected in cells transfected with the single constructs and thicker band (presumably made of two closely-migrating bands) were seen in cells transfected with both the YN and YC fusion constructs (Figure 5.5). These data demonstrate that the correct proteins are expressed and that these proteins are stable.

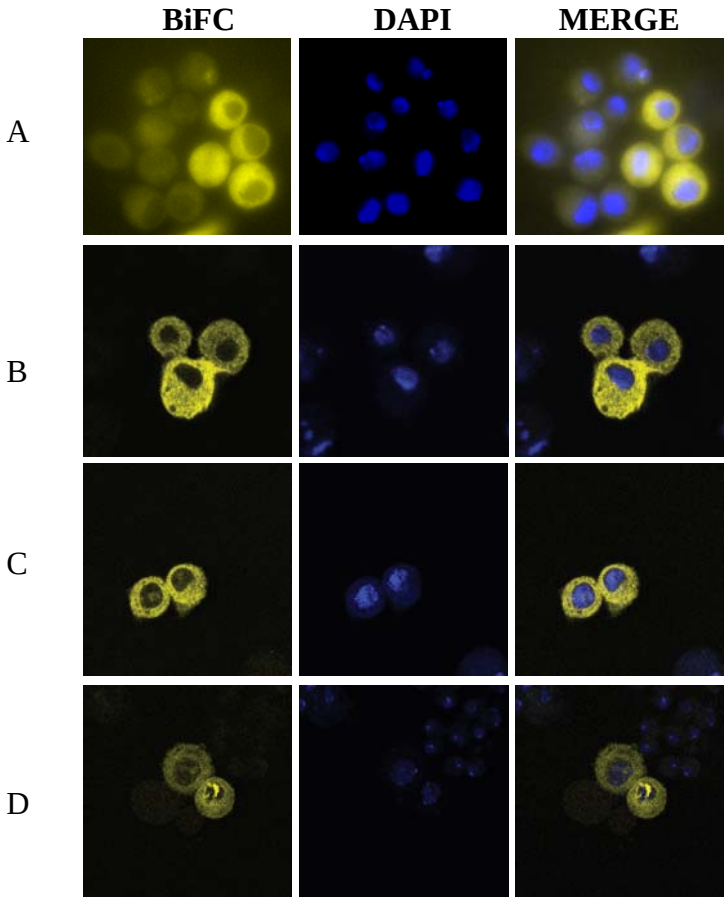


**Figure 5.3 Visualization of the RpS18 and RpL11 interaction using the BiFC assay**. The YFP signal is visulaized in cells expressing RpS18-YN and RpL11-YC. S2 cells were co-transfected with pUAST-RpS18-YN, pUAST-RpL11-YC and p-Act-GAL4. The top two rows (A and B) show examples of cells with the typical cytoplasmic YFP signal. The bottom rows (C and D) show example of cells with the less frequent nucleolar signal (about 10% of the transfected cells). YFP signals are shown on the left, DAPI staining in the middle and the merged image on the right. (A) Epifluorescence imaging using a GFP filter. (B), (C) and (D) confocal microscope images with 40 X oil immersion objective.

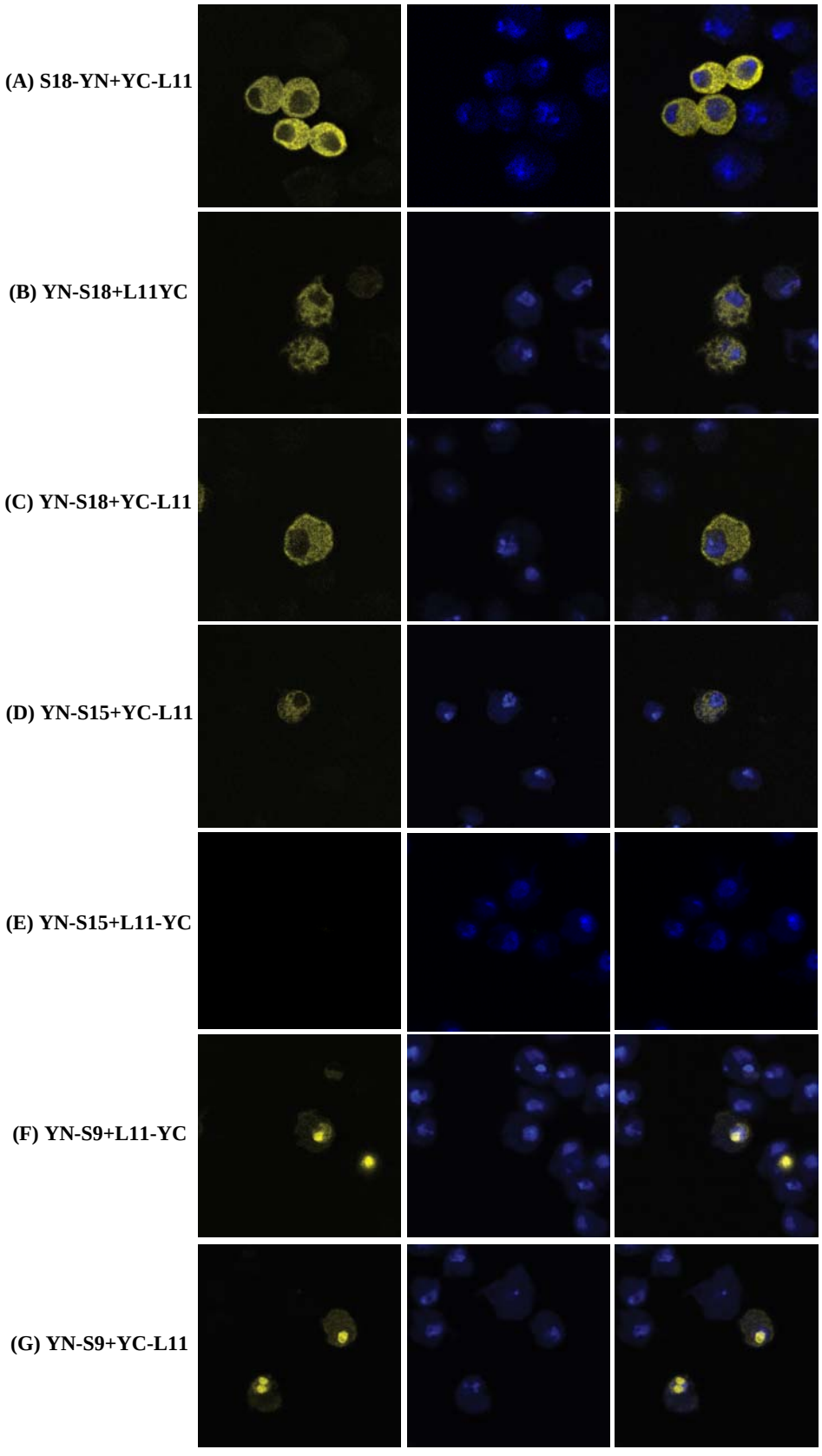
BiFC
DAPI
MERGE
(A) S18-YN+YC-L11
(B) YN-S18+L11YC
(C) YN-S18+YC-L11
(D) YN-S15+YC-L11
(E) YN-S15+L11-YC
(F) YN-S9+L11-YC
(G) YN-S9+YC-L11

**Figure 5.4 Visualization of the interaction between RpS18, RpS15 and RpS9 and RpL11.** Co-expression in S2 cells of different combinations of RPs fused with BiFC fragments with different orientations alongside p-Act-GAL4. BiFC signals are shown on the left, DAPI staining in the middle and the merged image on the right. The YFP signal becomes prominent in the cytoplasm when pUAST- RpS18-YN pairs with pUAST- YC -RpL11 (A) and becomes faint in the cytoplasm when pUAST-YN-RpS18 pairs with pUAST- RpL11-YC (B) or with pUAST- YC-RpL11 (C ).Similar to (C), when pUAST-YN-RpS15 pairs with pUAST- YC-RpL11, a weak YFP signal is observed in the cytoplasm ,and this becomes undetectable when paired with pUAST- RpL11-YC (D). The YFP signal is mostly in the nucleolus in cells expressing pUAST- YN RpS9 and pUAST- RpL11-YC (F) or pUAST- YN RpS9 and pUAST- YC -RpL11 (G). The images were taken with a confocal microscope with 40 X oil immersion objective

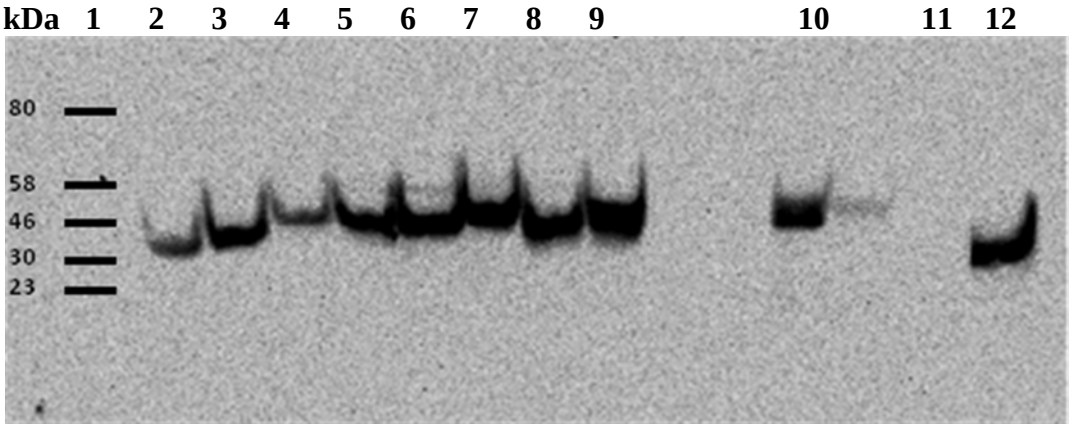


**Figure 5.5 The BiFC-tagged RPs are well expressed in S2 cells**.

Western blot of cell extracts from cells transfected with the constructs indicated. The fusion proteins were detected with a primary antibody against GFP. Protein ladder (lane 1); YC-RpL11 and RpL11-YC (lanes 2-3), expected size 31.7 kDa; YN-RpS18 and RpS18-YN (lanes 4- 5) ,expected size 35.8 kDa; YN-RpS15 (lane 6), expected size 35 kDa; YN-RpS9 (lane 7), expected size 40.5 kDa, YN-RpS15 + RpL11-YC (lane 8); YN-RpS9 + RpL11-YC (lane 9); RpS18-YN + RpL11-YC (lane 10); untransfected S2 cells (lane 11) as a negative control; EGFP (lane 12) ,expected size 27 kDa.

Transfection efficiency was low (~ 10%); this is probably due to the need to have three plasmids co-transfected for expression of the reporters (pUAST-RpS18-YN, pUAST-RpL11-YC and pBS-Act-GAL4). As expected, no BiFC signal was produced if any one of the three constructs was omitted, suggesting that the YFP signals we observe are specific and originate from the expected interaction between the BiFC fragments (Figure 5.6 B-D).

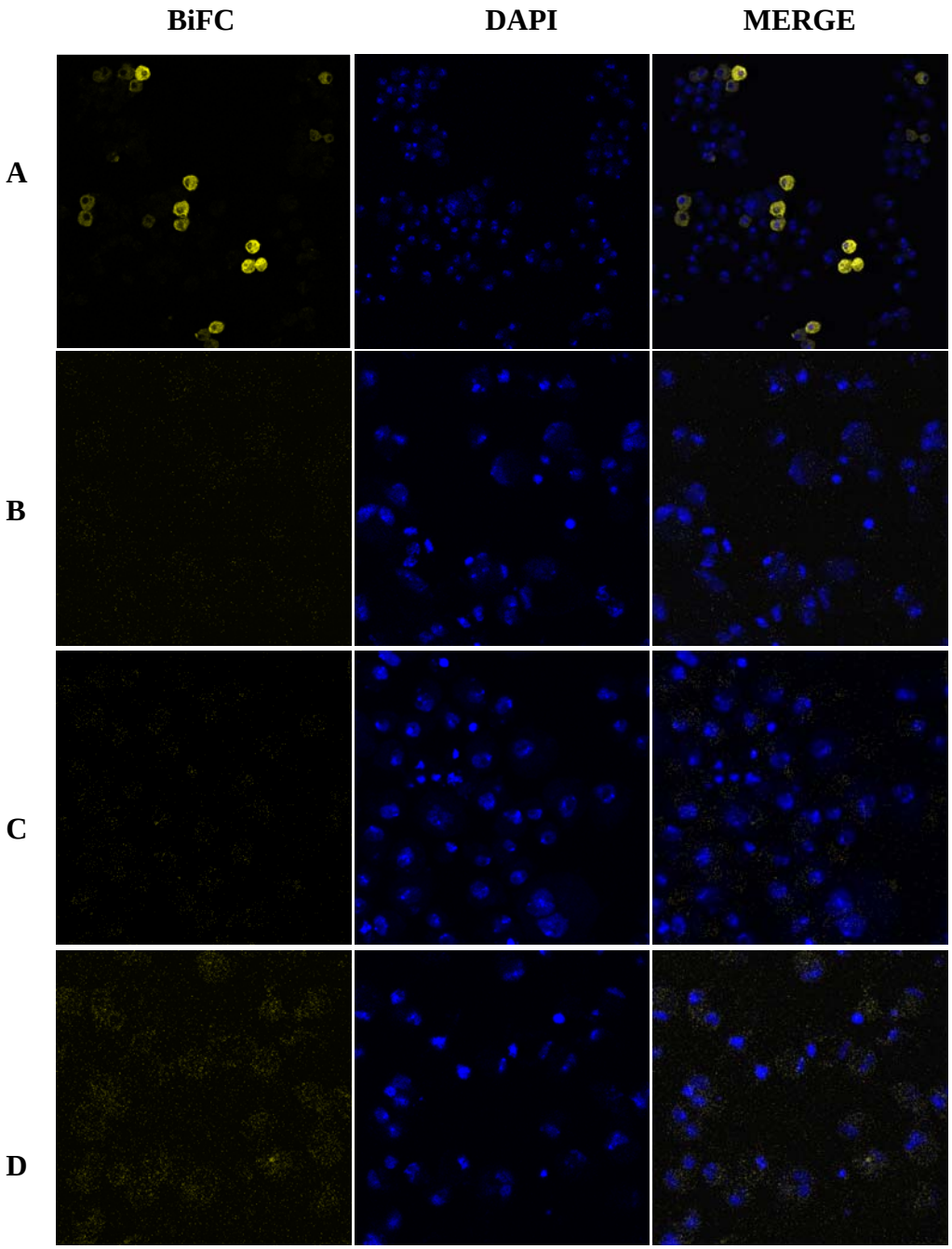


**Figure 5.6 YFP fluorescence is produced only in cells expressing both BiFC fragments**. (A) Imaging of YFP in S2 cells cotransfected with RpS18YN, RpL11YC and the Gal4 expressing plasmid. (B-D) No YFP fluorescence was observed in cells transfected without one of the three plasmids :( B) No RpL11-YC, (C) No RpS18-YN and (D) No Gal4. YFP imaging is shown on the left, DAPI staining in the middle and the merged image on the right. The images were taken with the confocal microscope with a 20 X objective.

#### 5.2.2.1 BiFC tagged RPs are incorporated into functional ribosomes

After having established that RpS18-YN and RpL11-YC is the pair which gives the most intense BiFC complementation (Figure 5.3), I verify that these tagged RPs are in fact incorporated into functional 40S and 60S subunits. Given that GFP tagged versions of these two RPs can be incorporated into functional ribosomes (see Chapter 3), it was expected that tagging with the smaller YN and YC peptides should also not prevent ribosome incorporation.

As previously observed with the GFP tagged proteins, we found that both RpS18-YN and RpL11-YC are present in polysome fractions (Figure 5.7). The Western blot analysis showed single bands of the expected size (RpS18-YN being 35.8 kDa and RpL11-YC 31.7 kDa) and two bands of the correct size when cotransfected with both BiFC constructs. These data indicate that RpL11-YC and RpS18-YN are functional and are efficiently incorporated into functional ribosomes.

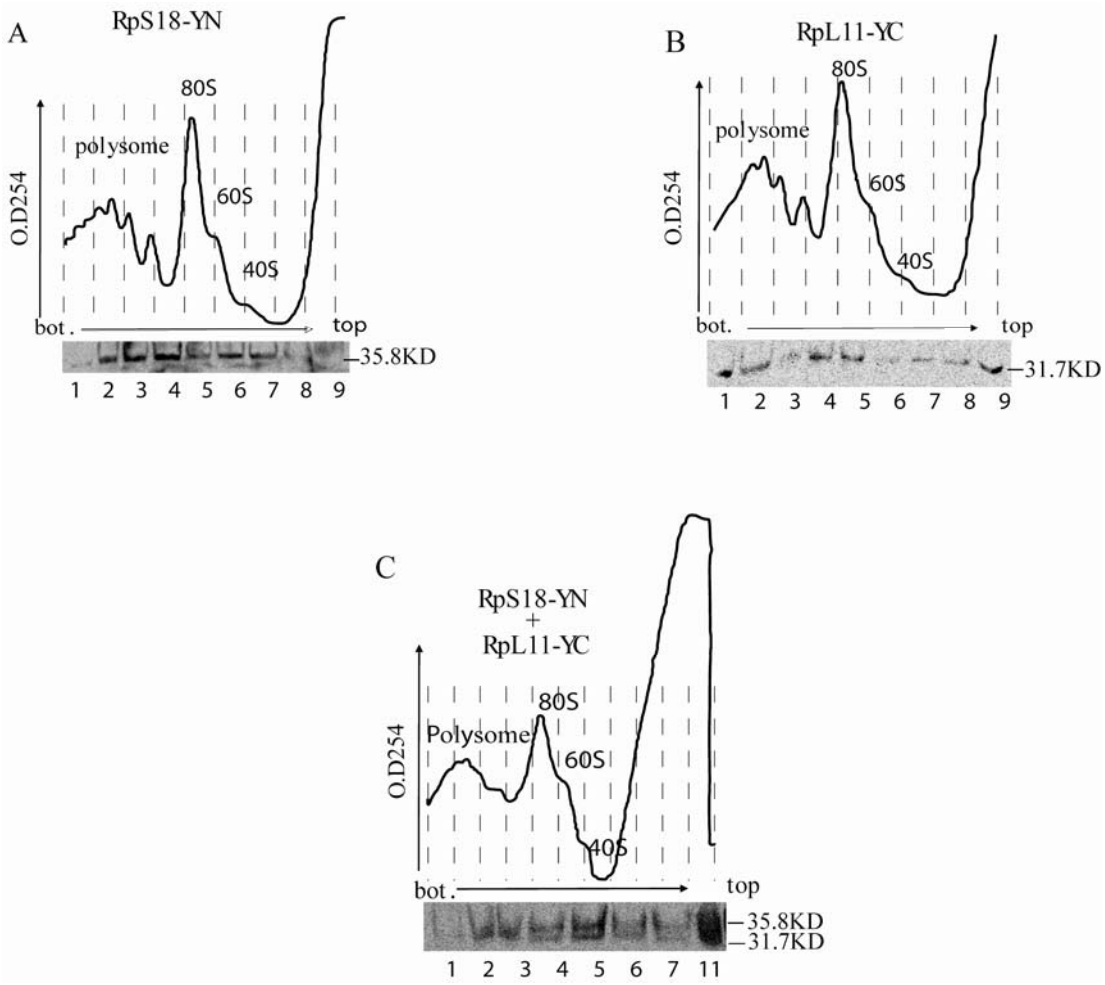


**Figure 5.7 Polysome analysis of S2 cells expressing BiFC-tagged RpS18 and RpL11**. The top portion of each panel shows the OD254 profile of the sucrose gradient (10-50%) fractionation of the total cell extract from cells transfected with the constructs indicated. The bottom portion of each panel shows the result of Western blotting with anti-GFP. (A) Polysome analysis of S2 cells transfected with RpS18-YN; (B) Polysome analysis of S2 cells transfected with RpL11-YC; (C) Polysome analysis of S2 cells cotransfected with RpL11-YC and RpS18-YN. (This experiment was done with technical assistence of Preethi Ramanathan)

Although a number of studies have confirmed that BiFC is primarily driven by the association of interacting proteins, it was also reported that, if expressed at a sufficiently high level, the YN and YC peptides can complement even when they are fused to proteins not normally interact with each other(Kerppola, 2008). To assess whether the BiFC signal we have detected is an artefact of over-expression, we analysed the expression and subcellular distribution of the BiFC tagged RPs by immunostaining of transfected cells; this was done with either a monoclonal antibody specific for the YC fragment or a polyclonal antibody that recognises both YC and YN. The assay revealed that both RpS18-YN and RpL11-YC are present throughout the cell and are particularly concentrated in the nucleus (Figure 5.8). The monoclonal antibody is specific for the YC peptide so there was no staining in cells expressing only RpS18-YN - the immunogenic epitope is in the YC fragment. The sub-cellular distribution of the BiFC-tagged RPs is similar to that of GFP alone, which shows an intense nuclear signal (Figure 5.8 F). In conclusion, I have found that the BiFC-tagged RPs are mostly concentrated in the nucleoplasm. Instead, the BiFC signal is most intense in the cytoplasm and almost absent in the nucleoplasm. Therefore, these results indicate that the YFP fluorescence detected in the cytoplasm is not likely to be an artefact of over-expression and suggests it is the result of ribosomal subunit interaction. In addition, Cells were transfected with BiFC constructs that express only the free YN and YC peptides and found that most cells had only a weak signal in the nucleoplasm; some cells showed a very weak cytoplasmic signal but this was much dimmer than the signal seen in cells expressing the RpS18-YN and RpL11-YC pair (Figure5.9, compare panels A and B with C). In addition, while in some cells transfected with the RpS18-YN and RpL11-YC pair, we detected a clear nucleolus

signal, none of the cells transfected with the free YN and YC pair produced a nucleolar signal (Figure 5.9). This amplies that the BiFC signal in the nucleolus seems not to be an artefact of over-expression or of the non-specific association between BiFC fragments , as mentioned above, the nucleolus BiFC has been observed in less than 10% of S2 cells transfected with the RpS18-YN and RpL11-YC pair (Figure 5.3 C-D) but becomes more prominent when S2 cell are transfected with YN- RpS9 and RpL11-YC or YC-RpL11 (Figure 5.4 F-G). The nucleolus is a non-membrane bound structure and it is not a stable component of cells and can exist only in certain stages of cell live during the cell cycle (Cmarko et al., 2008). This may explain the low frequency of the BiFC signal in the nucleolus compared with the cytoplasmic signal. The signal in the nucleolus is more difficult to explain as the spatial and temporal organisation of the early stage of ribosome biogenesis(90S preribosome) are still largely unknown (Perez-Fernandez et al., 2007).

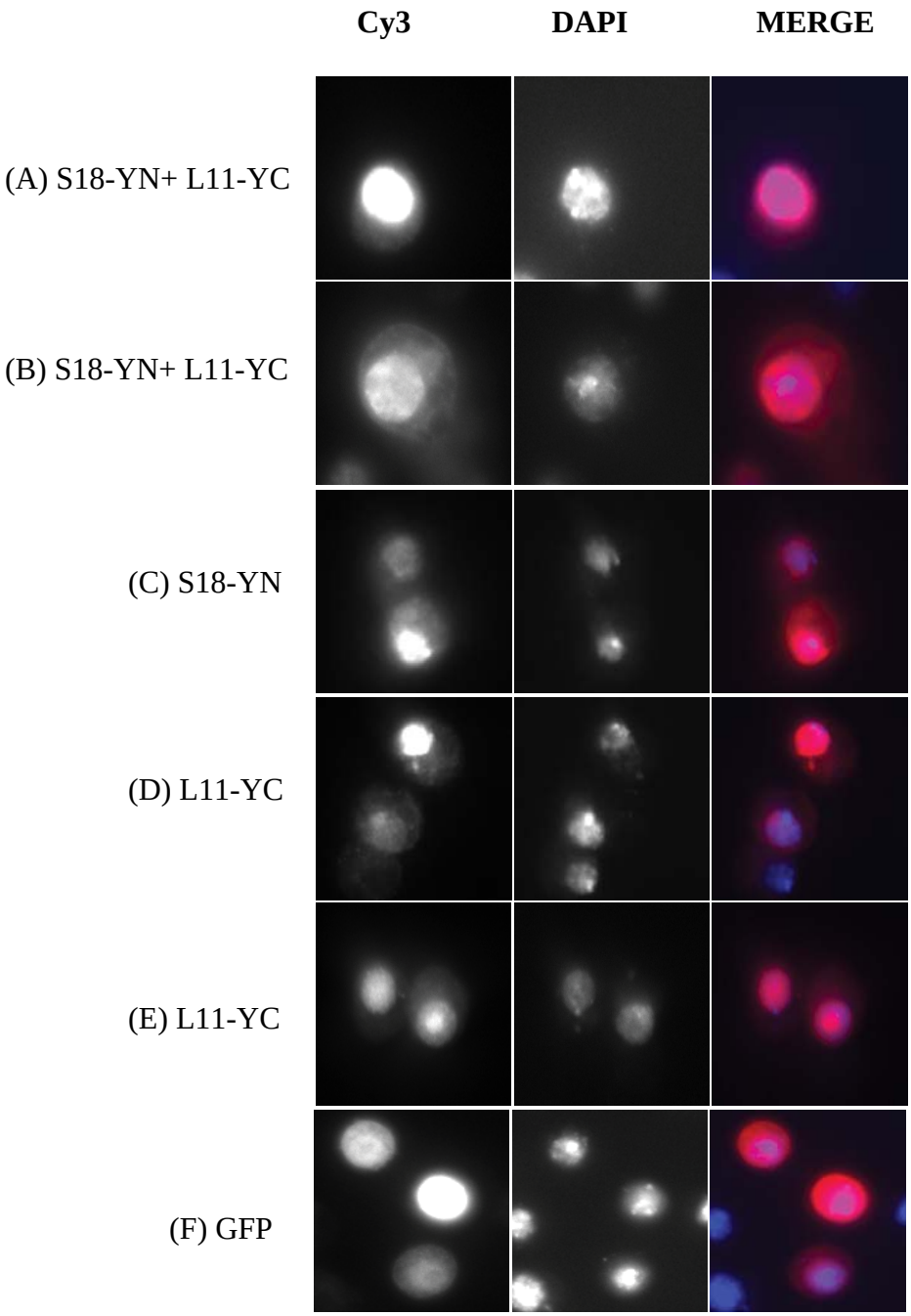
Cy3
DAPI
MERGE
(A) S18-YN+ L11-YC
(B) S18-YN+ L11-YC
(C) S18-YN
(D) L11-YC
(E) L11-YC
(F) GFP

**Figure 5.8 Sub-cellular distribution of BiFC-tagged RPs.** Immunostaining of cells transfected with the constructs indicated, using a polyclonal antibody against YFP and a monoclonal against the YC fragment. The primary antibody was detected with a Cy3 conjugated secondary antibody. (A) and (B) pUAST-RpS18.YN + pUAST RpL11.YC detected with the polyclonal or monoclonal antibody against YFP respectively. (C) and (D) pUAST-RpS18.YN and pUAST RpL11.YC respectively detected with the polyclonal antibody against YFP .(E) pUAST RpL11.YC detected with monoclonal antibody against YFP. (F) GFP only as a positive control. Cy3signals are shown on the left, DAPI staining in the middle and the merged image on the right. The images were taken with a confocal microscope with 40 X oil immersion objective.

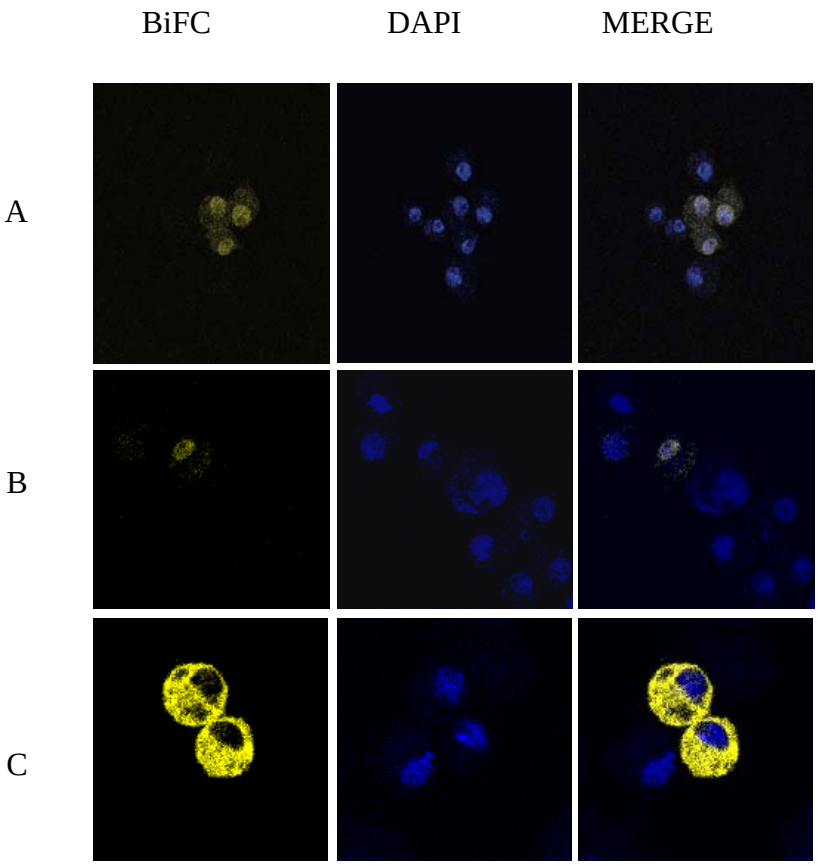


**Figure 5.9 Sub-cellular distribution of unfused BiFC fragments.** (A) and (B) confocal microscope imaging of YFP fluorescence in cells co-transfected with constructs expressing pUAST- YN and pUAST-YC along with the GAL4 driver where the YFP signal was very weak in nucleoplasm. (C) confocal microscope imaging of YFP fluorescence in cells transfected with pUAST-RpS18-YN and pUAST-RpL11-YC using the same driver (Gal4) .BiFC signals are shown on the left, DAPI staining in the middle and the merged image on the right. The images were taken with a confocal microscope with 40 X oil immersion objective

#### 5.2.2.2 Translation inhibition affects the RP-dependent BiFC signal

To test whether the BiFC signal is genuinely due to the joining of ribosome subunits during translation, I assessed whether the intensity of the YFP signal and its subcellular distribution is affected by well known drugs that affect translation. I treated the transfected cells with three protein synthesis inhibitors that have different mechanisms of action: cycloheximide (CHX), puromycin, and emetine (EME). Cells were treated with different concentrations of the inhibitors and for different lengths of time. I found that cycloheximide and puromycin were highly toxic; upon adding the drugs, the cells rapidly detached from the cover slip and could not be analysed. However, upon treatment with emetine at 20μg/ml, the cells were still alive and stayed attached to the coverslip so it was possible to investigate the effect of this drug. I found that cells treated with emetine, 12h before fixation, showed a clear change in the pattern of YFP signal: the cytoplasmic signal was more intense than in untreated cells and the nucleolar signal was apparent in most cells (Figure 5.10 A) .While in untreated samples only about 10% of cells show fluorescence in the nucleolus, in the sample treated with emetine most cells show a very intense nucleolar YFP fluorescence. Emetine inhibits translation elongation, prevents ribosome polysome breakdown and increases ribosome density on the mRNA yielding larger polysomes (Grollman, 1968). The increase in BiFC fluorescence and the patchy pattern might be due to emetine keeping the ribosome subunits joined and to an increase in the focal concentration of ribosomes. The increase in the signal in the nucleolus is more difficult to explain, but it suggests that ribosome subunits can interact in the

nucleolus. Alternatively, emetine might also bind the 90S subunit, perhaps stabilizing an interaction between nascent pre-40S and 60S particles.

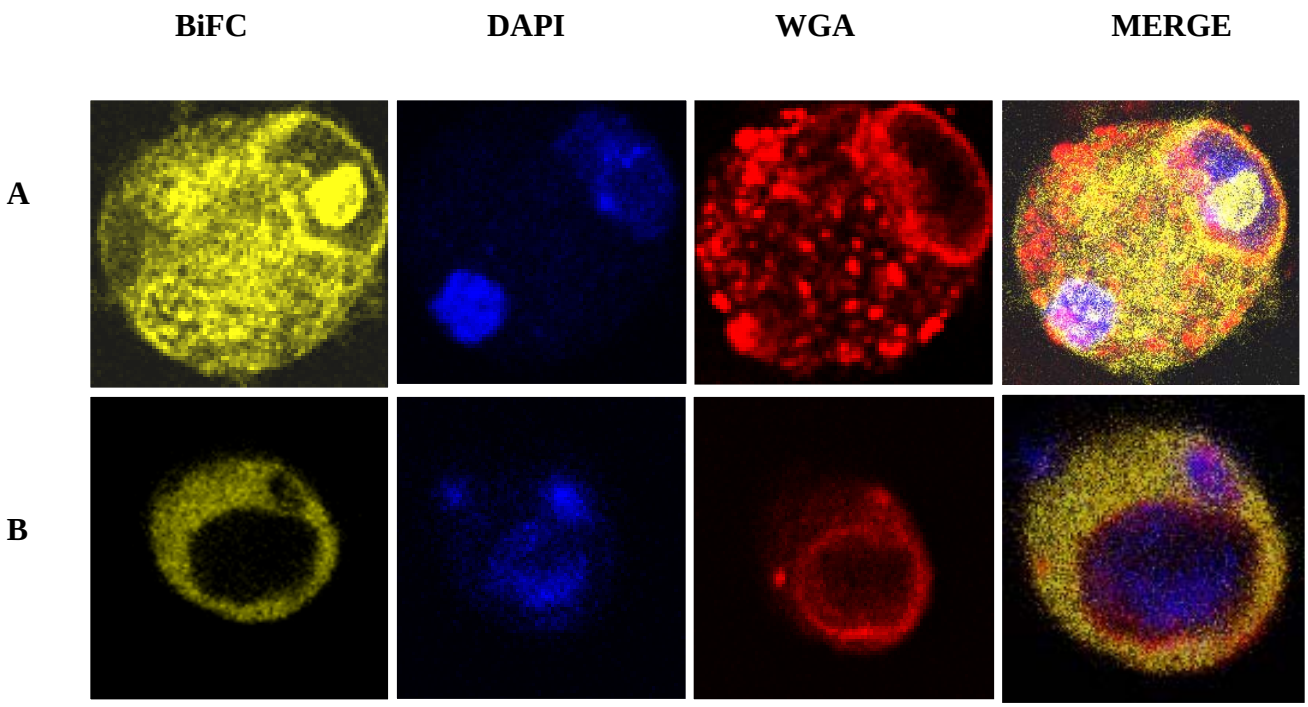


**Figure 5.10 Emetine treatment affects the intracellular localization of the BiFC signal**. (A) and (B) confocal microscope imaging of YFP fluorescence in cells co-transfected with constructs expressing pUAST-RpS18-YN, pUAST-RpL11-YC and pBS-Act-GAL4 .In (A) S2 cells were treated with 20 µg/ml emetine 12h before cell fixation and showed a clear change in the pattern of the YFP signal: the cytoplasmic signal was more intense than in untreated cells (B) and the nucleolar signal become more apparent and intense.The panels on the left show BiFC signals ,the panels in the second column show DAPI staining, the panels in the third column show wheat germ agglutinin (WGA) staining, and the panels on the right show merged pictures. The images were taken with a confocal microscope with 40 X oil immersion objective

#### 5.2.2.3 Inhibition of ribosome export enhances the interaction of RPs in the nucleus

Ribosomal subunits are synthesized and assembled in the nucleolus, but it is believed that they do not interact until export to the cytoplasm. The export of ribosomal subunits can be inhibited by Leptomycin B (LMB). This drug inhibits nuclear export by covalently binding to a cysteine residue in the central region of Crm1 (exportin1), which is the major receptor for the export of proteins out of the nucleus (Hutten and Kehlenbach, 2007; Kudo et al., 1999). Our observation indicates that ribosome subunits might interact in the nucleolus, therefore, I reasoned that it might be possible to force the subunits to interact in the nucleus by blocking nuclear export so increasing the nuclear pool of ribosomal subunits. Following 5 hours of treatment with LMB, I found that most of the transfected cells (more than 80%) showed a clear signal inside the nucleus, with apparent accumulation around the nuclear periphery (Figure5.11). Therefore, it is likely that ribosomal subunits are competent to interact in the nucleus, but normally do not because they are rapidly exported. This observation further indicates that the BiFC signal originates from ribosomal subunits interaction and not from the interaction of free RPs

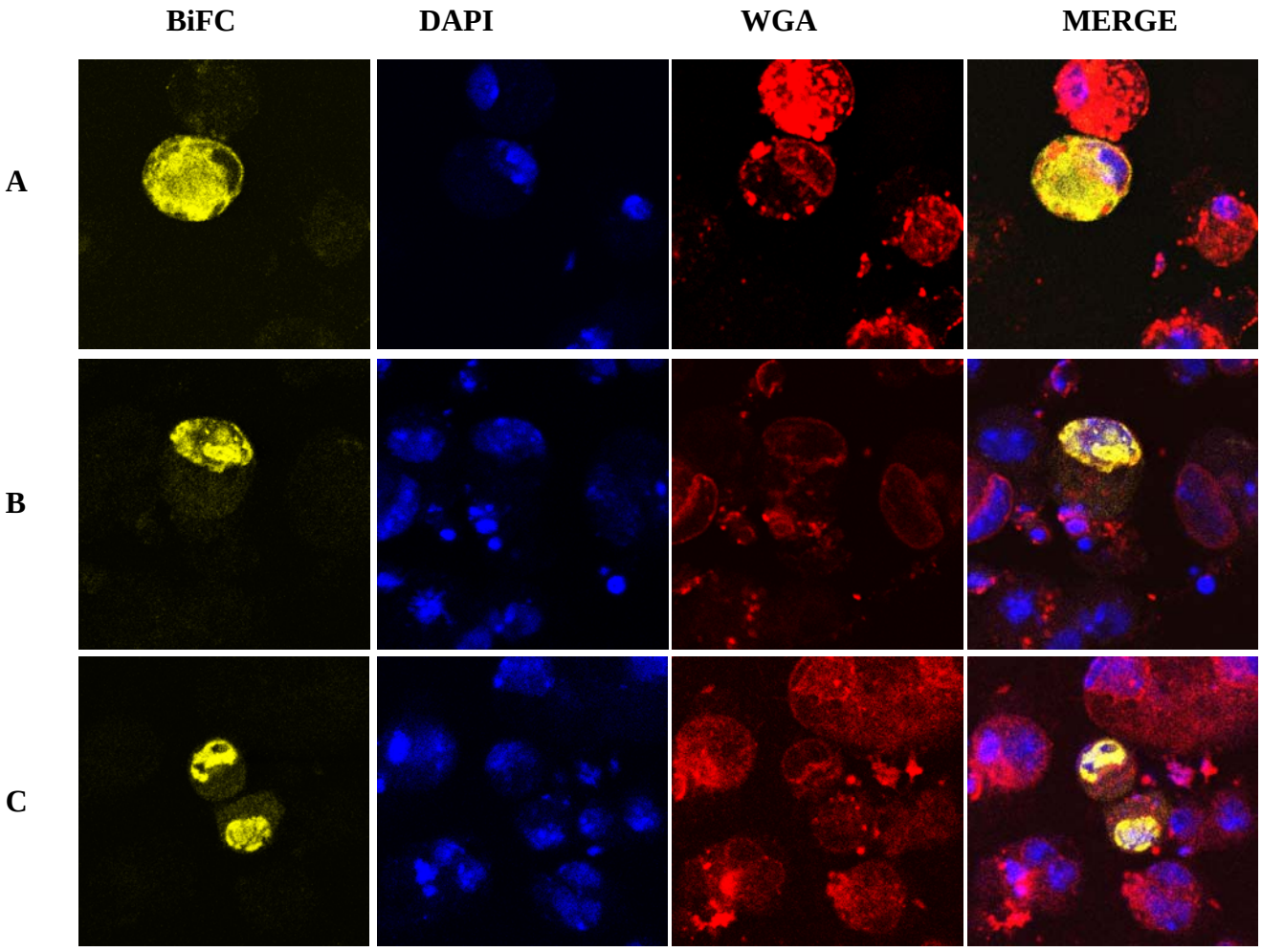


**Figure 5.11 Leptomycin B (LMB) affects the intracellular localization of the BiFC signal**. Confocal microscope imaging of YFP fluorescence in cells co-transfected with constructs expressing pUAST-RpS18-YN, pUAST-RpL11-YC and pBS-Act-GAL4. (A) shows the cytoplasmic YFP signal in untreated S2 cells as a positive control; the YFP signal is restricted inside the nucleus, with apparent accumulation around the nuclear periphery when the S2 cells are treated with Leptomycin B (LMB). (B) and (C) BiFC fluorescence in S2 cells treated with 50 nM and 100 nM LMB respectively 5h before cell fixation. The panels on the left show BiFC signals, the panels in the second column show DAPI staining, the panels in the third column show WGA staining, and the panels on the right show merged pictures. The images were taken with a confocal microscope with 40 × oil immersion objective

### 5.2.3 Visualization of ribosome subunit interaction in transgenic flies expressing BiFC-tagged ribosomal proteins

As the BiFC method I have developed was successful in S2 cells, I was interested to investigate whether the same method could be applied in flies. In particular, I was interested to know whether the ribosome subunits can interact in the nucleolus in flies and whether this interaction occurs only in a subset of cell types or if it is a general feature of all cell types. I also expected that, in flies, such a method would allow the study of ribosome subunit interactions in a more physiological context and also to investigate how the interaction is affected by mutant genetic backgrounds. In addition, such a technique would allow tracking of ribosome subunit interaction in highly polarized cells such as neurons, in which translation of some mRNAs is believed to be restricted to synapses and to be dependent on neuronal activity (Alvarez et al., 2000).

To test whether the technique worked in flies, I generated transgenic flies carrying UAS constructs expressing RpS18-YN and RpL11-YC (the pair that worked better in S2 cells). I then crossed the two individual transgenic strains and generated a double insert line expressing both RpS18-YN and RpL11-YC.

Transgenic flies were generated by standard P element-mediated germ line transformation (see Materials and Methods). Single-insert lines of the constructs pUAS-RpS18-YN and pUAS-RpL11-YC were established on the X, 2$^{nd}$, and 3$^{rd}$ chromosomes (Appendix III, table 5). Strains carrying both transgenes were generated by crossing the *P[W$^{+}$=UAS-RpS18:YN]*(K4.M2) transgene on the 2$^{nd}$ chromosome with the *P[W$^{+}$=UAS-RpL11-YC]*(K5.M4) on the 3$^{rd}$ chromosome using standard genetics protocols: first I crossed each transgenic line with a double balancer strain to

mark the second and third chromosomes, then I screened for flies carrying both transgenes by scoring for the absence of the balancers' dominant markers (Figure 5.12). The presence of both constructs was verified by single-fly PCR using primers specific for either the YN or YC fragments (Figure 5.13): bands of the size expected for the RPs tagged with YN and YC fragments can be seen in the recombinant flies carrying the correct transgenes.

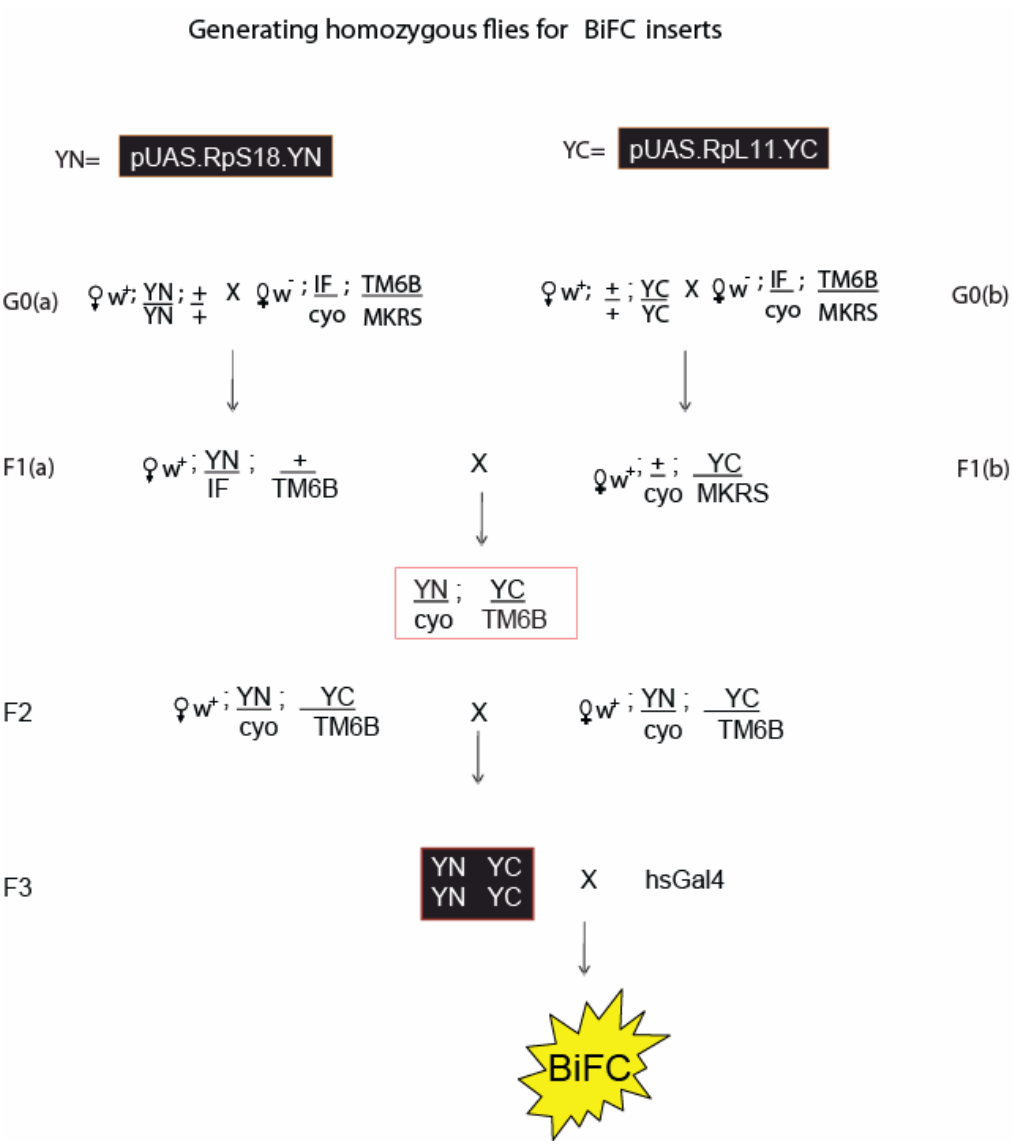


**Figure 5.12 Schematic of the protocol used for generating double-insert homozygous flies carrying the BiFC RPs pair**. In the G0 cross, a homozygous red eyed male with *pUAS-RpS18-YN* on the 2nd chromosome (cross **a**) and with pUAS-RpL11-YC on the 3rd chromosome (cross **b**) were crossed with double-balancer virgin females. Red eye males from the F1 (a) progeny, with *IF* and *TM6B* markers, were crossed with red-eye virgin females with *Cyo* and *MKRS* of the F1(b) progeny. Then F2 flies with the indicated genotypes were crossed to produce F3 flies homozygous for both inserts, which were selected for by the absence of both *Cyo and TM6B* dominant markers. The strain was initially verified by crossing with heat-shock Gal4 and by production of YFP fluorescence in the salivary glands.

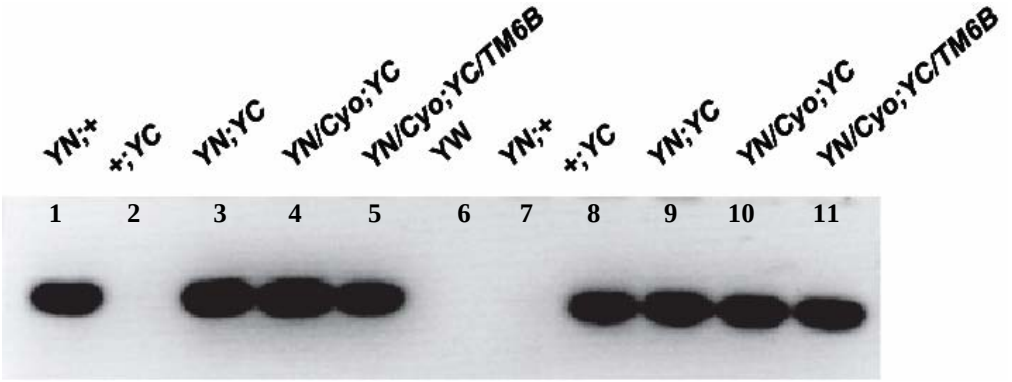


**Figure 5.13 PCR validation of the BiFC transgenic fly lines.**

PCR assay of genomic DNA isolated from five flies with the genotypes indicated. The PCRs were with primers specific for either the YN fragment (lanes 1-6) or for the YC fragment (lanes 6–11). Single bands of the expected sizes are visible; no bands are present in the negative *yw* control or in transgenic flies lacking the corresponding insert. (YN = RpS18-YN (939bp)), (YC = RpL11-YC (834bp)).

#### 5.2.3.1 BiFC analysis in *D. melanogaster* Salivary glands

After generating homozygous flies carrying both BiFC inserts (UAS-RpS18-YN on the 2nd chromosome and UAS-RpL11-YC on the 3rd chromosome), I tested whether co-expression of the two tagged ribosomal proteins produces BiFC complementation, as predicted by our study in S2 cells. To express the BiFC-reporters I crossed the strain carrying the BiFC transgenes with a heat shock -Gal4 driver – this driver is constitutively expressed in salivary glands and a high level of expression can be induced by deliberate heat-shock. First I assessed whether YFP fluorescence could be detected in salivary glands, which, because of their large size, we anticipated should be the best place to start our search. Following an extensive optimization of the heat-shock conditions (Material and Methods), we found that the best condition was to heat-shock larvae (early 3rd instars larvae before they start crawling out of the food) two days before dissection. The larvae were raised at 18°C because the lower temperature is expected to facilitate BiFC complementation and fluorophore maturation (Shyu et al., 2008).

Confocal microscope imaging of fixed salivary glands revealed a strong BiFC signal both in the cytoplasm and in the nucleolus in permeabilized salivary glands (Figure 5.14A). A similar pattern was observed in salivary glands that were fixed without detergent (non- permeabilized) (Figure 5.14B). There was no BiFC fluorescence in control experiments in which pUAS-RpS18-YN or pUAS-RpL11-YC are expressed individually (Figure 5.15). These results are consistent with our earlier study in S2 cells and indicate that, with this technique, it is possible to visualize ribosome subunit interaction in flies. A key finding is that the nucleolus showed an intense BiFC

fluorescence in all cells, suggesting that ribosomal subunits might interact before export to the cytoplasm.

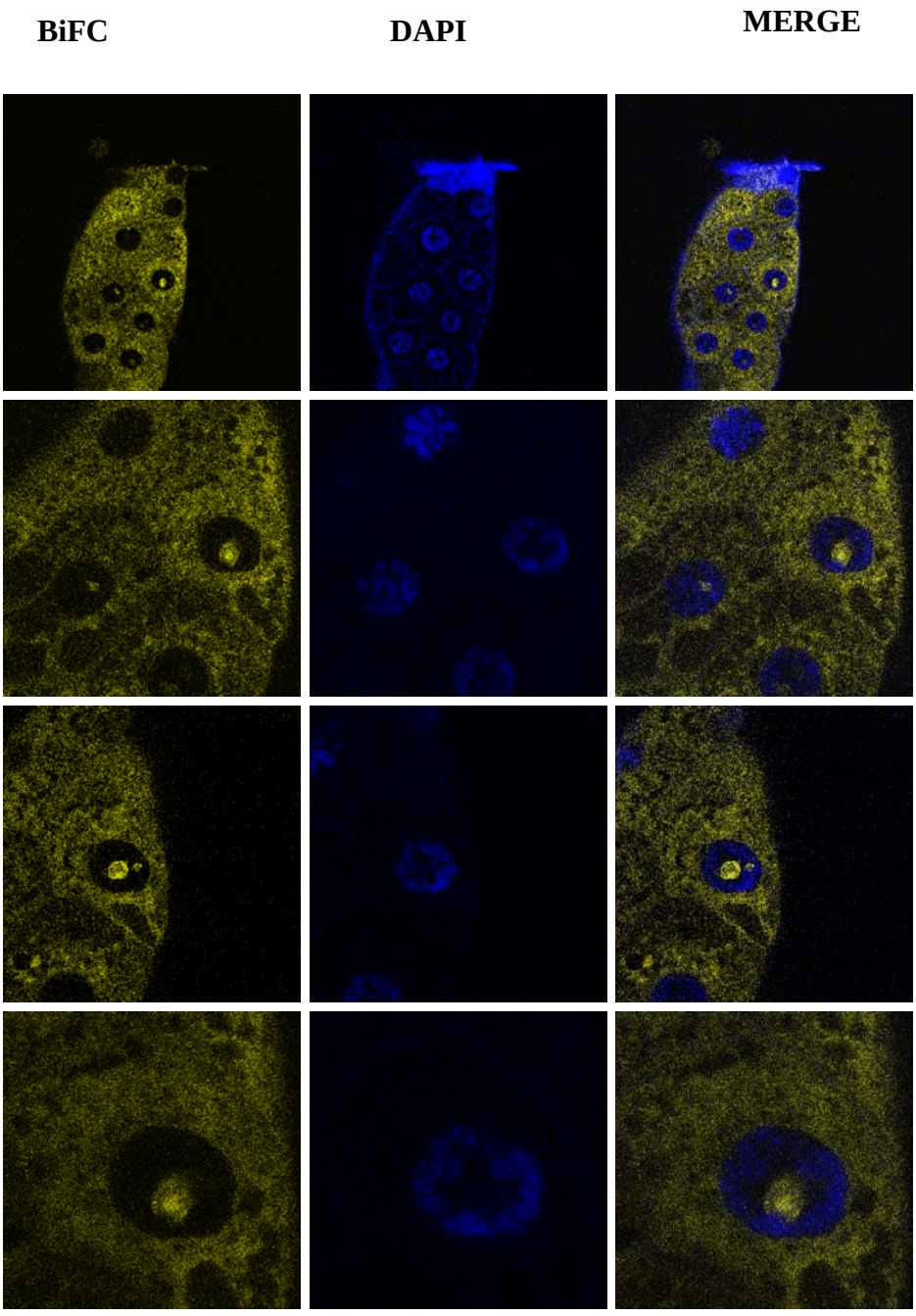


**Figure 5.14A BiFC analysis of ribosomal subunit interactions in permeabilized salivary glands.(legend next page)**

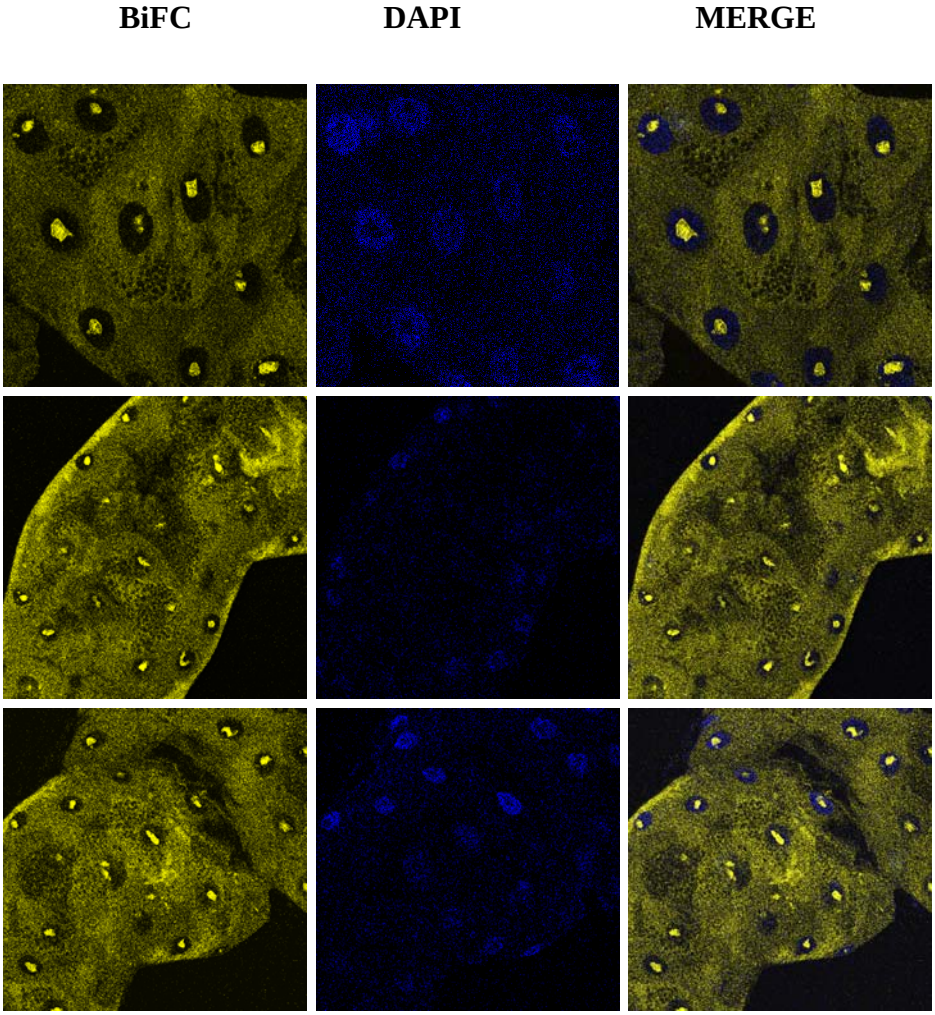


**Figure 5.14B BiFC analysis of ribosomal subunit interactions in non-permeabilized salivary glands.**(**A**) Confocal images of salivary glands expressing the BiFC reporters RpS18-YN and RpL11-YC. High level of expression was driven by a heat-shock Gal4 driver and by two 30 min. pulses of heat-shock with a 3 hour gap in between. Salivary glands were dissected from crawling 3$^{rd}$ instar larvae kept at 18 $^{0}$C and were fixed in 4% formaldehyde and permeabilized with 10% Triton X-100. (B) Same as above but salivary glands were not permeabilized with Triton.The images were taken with a confocal microscope with 40 × oil immersion objective.The left column shows the YFP signal (BiFC complementation), the middle column shows DAPI (DNA signal) and the right column shows a merge of the BiFC and DAPI pictures on the left.

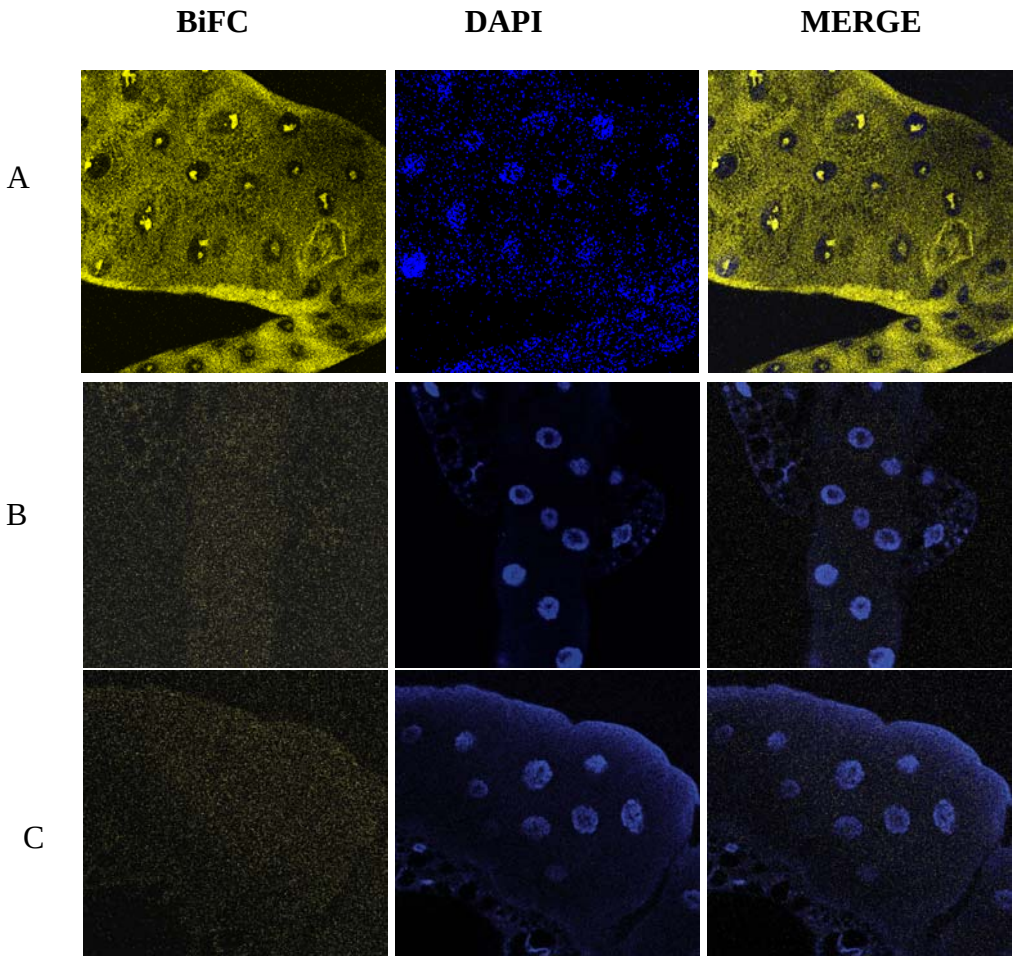


**Figure 5.15 YFP fluorescence is produced only in salivary glands expressing both BiFC fragments.** (A) BiFC fluorescence observed when the double insert line expressing pUAS-RpS18-YN and pUAS-RpL11-YC crossed with a heat shock-Gal4 driver. YFP signal disappears when the single insert transgene expressing either pUAS-RpS18-YN (B) or pUAS-RpL11-YC (C) is crossed with a heat shock-Gal4 driver. YFP signals (left column), DAPI staining (middle column) and the merged image (right column). The images were taken with a confocal microscope with 40 × oil immersion objective.

### 5.2.3.2 Transgenes inserts (BiFC tagged Rps) are functional

Since BiFC -tagged RPs are found in the polysome fraction in S2 cells (Figure 5.7), I expected these proteins to be functional. To verify the functionality of these proteins, I tested whether expression of RpS18-YN and RpL11-YC can rescue the lethal phenotype of mutations of the corresponding endogenous genes. As reviewed in the Introduction, in *Drosophila* RP genes are present in single copies and essential for viability. We were able to obtain homozygous lethal mutants for RpS18 and RpL11. The RpS18 mutant (*RpS18*$^{c02853}$*/Cyo* ; + ) was obtained from Exelixis and that for RpL11 (*RpL11*$^{k16914}$*/Cyo ;* + ) from the *Drosophila* Stock Center (Bloomington, IN) (see Appendix III,table 3). To assess whether expression of the tagged proteins can rescue lethality, I crossed flies carrying a lethal mutation on the endogenous ribosomal proteins, both located on the second chromosome, with a transgenic line on the third chromosome, expressing either RpS18-YN(K4-M3) or RpL11-YC(K5-M4) (see Appendix III, table 4). I followed the standard genetic protocol for testing mutation complementation (Materials and Methods). The presence of (*RpS18*$^{c02853}$) (Figure 5.16) and (*RpL11*$^{k16914}$) (Figure 5.17) on the second chromosome in F3 progeny was assessed by the lack of dominant markers from the balancer chromosomes as evidence for rescuing the lethality of the homozygous mutation on the second chromosome by the fused ribosomal protein on the third chromosome under the constitutive induction of the Actine-Gal4 on the third chromosome as a driver (Figures 5.16 and 5.17). The number of rescued flies was within the theoretically expected value of 6% , the scores for F3 progeny lacking the balancers dominant markers were 11 and 7 flies for RpL11 and RpS18 respectively (Appendix III ,table 6 and7) ,the rescued adults found to be survive at room temperature. These

genetic data demonstrate that both the RpS18-YN and RpL11-YC proteins can rescue mutant alleles of the endogenous genes. These data, together with the observation that these proteins are associated with polysomes in S2 cells, indicate that the tagged-RPs are functional components of ribosomal subunits.

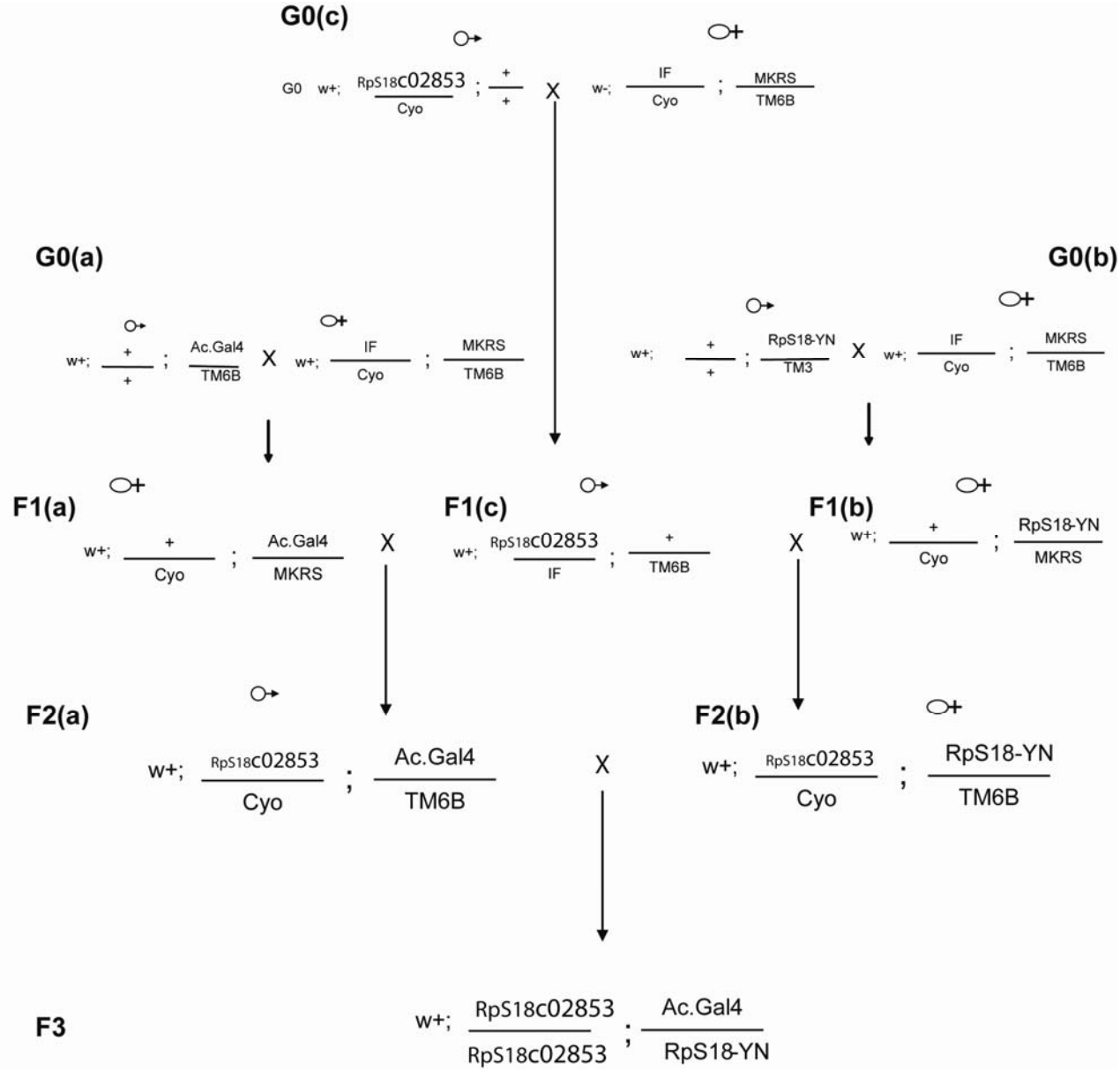


**Figure 5.16 Expression of RpS18-YN rescues a lethal mutation in the RpS18 locus**. In the G0 crosses,G0(a) (+;*Actin Gal4* ), G0(b) (+*;RpS18-YN* ) and G0(c) (*RpS18*$^{c02853}$;+ ) were crossed with double balancer virgin females. Virgin females with Cyo and MKRS from the F1(a) and F1b progeny were crossed with IF;TM6B F1(c) male progeny. In the final F2 cross, Cyo;TM6B (bothF2(a) and F2(b)) were crossed with each other. F3 progeny was scored for flies lacking the dominant markers Cyo;TM6B.

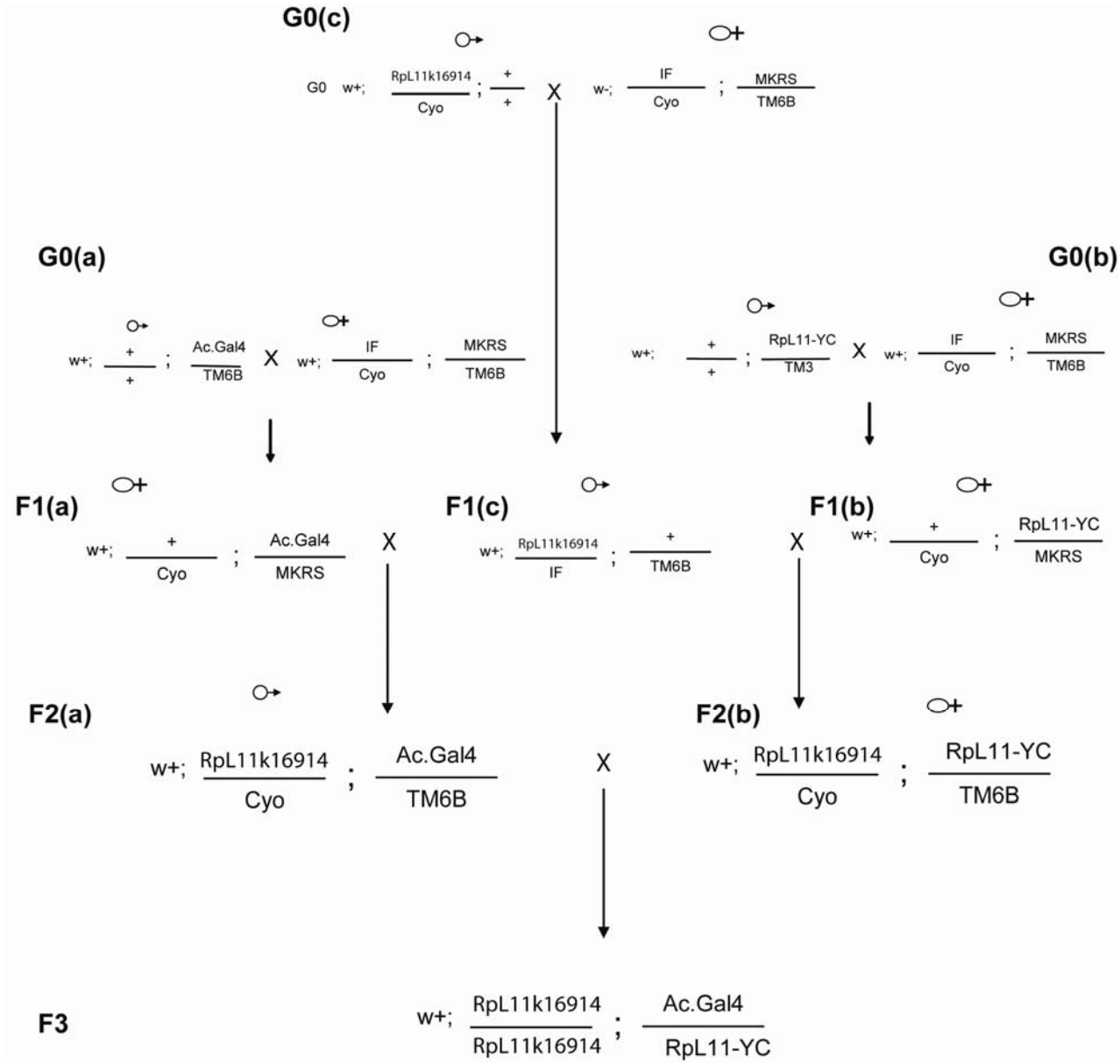


**Figure 5.17 Expression of RpL11-YC rescues a lethal mutation in the RpL11 locus.** In the G0 crosses, G0(a)(+;*Actin Gal4*) ,G0(b) (*+;RpL11-YC* ) and G0(c) (*RpL11k16914*;+ ) were crossed with double balancer virgin females. Virgin females with Cyo and MKRS from the F1(a) and F1(b) progeny were crossed with IF;TM6B F1(c) male progeny. In the final F2 cross, Cyo;TM6B (bothF2(a) and F2(b)) were crossed with each other. F3 progeny were scored for flies lacking the dominant markers Cyo;TM6B.

### 5.2.4 Generation of a fly strain expressing both Rps18-GFP and RpL11-RFP

An alternative approach to visualize the interaction between RpS18 and RpL11 is to use FRET. To do this, I have generated a strain of flies that express both RpS18-GFP and RpL11-RFP. GFP and RFP can be used as an efficient FRET pair due to their minimal emission overlap (Muller-Taubenberger and Anderson, 2007). First I generated transgenic lines with a single-insert RpS18-GFP and RpL11-RFP on the X, 2nd, and 3rd chromosomes (see Appendix III, table 4). Then a line carrying both transgenes was established by crossing *P[W+=UAS-RpS18:GFP]*(K2.M1) on the 2nd chromosome with *P[W+=UAS-RpL11:RFP]*(K3.M2) on the 3rd chromosome using standard genetics protocols (Figure 5.18). The presence of the inserts was verified by crossing the homozygote line with the SG -Gal4 line and by inspecting for the presence of GFP and RFP fluorescence in the salivary glands of 3rd instar larvae ( this was done in intact larvae, under a fluorescence microscope). The strain shows both GFP and RFP fluorescence, indicating the presence of both transgenes. To further characterize this strain; I crossed it with the SG-Gal4 driver and investigated the subcellular localization of the two proteins in salivary glands by confocal microscopy. The imaging showed that both proteins are highly abundant in the cytoplasm and nucleolus (Figure 5.19). A less intense signal was also detected in the nucleoplasm; the two proteins, as expected, show similar sub-cellular distributions.

Future work shall investigate whether these two proteins generate FRET and whether these interactions can be used to track ribosomal subunit interaction in cells.

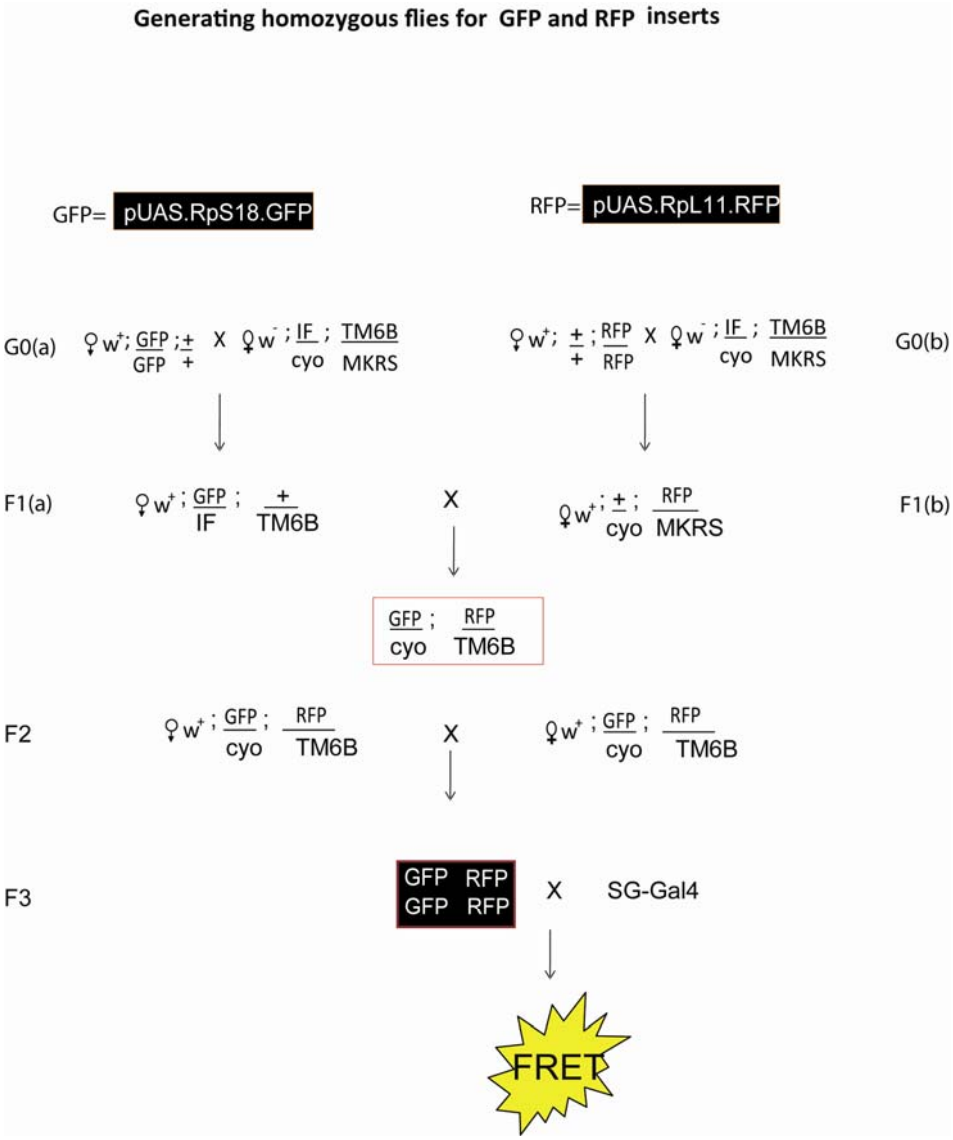


**Figure 5.18 Schematic of the protocol used for generating double-insert homozygous flies carrying the RPs tagged with FP**. In the G0 cross, a homozygous red eyed male with *pUAS-RpS18-GFP* on the 2nd chromosome (cross **a**) and with pUAS-RpL11-RFP on the 3rd chromosome (cross **b**) was crossed with double-balancer virgin females. Red eye males from the F1 (a) progeny, with *IF* and *TM6B* markers, were crossed with red-eye virgin females with *Cyo* and *MKRS* of the F1(b) progeny. Then F2 flies with the indicated genotypes were crossed to produce F3 flies homozygous for both inserts, which were selected for by the absence of both *Cyo* and *TM6B* dominant markers. The strain was initially verified by crossing with SG- Gal4 and by the production of both GFP and RFP fluorescence in the salivary glands.

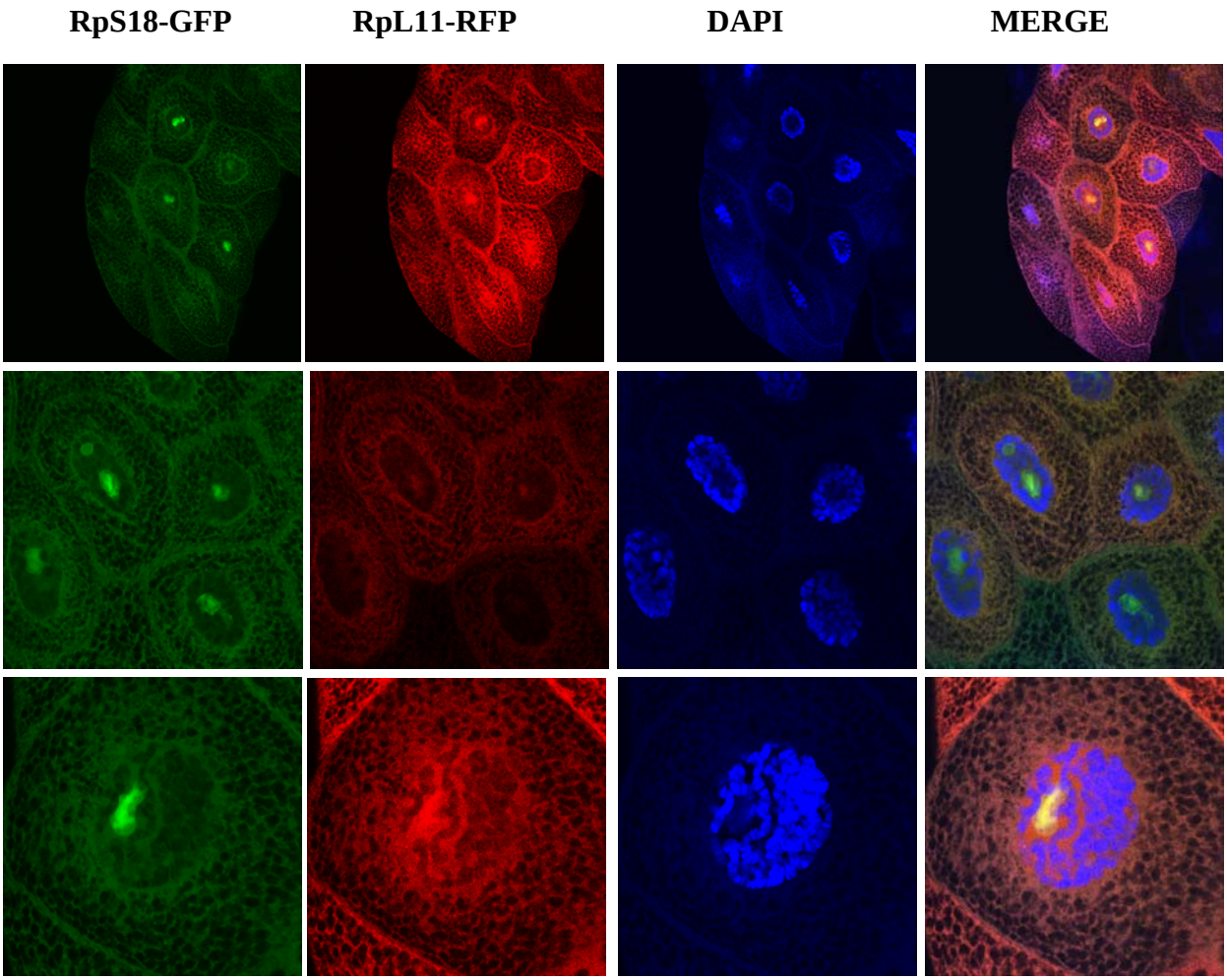


**Figure 5.19 RpS18-GFP co-localizes with RpL11-RFP in salivary glands.**
Confocal microscope images of cells expressing both RpS18 and RpL11. Images of different cells at diverse magnification are shown. The columns show the GFP signal in green (RpS18), the RFP signal (RpL11) in red and the DNA in blue (DAPI). The pictures in the column on the right show a merge of the images on the left. The images were taken with a confocal microscope with 40 × oil immersion objective.

## 5.3 Discussion

In this chapter I have reported data demonstrating that the BiFC technique is a powerful tool to visualize ribosome subunit interaction in both cells in culture and in *Drosophila* salivary glands. To optimize the BiFC approach, different combinations of RPs fused with the BiFC fragments at either the C- or N-terminus have been tested. I found that the best BiFC signal is produced by tagging RpL11 with the YC fragment at the C-terminal end (pUAS-RpL11-YC) and RpS18 with the YN fragment at the C-terminal end (pUAS-RpS18-YN). These two tagged RPs appear to be incorporated into functional ribosomal 40S and 60S subunits, because they associate with polysome fractions. In addition, I found that expression of RpS18-YN and RpL11-YC in flies complements lethal mutations in the endogenous RPs genes.

By tagging RPs located at the interface between the two subunits using the optimal pair of pUAS-RpS18-YN and pUAS-RpL11-YC, we were able to detect a strong YFP signal in the cytoplasm but not in the nucleoplasm, in spite of the fact that both proteins are abundant throughout the cell. The cytoplasmic signal is likely to be originating from the interaction between 60S and 40S during translation. Our observation, that the signal is enhanced by emetine, a drug that increases ribosome number on mRNA by stopping elongation, may support this conclusion. The finding that the interaction is most apparent in the cytoplasm is in agreement with the current view that ribosome subunits interact only during translation in the cytoplasm. However, I also found that, in some S2 cells and in all salivary gland nuclei, there was also a clear BiFC signal in the nucleolus, suggesting that the subunits might interact prior to nuclear export under certain conditions.

The BiFC signal in the nucleolus is, as is that in the cytoplasm, enhanced by incubation of the transfected cells with emetine. Although these observation suggest that ribosomal subunits can interact in the nucleolus, we cannot exclude the possibility that nucleolar signal is due to either an interaction between RpS18 and RpL11 in the pre-90S ribosome or to the very high local concentration of the RPs. Further indication that the ribosomal subunits can interact in the nucleus is the observation that, upon treatment with leptomycin B (LMB), a clear BiFC signal is also present in the nucleoplasm. An unexpected observation was that cotransfection of S2 cell with RpS9-YN and RpL11-YC produced an apparent BiFC signal in the nucleolus, while we expcetd this combination of RPs to work as a negative control because of RpS9 position on the solvent side, which should prevent interaction with RpL11-YC. This pair of BiFC-fusions, however, as expected did not complement in the cytoplasm. These observations might indicate that nucleolar ribosomal subunits have a different conformation than that in cytoplasmic 80S.

# Chapter 6. Discussion and Conclusion

## 6.1 Development of a new experimental technique to visualize translation

Although ribosomal subunits are assembled in the nucleolus, it is believed that they interact only during translation, in the cytoplasm. The present study aimed to find out whether ribosomal subunits can also interact in the nucleus and nucleolus. To address this issue, I have tagged both 40S and 60S RPs; and, in particular, I studied proteins located at the interface between the two subunits, which are predicted to interact upon subunits joining upon formation of the 80S. To visualize the interaction, initially we planned to tag 40S RPs with GFP and 60S RPs with RFP and use microscopy FRET assays to measure the interaction between the proteins. The FRET technique is the most frequently used technique to measure protein-protein interactions, however, we found it difficult to implement FRET in the laboratory (we could not measure GFP-RFP FRET with our microscope set-up). Therefore, as an alternative to FRET, in this project I decided to use BiFC, which is a technique that also allows imaging of protein–protein interactions and is a relatively simple alternative to FRET (Hu et al., 2002) (see Materials and Methods). Compared to FRET, BiFC shows essentially no background; in agreement with previous studies, I found very little YFP fluorescence in S2 cells expressing the YN and the YC peptides alone, not fused to any interacting proteins. To develop such assay, I have tagged several 40S RPs with the YN fragment and RpL11 with the YC fragment. Using this strategy in S2 cells, I found that the RpS18-YN and RpL11-YC pair produces the best BiFC signal (Figure 5.3). As reviewed in the Introduction, these two proteins appear to interact in cryo-EM

reconstructions of both the yeast and mammalian 80S (Chandramouli et al., 2008; Spahn et al., 2001). In contrast, we found only a minimal BiFC signal when using RpS9-YN and RpL11-YC; this is in agreement with the fact that RpS9 is located away from RpL11 in the 80S.

In summary, the assay I have developed appears to be a very sensitive procedure to visualize the interaction of ribosome subunits in cells, and, as discussed below, in transgenic flies. The BiFC assay probably worked very efficiently in *Drosophila* because both S2 cells and flies are grown at low temperatures, and it is known that maturation of the YN-YC complex to produce an active fluorophore is enhanced by low temperature; this is a limitation in animal cells, but not in *Drosophila* because flies are healthy at temperatures as low as 17°C. Consistent with low temperatures improving complementation, I found that the BiFC signal is increased by incubation at 18°C, for both transfected S2 cells and transgenic flies. I found that the BiFC complementation was affected by whether the tag was at the N- or C-terminus of the RPs, but, contrary to what has been reported for FRET, both orientations allowed complementation, with the only difference being in the intensity of the signal observed (Figure 5.4).

## 6.2 Do ribosomal subunits interact in the nucleus?

My data clearly indicate that the BiFC approach I have developed can be used to visualize the interaction of ribosome subunits in both S2 cells and in the *Drosophila* salivary gland. With this technique I found that the 60S and 40S subunits interact primarily in the cytoplasm, as expected; this is in agreement with the current view that ribosome subunits interact only during translation in the cytoplasm. However, I also found that in S2 cells and *Drosophila* salivary glands there was a clear signal also in

the nucleolus, suggesting that the subunits, at least under certain conditions, might interact prior to nuclear export. As mentioned above, the most intense BiFC signal was produced by the RpS18-YN and RpL11-YC pair, both in S2 cells and fly tissues (Figures 5.3 and 5.14). We are confident that the signal originates from genuine subunit interaction because both tagged RPs are incorporated into polysomal ribosomes; the functionality of the tagged RPs is also supported by genetic studies as the tagged proteins can rescue lethality mutations of the endogenous genes (Figures 5.16 and 5.17).

The fact that the signal is most intense in the cytoplasm is consistent with it originating by subunits joining during translation; it is unlikely that the BiFC signal we detected in the cytoplasm and nucleolus is due to the association of free RPs, because we found, by immunostaining, that the tagged RPs (presumably not associated with other RPs) are most concentrated in the nucleoplasm, yet we detected no obvious BiFC signal in this location. Furthermore, as mentioned above, co-expression of the YN and YC peptides alone, when not fused to interacting proteins, produces only a weak signal in the nucleoplasm, which is where the two peptides are most abundant in transfected cells. Therefore, we propose that the absence of a BiFC signal in the nucleoplasm of cells expressing S18-YN and L11-YC is due either to the ribosomal subunits not interacting in the nucleoplasm, in agreement with the currently accepted understanding that the translation is restricted to the cytoplasm; and consistent, with Bohnsack et Al. (2002) which suggested that translation can not occur in the nucleus because the vast majority of translation factores are actively excluded from the nucleus (Bohnsack et al., 2002). However, this does not eliminate the possibility that the ribosomal subunits can interact in the nucleus, because BiFC is known to require maturation after the initial YC/YN interaction, before producing

YFP fluorescence, so that the 80S that form in the nucleoplasm might not remain in this location sufficiently long to allow the maturation of the YFP fluorophore. The observation that there is a delay between YN and YC interaction and maturation of the YFP fluorophore is in consistent with this latter interpretation (Kerppola, 2006a).

We also did not observe a BiFC signal at transcription sites. This observation could be interpreted as evidence that ribosomes are not present at these sites. However, I found that the tagged RPs accumulate at these sites (see also section below) in agreement with previous studies (Brogna et al., 2002); it is feasible that the 80S that assemble at the site of transcription, similarly to the 80S forming in the nucleoplasm, do not accumulate there long enough for the YFP fluorescence to develop.

A key finding made during my PhD is that, in both S2 cells and in salivary glands, ribosomal subunits appear to interact in the nucleolus. The key issue is whether the interaction is between mature 40S and 60S subunits or whether instead it is caused by interaction between RpS18 and RpL11 in the 90S pre-ribosome (Ferreira-Cerca et al., 2007; Zhang et al., 2007). Our observation that the BiFC signal is enhanced by emetine treatment indicates that the interaction is translation-dependent as that in the cytoplasm - emetine is a drug that blocks translation elongation and increases ribosome number on polysomes (Grollman, 1968). Not all nuclei show a nucleolar signal in transfected cells; the nucleolus is a dynamic structure that breaks down during cell division (Cmarko et al., 2008) and perhaps in S2 cells the subunits interact in the nucleolus only during certain stages of the cell cycle. However, all salivary gland cells have nucleolus; salivary glands differentiate without further cell division and increase in size due to several cycles of endoreplication of the chromosomes, which become polytenic and very large (Andrew et al., 2000). In salivary glands all

cells show a prominent BiFC signal in the nucleolus. The nucleolar BiFC signal in the salivary glands is not affected by treatment with Actinomycin D at concentrations that block Pol I transcription, suggesting that the signal does not originate from the interaction of RPs associated with nascent rRNA or with the 90S pre-ribosome. Instead the recruitment of free RPs, tagged with either GFP or RFP, to the nucleolus is prevented by treatment with Actinomycin D (unpublished data from other members of the group). Furthermore, even if the two RPs did interact in the 90S subunit, we would not expect to see a BiFC signal because the maturation of the BiFC signal requires hours (12-36 hours) (Kerppola, 2006a); yet the 90S subunit is a transient structure existing for only a short time. Thus the signal is most likely not going to be due to an interaction between proteins that just transit the nucleolus. Instead, for us to detect the signal, the interaction has to be between factors that are stably associated with the nucleolus. Alternatively, the initial interaction between BiFC fragments could happen outside the nucleolus, followed by relocation of the complex to the nucleolus: assuming that the BiFC interaction is irreversible, it can be envisaged that, upon interaction of RpL11-YC and RpS18-YN, the maturation of 90S is stopped, leading to an accumulation of 90S which cannot be further processed because of the interaction between the pre-40S and pre-60S domains. Such events should impair ribosome biogenesis and have a negative effect on growth; however, contrary to this scenario, I found no evidence of overexpession of these BiFC tagged proteins having a negative effect on growth in both S2 cells and in flies. In addition, the 90S might not always be formed. It has been reported that in actively growing cells the nascent rRNA is cleaved in the internal transcribed spacer I (ITS1), thereby immediately releasing pre-40S particles without prior 90S particle formation (Osheim et al., 2004). The salivary glands are some of the most metabolically active cells in the *Drosophila*

larva, they synthesize a great amount of glue proteins - these proteins form a sticky matrix that allows the larva to adhere itself to solid surfaces to prepare for pupation (Andrew et al., 2000). Ribosome biogenesis is expected to be very active in these cells; these cells have very large nucleoli. Since the salivary gland is a very metabolically active tissue, the other possible explanation for nucleolar BiFC is that the pre-ribosome subunits (pre-40S and pre-60S) can interact in the nucleolus for translation or for some yet unknown function, maybe related to a specific requirement of these unusually highly metabolically active cells. The recent reports that the immature pre-40S can be used in translation initiation in *S. cerevisiae* (Soudet et al., 2009) and the presence of mRNA in the nucleolus of the plant cell (Kim et al., 2009) are consistent with our view that pre-ribosomal subunits might also interact in the nucleolus forming ribosomes capable of binding mRNA.

## 6.3 Tagged RPs show the expected subcellular distribution in S2 cells and salivary glands

As reviewed in the Introduction (Chapter 1), RPs are synthesized in the cytoplasm and rapidly imported into the nucleus where they accumulate in the nucleolus and associate with rRNA, launching the early stage of pre-ribosome assembly (90S pre-ribosome) before they are exported back as a ribosomal subunit component (Pre-40S or Pre-60S) to the cytoplasm where they interact together forming functional ribosome 80S. The pattern of sub-cellular distribution of the tagged-RPs used in this study is similar to what has been reported by other studies in other eukaryotes (Jakel and Gorlich, 1998; Kruger et al., 2007; Lam et al., 2007; Plafker and Macara, 2002). I found that RPs are concentrated in the nucleolus and cytoplasm, and, to a lesser extent, also in the nucleoplasm. Interestingly, I found no evidence to indicate that over-expression of tagged RPs has any detrimental effects on the viability of the

transgenic larvae and the growth of the transfected S2 cells. The data, therefore, indicate that over-expression of tagged RPs provides a feasible tool to track ribosomal subunits in *Drosophila* cells (see Chapter 3).

## 6.4 RPs accumulate at active transcription sites on polytene chromosomes

One of the aims of my project was to verify that RPs associate with transcription sites on the polytene chromosomes of *Drosophila*, as indicated by the previous study of Brogna et al. in which endogenous RPs were visualized by immunostaining at these sites (Brogna et al., 2002). Here, using transgenic flies expressing tagged RPs (RpS9-GFP, RpS18-GFP, and RpL11-RFP), we also found that the RPs colocalize with Pol II at transcription sites (interbands) of polytene chromosomes; visualization was with antibodies specific for either GFP or RFP. My results are in agreement with results previously reported by Brogna et al. and confirm that RPs are present at active sites of transcription. It has been argued that the antibodies used by Brogna et al. were not sufficiently specific and that the signal at transcription sites might have been due to cross reaction (Dahlberg and Lund, 2004); here, however, I have used primary antibodies directed against the GFP or RFP tag, and I can rigorously exclude the possibility that the staining was due to some residual cross-reactivity, because there were no signals observed in flies that were not expressing the tagged RPs under investigation.

These observations are consistent with the view that translation may occur at these sites as suggested by previous studies (see Introduction, Chapter I). However, given that we did not find evidence of subunit interaction at these sites, the issue of whether translation is occurring remains to be resolved. Alternative explanations as to why

RPs are associated with chromatin need also to be explored; for example, the chromosome association might be due to some non-ribosomal function of these RPs**.** As reviewed in the Introduction, several RPs are known to have extra-ribosomal functions, for instance, having a role in apoptosis, DNA repair and transcription (Lindstrom, 2009; Wool et al., 1995). It is even possible that association with the chromatin is an artefact of over-expression. In fact a recent study has suggested that even endogenous RPs are produced in excess and that those that fail to be incorporated into ribosomes accumulate in the nucleoplasm, where they are subject to proteosome degradation (Lam et al., 2007).

## 6.5 Conclusion

My PhD project aim was to visualize functional ribosomes in eukaryotes. To do this I have developed a BiFC-based imaging technique to visualize the interaction of ribosome subunits in intact cells, either fixed or live (we are now writing it up a manuscript for publication). With this technique I discovered that ribosomal subunits might also interact in the nucleolus and not only in the cytoplasm as currently believed**.** I expect this technique to become a powerful tool to visualize translation in cells; for example, on the basis of preliminary work (by other students in the lab) this technique can be used to visualize translation in highly polarized cells such as neurons. However, the limitation of this BiFC-based assay is that the complementation between the YN and YC fragments is most probably irreversible and therefore the procedure, while very sensitive, is not suitable for analysing dynamic or quantitative changes in subunit interaction (Kerppola, 2008). On the basis of the information we have gained with the BiFC-based assay and the other transgenes I have generated, we are trying to visualize the interaction using FRET assays: in collaboration with collegues with expertises in FRET, we are trying to visualize

interaction between S18-GFP and L11-RFP using FLIM - in this assay GFP acts as a donor and RFP as an acceptor, and we look for changes in the fluorescence life-time of GFP (Festy et al., 2007).In conclusion, I have shown that the BiFC is a powerfull technique to visualize ribosomal subunit interaction in cells. In future, I expect that by using multicolour BiFC assays should be possible to visualize mRNA and ribosome complexes for instance by labelling the nuclear and cytoplasmic cab binding protein in conjunction with the ribosomal subunits should allow visualization of translation at different stages of mRNA maturation; and should also make possible to give a definitive answer to the issue of wether translation can occur in the nucleolus, as suggested by my findings.

# References

Acker, M.G., and Lorsch, J.R. (2008). Mechanism of ribosomal subunit joining during eukaryotic translation initiation. Biochemical Society transactions *36*, 653-657.

Allen, S.H., and Wong, K.P. (1978). Conformation of ribosomal proteins free in solution and bound to ribosomal RNA. Biochemistry *17*, 3971-3978.

Alonso, J., and Santaren, J.F. (2006). Characterization of the Drosophila melanogaster ribosomal proteome. J Proteome Res *5*, 2025-2032.

Alvarez, J., Giuditta, A., and Koenig, E. (2000). Protein synthesis in axons and terminals: significance for maintenance, plasticity and regulation of phenotype. With a critique of slow transport theory. Progress in neurobiology *62*, 1-62.

Amrani, N., Ganesan, R., Kervestin, S., Mangus, D.A., Ghosh, S., and Jacobson, A. (2004). A faux 3'-UTR promotes aberrant termination and triggers nonsense-mediated mRNA decay. Nature *432*, 112-118.

Amrani, N., Sachs, M.S., and Jacobson, A. (2006). Early nonsense: mRNA decay solves a translational problem. Nature reviews *7*, 415-425.

Andersen, J.S., Lam, Y.W., Leung, A.K., Ong, S.E., Lyon, C.E., Lamond, A.I., and Mann, M. (2005). Nucleolar proteome dynamics. Nature *433*, 77-83.

Andrew, D.J., Henderson, K.D., and Seshaiah, P. (2000). Salivary gland development in Drosophila melanogaster. Mechanisms of development *92*, 5-17.

Arava, Y., Boas, F.E., Brown, P.O., and Herschlag, D. (2005). Dissecting eukaryotic translation and its control by ribosome density mapping. Nucleic acids research *33*, 2421-2432.

Atmakuri, K., Ding, Z., and Christie, P.J. (2003). VirE2, a type IV secretion substrate, interacts with the VirD4 transfer protein at cell poles of Agrobacterium tumefaciens. Molecular microbiology *49*, 1699-1713.

Ban, N., Nissen, P., Hansen, J., Moore, P.B., and Steitz, T.A. (2000). The complete atomic structure of the large ribosomal subunit at 2.4 A resolution. Science *289*, 905-920.

Behm-Ansmant, I., Gatfield, D., Rehwinkel, J., Hilgers, V., and Izaurralde, E. (2007). A conserved role for cytoplasmic poly(A)-binding protein 1 (PABPC1) in nonsense-mediated mRNA decay. The EMBO journal *26*, 1591-1601.

Belgrader, P., Cheng, J., and Maquat, L.E. (1993). Evidence to implicate translation by ribosomes in the mechanism by which nonsense codons reduce the nuclear level of

human triosephosphate isomerase mRNA. Proceedings of the National Academy of Sciences of the United States of America *90*, 482-486.

Belgrader, P., Cheng, J., Zhou, X., Stephenson, L.S., and Maquat, L.E. (1994). Mammalian nonsense codons can be cis effectors of nuclear mRNA half-life. Molecular and cellular biology *14*, 8219-8228.

Bensadoun, A., and Weinstein, D. (1976). Assay of proteins in the presence of interfering materials. Analytical biochemistry *70*, 241-250.

Benton, R., Sachse, S., Michnick, S.W., and Vosshall, L.B. (2006). Atypical membrane topology and heteromeric function of Drosophila odorant receptors in vivo. PLoS Biol *4*, e20.

Berget, S.M., Moore, C., and Sharp, P.A. (1977). Spliced segments at the 5' terminus of adenovirus 2 late mRNA. Proceedings of the National Academy of Sciences of the United States of America *74*, 3171-3175.

Beringer, M., and Rodnina, M.V. (2007). The ribosomal peptidyl transferase. Mol Cell *26*, 311-321.

Bhat, R.A., Lahaye, T., and Panstruga, R. (2006). The visible touch: in planta visualization of protein-protein interactions by fluorophore-based methods. Plant methods *2*, 12.

Bischof, J., Maeda, R.K., Hediger, M., Karch, F., and Basler, K. (2007). An optimized transgenesis system for Drosophila using germ-line-specific phiC31 integrases. Proceedings of the National Academy of Sciences of the United States of America *104*, 3312-3317.

Bohnsack, M.T., Regener, K., Schwappach, B., Saffrich, R., Paraskeva, E., Hartmann, E., and Gorlich, D. (2002). Exp5 exports eEF1A via tRNA from nuclei and synergizes with other transport pathways to confine translation to the cytoplasm. The EMBO journal *21*, 6205-6215.

Brand, A.H., and Perrimon, N. (1993). Targeted gene expression as a means of altering cell fates and generating dominant phenotypes. Development (Cambridge, England) *118*, 401-415.

Brodsky, A.S., and Silver, P.A. (2000). Pre-mRNA processing factors are required for nuclear export. RNA (New York, NY *6*, 1737-1749.

Brogna, A., Ferrara, R., Bucceri, A.M., Lanteri, E., and Catalano, F. (1999). Influence of aging on gastrointestinal transit time. An ultrasonographic and radiologic study. Invest Radiol *34*, 357-359.

Brogna, S., Sato, T.A., and Rosbash, M. (2002). Ribosome components are associated with sites of transcription. Mol Cell *10*, 93-104.

Brogna, S., and Wen, J. (2009). Nonsense-mediated mRNA decay (NMD) mechanisms. Nature structural & molecular biology *16*, 107-113.

Buhler, M., Steiner, S., Mohn, F., Paillusson, A., and Muhlemann, O. (2006). EJC-independent degradation of nonsense immunoglobulin-mu mRNA depends on 3' UTR length. Nature structural & molecular biology *13*, 462-464.

Carter, M.S., Li, S., and Wilkinson, M.F. (1996). A splicing-dependent regulatory mechanism that detects translation signals. The EMBO journal *15*, 5965-5975.

Chamieh, H., Ballut, L., Bonneau, F., and Le Hir, H. (2008). NMD factors UPF2 and UPF3 bridge UPF1 to the exon junction complex and stimulate its RNA helicase activity. Nature structural & molecular biology *15*, 85-93.

Chandramouli, P., Topf, M., Menetret, J.F., Eswar, N., Cannone, J.J., Gutell, R.R., Sali, A., and Akey, C.W. (2008). Structure of the mammalian 80S ribosome at 8.7 A resolution. Structure *16*, 535-548.

Chang, J.C., and Kan, Y.W. (1979). beta 0 thalassemia, a nonsense mutation in man. Proceedings of the National Academy of Sciences of the United States of America *76*, 2886-2889.

Cheng, J., Belgrader, P., Zhou, X., and Maquat, L.E. (1994). Introns are cis effectors of the nonsense-codon-mediated reduction in nuclear mRNA abundance. Molecular and cellular biology *14*, 6317-6325.

Cheng, J., and Maquat, L.E. (1993). Nonsense codons can reduce the abundance of nuclear mRNA without affecting the abundance of pre-mRNA or the half-life of cytoplasmic mRNA. Molecular and cellular biology *13*, 1892-1902.

Choesmel, V., Bacqueville, D., Rouquette, J., Noaillac-Depeyre, J., Fribourg, S., Cretien, A., Leblanc, T., Tchernia, G., Da Costa, L., and Gleizes, P.E. (2007). Impaired ribosome biogenesis in Diamond-Blackfan anemia. Blood *109*, 1275-1283.

Chow, L.T., Gelinas, R.E., Broker, T.R., and Roberts, R.J. (1977). An amazing sequence arrangement at the 5' ends of adenovirus 2 messenger RNA. Cell *12*, 1-8.

Chu, S., Archer, R.H., Zengel, J.M., and Lindahl, L. (1994). The RNA of RNase MRP is required for normal processing of ribosomal RNA. Proceedings of the National Academy of Sciences of the United States of America *91*, 659-663.

Cmarko, D., Smigova, J., Minichova, L., and Popov, A. (2008). Nucleolus: the ribosome factory. Histology and histopathology *23*, 1291-1298.

Colgan, D.F., and Manley, J.L. (1997). Mechanism and regulation of mRNA polyadenylation. Genes & development *11*, 2755-2766.

Conti, E., and Izaurralde, E. (2005). Nonsense-mediated mRNA decay: molecular insights and mechanistic variations across species. Curr Opin Cell Biol *17*, 316-325.

Culbertson, M.R., Underbrink, K.M., and Fink, G.R. (1980). Frameshift suppression Saccharomyces cerevisiae. II. Genetic properties of group II suppressors. Genetics *95*, 833-853.

Dahlberg, J.E., and Lund, E. (2004). Does protein synthesis occur in the nucleus? Curr Opin Cell Biol *16*, 335-338.

Dahlberg, J.E., Lund, E., and Goodwin, E.B. (2003). Nuclear translation: what is the evidence? RNA (New York, NY *9*, 1-8.

Dai, M.S., and Lu, H. (2004). Inhibition of MDM2-mediated p53 ubiquitination and degradation by ribosomal protein L5. J Biol Chem *279*, 44475-44482.

Dai, M.S., Sears, R., and Lu, H. (2007). Feedback regulation of c-Myc by ribosomal protein L11. Cell cycle (Georgetown, Tex *6*, 2735-2741.

Degot, S., Le Hir, H., Alpy, F., Kedinger, V., Stoll, I., Wendling, C., Seraphin, B., Rio, M.C., and Tomasetto, C. (2004). Association of the breast cancer protein MLN51 with the exon junction complex via its speckle localizer and RNA binding module. J Biol Chem *279*, 33702-33715.

Deshmukh, M., Stark, J., Yeh, L.C., Lee, J.C., and Woolford, J.L., Jr. (1995). Multiple regions of yeast ribosomal protein L1 are important for its interaction with 5 S rRNA and assembly into ribosomes. J Biol Chem *270*, 30148-30156.

Duffy, J.B. (2002). GAL4 system in Drosophila: a fly geneticist's Swiss army knife. Genesis *34*, 1-15.

Eberle, A.B., Stalder, L., Mathys, H., Orozco, R.Z., and Muhlemann, O. (2008). Posttranscriptional gene regulation by spatial rearrangement of the 3' untranslated region. PLoS Biol *6*, e92.

Ferreira-Cerca, S., Poll, G., Gleizes, P.E., Tschochner, H., and Milkereit, P. (2005). Roles of eukaryotic ribosomal proteins in maturation and transport of pre-18S rRNA and ribosome function. Mol Cell *20*, 263-275.

Ferreira-Cerca, S., Poll, G., Kuhn, H., Neueder, A., Jakob, S., Tschochner, H., and Milkereit, P. (2007). Analysis of the in vivo assembly pathway of eukaryotic 40S ribosomal proteins. Mol Cell *28*, 446-457.

Festy, F., Ameer-Beg, S.M., Ng, T., and Suhling, K. (2007). Imaging proteins in vivo using fluorescence lifetime microscopy. Mol Biosyst *3*, 381-391.

Freeman, M. (1996). Reiterative use of the EGF receptor triggers differentiation of all cell types in the Drosophila eye. Cell *87*, 651-660.

Gatfield, D., and Izaurralde, E. (2004). Nonsense-mediated messenger RNA decay is initiated by endonucleolytic cleavage in Drosophila. Nature *429*, 575-578.

Gatfield, D., Unterholzner, L., Ciccarelli, F.D., Bork, P., and Izaurralde, E. (2003). Nonsense-mediated mRNA decay in Drosophila: at the intersection of the yeast and mammalian pathways. The EMBO journal *22*, 3960-3970.

Gazda, H.T., Zhong, R., Long, L., Niewiadomska, E., Lipton, J.M., Ploszynska, A., Zaucha, J.M., Vlachos, A., Atsidaftos, E., Viskochil, D.H., *et al.* (2004). RNA and

protein evidence for haplo-insufficiency in Diamond-Blackfan anaemia patients with RPS19 mutations. Br J Haematol *127*, 105-113.

Giorgi, C., Yeo, G.W., Stone, M.E., Katz, D.B., Burge, C., Turrigiano, G., and Moore, M.J. (2007). The EJC factor eIF4AIII modulates synaptic strength and neuronal protein expression. Cell *130*, 179-191.

Goldstein, D.J. (1970). Aspects of scanning microdensitometry. I. Stray light (glare). Journal of microscopy *92*, 1-16.

Greenspan, R.J. (2004). E pluribus unum, ex uno plura: quantitative and single-gene perspectives on the study of behavior. Annual review of neuroscience *27*, 79-105.

Grollman, A.P. (1968). Inhibitors of protein biosynthesis. V. Effects of emetine on protein and nucleic acid biosynthesis in HeLa cells. J Biol Chem *243*, 4089-4094.

Hachet, O., and Ephrussi, A. (2004). Splicing of oskar RNA in the nucleus is coupled to its cytoplasmic localization. Nature *428*, 959-963.

Hagiwara, M., and Nojima, T. (2007). Cross-talks between transcription and post-transcriptional events within a 'mRNA factory'. Journal of biochemistry *142*, 11-15.

Halic, M., Becker, T., Frank, J., Spahn, C.M., and Beckmann, R. (2005). Localization and dynamic behavior of ribosomal protein L30e. Nature structural & molecular biology *12*, 467-468.

Han, K. (1996). An efficient DDAB-mediated transfection of Drosophila S2 cells. Nucleic acids research *24*, 4362-4363.

Hartley, J.L., Temple, G.F., and Brasch, M.A. (2000). DNA cloning using in vitro site-specific recombination. Genome research *10*, 1788-1795.

He, F., Brown, A.H., and Jacobson, A. (1997). Upf1p, Nmd2p, and Upf3p are interacting components of the yeast nonsense-mediated mRNA decay pathway. Molecular and cellular biology *17*, 1580-1594.

Heix, J., Vente, A., Voit, R., Budde, A., Michaelidis, T.M., and Grummt, I. (1998). Mitotic silencing of human rRNA synthesis: inactivation of the promoter selectivity factor SL1 by cdc2/cyclin B-mediated phosphorylation. The EMBO journal *17*, 7373-7381.

Henras, A.K., Soudet, J., Gerus, M., Lebaron, S., Caizergues-Ferrer, M., Mougin, A., and Henry, Y. (2008). The post-transcriptional steps of eukaryotic ribosome biogenesis. Cell Mol Life Sci *65*, 2334-2359.

Hentze, M.W., and Kulozik, A.E. (1999). A perfect message: RNA surveillance and nonsense-mediated decay. Cell *96*, 307-310.

Hiatt, S.M., Shyu, Y.J., Duren, H.M., and Hu, C.D. (2008). Bimolecular fluorescence complementation (BiFC) analysis of protein interactions in Caenorhabditis elegans. Methods (San Diego, Calif *45*, 185-191.

Hodgkin, J., Papp, A., Pulak, R., Ambros, V., and Anderson, P. (1989). A new kind of informational suppression in the nematode Caenorhabditis elegans. Genetics *123*, 301-313.

Holbrook, J.A., Neu-Yilik, G., Hentze, M.W., and Kulozik, A.E. (2004). Nonsense-mediated decay approaches the clinic. Nature genetics *36*, 801-808.

Hosoda, N., Kim, Y.K., Lejeune, F., and Maquat, L.E. (2005). CBP80 promotes interaction of Upf1 with Upf2 during nonsense-mediated mRNA decay in mammalian cells. Nature structural & molecular biology *12*, 893-901.

Hu, C.D., Chinenov, Y., and Kerppola, T.K. (2002). Visualization of interactions among bZIP and Rel family proteins in living cells using bimolecular fluorescence complementation. Mol Cell *9*, 789-798.

Huang, S. (2002). Building an efficient factory: where is pre-rRNA synthesized in the nucleolus? The Journal of cell biology *157*, 739-741.

Hui, J. (2009). Regulation of mammalian pre-mRNA splicing. Science in China *52*, 253-260.

Hurt, E., Hannus, S., Schmelzl, B., Lau, D., Tollervey, D., and Simos, G. (1999). A novel in vivo assay reveals inhibition of ribosomal nuclear export in ran-cycle and nucleoporin mutants. The Journal of cell biology *144*, 389-401.

Hutten, S., and Kehlenbach, R.H. (2007). CRM1-mediated nuclear export: to the pore and beyond. Trends in cell biology *17*, 193-201.

Iborra, F.J., Escargueil, A.E., Kwek, K.Y., Akoulitchev, A., and Cook, P.R. (2004). Molecular cross-talk between the transcription, translation, and nonsense-mediated decay machineries. Journal of cell science *117*, 899-906.

Iborra, F.J., Jackson, D.A., and Cook, P.R. (2001). Coupled transcription and translation within nuclei of mammalian cells. Science *293*, 1139-1142.

Inada, T., Winstall, E., Tarun, S.Z., Jr., Yates, J.R., 3rd, Schieltz, D., and Sachs, A.B. (2002). One-step affinity purification of the yeast ribosome and its associated proteins and mRNAs. RNA (New York, NY *8*, 948-958.

Ishigaki, Y., Li, X., Serin, G., and Maquat, L.E. (2001). Evidence for a pioneer round of mRNA translation: mRNAs subject to nonsense-mediated decay in mammalian cells are bound by CBP80 and CBP20. Cell *106*, 607-617.

Jakel, S., and Gorlich, D. (1998). Importin beta, transportin, RanBP5 and RanBP7 mediate nuclear import of ribosomal proteins in mammalian cells. The EMBO journal *17*, 4491-4502.

Jensen, T.H., Dower, K., Libri, D., and Rosbash, M. (2003). Early formation of mRNP: license for export or quality control? Mol Cell *11*, 1129-1138.

Kapp, L.D., and Lorsch, J.R. (2004). The molecular mechanics of eukaryotic translation. Annual review of biochemistry *73*, 657-704.

Kashima, I., Yamashita, A., Izumi, N., Kataoka, N., Morishita, R., Hoshino, S., Ohno, M., Dreyfuss, G., and Ohno, S. (2006). Binding of a novel SMG-1-Upf1-eRF1-eRF3 complex (SURF) to the exon junction complex triggers Upf1 phosphorylation and nonsense-mediated mRNA decay. Genes & development *20*, 355-367.

Kebaara, B.W., and Atkin, A.L. (2009). Long 3'-UTRs target wild-type mRNAs for nonsense-mediated mRNA decay in Saccharomyces cerevisiae. Nucleic acids research.

Kerppola, T.K. (2006a). Design and implementation of bimolecular fluorescence complementation (BiFC) assays for the visualization of protein interactions in living cells. Nature protocols *1*, 1278-1286.

Kerppola, T.K. (2006b). Visualization of molecular interactions by fluorescence complementation. Nature reviews *7*, 449-456.

Kerppola, T.K. (2008). Bimolecular fluorescence complementation (BiFC) analysis as a probe of protein interactions in living cells. Annual review of biophysics *37*, 465-487.

Kertesz, S., Kerenyi, Z., Merai, Z., Bartos, I., Palfy, T., Barta, E., and Silhavy, D. (2006). Both introns and long 3'-UTRs operate as cis-acting elements to trigger nonsense-mediated decay in plants. Nucleic acids research *34*, 6147-6157.

Kim, S.H., Koroleva, O.A., Lewandowska, D., Pendle, A.F., Clark, G.P., Simpson, C.G., Shaw, P.J., and Brown, J.W. (2009). Aberrant mRNA transcripts and the nonsense-mediated decay proteins UPF2 and UPF3 are enriched in the Arabidopsis nucleolus. Plant Cell *21*, 2045-2057.

Kim, S.Y., Lee, M.Y., Cho, K.C., Choi, Y.S., Choi, J.S., Sung, K.W., Kwon, O.J., Kim, H.S., Kim, I.K., and Jeong, S.W. (2003). Alterations in mRNA expression of ribosomal protein S9 in hydrogen peroxide-treated neurotumor cells and in rat hippocampus after transient ischemia. Neurochemical research *28*, 925-931.

Kressler, D., de la Cruz, J., Rojo, M., and Linder, P. (1997). Fal1p is an essential DEAD-box protein involved in 40S-ribosomal-subunit biogenesis in Saccharomyces cerevisiae. Molecular and cellular biology *17*, 7283-7294.

Kruger, T., Zentgraf, H., and Scheer, U. (2007). Intranucleolar sites of ribosome biogenesis defined by the localization of early binding ribosomal proteins. The Journal of cell biology *177*, 573-578.

Kudo, N., Matsumori, N., Taoka, H., Fujiwara, D., Schreiner, E.P., Wolff, B., Yoshida, M., and Horinouchi, S. (1999). Leptomycin B inactivates CRM1/exportin 1 by covalent modification at a cysteine residue in the central conserved region. Proceedings of the National Academy of Sciences of the United States of America *96*, 9112-9117.

Lam, Y.W., Lamond, A.I., Mann, M., and Andersen, J.S. (2007). Analysis of nucleolar protein dynamics reveals the nuclear degradation of ribosomal proteins. Curr Biol *17*, 749-760.

Lambertsson, A. (1998). The minute genes in Drosophila and their molecular functions. Adv Genet *38*, 69-134.

Lambertsson, A.G. (1975). The ribosomal proteins of drosophila melanogaster. IV. Characterization by two-dimensional gel electrophoresis of the ribosomal proteins from nine postembryonic developmental stages. Mol Gen Genet *139*, 133-144.

Landy, A. (1989). Dynamic, structural, and regulatory aspects of lambda site-specific recombination. Annual review of biochemistry *58*, 913-949.

Le Hir, H., Gatfield, D., Izaurralde, E., and Moore, M.J. (2001). The exon-exon junction complex provides a binding platform for factors involved in mRNA export and nonsense-mediated mRNA decay. The EMBO journal *20*, 4987-4997.

Le Hir, H., Izaurralde, E., Maquat, L.E., and Moore, M.J. (2000). The spliceosome deposits multiple proteins 20-24 nucleotides upstream of mRNA exon-exon junctions. The EMBO journal *19*, 6860-6869.

Leger-Silvestre, I., Milkereit, P., Ferreira-Cerca, S., Saveanu, C., Rousselle, J.C., Choesmel, V., Guinefoleau, C., Gas, N., and Gleizes, P.E. (2004). The ribosomal protein Rps15p is required for nuclear exit of the 40S subunit precursors in yeast. The EMBO journal *23*, 2336-2347.

Lejeune, F., Ishigaki, Y., Li, X., and Maquat, L.E. (2002). The exon junction complex is detected on CBP80-bound but not eIF4E-bound mRNA in mammalian cells: dynamics of mRNP remodeling. The EMBO journal *21*, 3536-3545.

Li, B., Wachtel, C., Miriami, E., Yahalom, G., Friedlander, G., Sharon, G., Sperling, R., and Sperling, J. (2002). Stop codons affect 5' splice site selection by surveillance of splicing. Proceedings of the National Academy of Sciences of the United States of America *99*, 5277-5282.

Lim, S.K., and Maquat, L.E. (1992). Human beta-globin mRNAs that harbor a nonsense codon are degraded in murine erythroid tissues to intermediates lacking regions of exon I or exons I and II that have a cap-like structure at the 5' termini. The EMBO journal *11*, 3271-3278.

Lindstrom, M.S. (2009). Emerging functions of ribosomal proteins in gene-specific transcription and translation. Biochemical and biophysical research communications *379*, 167-170.

Lopez, C.D., Martinovsky, G., and Naumovski, L. (2002). Inhibition of cell death by ribosomal protein L35a. Cancer letters *180*, 195-202.

Lygerou, Z., Allmang, C., Tollervey, D., and Seraphin, B. (1996). Accurate processing of a eukaryotic precursor ribosomal RNA by ribonuclease MRP in vitro. Science *272*, 268-270.

Maguire, B.A., and Zimmermann, R.A. (2001). The ribosome in focus. Cell *104*, 813-816.

Malygin, A.A., Parakhnevitch, N.M., Ivanov, A.V., Eperon, I.C., and Karpova, G.G. (2007). Human ribosomal protein S13 regulates expression of its own gene at the splicing step by a feedback mechanism. Nucleic acids research *35*, 6414-6423.

Mangiarotti, G. (1999). Coupling of transcription and translation in Dictyostelium discoideum nuclei. Biochemistry *38*, 3996-4000.

Mangiarotti, G., and Chiaberge, S. (1997). Reconstitution of functional eukaryotic ribosomes from Dictyostelium discoideum ribosomal proteins and RNA. J Biol Chem *272*, 19682-19687.

Maquat, L.E. (1995). When cells stop making sense: effects of nonsense codons on RNA metabolism in vertebrate cells. RNA (New York, NY *1*, 453-465.

Maquat, L.E. (2004). Nonsense-mediated mRNA decay: splicing, translation and mRNP dynamics. Nature reviews *5*, 89-99.

Maquat, L.E., and Li, X. (2001). Mammalian heat shock p70 and histone H4 transcripts, which derive from naturally intronless genes, are immune to nonsense-mediated decay. RNA (New York, NY *7*, 445-456.

Marygold, S.J., Roote, J., Reuter, G., Lambertsson, A., Ashburner, M., Millburn, G., Harrison, P., Yu, Z., Kenmochi, N., Kaufman, T.C., *et al.* (2007). The ribosomal protein genes and Minute loci of Drosophila melanogaster. Genome Biol *8*, R216.

McConkey, E.H., Bielka, H., Gordon, J., Lastick, S.M., Lin, A., Ogata, K., Reboud, J.P., Traugh, J.A., Traut, R.R., Warner, J.R., *et al.* (1979). Proposed uniform nomenclature for mammalian ribosomal proteins. Mol Gen Genet *169*, 1-6.

McGlincy, N.J., and Smith, C.W. (2008). Alternative splicing resulting in nonsense-mediated mRNA decay: what is the meaning of nonsense? Trends Biochem Sci *33*, 385-393.

Mendell, J.T., and Dietz, H.C. (2001). When the message goes awry: disease-producing mutations that influence mRNA content and performance. Cell *107*, 411-414.

Merryman, C., Moazed, D., Daubresse, G., and Noller, H.F. (1999). Nucleotides in 23S rRNA protected by the association of 30S and 50S ribosomal subunits. Journal of molecular biology *285*, 107-113.

Mitchell, P., Osswald, M., and Brimacombe, R. (1992). Identification of intermolecular RNA cross-links at the subunit interface of the Escherichia coli ribosome. Biochemistry *31*, 3004-3011.

Moore, M.J. (2005). From birth to death: the complex lives of eukaryotic mRNAs. Science *309*, 1514-1518.

Moore, M.J., and Proudfoot, N.J. (2009). Pre-mRNA processing reaches back to transcription and ahead to translation. Cell *136*, 688-700.

Morell, M., Espargaro, A., Aviles, F.X., and Ventura, S. (2007). Detection of transient protein-protein interactions by bimolecular fluorescence complementation: the Abl-SH3 case. Proteomics *7*, 1023-1036.

Muhlemann, O., Mock-Casagrande, C.S., Wang, J., Li, S., Custodio, N., Carmo-Fonseca, M., Wilkinson, M.F., and Moore, M.J. (2001). Precursor RNAs harboring nonsense codons accumulate near the site of transcription. Mol Cell *8*, 33-43.

Muhlrad, D., and Parker, R. (1999). Aberrant mRNAs with extended 3' UTRs are substrates for rapid degradation by mRNA surveillance. RNA (New York, NY *5*, 1299-1307.

Muller-Taubenberger, A., and Anderson, K.I. (2007). Recent advances using green and red fluorescent protein variants. Appl Microbiol Biotechnol *77*, 1-12.

Nakao, A., Yoshihama, M., and Kenmochi, N. (2004). RPG: the Ribosomal Protein Gene database. Nucleic acids research *32*, D168-170.

Nathanson, L., Xia, T., and Deutscher, M.P. (2003). Nuclear protein synthesis: a re-evaluation. RNA (New York, NY *9*, 9-13.

Ni, J.Q., Liu, L.P., Hess, D., Rietdorf, J., and Sun, F.L. (2006). Drosophila ribosomal proteins are associated with linker histone H1 and suppress gene transcription. Genes & development *20*, 1959-1973.

O'Hare, K., and Rubin, G.M. (1983). Structures of P transposable elements and their sites of insertion and excision in the Drosophila melanogaster genome. Cell *34*, 25-35.

Osheim, Y.N., French, S.L., Keck, K.M., Champion, E.A., Spasov, K., Dragon, F., Baserga, S.J., and Beyer, A.L. (2004). Pre-18S ribosomal RNA is structurally compacted into the SSU processome prior to being cleaved from nascent transcripts in Saccharomyces cerevisiae. Mol Cell *16*, 943-954.

Palacios, I.M., Gatfield, D., St Johnston, D., and Izaurralde, E. (2004). An eIF4AIII-containing complex required for mRNA localization and nonsense-mediated mRNA decay. Nature *427*, 753-757.

Perez-Fernandez, J., Roman, A., De Las Rivas, J., Bustelo, X.R., and Dosil, M. (2007). The 90S preribosome is a multimodular structure that is assembled through a hierarchical mechanism. Molecular and cellular biology *27*, 5414-5429.

Pisarev, A.V., Hellen, C.U., and Pestova, T.V. (2007). Recycling of eukaryotic posttermination ribosomal complexes. Cell *131*, 286-299.

Pisareva, V.P., Pisarev, A.V., Hellen, C.U., Rodnina, M.V., and Pestova, T.V. (2006). Kinetic analysis of interaction of eukaryotic release factor 3 with guanine nucleotides. J Biol Chem *281*, 40224-40235.

Plafker, S.M., and Macara, I.G. (2002). Ribosomal protein L12 uses a distinct nuclear import pathway mediated by importin 11. Molecular and cellular biology *22*, 1266-1275.

Pulak, R., and Anderson, P. (1993). mRNA surveillance by the Caenorhabditis elegans smg genes. Genes & development *7*, 1885-1897.

Qian, L., Theodor, L., Carter, M., Vu, M.N., Sasaki, A.W., and Wilkinson, M.F. (1993). T cell receptor-beta mRNA splicing: regulation of unusual splicing intermediates. Molecular and cellular biology *13*, 1686-1696.

Ramakrishnan, V. (2002). Ribosome structure and the mechanism of translation. Cell *108*, 557-572.

Robledo, S., Idol, R.A., Crimmins, D.L., Ladenson, J.H., Mason, P.J., and Bessler, M. (2008). The role of human ribosomal proteins in the maturation of rRNA and ribosome production. RNA (New York, NY *14*, 1918-1929.

Rodnina, M.V., and Wintermeyer, W. (2001). Fidelity of aminoacyl-tRNA selection on the ribosome: kinetic and structural mechanisms. Annual review of biochemistry *70*, 415-435.

Rodnina, M.V., and Wintermeyer, W. (2009). Recent mechanistic insights into eukaryotic ribosomes. Curr Opin Cell Biol *21*, 435-443.

Rosado, I.V., Kressler, D., and de la Cruz, J. (2007). Functional analysis of Saccharomyces cerevisiae ribosomal protein Rpl3p in ribosome synthesis. Nucleic acids research *35*, 4203-4213.

Rubbi, C.P., and Milner, J. (2003). Disruption of the nucleolus mediates stabilization of p53 in response to DNA damage and other stresses. The EMBO journal *22*, 6068-6077.

Rubin, G.M., and Spradling, A.C. (1982). Genetic transformation of Drosophila with transposable element vectors. Science *218*, 348-353.

Ruiz-Echevarria, M.J., Gonzalez, C.I., and Peltz, S.W. (1998). Identifying the right stop: determining how the surveillance complex recognizes and degrades an aberrant mRNA. The EMBO journal *17*, 575-589.

Saka, Y., Hagemann, A.I., Piepenburg, O., and Smith, J.C. (2007). Nuclear accumulation of Smad complexes occurs only after the midblastula transition in Xenopus. Development (Cambridge, England) *134*, 4209-4218.

Sambrook, J., Fritsch, E.F., and Maniatis, T. (1989). Molecular Cloning: A Laboratory Manual (Second Edition) (New York, Cold Spring Harbor Laboratory Press).

Sayani, S., Janis, M., Lee, C.Y., Toesca, I., and Chanfreau, G.F. (2008). Widespread impact of nonsense-mediated mRNA decay on the yeast intronome. Mol Cell *31*, 360-370.

Schluenzen, F., Tocilj, A., Zarivach, R., Harms, J., Gluehmann, M., Janell, D., Bashan, A., Bartels, H., Agmon, I., Franceschi, F., *et al.* (2000). Structure of functionally activated small ribosomal subunit at 3.3 angstroms resolution. Cell *102*, 615-623.

Schneider, D.A., Michel, A., Sikes, M.L., Vu, L., Dodd, J.A., Salgia, S., Osheim, Y.N., Beyer, A.L., and Nomura, M. (2007). Transcription elongation by RNA polymerase I is linked to efficient rRNA processing and ribosome assembly. Mol Cell *26*, 217-229.

Schroder, P.A., and Moore, M.J. (2005). Association of ribosomal proteins with nascent transcripts in S. cerevisiae. RNA (New York, NY *11*, 1521-1529.

Schubert, U., Anton, L.C., Gibbs, J., Norbury, C.C., Yewdell, J.W., and Bennink, J.R. (2000). Rapid degradation of a large fraction of newly synthesized proteins by proteasomes. Nature *404*, 770-774.

Sekar, R.B., and Periasamy, A. (2003). Fluorescence resonance energy transfer (FRET) microscopy imaging of live cell protein localizations. The Journal of cell biology *160*, 629-633.

Shi, Y., Zhai, H., Wang, X., Han, Z., Liu, C., Lan, M., Du, J., Guo, C., Zhang, Y., Wu, K., *et al.* (2004). Ribosomal proteins S13 and L23 promote multidrug resistance in gastric cancer cells by suppressing drug-induced apoptosis. Experimental cell research *296*, 337-346.

Shopland, L.S., and Lis, J.T. (1996). HSF recruitment and loss at most Drosophila heat shock loci is coordinated and depends on proximal promoter sequences. Chromosoma *105*, 158-171.

Shuman, S. (2001). Structure, mechanism, and evolution of the mRNA capping apparatus. Progress in nucleic acid research and molecular biology *66*, 1-40.

Shyu, Y.J., Hiatt, S.M., Duren, H.M., Ellis, R.E., Kerppola, T.K., and Hu, C.D. (2008). Visualization of protein interactions in living Caenorhabditis elegans using bimolecular fluorescence complementation analysis. Nature protocols *3*, 588-596.

Shyu, Y.J., Liu, H., Deng, X., and Hu, C.D. (2006). Identification of new fluorescent protein fragments for bimolecular fluorescence complementation analysis under physiological conditions. BioTechniques *40*, 61-66.

Singh, G., Rebbapragada, I., and Lykke-Andersen, J. (2008). A competition between stimulators and antagonists of Upf complex recruitment governs human nonsense-mediated mRNA decay. PLoS Biol *6*, e111.

Sirri, V., Urcuqui-Inchima, S., Roussel, P., and Hernandez-Verdun, D. (2008). Nucleolus: the fascinating nuclear body. Histochem Cell Biol *129*, 13-31.

Soudet, J., Gelugne, J.P., Belhabich-Baumas, K., Caizergues-Ferrer, M., and Mougin, A. (2009). Immature small ribosomal subunits can engage in translation initiation in Saccharomyces cerevisiae. The EMBO journal.

Spahn, C.M., Beckmann, R., Eswar, N., Penczek, P.A., Sali, A., Blobel, G., and Frank, J. (2001). Structure of the 80S ribosome from Saccharomyces cerevisiae--tRNA-ribosome and subunit-subunit interactions. Cell *107*, 373-386.

Stamm, S., Ben-Ari, S., Rafalska, I., Tang, Y., Zhang, Z., Toiber, D., Thanaraj, T.A., and Soreq, H. (2005). Function of alternative splicing. Gene *344*, 1-20.

Thermann, R., Neu-Yilik, G., Deters, A., Frede, U., Wehr, K., Hagemeier, C., Hentze, M.W., and Kulozik, A.E. (1998). Binary specification of nonsense codons by splicing and cytoplasmic translation. The EMBO journal *17*, 3484-3494.

Tschochner, H., and Hurt, E. (2003). Pre-ribosomes on the road from the nucleolus to the cytoplasm. Trends in cell biology *13*, 255-263.

van Beekvelt, C.A., de Graaff-Vincent, M., Faber, A.W., van't Riet, J., Venema, J., and Raue, H.A. (2001). All three functional domains of the large ribosomal subunit protein L25 are required for both early and late pre-rRNA processing steps in Saccharomyces cerevisiae. Nucleic acids research *29*, 5001-5008.

Venema, J., and Tollervey, D. (1999). Ribosome synthesis in Saccharomyces cerevisiae. Annual review of genetics *33*, 261-311.

Veuthey, A.L., and Bittar, G. (1998). Phylogenetic relationships of fungi, plantae, and animalia inferred from homologous comparison of ribosomal proteins. J Mol Evol *47*, 81-92.

Warner, J.R. (1999). The economics of ribosome biosynthesis in yeast. Trends Biochem Sci *24*, 437-440.

Warner, J.R., and McIntosh, K.B. (2009). How common are extraribosomal functions of ribosomal proteins? Mol Cell *34*, 3-11.

Weeks, J.R., Hardin, S.E., Shen, J., Lee, J.M., and Greenleaf, A.L. (1993). Locus-specific variation in phosphorylation state of RNA polymerase II in vivo: correlations with gene activity and transcript processing. Genes & development *7*, 2329-2344.

Wells, S.E., Hillner, P.E., Vale, R.D., and Sachs, A.B. (1998). Circularization of mRNA by eukaryotic translation initiation factors. Mol Cell *2*, 135-140.

Weng, Y., Czaplinski, K., and Peltz, S.W. (1996). Identification and characterization of mutations in the UPF1 gene that affect nonsense suppression and the formation of the Upf protein complex but not mRNA turnover. Molecular and cellular biology *16*, 5491-5506.

West, M., Hedges, J.B., Chen, A., and Johnson, A.W. (2005). Defining the order in which Nmd3p and Rpl10p load onto nascent 60S ribosomal subunits. Molecular and cellular biology *25*, 3802-3813.

Wimberly, B.T., Brodersen, D.E., Clemons, W.M., Jr., Morgan-Warren, R.J., Carter, A.P., Vonrhein, C., Hartsch, T., and Ramakrishnan, V. (2000). Structure of the 30S ribosomal subunit. Nature *407*, 327-339.

Wool, I.G. (1979). The structure and function of eukaryotic ribosomes. Annual review of biochemistry *48*, 719-754.

Wool, I.G. (1996). Extraribosomal functions of ribosomal proteins. Trends Biochem Sci *21*, 164-165.

Wool, I.G., Chan, Y.L., and Gluck, A. (1995). Structure and evolution of mammalian ribosomal proteins. Biochem Cell Biol *73*, 933-947.

Wool, I.G., Chan, Y.L., Gluck, A., and Suzuki, K. (1991). The primary structure of rat ribosomal proteins P0, P1, and P2 and a proposal for a uniform nomenclature for mammalian and yeast ribosomal proteins. Biochimie *73*, 861-870.

Yusupov, M.M., Yusupova, G.Z., Baucom, A., Lieberman, K., Earnest, T.N., Cate, J.H., and Noller, H.F. (2001). Crystal structure of the ribosome at 5.5 A resolution. Science *292*, 883-896.

Zemp, I., and Kutay, U. (2007). Nuclear export and cytoplasmic maturation of ribosomal subunits. FEBS letters *581*, 2783-2793.

Zhang, J., Harnpicharnchai, P., Jakovljevic, J., Tang, L., Guo, Y., Oeffinger, M., Rout, M.P., Hiley, S.L., Hughes, T., and Woolford, J.L., Jr. (2007). Assembly factors Rpf2 and Rrs1 recruit 5S rRNA and ribosomal proteins rpL5 and rpL11 into nascent ribosomes. Genes & development *21*, 2580-2592.

Zhang, J., and Maquat, L.E. (1996). Evidence that the decay of nucleus-associated nonsense mRNA for human triosephosphate isomerase involves nonsense codon recognition after splicing. RNA (New York, NY *2*, 235-243.

Zhang, J., Sun, X., Qian, Y., LaDuca, J.P., and Maquat, L.E. (1998). At least one intron is required for the nonsense-mediated decay of triosephosphate isomerase mRNA: a possible link between nuclear splicing and cytoplasmic translation. Molecular and cellular biology *18*, 5272-5283.

Zhang, S., Ma, C., and Chalfie, M. (2004). Combinatorial marking of cells and organelles with reconstituted fluorescent proteins. Cell *119*, 137-144.

Zhang, S., Ruiz-Echevarria, M.J., Quan, Y., and Peltz, S.W. (1995). Identification and characterization of a sequence motif involved in nonsense-mediated mRNA decay. Molecular and cellular biology *15*, 2231-2244.

Zhimulev, I.F., Belyaeva, E.S., Semeshin, V.F., Koryakov, D.E., Demakov, S.A., Demakova, O.V., Pokholkova, G.V., and Andreyeva, E.N. (2004). Polytene chromosomes: 70 years of genetic research. Int Rev Cytol *241*, 203-275.

Zhou, Z., Licklider, L.J., Gygi, S.P., and Reed, R. (2002). Comprehensive proteomic analysis of the human spliceosome. Nature *419*, 182-185.

# Appendixes

## Appendix I.

## Recipes for *E. coli* growth media

### LB broth

Dissolve 10 g Bacto-tryptone, 5 g yeast extract, and 10 g NaCl in 800 ml $dH_2O$. Adjust pH to 7.5 with NaOH, bring the volume to 1L with $dH_2O$, transfer to a bottle and sterilize by autoclaving at 121°C for 15 minutes. Add antibiotics to cold media at the required concentration just before using it.

### Agar-LB plates

Dissolve 10 g Bacto-tryptone, 5 g yeast extract, 10 g NaCl and 10 g agar are dissolved in 800 mL of $dH_2O$. Adjust pH to 7.5 with NaOH, bring the volume to 1 L with $dH_2O$, transfer to a bottle and sterilize by autoclaving at 121°C for 15 minutes. Cool the media to about 60°C, add the required antibiotic (for example, 1 ml of 100 mg/ml ampicillin) and pour 25-30 ml/plate (9 cm Petri dishes). Plates can be stored at 4 °C for up to 4 weeks.

### SOC

Dissolve 20 g Bacto-tryptone, 5 g yeast extract, 0.6 g NaCl and 0.18 g KCl in 970 ml of $dH_2O$ and sterilize by autoclaving at 121°C for 15 minutes (before autoclaving, the media can be aliquoted into 20 ml glass bottles for convenience). Before using it, add the following (for 20 ml aliquot): 200 μL of 1 M $MgCl_2$, 200 μl of 1 M $MgSO_4$ and 240 μl of 30% glucose

## Appendix II.

## Ribosomal Proteins (RPs) cDNA nucleotide and amino acids sequences

The sequences of the primers used for Gateway cloning are reported below (the gene specific sequence is underlined; ATG and Kozak sequences are in italic. In bold are the Gateway recombination sequences (see Material and Methods). Primers have four guanines at the 5' end as required by the Gateway procedure

### RpS9

**DEFINITION** *Drosophila melanogaster* Ribosomal protein S9
**ACCESSION** NM_168350
**ORGANISM** *Drosophila melanogaster* (fruit fly)
**Translation**="MVNGRIPSVFSKTYVTPRRPYEKARLDQELKIIGEYGLRNKREVWRVKYALAKIRK
AARELLTLDEKDEKRLFQGNALLRRLVRIGVLDESRMKLDYVLGLKIEDFLERRLQTQVFKLGLAKSIH
HARVLIRQRHIRVRKQVVNIPSFVVRLDSQKHIDFSLKSPFGGGRPGRVKRKNLKKNQGGGGGAAEEEE
D

**cDNA sequence**

ATGGTGAACGGCCGCATACCCTCGGTCTTCTCGAAGACCTACGTGACTCCCCGTCGCCCCTATGAGAAG
GCGCGTCTGGACCAGGAGTTGAAGATCATCGGCGAGTATGGTCTGCGCAACAAGCGCGAAGTGTGGCGC
GTCAAGTACGCCCTGGCTAAGATCCGTAAGGCCGCTCGTGAGCTGCTGACCCTCGACGAGAAGGACGAG
AAGCGTCTGTTCCAGGGTAATGCCCTGCTGCGCCGTCTGGTCCGTATCGGTGTCCTGGACGAGTCCCGC
ATGAAGCTCGATTACGTGCTGGGTCTGAAGATTGAGGACTTCTTGGAGCGTCGTCTGCAGACGCAGGTG
TTCAAGCTGGGACTTGCCAAGTCCATCCATCATGCTCGCGTCCTGATCCGTCAGCGTCACATTCGTGTC
CGCAAGCAGGTGGTCAACATCCCGTCGTTCGTCGTGCGCCTGGACTCCCAGAAGCACATCGACTTCTCC
CTGAAGTCGCCCTTCGGCGGCGGCCGTCCCGGTCGCGTCAAGAGGAAGAACCTGAAGAAGAACCAGGGC
GGTGGCGGTGGAGCTGCTGAAGAGGAGGAGGACTAA

**Gateway Primer**
RpS9.att.start.Fow
GGGG**ACAAGTTTGTACAAAAAAGCAGGCT**TC*acc*<u>*atg*GTGAACGGCCGCAT
ACC</u>

RpS9.att.stop.Rev
GGGG**ACCACTTTGTACAAGAAAGCTGGGT**<u>CGTCCTCCTCCTCTTCAGCA</u>

.

# RpS15

**DEFINITION** *Drosophila melanogaster* Ribosomal protein S15
**ACCESSION** NM_137292
**Translation**"MADQVDENLKKKRTFKKFTYRGVDLDQLLDMPNNQLVELMHSRARRRFSRGLKRKPM
ALIKKLRKAKKEAPPNEKPEIVKTHLRNMIIVPEMTGSIIGVYNGKDFGQVEVKPEMIGHYLGEFALTY
KPVKHGRPGIGATHSSRFIPLK"
**cDNA sequence**

ATGGCCGATCAAGTCGATGAAAATCTGAAGAAGAAGCGTACCTTCAAGAAGTTCACCTACCGCGGTGTC
GACTTGGACCAGCTTCTGGACATGCCCAACAACCAGCTGGTGGAGCTGATGCACAGCCGTGCCCGCAGG
CGTTTCTCCCGCGGACTGAAGCGCAAGCCAATGGCTCTGATCAAGAAGCTGCGCAAGGCCAAGAAGGAG
GCACCGCCAAATGAGAAGCCCGAGATTGTCAAGACCCACCTGAGGAACATGATCATCGTACCCGAGATG
ACCGGCTCCATCATTGGCGTCTACAACGGCAAGGACTTCGGACAGGTGGAGGTCAAGCCCGAGATGATC
GGTCACTACCTGGGCGAGTTCGCCCTGACCTACAAGCCCGTCAAGCACGGTCGTCCTGGTATCGGTGCC
ACCCACAGCTCCCGTTTCATTCCTCTGAAGTGA

**Gateway Primer**
RpS15.att.start.Fow
GGGG**ACAAGTTTGTACAAAAAAGCAGGCT**TC*acc*<u>*atg*</u><u>GCCGATCAAGTCGATGAAAA</u>

RpS15.att.stop.Rev
GGGG**ACCACTTTGTACAAGAAAGCTGGGT**<u>CCTTCAGAGGAATGAAACG</u>

# RpS18

**DEFINITION** *Drosophila melanogaster* Ribosomal protein S18
**ACCESSION** NM_166383
**Translation**
"MSLVIPEKFQHILRIMNTNIDGKRKVGIAMTAIKGVGRRYSNIVLKKADVDLTKRAGECTEEEVDKVV
TIISNPLQYKVPNWFLNRQKDIIDGKYWQLTSSNLDSKLRDDLERLKKIRSHRGLRHYWGLRVRGQHTK
TTGRRGRTVGVSKKK"
**cDNA sequence**

ATGTCGCTCGTCATCCCAGAGAAGTTCCAGCACATCCTGCGTATCATGAATACGAACATCGACGGCAAG
CGCAAGGTTGGCATCGCCATGACCGCCATCAAGGGAGTGGGTCGCCGCTACTCCAACATTGTGCTGAAG
AAGGCCGATGTCGATCTTACCAAGCGCGCCGGTGAGTGCACCGAGGAGGAGGTCGACAAGGTGGTGACC
ATCATCTCGAACCCTCTGCAGTACAAGGTGCCCAACTGGTTCCTCAACAGGCAGAAGGACATCATCGAT
GGCAAGTACTGGCAGCTGACCTCCTCCAACTTGGACTCGAAGCTGCGTGACGATCTGGAGCGTCTGAAG
AAGATCCGCTCCCACCGTGGTCTGCGTCACTACTGGGGCCTCCGTGTGCGTGGCCAGCACACCAAGACC
ACCGGTCGTCGTGGTCGCACCGTGGGTGTGTCCAAGAAGAAGTAA

**Gateway Primer**
RpS18.att.start.Fow
GGGG**ACAAGTTTGTACAAAAAAGCAGGCT**TC*acc*<u>*atg*</u><u>TCGCTCGTCATCCCAGA</u>

RpS18.att.stop.Rev
GGGG**ACCACTTTGTACAAGAAAGCTGGGT**<u>CCTTCTTCTTGGACACACCCAC</u>

# RpS13

DEFINITION  *Drosophila melanogaster* Ribosomal protein S13.
ACCESSION   AY058536
translation="MGRMHAPGKGISQSALPYRRTVPSWLKLNADDVKEQIKKLGKKG
LTPSKIGIILRDSHGVAQVRFVNGNKILRIMKSVGLKPDIPEDLYHMIKKAVAIRKHL
ERNRKDKDGKFRLILVESRIHRLARYYKTKSVLPPNWKYESSTASALVA"
**cDNA sequence**

ATGGGTCGTATGCACGCTCCTGGCAAGGGTATTTCCCAATCAGCCCTCCCCTACAGACGCACTGTCCCA
TCCTGGCTGAAACTGAACGCAGATGATGTCAAGGAGCAGATTAAGAAGCTGGGCAAGAAGGGTCTGACT
CCCTCCAAAATCGGCATCATCCTGCGTGACTCGCACGGAGTTGCCCAGGTGCGTTTCGTCAACGGAAAC
AAGATCCTGCGCATCATGAAGTCGGTGGGTCTGAAGCCCGACATTCCCGAGGATCTGTACCACATGATC
AAGAAGGCCGTCGCCATCCGCAAGCACTTGGAGCGCAACCGCAAGGACAAGGACGGCAAGTTCCGTCTG
ATTCTGGTCGAGTCCAGGATCCACCGCCTGGCCCGCTACTACAAGACCAAGAGCGTCCTGCCCCCCAAC
TGGAAATACGAGTCGAGCACTGCCTCCGCCCTGGTTGCCTAA

**Gateway Primer**
RpS13.att.start.Fow
GGGG**ACAAGTTTGTACAAAAAAGCAGGCT**TC*accatg*GTGAACGGCCGCAT
ACC

RpS13.att.stop.Rev
GGGG**ACCACTTTGTACAAGAAAGCTGGGT**CGTCCTCCTCCTCTTCAGCA

# RpS5a

DEFINITION  *Drosophila melanogaster* Ribosomal protein S15a.
ACCESSION  AY075368
translation="MAEVAENVVETFEEPAAPMEAEVAETILETNVVSTTELPEIKLF
GRWSCDDVTVNDISLQDYISVKEKFARYLPHSAGRYAAKRFRKAQCPIVERLTCSLMM
KGRNNGKKLMACRIVKHSFEIIHLLTGENPLQILVSAIINSGPREDSTRIGRAGTVRR
QAVDVSPLRRVNQAIWLLCTGAREAAFRNIKTIAECLADELINAAKGSSNSYAIKKKD
ELERVAKSNR"

**cDNA sequence**

ATGGCCGAAGTTGCTGAAAACGTGGTGGAGACCTTCGAGGAGCCAGCGGCACCTATGGAAGCCGAGGTG
GCCGAGACGATCCTGGAGACAAATGTGGTGTCCACCACTGAGCTGCCGGAGATCAAGCTGTTCGGCCGC
TGGTCTTGCGACGATGTCACCGTTAACGACATCTCTCTGCAGGATTACATCTCGGTGAAGGAGAAGTTT
GCCCGCTATCTTCCCCATTCCGCCGGACGTTATGCCGCCAAGCGTTTCCGCAAGGCCCAGTGCCCCATT
GTGGAGCGTTTGACCTGCTCCCTGATGATGAAGGGTCGCAACAACGGCAAGAAGCTGATGGCCTGCCGC
ATCGTCAAGCACTCGTTCGAGATCATTCATCTGCTCACCGGGGAGAACCCTCTGCAGATCCTGGTCAGC
GCCATCATCAACTCGGGACCCCGTGAGGACTCCACCCGTATTGGACGTGCCGGTACCGTCCGTCGCCAG
GCCGTCGATGTGTCGCCCCTGCGTCGCGTCAACCAGGCTATCTGGCTGCTGTGCACTGGAGCTCGTGAG
GCTGCCTTCAGGAACATCAAGACCATCGCCGAGTGCCTGGCTGATGAGCTGATCAACGCTGCTAAGGGA
TCTTCCAACTCGTACGCCATCAAGAAGAAGGATGAGTTGGAGCGTGTCGCCAAGTCCAACCGTTAA

**Gateway Primer**

RpS5a.att.start.Fow

GGGG**ACAAGTTTGTACAAAAAAGCAGGCT**TC*acc*<u>*atg*</u><u>GTGAACGGCCGCAT</u>
<u>ACC</u>

RpS5a.att.stop.Rev

GGGG**ACCACTTTGTACAAGAAAGCTGGGT**<u>CGTCCTCCTCCTCTTCAGCA</u>

# RpS2

**DEFINITION** *Drosophila melanogaster* Ribosomal protein S2.
**ACCESSION** AY094799
translation="MADEAPARSGFRGGFGSRGGRGGRGRGRGRWARGRGKEDSKEWV
QRTRFKAFVAIGDNNGHIGLGVKCSKEVATAIRGAIILAKLSVVPVRRGYWGNKIGKP
HTVPCKVTGKCGSVSVRLIPAPRGTGIVSAPVPKKLLTMAGIEDCYTSARGSTGTLGN
FAKATYAAIAKTYAYLTPDLWKEMPLGSTPYQAYSDFLSKPTPRLHADA"
**cDNA sequence**

ATGGCGGACGAAGCTCCAGCCCGTAGTGGATTCCGTGGCGGATTTGGCTCTCGTGGTGGTCGTGGTGGA
CGCGGTCGTGGCCGTGGACGCTGGGCCCGTGGACGTGGAAAGGAGGACTCCAAGGAGTGGGTGCCAGTG
ACCAAGCTGGGACGCCTGGTGCGCGAGGGCAAGATCAAGTCTTTGGAGGAGATCTACCTGTACTCGCTT
CCCATCAAAGAGTTCGAGATCATCGACTTCTTCCTGGGATCCTCGCTGAAGGATGAGGTGCTGAAGATC
ATGCCCGTCCAGAAGCAGACCCGTGCTGGTCAGCGTACCCGTTTCAAGGCCTTCGTTGCCATCGGCGAC
AACAATGGCCACATTGGTCTGGGCGTTAAGTGCAGCAAGGAAGTGGCCACCGCCATCCGTGGTGCCATC
ATTCTGGCCAAGCTCTCCGTGGTGCCCGTGCGCCGTGGCTACTGGGGCAACAAGATCGGCAAGCCCCAC
ACCGTGCCCTGCAAGGTCACCGGCAAGTGCGGTTCCGTCTCCGTGCGCCTCATCCCCGCTCCCCGTGGT
ACTGGCATTGTCTCGGCCCCCGTGCCCAAGAAGCTGCTGACCATGGCCGGTATTGAGGATTGCTACACC
TCGGCCCGTGGCTCCACTGGAACCCTCGGCAACTTCGCCAAGGCTACATATGCCGCCATCGCCAAGACG
TACGCGTACTTGACCCCCGATCTGTGGAAGGAGATGCCTCTGGGCTCCACTCCTTACCAGGCATACTCG
GACTTCCTGTCCAAGCCCACTCCTCGTCTGCACGCCGATGCCTAA

**Gateway Primer**
RpS2.att.start.Fow
GGGG**ACAAGTTTGTACAAAAAAGCAGGCT**TC*accatg*GTGAACGGCCGCAT
ACC

RpS2.att.stop.Rev
GGGG**ACCACTTTGTACAAGAAAGCTGGGT**CGTCCTCCTCCTCTTCAGCA

# RpL11

**DEFINITION** *Drosophila melanogaster* Ribosomal protein L11
**ACCESSION** NM_057706

**TRANSLATION**="MAAVTKKIKRDPAKNPMRDLHIRKLCLNICVGESGDRLTRAAKV
LEQLTGQQPVFSKARYTVRSFGIRRNEKIAVHCTVRGAKAEEILERGLKVREYELRRE
NFSSTGNFGFGIQEHIDLGIKYDPSIGIYGLDFYVVLGRPGYNVNHRKRKSGTVGFQH
RLTKEDAMKWFQQKYDGIILNTKK"
**cDNA sequence**

ATGGCGGCGGTTACCAAGAAGATTAAGCGCGATCCCGCGAAGAACCCGATGAGGGATCTGCACATCCGC
AAACTCTGCCTGAACATCTGCGTGGGCGAGTCCGGTGACAGGCTGACCCGTGCCGCCAAGGTGCTGGAG
CAGCTGACTGGTCAGCAGCCAGTGTTCTCCAAGGCCCGCTACACGGTCCGTTCGTTCGGTATTCGCCGT
AACGAGAAGATCGCTGTCCACTGCACGGTGCGCGGCGCCAAGGCTGAGGAGATTCTGGAGCGTGGCCTG
AAGGTGCGCGAGTACGAGCTGCGTCGGGAGAACTTCTCCTCCACCGGCAACTTCGGTTTCGGCATCCAG
GAACACATCGATCTGGGCATCAAGTACGATCCCTCCATCGGTATCTATGGTCTGGACTTCTACGTCGTC
CTCGGCCGCCCTGGCTACAATGTGAACCACAGGAAGCGCAAGTCCGGCACTGTCGGCTTCCAGCACCGC
CTCACCAAGGAGGATGCCATGAAGTGGTTCCAGCAGAAATACGATGGTATCATCTTGAACACCAAGAAG
TAG

**Gateway Primer**

RpL11.att.start.Fow
GGGG**ACAAGTTTGTACAAAAAAGCAGGCT**TC*accatg*GCGGCGGTTACCAA
G

RpL11.att.stop.Rev
GGGG**ACCACTTTGTACAAGAAAGCTGGGT**CCTTCTTGGTGTTCAAGATG

# RpL36

DEFINITION  *Drosophila melanogaster* Ribosomal protein L36.
ACCESSION   AY070831

translation="MAVRYELAIGLNKGHKTSKIRNVKYTGDKKVKGLRGSRLKNIQT
RHTKFMRDLVREVVGHAPYEKRTMELLKVSKDKRALKFLKRRLGTHIRAKRKREELSN
ILTQLRKAQTHAK"

**cDNA sequence**

ATGGCAGTGCGCTACGAGCTGGCTATTGGCCTGAACAAGGGCCACAAGACCTCGAAGATCAGGAATGTG
AAGTACACCGGCGACAAGAAGGTCAAGGGTCTGCGCGGATCGCGCTTGAAGAACATCCAAACCCGCCAC
ACCAAGTTCATGCGCGACTTGGTCCGCGAGGTCGTTGGCCACGCTCCCTATGAGAAGCGCACCATGGAG
TTGCTGAAGGTGTCCAAGGATAAGAGGGCCCTGAAGTTCCTCAAGCGCCGCCTGGGCACCCACATCCGT
GCCAAGAGGAAGCGTGAGGAGTTGTCCAACATCCTCACCCAGCTGAGGAAGGCCCAGACCCACGCCAAG
TAA

**Gateway Primer**

RpL36.att.start.Fow

GGGG**ACAAGTTTGTACAAAAAAGCAGGCT**TC*acc*<u>*atg*</u><u>GTGAACGGCCGCAT</u>
<u>ACC</u>

RpL36.att.stop.Rev

GGGG**ACCACTTTGTACAAGAAAGCTGGGT**<u>CGTCCTCCTCCTCTTCAGCA</u>

# RpL32

DEFINITION  *Drosophila melanogaster* Ribosomal protein L32.
ACCESSION   BT011442

translation="MDTAQEASPTCFKMTIRPAYRPKIVKKRTKHFIRHQSDRYAKLS
HKWRKPKGIDNRVRRRFKGQYLMPNIGYGSNKRTRHMLPTGFKKFLVHNVRELEVLLM
QNRVYCGEIAHGVSSKKRKEIVERAKQLSVRLTNPNGRLRSQENE"
**cDNA sequence**

ATGACCATCCGCCCAGCATACAGGCCCAAGATCGTGAAGAAGCGCACCAAGCACTTCATCCGCCACCAG
TCGGATCGATATGCTAAGCTGTCGCACAAATGGCGCAAGCCCAAGGGTATCGACAACAGAGTGCGTCGC
CGCTTCAAGGGACAGTATCTGATGCCCAACATCGGTTACGGATCGAACAAGCGCACCCGCCACATGCTG
CCCACCGGATTCAAGAAGTTCCTGGTGCACAACGTGCGCGAGCTGGAGGTCCTGCTCATGCAGAACCGC
GTTTACTGCGGCGAGATCGCCCACGGCGTCTCCTCCAAGAAGCGCAAGGAGATTGTCGAGCGCGCCAAG
CAGCTGTCGGTCCGCCTCACCAACCCCAACGGTCGCCTGCGTTCTCAAGAGAACGAGTAA

**Gateway Primer**
RpL32.att.start.Fow
GGGG**ACAAGTTTGTACAAAAAAGCAGGCT**TC*acc*<u>*atg*</u><u>GTGAACGGCCGCAT</u>
<u>ACC</u>

RpL32.att.stop.Rev
GGGG**ACCACTTTGTACAAGAAAGCTGGGT**<u>CGTCCTCCTCCTCTTCAGCA</u>

# RpL23

DEFINITION  *Drosophila melanogaster* Ribosomal protein L23.
ACCESSION   BT031034

translation="MSKRGRGGTAGGKFRISLGLPVGAVMNCADNTGAKNLYVIAVHG
IRGRLNRLPAAGVGDLFVATVKKGKPELRKKVMPAVVIRQRKPFRRRDGVFIYFEDNA
GVIVNNKGEMKGSAITGPVAKECADLWPRIASNASSIA"
**cDNA sequence**

ATGTCGAAGAGAGGACGTGGAGGTACCGCGGGAGGCAAGTTCCGCATCTCCCTCGGTTTGCCCGTGGGC
GCCGTGATGAACTGTGCCGACAACACCGGAGCCAAGAACCTGTACGTGATCGCCGTCCACGGAATCCGC
GGTCGCCTTAACCGTCTGCCCGCCGCTGGTGTCGGCGACATGTTCGTGGCCACCGTGAAGAAGGGAAAG
CCCGAGCTCAGGAAGAAGGTCATGCCTGCCGTGGTTATTCGGCAGCGCAAACCGTTCAGGAGGAGGGAC
GGGGTGTTTATATACTTTGAGGACAATGCCGGGGTAATAGTAAACAACAAGGGCGAAATGAAGGGCTCG
GCCATCACTGGACCGGTGGCCAAGGAATGCGCCGATCTGTGGCCCCGTATTGCATCCAATGCAAGCTCT
ATAGCCTAA

**Gateway Primer**

RpL23.att.start.Fow
GGGG**ACAAGTTTGTACAAAAAAGCAGGCT**TC*acc*<u>*atg*</u><u>GTGAACGGCCGCAT
ACC</u>

RpL23.att.stop.Rev
GGGG**ACCACTTTGTACAAGAAAGCTGGGT**<u>CGTCCTCCTCCTCTTCAGCA</u>

# RpL8

DEFINITION  *Drosophila melanogaster* Ribosomal protein L8.
ACCESSION   AY071342
translation="MGRVIRAQRKGAGSVFKAHVKKRKGAAKLRSLDFAERSGYIRGV
VKDIIHDPGRGAPLAVVHFRDPYRYKIRKELFIAPEGMHTGQFVYCGRKATLQIGNVM
PLSQMPEGTIICNLEEKTGDRGRLARTSGNYATVIAHNQDTKKTRVKLPSGAKKVVPS
ANRAMVGIVAGGGRIDKPILKAGRAYHKYKVKRNSWPKVRGVAMNPVEHPHGGGNHQH
IGKASTVKRGTSAGRKVGLIAARRTGRIRGGKGDSKDK"

**cDNA sequence**

ATGGGTCGCGTTATTCGTGCACAGCGTAAGGGAGCTGGTTCCGTGTTCAAGGCGCACGTGAAGAAGCGC
AAGGGAGCCGCCAAGCTGCGTTCCCTGGACTTCGCCGAGCGTTCCGGCTACATCCGCGGAGTTGTCAAG
GACATCATCCACGATCCCGGCCGTGGCGCTCCTCTGGCCGTCGTCCACTTCCGCGACCCCTACCGCTAC
AAGATCCGCAAGGAGCTGTTCATCGCCCCCGAGGGCATGCACACCGGCCAGTTCGTGTACTGCGGCCGC
AAGGCCACCCTTCAGATCGGCAACGTGATGCCCCTCAGCCAGATGCCCGAGGGTACCATCATCTGCAAC
CTGGAGGAGAAGACCGGTGATCGCGGCCGTTTGGCCCGCACCTCTGGCAACTACGCCACCGTGATTGCC
CACAACCAGGACACCAAGAAGACGCGTGTCAAGCTGCCATCCGGCGCCAAGAAGGTCGTGCCCTCGGCC
AACCGCGCCATGGTTGGCATCGTCGCCGGCGGCGGTCGTATCGACAAGCCCATCCTGAAGGCCGGTCGT
GCCTACCACAAGTACAAGGTGAAGCGCAACAGCTGGCCTAAGGTGCGTGGTGTGGCCATGAACCCCGTG
GAGCATCCTCACGGTGGTGGTAACCATCAGCACATTGGTAAGGCCTCCACCGTCAAGCGAGGCACATCC
GCCGGTCGCAAGGTCGGTCTCATCGCTGCCCGTCGTACCGGTAGGATCCGTGGTGGCAAGGGCGACAGC
AAGGACAAGTAA

**Gateway Primer**

RpL8.att.start.Fow

GGGG**ACAAGTTTGTACAAAAAAGCAGGCT**TC*acc**atg***GTGAACGGCCGCAT
ACC

RpL8.att.stop.Rev

GGGG**ACCACTTTGTACAAGAAAGCTGGGT**CGTCCTCCTCCTCTTCAGCA

**(A) BiFC-YC (155-239)**

aaacagaaagtcatgaaccacgacaagcagaagaacggcatcaaggtgaacttcaagatccgccacaacatcgaggac
ggcagcgtgcagctcgccgaccactaccagcagaacacccccatcggcgacggccccgtgctgctgcccgacaaccac
tacctgagctaccagtccgccctgagcaaagaccccaacgagaagcgcgatcacatggtcctgctggagttcgtgaccgc
cgccgggatcactctcggcatggacgagctgtacaagtaa

**(B) BiFC-YN (1-154)**

agatccatcgccaccatggtgagcaagggcgaggagctgttcaccggggtggtgcccatcctggtcgagctggacggcg
acgtaaacggccacaagttcagcgtgtccggcgagggcgagggcgatgccacctacggcaagctgaccctgaagttcat
ctgcaccaccggcaagctgcccgtgccctggcccaccctcgtgaccaccttcggctacggcctgcagtgcttcgcccgct
accccgaccacatgaagcagcacgacttcttcaagtccgccatgcccgaaggctacgtccaggagcgcaccatcttcttca
aggacgacggcaactacaagacccgcgccgaggtgaagttcgagggcgacaccctggtgaaccgcatcgagctgaag
ggcatcgacttcaaggaggacggcaacatcctggggcacaagctggagtacaactacaacagccacaacgtctatatcat
g

**(C)**

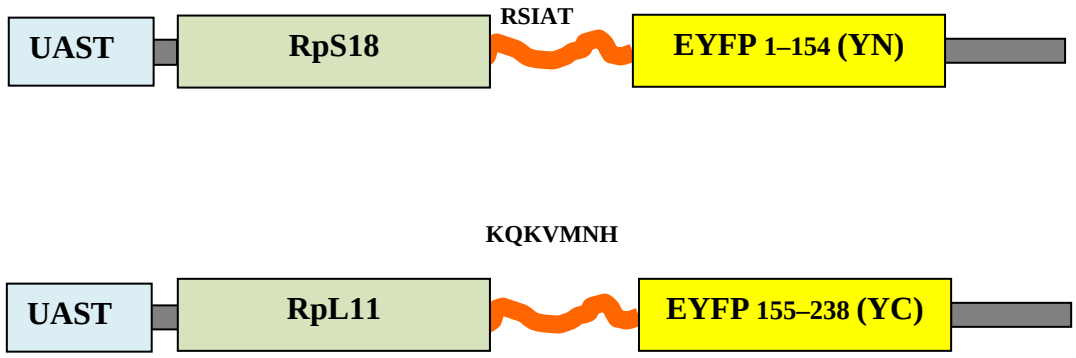


**Figure S1 Sequences of EYFP based BiFC fragments and schematic of the constructs.**

(A) BiFC-YC (155-239) sequence: the shaded region shows the linker sequence (KQKVMNH) and the red nucleotides indicate the C-terminal (155-239) fragment of YFP.

(B) BiFC-YN (1-154) sequence: the shaded region shows the linker sequence (RSIAT) and the red nucleotides indicate the N-terminal (1-154) fragment of YFP.

(C) Schematic of the pUAST-RpS18-YN and pUAST-RpL11-YC constructs.

## Appendix III. Primers, Constructs list and fly strains used in this study

### Table 1. Primers

| Primer cod | Primer name | Primer Sequences (5' to 3') |
|---|---|---|
| KJ1 | BamH1-RpS9.Fow | GGG GGA TCC ACC ATG GTG AAC GGC CGC ATA CCC |
| KJ2 | Bgl II-RpS9 Rev | GGG AGA TCT GTC CTC CTC CTC TTC AGC AGC |
| KJ3 | BamHI-RpS9 Rev | GGG GGA TCC TTA GTC CTC CTC CTC TTC AGC AGC |
| KJ4 | RpS9.att.start.Fow | GGGGACAAGTTTGTACAAAAAAGCAGGCTTCaccatgGT GAACGGCCGCATACC |
| KJ5 | RpS9.att.stop.Rev | GGGGACCACTTTGTACAAGAAAGCTGGGTCGTCCTC CTCCTCTTCAGCA |
| KJ6 | BamH1-RpS15.Fow | GGG GGA TCC ACC ATG GCC GAT CAA GTC GAT GAA |
| KJ7 | BamHI-RpS15 Rev | GGG GGA TCC TCA CTT CAG AGG AAT GAA ACG |
| KJ8 | RpS15.att.cds.fow | GGGGACAAGTTTGTACAAAAAAGCAGGCTTCACCAT GGCCGATCAAGTCGATGAAAA |
| KJ9 | RpS15.att.stop.rev | GGGGACAAGTTTGTACAAGAAAGCTGGGTCCTTCAG AGGAATGAAACG |
| KJ10 | Bgl II-RpS15 Rev | GGG AGA TCT CTT CAG AGG AAT GAA ACG |
| KJ11 | BamH1-RpS18.Fow | GGG GGA TCC ATG TCG CTC GTC ATC CCA GA ` |
| KJ12 | BamHI-RpS18 Rev | GGG GGA TCC TTA CTT CTT CTT GGA CAC ACC CAC |

| | | |
|---|---|---|
| **KJ13** | **RpS18.att.Start.Fow** | **GGGGACAAGTTTGTACAAAAAAGCAGGCTTCACCATGTCGCTCGCTCGTCATCCCAGAGA** |
| **KJ14** | **RpS18.att.sto.rev** | **GGGGACAAGTTTGTACAAGAAAGCTGGGTCCTTCTTCTTGGACACACCCAC** |
| **KJ15** | **Bgl II-RpS18 Rev** | **GGG AGA TCT CTT CTT CTT GGA CAC ACC CAC** |
| **KJ16** | **UASP Rev** | **GGCAAGGGTCGAGTCGATAG** |
| **KJ17** | **BamH1-RpL11 Fow** | **GGG GGA TCC ATG GCG GCG GTT ACC AAG** |
| **KJ18** | **BamHI- RpL11 Rev n-fusion** | **GGG GGA TCC CTA CTT CTT GGT GTT CAA GAT G** |
| **KJ19** | **Bgl II- RpL11 Rev** | **GGG AGA TCT CTT CTT GGT GTT CAA GAT G** |
| **KJ20** | **RpL11.att.start.Fow** | **GGGGACAAGTTTGTACAAAAAAGCAGGCTTCaccatgGCGGCGGTTACCAAG** |
| **KJ21** | **RpL11.att.stop.Rev** | **GGGGACCACTTTGTACAAGAAAGCTGGGTCCTTCTTGGTGTTCAAGATG** |
| **KJ22** | **RpL11.att.cds.fow** | **GGGGACAAGTTTGTACAAAAAAGCAGGCTTCACCATGGCGGTAGGTTCAACCAC** |
| **KJ23** | **UASPf** | **GGCAAGGGTCGAGTCGATAG** |
| **KJ24** | **GFPr** | **CTTCGGGCATGGCGGACTTG** |
| **KJ25** | **RFPr** | **GGACAGCTTCAAGTAGTCGG** |
| **KJ26** | **M13 forward** | **GTAAAACGACGGCCAG** |
| **KJ27** | **M13 Reverse** | **CAGGAAACAGCTATGAC** |

| | | |
|---|---|---|
| **KJ28** | **BamH-BiFC-YN Fow** | **GGG GGA TCC AGA TCC ATC GCC A** |
| **KJ29** | **Bgl II-BiFC-YN Rev** | **GGG AGA TCT CTA GGC CAT GAT ATA GAC** |
| **KJ30** | **BamH-BiFC-YC Fow** | **GGG GGA TCC AAA CAG AAA GTC ATG AAC** |
| **KJ31** | **Bgl II -BiFC-YC Rev** | **GGG AGA TCT TTA CTT GTA CAG CTC GTC** |
| **KJ32** | **BglII-BiFC-YN Fow N-fusion** | **GGG GGA TCC acc atg GTG AGC AAG GGC GAG** |
| **KJ33** | **BamH1-BiFC-YN Rev N-fusion** | **GGG GGA TCC GGT GGC GAT GGA TCT CAT GAT ATA GAC GTT GAG** |
| **KJ34** | **BglII -BiFC-YC Fow N-fusion** | **GGG GGA TCC acc atg GAC AAG CAG AAG AAC GGC** |
| **KJ35** | **BamH1-BiFC-YC Rev N-fusion** | **GGG GGA TCC GTG GTT CAT GAC TTT CTG TTT CTT GTA CAG CTC GTC CAT** |
| **KJ36** | **RpL36.att.Fow** | **GGGGACAAGTTTGTACAAAAAAGCAGGCTTCaccATG GCAGTGCGCTACGAGCT** |
| **KJ37** | **RpL36.att.Stop.Rev** | **GGGGACCACTTTGTACAAGAAAGCTGGGTcTTACTTG GCGTGGGTCTGGGC** |
| **KJ38** | **RpL36.att.Rev** | **GGGGACCACTTTGTACAAGAAAGCTGGGTcCTTGGCG TGGGTCTGGGC** |
| **KJ39** | **RpL8.att.Fow** | **GGGGACAAGTTTGTACAAAAAAGCAGGCTTCaccATG GGTCGCGTTATTCGTGCA** |
| **KJ40** | **RpL8.att.Stop.Rev** | **GGGGACCACTTTGTACAAGAAAGCTGGGTcTTACTTG TCCTTGCTGTCGCC** |
| **KJ41** | **RpL8.att.Rev** | **GGGGACCACTTTGTACAAGAAAGCTGGGTcCTTGTCC TTGCTGTCGCC** |

| | | |
|---|---|---|
| **KJ42** | **RpL32.att.Fow** | **GGGGACAAGTTTGTACAAAAAAGCAGGCTTCaccATGACCATCCGCCCAGCATACA** |
| **KJ43** | **RpL32.stt.stop.Rev** | **GGGGACCACTTTGTACAAGAAAGCTGGGTcTTACTCGTTCTCTTGAGAACG** |
| **KJ44** | **RpL32.stt.Rev** | **GGGGACCACTTTGTACAAGAAAGCTGGGTcCTCGTTCTCTTGAGAACG** |
| **KJ45** | **RpL23A.att.Fow** | **GGGGACAAGTTTGTACAAAAAAGCAGGCTTCaccATGCCACCCAAAAAGCCAACC** |
| **KJ46** | **RpL23A.att.stop.Rev** | **GGGGACCACTTTGTACAAGAAAGCTGGGTcTTATATGATGCCGATCTTGTT** |
| **KJ47** | **RpL23A.att.Rev** | **GGGGACCACTTTGTACAAGAAAGCTGGGTcTATGATGCCGATCTTGTT** |
| **KJ48** | **RpL23.att.Fow** | **GGGGACAAGTTTGTACAAAAAAGCAGGCTTCaccATGTCGAAGAGAGGACGTGGA** |
| **KJ49** | **RpL23.att.stop.Rev** | **GGGGACCACTTTGTACAAGAAAGCTGGGTcTTAGGCTATAGAGCTTGCATT** |
| **KJ50** | **RpL23.att.Rev** | **GGGGACCACTTTGTACAAGAAAGCTGGGTcGGCTATAGAGCTTGCATT** |
| **KJ51** | **RpS5a.att.Fow** | **GGGGACAAGTTTGTACAAAAAAGCAGGCTTCaccATGGCCGAAGTTGCTGAAAAC** |
| **KJ52** | **RpS5a.att.stop.Rev** | **GGGGACCACTTTGTACAAGAAAGCTGGGTcTTAACGGTTGGACTTGGCGAC** |
| **KJ53** | **RpS5a.att.Rev** | **GGGGACCACTTTGTACAAGAAAGCTGGGTcACGGTTGGACTTGGCGAC** |
| **KJ54** | **RpS13.att.Fow** | **GGGGACAAGTTTGTACAAAAAAGCAGGCTTCaccATGGGTCGTATGCACGCTCCT** |
| **KJ56** | **RpS13.att.stop.Rev** | **GGGGACCACTTTGTACAAGAAAGCTGGGTcTTAGGCAACCAGGGCGGAGGC** |
| **KJ57** | **RpS13.att.Rev** | **GGGGACCACTTTGTACAAGAAAGCTGGGTcGGCAACC** |

| | | |
|---|---|---|
| | | **AGGGCGGAGGC** |
| **KJ58** | **RpS11.att.Fow** | **GGGGACAAGTTTGTACAAAAAAGCAGGCTTCaccATG GCTGATCAGAACGAGCGC** |
| **KJ59** | **RpS11.att.stop.Rev** | **GGGGACCACTTTGTACAAGAAAGCTGGGTcCTAGTAC TTCTTGAAGCTCTT** |
| **KJ60** | **RpS11.att.Rev** | **GGGGACCACTTTGTACAAGAAAGCTGGGTcGTACTTC TTGAAGCTCTT** |
| **KJ61** | **RpS3.att.Fow** | **GGGGACAAGTTTGTACAAAAAAGCAGGCTTCaccATGA ATGCGAACCTTCCGATT** |
| **KJ62** | **RpS3.att.stop.Rev** | **GGGGACCACTTTGTACAAGAAAGCTGGGTcTTACAAA ACTTTCGCCTCGGA** |
| **KJ63** | **RpS3.att.Rev** | **GGGGACCACTTTGTACAAGAAAGCTGGGTcCAAAACT TTCGCCTCGGA** |
| **KJ64** | **RpS2.att.Fow** | **GGGGACAAGTTTGTACAAAAAAGCAGGCTTCaccATG GCGGACGAAGCTCCAGCC** |
| **KJ65** | **RpS2.att.stop.Rev** | **GGGGACCACTTTGTACAAGAAAGCTGGGTcTTAGGCA TCGGCGTGCAGACG** |
| **KJ66** | **RpS2.att.Rev** | **GGGGACCACTTTGTACAAGAAAGCTGGGTcGGCATCG GCGTGCAGACG** |
| **KJ67** | **KpnI-pTW Fow** | **GGG*GGTACC*GAGAACTCTGAATAGGGAATTG** |
| **KJ68** | **KpnI-pTW- Rev** | **GGG*GGTACC*AGATCCTCTAGCTTACGTCA** |
| **KJ69** | **Not1-YN-Fow** | **GGG GCGGCCGC ACC ATG GTG AGC AAG GGC GAG GAG** |
| **KJ70** | **Kpn1-YN-Rev** | **GGG GGTACC TTA CAT GAT ATA GAC GTT GTG** |
| **KJ71** | **Not1-YC-Fow** | **GGG GCGGCCGC ACC ATG GAC AAG CAG AAG AAC GGC** |

| | | |
|---|---|---|
| **KJ72** | **Kpn1-YC-Rev** | **GGG GGTACC TTA CTT GTA CAG CTC GTC CAT** |
| **KJ73** | **UAST - Rev** | **GTCACACCACAGAAGTAAGG** |
| **KJ74** | **UAST - Fow** | **CATGTCCGTGGGGTTTGA** |

**Table 2. Constructs list**

| Construct code | Construct name | Construct origin |
|---|---|---|
| K1 | pAWG-RpS9 | K.Jubran |
| K2 | pAWG-RpS15 | K.Jubran |
| K3 | pAWG-RpS18 | K.Jubran |
| K4 | pAWG-RpL11 | K.Jubran |
| K5 | pAGW-RpS9 | K.Jubran |
| K6 | pAGW-RpS15 | K.Jubran |
| K7 | pAGW-RpS18 | K.Jubran |
| K8 | pAGW-RpL11 | K.Jubran |
| K9 | pTWG-RpS9 | K.Jubran |
| K10 | pTWG-RpS15 | K.Jubran |
| K11 | pTWG-RpS18 | K.Jubran |
| K12 | pTWG-RpL11 | K.Jubran |
| K13 | pTWR-RpS9 | K.Jubran |
| K14 | pTWR-RpS15 | K.Jubran |
| K15 | pTWR-RpS18 | K.Jubran |
| K16 | pTWR-RpL11 | K.Jubran |
| K17 | pUAST-RpS18-YN | K.Jubran |
| K18 | pUAST-RpL11-YC | K.Jubran |
| K19 | pUAST-YN-RpS18 | K.Jubran |
| K20 | pUAST-YN-RpS15 | K.Jubran |
| K21 | pUAST-YN-RpS9 | K.Jubran |
| K22 | pUAST-YC-RpL11 | K.Jubran |
| K23 | pTWG-RpS5a | K.Jubran |
| K24 | pTWG-RpS13 | K.Jubran |
| K25 | pTWG-RpS11 | K.Jubran |
| K26 | pTWG-RpS2 | K.Jubran |
| K27 | pTWR-RpL36 | K.Jubran |
| K28 | pTWR-RpL8 | K.Jubran |
| K29 | pTWR-RpL32 | K.Jubran |
| K30 | pTWR-RpL23 | K.Jubran |
| K31 | pUAST.attB.WG | K.Jubran |
| K32 | pUAST.attB.WR | K.Jubran |
| K33 | pUAST.attB.WG-RpS5a | K.Jubran |
| K34 | pUAST.attB.WG-RpS13 | K.Jubran |
| K35 | pUAST.attB.WG-RpS11 | K.Jubran |
| K36 | pUAST.attB.WG-RpS2 | K.Jubran |
| K37 | pUAST.attB.WR-RpL36 | K.Jubran |
| K38 | pUAST.attB.WR-RpL8 | K.Jubran |
| K39 | pUAST.attB.WR-RpL32 | K.Jubran |
| K40 | pUAST.attB.WR-RpL23 | K.Jubran |
| K41 | pUAST.attB.YN | K.Jubran |

| | | |
|---|---|---|
| K42 | pUAST.attB.YC | K.Jubran |
| K43 | pERE-GAL 4 | K.Jubran |
| K44 | pB.S.Act.Gal4 | S.Brogna |
| K45 | pUAST.attB | A.Hidalgo |
| K46 | pAWG | Carnegie Institute |
| K47 | pAGW | Carnegie Institute |
| K48 | pTWG | Carnegie Institute |
| K49 | pTWR | Carnegie Institute |
| K50 | pAc5.1 | S.Brogna |
| K51 | pAc.RpS18-YN | K.Jubran |
| K52 | pAc.RpL11-YC | K.Jubran |
| K53 | pB.S-YN(for N-fusion) | K.Jubran |
| K54 | pB.S-YC(for N-fusion | K.Jubran |
| K55 | pBiFC-bFosYC155 | T. Kerppola |
| K56 | pBiFC-bJunYN155 | T. Kerppola |
| K57 | pBiFC-bFosZIPYC155 | T. Kerppola |
| K58 | pDONR-RpL36 | K.Jubran |
| K59 | pDONR-RpL8 | K.Jubran |
| K60 | pDONR-RpL32 | K.Jubran |
| K61 | pDONR-RpL23 | K.Jubran |
| K62 | pDONR-RpS5a | K.Jubran |
| K63 | pDONR-RpS13 | K.Jubran |
| K64 | pDONR-RpS11 | K.Jubran |
| K65 | pDONR-RpS2 | K.Jubran |
| K66 | pDONR-RpS3 | K.Jubran |
| K67 | pDONR-RpL30 | K.Jubran |
| K68 | pDONR-RpL23A | K.Jubran |
| K69 | pDONR-RpS9 | K.Jubran |
| K70 | pDONR-RpS15 | K.Jubran |
| K71 | pDONR-RpS18 | K.Jubran |
| K72 | pDONR-RpL11 | K.Jubran |

**Table 3.Fly stocks**

| Genotype | Origin | Stock No. |
|---|---|---|
| *w+; IF/ CyO ; TM6B/MKRS* | A. Hidalgo lab | |
| *yw (*wild tipe) | A. Hidalgo lab | |
| Act5C-GAL4]25FO1/CyO | Bloomington | 4414 |
| Act5C-GAL4]17bFO1/TM6B | Bloomington | 3954 |
| gmrGal4 MF815/ gmrGal4 MF815 | A. Hidalgo lab | gmrGal4 |
| RpL11[k16914]/CyO | Bloomington | 11208 |
| yw;crol$^{2}$cn$^{1}$/CyO y$^{+}$;P[w+;GAL-4]699hII | Pier Paolo D'Avino (Cambridge) | (SG-Gal4)#78 |
| Dmel\RpS18$^{c02853}$ from Exelixi Harvard c02853 | Exelixi | |
| RpS5a[1] f[1]/FM6 | Bloomington | 72 |
| RpS5a[2]/FM6 | Bloomington | 73 |
| M(2)53[1]/SM5 | Bloomington | 346 |
| y[1] w[*]; P[w[+mC]=lacW]RpS13[1]/CyO | Bloomington | 2246 |
| Df(3R)X3F, P[ry[+t7.2]=RP49]mtg[P2] e[1]/TM3, Sb[1] | Bloomington | 2352 |
| Df(1)su(s)83, y[1] cho[1] ras[1] v[1]/Dp(1;Y)y[2]sc/C(1)DX, y[1] f[1] | Bloomington | 3370 |
| sop[PRW1]/CyO; ry[506] | Bloomington | 6262 |
| y[1] w[67c23]; P[w[+mC]=lacW]sop[k01215]/CyO | Bloomington | 10499 |
| y[1] w[67c23]; P[w[+mC]=lacW]RpS13[k09614]/CyO | Bloomington | 10910 |

| | | |
|---|---|---|
| y[1] w[67c23];<br>P[w[+mC]=lacW]RpL11[k16914]/CyO | Bloomington | 11208 |
| w[67c23] P[w[+mC]=lacW]G0213a<br>P[lacW]G0213b, l(1)G0213[G0213]/FM7c | Bloomington | 11952 |
| P[w[+mC]=lacW]RpL36[G0471]<br>w[67c23]/FM7c | Bloomington | 12266 |
| w[1118];<br>PBac[w[+mC]=RB]RpS15[e01611]/CyO | Bloomington | 17971 |

**Table 4.Transgene lines used in this study**

| **line** | **description** | **origin** | Refer as |
|---|---|---|---|
| *w+;UAS.RpS9-GFP* | pUAS.RpS9.GFP<br>Strain yw | K.Jubran | K1(M1-M10)<br>The best was (K1-M9) |
| *w+;UAS.RpS18-GFP* | pUAS.RpS18-GFP<br>Strain yw | K.Jubran | K2(M1-M10)<br>The best was (K2-M2) |
| *w+;UAS.RpL11-RFP* | pUAS.RpL11-RFP<br>Strain yw | K.Jubran | K3(M1-M10)<br>The best was (K3-M2) |
| *w+;UAS.RpS18-YN/CyO*<br>*w+;UAS.RpS18-YN/ TM3* | UAS RpS18-YN<br>Strain yw | K.Jubran | K4(M1-M10) The line used to generate BiFC line was (K4-M2) |
| *w+;UAS.RpL11-YC/CyO*<br>*w+;UAS.RpL11-YC/ TM3* | UAS RpL11-YC<br>Strain yw | K.Jubran | K5(M1-M10) The line used to generate BiFC line was (K5-M4) |
| *w+; UAS.RpS18-YN;UAS.RpL11-YC* | UAS-RpS18-YN (2),<br>UAS RpL11-YC (3) | K.Jubran | BiFC line<br>(K4-M2)X(K5-M4) |
| *w+;UAS.attB.RpL36[2R51C] /CyO* | UAS.attB.RpL36-RFP<br>Strain 24482(2R51C) | K.Jubran | K6 |
| *w+;UAS.attB.RpL8[2R51C] /CyO* | UAS.attB.RpL8-RFP<br>Strain 24482(2R51C) | K.Jubran | K7 |
| *w+;UAS.attB.RpL32[2R51C ]/CyO* | UAS.attB.RpL32-RFP<br>Strain 24482(2R51C) | K.Jubran | K8 |
| *w+;UAS.attB.RpL23[2R51C ]/CyO* | UAS.attB.RpL23-RFP<br>Strain 24482(2R51C) | K.Jubran | K9 |
| *w+;UAS.RpS15-GFP/CyO*<br>*w+;UAS.RpS15-GFP/ TM3* | pUAS.RpS15.GFP<br>Strain yw | K.Jubran | K10(M1-M10) |
| *w+;UAS.attB.RpS5a[58A ]/CyO* | UAS.attB.RpS5a-GFP<br>Strain 24484(58A) | K.Jubran | K11 |

| | | | |
|---|---|---|---|
| *w+;UAS.attB.RpS13[58A ]/CyO* | UAS.attB.RpS13-GFP Strain 24484(58A) | K.Jubran | K12 |
| *w+;UAS.attB.RpS11[58A ]/CyO* | UAS.attB.RpS11-GFP Strain 24484(58A) | K.Jubran | K13 |
| *w+;UAS.attB.RpS2[58A ]/CyO* | UAS.attB.RpS2-GFP Strain 24484(58A) | K.Jubran | K14 |
| *w+; UAS.RpS18-GFP;UAS.RpL11-RFP* | UAS-RpS18-GFP (2), UAS RpL11-RFP (3) | K.Jubran | FRET line (K2-M1)X(K3-M2) |

**Table 5.Transgene lines with insert at different locations .**

| line | Insert location | Refer as | comments |
|---|---|---|---|
| *w+;UAS.RpS15-GFP/ TM6B* | **3rd** | K10-M1 | C-terminal .balancer used for 3rd Chr. was TM6B(sb) |
| *w+;UAS.RpS15-GFP/ TM6B* | **3rd** | K10-M2 | C-terminal .balancer used for 3rd Chr. was TM6B(sb) |
| *w+;UAS.RpS15-GFP/CyO* | **2nd** | K10-M3 | C-terminal. balancer used for 2nd Chr. was cyo |
| *w+;UAS.RpS15-GFP/CyO* | **2nd** | K10-M4 | C-terminal. balancer used for 2nd Chr. was *cyo* |
| *w+;UAS.RpS15-GFP/ TM6B* | **3rd** | K10-M5 | C-terminal .balancer used for 3rd Chr. was TM6B(sb) |
| *w+;UAS.RpS15-GFP/CyO* | **2nd** | K10-M6 | C-terminal. balancer used for 2nd Chr. was cyo |
| *w+;UAS.RpS15-GFP/CyO* | **2nd** | K10-M7 | C-terminal. balancer used for 2nd Chr. was cyo |
| *w+;UAS.RpS15-GFP/FM7i* | **x** | K10-M8 | C-terminal balancer used for X Chr was *FM7i;* |
| *w+;UAS.RpS15-GFP/ TM6B* | **3rd** | K10-M9 | C-terminal .balancer used for 3rd Chr. was TM6B(sb) |
| *w+;UAS.RpS15-GFP/CyO* | **2nd** | K10-F10 | C-terminal. balancer used for 2nd Chr. was cyo |
| *w+;UAS.RpS18-YN/CyO* | **2nd** | K4-M1 | C-terminal. balancer used for 2nd Chr. was cyo |
| *w+;UAS.RpS18-YN/CyO* | **2nd** | K4-M2 | C-terminal. balancer used for 2nd Chr. was cyo |

| | | | |
|---|---|---|---|
| *w+;UAS.RpS18-YN/ TM6B* | **3rd** | K4-M3 | C-terminal .balancer used for 3rd Chr. was TM6B(sb) |
| *w+;UAS.RpS18-YN/ TM6B* | **3rd** | K4-M4 | C-terminal .balancer used for 3rd Chr. was TM6B(sb) |
| *w+;UAS.RpS18-YN/ TM6B* | **3rd** | K4-M5 | C-terminal .balancer used for 3rd Chr. was TM6B(sb) |
| *w+;UAS.RpS18-YN/ TM6B* | **3rd** | K4-M6 | C-terminal .balancer used for 3rd Chr. was TM6B(sb) |
| *w+;UAS.RpS18-YN/ TM6B* | **3rd** | K4-M7 | C-terminal .balancer used for 3rd Chr. was TM6B(sb) |
| *w+;UAS.RpS18-YN/CyO* | **2nd** | K4-M8 | C-terminal. balancer used for 2nd Chr. was cyo |
| *w+;UAS.RpS18-YN/CyO* | **2nd** | K4-M9 | C-terminal. balancer used for 2nd Chr. was cyo |
| *w+;UAS.RpS18-YN/ TM6B* | **3rd** | K4-M10 | C-terminal .balancer used for 3rd Chr. was TM6B(sb) |
| *w+;UAS.RpL11-YC/ TM6B* | **3rd** | K5-M1 | C-terminal .balancer used for 3rd Chr. was TM6B(sb) |
| *w+;UAS.RpL11-YC/CyO* | **2nd** | K5-M2 | C-terminal. balancer used for 2nd Chr. was cyo |
| *w+;UAS.RpL11-YC/CyO* | **2nd** | K5-M3 | C-terminal. balancer used for 2nd Chr. was cyo |
| *w+;UAS.RpL11-YC/ TM6B* | **3rd** | K5-M4 | C-terminal .balancer used for 3rd Chr. was TM6B(sb) |
| *w+;UAS.RpL11-YC/CyO* | **2nd** | K5-M5 | C-terminal. balancer used for 2nd Chr. was cyo |
| *w+;UAS.RpL11-YC/CyO* | **2nd** | K5-M6 | C-terminal. balancer used for 2nd Chr. was cyo |
| *w+;UAS.RpL11-YC/ TM6B* | **3rd** | K5-M7 | C-terminal .balancer used for 3rd Chr. |

| | | | |
|---|---|---|---|
| | | | was TM6B(sb) |
| *w+;UAS.RpL11-YC/ TM6B* | **3rd** | K5-M8 | C-terminal .balancer used for 3rd Chr. was TM6B(sb) |
| *w+;UAS.RpL11-YC/ TM6B* | **3rd** | K5-M9 | C-terminal .balancer used for 3rd Chr. was TM6B(sb) |
| *w+;UAS.RpL11-YC/ TM6B* | **3rd** | K5-M10 | C-terminal .balancer used for 3rd Chr. was TM6B(sb) |

**Table 6. Expression of RpL11-YC rescues a lethal mutation in the RpL11 locus**

| **Cyo; RpL11-YC** | **Cyo;TM6B** | **M ; TM6B** | ***M ; RpL11-YC** | |
|---|---|---|---|---|
| Cyo ; RpL11-YC / M ; Ac.Gal4 (B2) | Cyo ; TM6B / M ; Ac.Gal4 (D2) | | M ; RpL11-YC / M ; Ac.Gal4 (A) | **M ; Ac.Gal4** |
| Cyo ; RpL11-YC / M ; TM6B (C2) | | | | **M ; TM6B** |
| | | | M ; RpL11-YC / Cyo ; TM6B (C1) | **Cyo;TM6B** |
| | | M ; TM6B / Cyo ; Ac.Gal4 (D1) | M ; RpL11-YC / Cyo ; Ac.Gal4 (B1) | **Cyo ;Ac.Gal4** |

***M**= RpL11k16914

**Table 6.** Rescue of the lethality of mutated flies homozygous for disrupted RpL11 by RpL11-YC transgenes. (A)the number of rescued flies, which was within the theoretically expected value of 11 flies. The number of other phenotypic , (B1) +(B2)=81 and ,(C1)+(C2) +(D1)+(D2)=102.

**Table 7. Expression of RpS18-YN rescues a lethal mutation in the RpS18 locus**

| **Cyo; RpS18-YN** | **Cyo;TM6B** | **M ; TM6B** | ***M ; RpS18-YN** | |
|---|---|---|---|---|
| Cyo ; RpS18-YN / M ; Ac.Gal4 (B2) | Cyo ; TM6B / M ; Ac.Gal4 (D2) | | M ; RpS18-YN / M ; Ac.Gal4 (A) | **M ; Ac.Gal4** |
| Cyo ; RpS18-YN / M ; TM6B (C2) | | | | **M ; TM6B** |
| | | | M ; RpS18-YN / Cyo ; TM6B (C1) | **Cyo;TM6B** |
| | | M ; TM6B / Cyo ; Ac.Gal4 (D1) | M ; RpS18-YN / Cyo ; Ac.Gal4 (B1) | **Cyo ;Ac.Gal4** |

***M** =RpS18c02853

**Table 7.** Rescue of the lethality of mutated flies homozygous for disrupted RpS18 by RpS18-YN transgenes. (A)the number of rescued flies which was within the theoretically expected value of 7 fly. The number of other phenotypic , (B1) +(B2)=56 fly and ,(C1)+(C2) +(D1)+(D2)=73 fly.

,